# BIOCATALYTIC PRODUCTION OF BIODIESEL AND BIOETHANOL FROM PALM-OIL FEEDSTOCK

**MS. MARISA RAITA**

**ID: 53920003**

**A THESIS SUBMITTED AS A PART OF THE REQUIREMENTS
FOR THE DEGREE OF DOCTOR OF PHILOSOPHY
IN ENERGY TECHNOLOGY**

**THE JOINT GRADUATE SCHOOL OF ENERGY AND ENVIRONMENT
AT KING MONGKUT'S UNIVERSITY OF TECHNOLOGY THONBURI**

**2ND SEMESTER 2013**

# Biocatalytic Production of Biodiesel and Bioethanol from Palm-Oil Feedstock

Ms. Marisa Raita
ID: 53920003

A Thesis Submitted as a Part of the Requirements
for the Degree of Doctor of Philosophy
in Energy Technology

The Joint Graduate School of Energy and Environment
at King Mongkut's University of Technology Thonburi

2nd Semester 2013

Thesis Committee

| | |
|---|---|
| ( Assoc. Prof. Dr. Navadol Laosiripojana ) | Advisor |
| ( Dr. Verawat Champreda ) | Co-advisor |
| ( Asst. Prof. Dr. Worapon Kiatkittipong ) | Member |
| ( Dr. Niran Roongsawang ) | Member |
| ( Prof. Dr. Poonsuk Prasertsan ) | External Examiner |

**Thesis Title**: Biocatalytic Production of Biodiesel and Bioethanol from Palm-Oil Feedstock

**Student's name, organization and telephone/fax numbers/email**

Miss Marisa Raita
The Joint Graduate School of Energy and Environment (JGSEE)
King Mongkut's University of Technology Thonburi
126 Pracha Uthit Rd., Bangmod, Tungkru, Bangkok 10140, Thailand
Telephone: 0-85-3639161
Email: marisabkk28@gmail.com

**Co-advisor's name, organization and telephone/fax numbers/email**

Dr. Verawat Champreda
National Center for Genetic Engineering and Biotechnology
113 Phahonyothin Rd., Klong Luang, Pathumthani 12120, Thailand
Telephone: 02-564-6700 ext 3473
Email: verawat@biotec.or.th

**Advisor's name, organization and telephone/fax numbers/email**

Assoc. Prof. Dr. Navadol Laosiripojana
The Joint Graduate School of Energy and Environment (JGSEE)
King Mongkut's University of Technology Thonburi
126 Pracha Uthit Rd., Bangmod, Tungkru, Bangkok 10140, Thailand
Telephone: 02-872-6736 ext 4146
Email: navadol_l@jgsee.kmutt.ac.th

**Topic:** Biocatalytic Production of Biodiesel and Bioethanol from Palm-Oil Feedstock

**Name of Student:** Miss Marisa Raita **Student ID:** 53920003
**Name of Advisor:** Assoc. Prof. Dr. Navadol Laosiripojana
**Name of Co-Advisor:** Dr. Verawat Champreda

## ABSTRACT

Palm oil is a potent feedstock for the production of biodiesel, while the cellulosic waste from palm oil processing represents an underused biomass for valorization. In this study, conversion of oil palm-derived feedstock to biodiesel and bioethanol using novel biocatalysts and genetically modified ethanolgen has been investigated. In this part, the work is focused on development of an efficient biocatalytic process for biodiesel production from palm oil using novel biocatalyst designs i.e. crosslinked protein-coated microcrystalline lipase (CL-PCMC lipase) and magnetic nanoparticle lipase with modified covalent linkage. The zwitterionic glycine (Gly) was found to be a superior core matrix component from the screening of various organic/inorganic solid-state buffer compared to the conventional insert $K_2SO_4$ for synthesis of immobilized *Thermomyces lanuginosus* lipase with the highest catalytic performance towards esterification of palmitic acid, transesterification of refined palm oil and co-ester/transesterification of crude palm oil with the fatty acid methyl ester (FAME) yield of $\geq$ 95% (mol/mol) from the optimized reaction containing at 4:1 [MtOH]/[FFA] with 20% of the CL-PCMC-lipase/Gly in the presence of tert-butanol as a co-solvent and incubated at 50 °C for 6 h. The high performance of the biocatalyst could be related to the control of enzyme ionization state by glycine which can act as solid-state buffer. Esterification of palm fatty acid distillate using ethanol as a nucleophile led to the highest fatty acid ethyl ester yield of > 95% based on molar basis. The reaction kinetics on esterification followed the Ping-Pong Bi-Bi model and key kinetic parameters were obtained for further reaction up-scaling. Immobilization of the lipase on magnetic nanoparticle was investigated as another potent biocatalyst design with high reactive surface area and simple separation by magnetization. Modification of covalent linkage between the iron core matrix and the enzyme in the form of $Fe_3O_4$-AP-EN-lipase showed the superior catalytic performance toward transesterification of RPO. The optimal reaction contained 23.2% w/w enzyme loading and 4.7:1 methanol to oil molar ratio with 3.4% water content in the presence of 1:1 (v/v) *tert*-butanol to oil obtained from

experimental design optimization using central composite design (CCD) approach. Under the predicted optimal condition, the maximal FAME yield of 97.2% was achieved after incubation at 50 °C for 24 h, which was slightly lower than the predicted yield. Both microcrystalline lipase and magnetic nanoparticle lipase showed high operational stability and could be used in consecutive batches or continuous process.

Another part of the study was focused on the conversion of palm kernel cake (PKC), a mannnan rich by-product to ethanol by using genetically engineered thermophilic bacterium *Geobacillus thermoglucosidasius* TM242. The highest fermentable sugars of 28.3 g/L was obtained from 5% PKC pretreated conditions at 4.5 bar (148 °C) for 15 min using 1.67 %v/w of Advanced Enzymes Technology mannanase (AET mannanase) and 10.38 FPU/g glucan of Cellic Ctec2 cellulase. Fermentation of the PKC hydrolysate led to the maximal ethanol concentration with 9.9 g/L (92.4% of theoretical yield based on the total sugars in 5% PKC) after incubation at 60 °C for 48 h whereas a lower ethanol concentration was obtained using *S. cerevisiae*. The higher ethanol yield from TM242 was due to the ability of the bacteria on converting both hexose and pentose sugars together with the short-chain glucose and mannose oligomers to ethanol.
The *G. thermoglucosidasius* TM242 is thus a promising alternative microorganism for improvement of bioethanol production from lignocellulosic biomass from PKC and other lignocellulosic biomass. Overall the work provides efficient approaches for improvement of biodiesel and bioethanol production from oil palm-derived products by biotechnological processes using novel biocatalysts and ethanologen which can lead to increasing economic competitiveness of the biofuel industry.

**Keywords:** Biodiesel, Bioethanol, Cross-linked protein coated microcrystalline (CL-PCMC), *Geobacillus thermoglucosidasius*, Immobilized lipase, Magnetic nanoparticle, Palm oil, Palm kernel cake

## ACKNOWLEDGEMENTS

First and foremost, I would like to express my gratitude to my supervisors, Assoc. Prof. Dr. Navadol Laosiripojana (JGSEE) and co-supervisor, Dr. Verawat Champreda (BIOTEC, NSTDA) for their useful comments, remarks and engagement throughout the learning process of this thesis.

As most of my work was done at the National Center for Genetic Engineering and Biotechnology (BIOTEC), National Science and Technology Development Agency (NSTDA), I would like to say thank you so much to everyone at the Enzyme Technology Laboratory. Everybody there was an important part of my success as they always kindly helped and encourage me to finish my work especially, Dr. Pattanop kanokratana, Ms. Thanaporn Laothanachareon, Mr. Sarunyou Wongwilaiwalin, and Ms. Jantima Arnthong. Including, I would like to thank Ms. Ubonwan Chaiyo, Ms. Luksana Piromsphon, and Ms. Chayani Sangsue for experimental help at the environmental laboratory.

I would like to deeply thank Prof. David Leak from the Department of Biology and Biochemistry University of Bath Claverton for giving me the good opportunity for research training in the UK as well as Dr. Christopher Ibenegbu for willing help, valuable suggestion and encouragement through 5 months in the UK.

I would like to also thank the committee members, Asst. Prof. Dr. Worapon Kiatkittipong, and Dr. Niran Roongsawang, for their valuable advice and suggestions, and the external examiner, Prof. Dr. Poonsuk Prasertsan, for her kind and valuable comments and suggestions. I acknowledge the financial support from the Royal Golden Jubilee Scholarship (RGJ) and the Joint Graduate School of Energy and Environment (JGSEE).

Finally, I would like to express my warm thanks to my family for their moral support, which has played an important role in my achievements.

# CONTENTS

## CONTENTS (Cont')

**CONTENTS (Cont')**

**CONTENTS (Cont')**

**CONTENTS (Cont')**

**CONTENTS (Cont')**

# LIST OF TABLES

## LIST OF TABLES (Cont')

## LIST OF TABLES (Cont')

# LIST OF FIGURES

## LIST OF FIGURES (Cont')

## LIST OF FIGURES (Cont')

## LIST OF FIGURES (Cont')

# LIST OF ABBREVIATIONS

| | | |
|---|---|---|
| AET | = | advanced enzymes technology |
| AOX | = | alcohol oxidase |
| APTES | = | aminopropyl trimethoxysilane |
| AREP | = | acetone rinsed enzyme preparation |
| BMGY | = | buffered minimal glycerol yeast |
| BMMY | = | buffered minimal methanol yeast |
| BSPs | = | biomass support particle |
| CA | = | *Candida antarctica* |
| CAPSO | = | 3-(cyclohexylamino)-2-hydroxy-1-propanesulfonic acid |
| CBP | = | consolidated bioprocessing process |
| CLEAs | = | cross-linked enzyme aggregates |
| CLECs | = | cross-linked enzyme crystals |
| CL-PCMCs | = | cross linked protein-coated microcrystals |
| CPO | = | crude palm oil |
| *E*a | = | activation energy |
| EDC | = | 1-ethyl-3-(3-dimethylaminopropyl) carbodiimide solution |
| EPFB | = | empty palm fruit bunch |
| EtOH | = | ethanol |
| FAEE | = | fatty acid ethyl ester |
| FAME | = | fatty acid methyl ester |
| FFAs | = | free fatty acids |
| FTIR | = | fourier-Transformed Infrared Spectroscopy |
| GA | = | glutaraldehyde |
| GPI | = | glycosylphosphatidylinositol |
| HEPES | = | 4-(2-hydroxyethyl)piperazine-1-ethanesulfonic acid |
| IC | = | Ion chromatography |
| MeOH | = | methanol |
| MES | = | 2-morpholinoethanesulfonic acid |
| MOPS | = | 3-morpholinepropanesulfonic acid |
| NHS | = | N-hydroxysuccinimide |
| PCMCs | = | protein-coated microcrystals |

**LIST OF ABBREVIATIONS (Cont')**

| | | |
|---|---|---|
| PFAD | = | palm fatty acid distillate |
| PKC | = | palm kernel cake |
| PVDF | = | polyvinylidene fluoride |
| RPO | = | refined palm olein |
| SDS-PAGE | = | sodium dodecyl sulfate polyacrylamide gel electrophoresis |
| SEM | = | scanning electron microscope |
| SHF | = | separated hydrolysis fermentation |
| SPY | = | salt peptone yeast extract |
| SSCF | = | simultaneous saccharification and co-fermentation processes |
| TAPS | = | [(2-hydroxy-1,1-bis(hydroxymethyl)ethyl)amino]-1-propanesulfonic acid |
| *t*-BuOH | = | tert-butanol |
| TL | = | *Thermomyces lanuginosus* |
| TSA | = | tryptone soya agar |
| XRD | = | X-ray diffraction |
| YPD | = | yeast peptone dextrose |

# CHAPTER 1
## INTRODUCTION

### 1.1 Rationale/Problem Statement

Nowadays, fossil fuels, such as diesel and gasoline, are key energy sources for industry and automobiles. The problems on increasing price of petroleum fuels and their environmental impact have led to the finding of new renewable fuel in order to overcome these problems. Several alternative renewable fuels are widely used including bioethanol and biodiesel while some are being developed for future use such as second generation biofuels. Among the conventional fuels, diesel is a key petroleum-based fuel used in diesel engines e.g. heavy trucks, city transport buses, locomotives, electric generators, and also in industrial sectors. While, bioethanol is mainly used for gasoline mixture in transportation sectors. Searching for alternative sources to replace the petroleum fuels is thus important for solving the current energy problem worldwide.

Oil palm is currently the largest supply of feedstock in many tropical and subtropical countries, such as Thailand, Malaysia and Indonesia, for the utilization in oil consumption and biofuel production. The main components after industrial palm oil processing are approximately 20% of crude palm oil and 80% of biomass. These products, by-product and residues are illustrated in Figure 1 [1], allowing utilization on several possible applications, especially biodiesel and bioethanol production. Typically, refined palm olein (RPO) obtained from refinery of crude palm oil after separation of palm fatty acid distillate (PFAD) is the major feedstock for alkali-catalyzed transesterification into industrial section. The fluctuating price of edible palm oil during 2006 in Asia was observed related to rapid demand both domestic and export trade, including competitive problems between food and fuel [2]. Interests on using crude palm oil (CPO) and palm fatty acid distillate (PFAD), a by-product from palm oil processing has been increasing for reducing the feedstock cost and enhancing the value added by-product in biodiesel industry. Moreover, the large proportion of residues e.g. empty palm fruit bunch (EPFB), palm fiber (PF), and palm kernel cake (PKC) after palm oil processing is also considered a challenge resource for future feasible production of lignocellulosic ethanol.

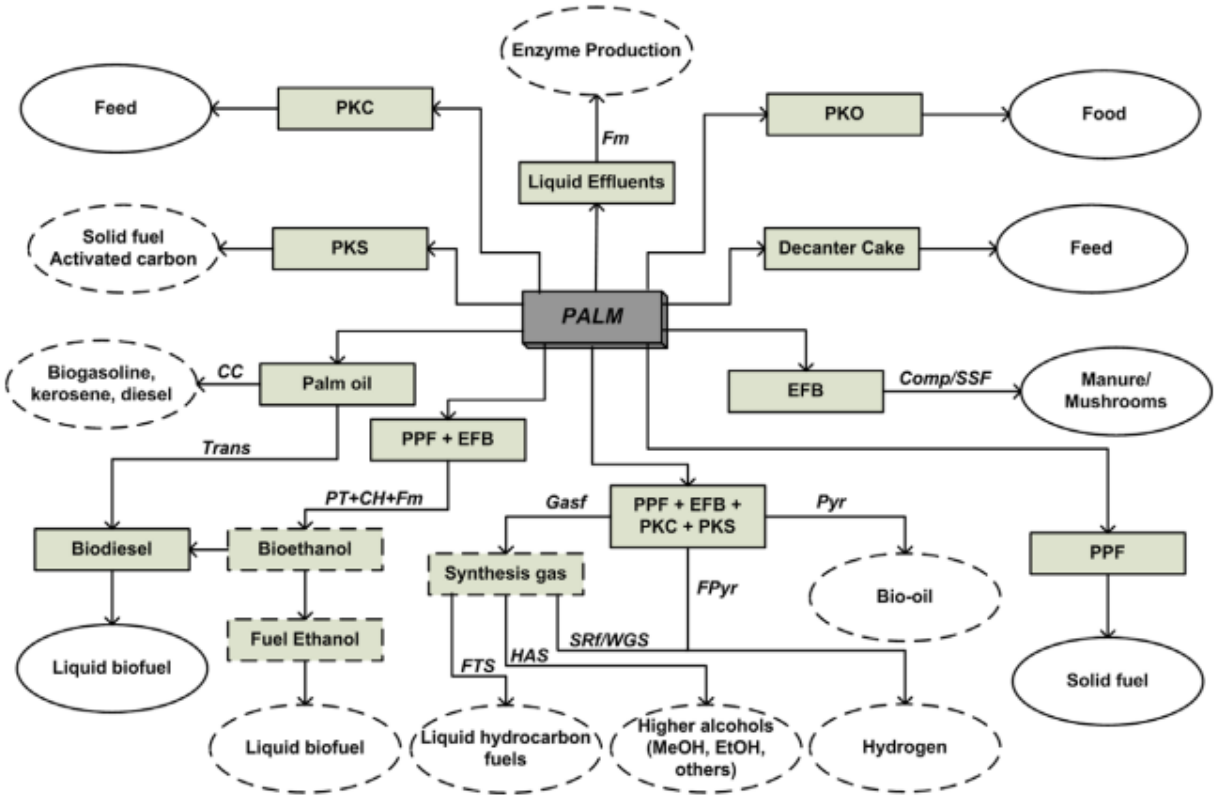


**Figure 1.1** The products and residues obtained during a refined palm oil processing [1].

Biodiesel is a potent alternative for replacing conventional diesel fuel. It has comparable properties to conventional diesel but has several environmental advantages as it is carbon-neutral which can help reducing the emissions of carbon monoxide to the atmosphere and has lower unburned hydrocarbons, particulate matter and other pollutants [3]. This alternative fuel can be produced from transesterification and esterification of vegetable oils or free fatty acids (FFAs) with short chain alcohols in catalytic reaction using bases, acids, or enzymes as the catalysts.

There are several vegetable oils which are used as raw materials for synthesis of biodiesel such as soybean oil, sunflower oil, rapeseed oil and palm oil. The homogeneous acid catalyzed process is energy intensive and has difficulties in catalyst recovery, waste treatment, and corrosion of the equipment which lead to an increase in the overall cost of the process. Likewise, the use of base catalysts in process e.g. sodium hydroxide, and potassium hydroxide results in the undesirable product from saponification containing high free fatty acid in the reaction. These limitations can be overcome by using biocatalytic process that performs under mild reaction conditions with no chemical waste, and allows ease of by-product recovery making it as an efficient and environmentally friendly process.

The way to develop biocatalysts for biodiesel production has focused on the cost reduction for enzymes and improvement of the enzyme's operational time and reusability which would benefit the commercialization of the biocatalytic process for biodiesel synthesis in the future. Lipases can be used for synthesis of biodiesel. This enzyme can work in non-aqueous system in transesterification and esterification processes. Free and immobilized lipases have been reported for catalyzing reaction in biodiesel synthesis. Immobilized lipases have been used with several advantages over the free lipase including their reusability and higher stability which lead to increasing cost-effectiveness of the biocatalytic process.

Several methods on lipase immobilization e.g. adsorption, covalent bonding, entrapment, and microcrystalline enzymes such as protein-coated microcrystals (PCMCs) and cross linked protein-coated microcrystals (CL-PCMCs) have been reported [4, 5]. Among these biocatalyst designs, the microcrystalline enzymes have been shown as potent alternative biocatalyst designs with higher stability, catalytic efficiency, and reusability in aqueous and/or non-aqueous media [6]. The solid carriers have been shown to have important influences on catalytic performance of the biocatalysts. A variety of solid supports has been reported for lipase immobilization e.g. acrylic resin, hydrophobic sol gel, textile membrane, and magnetic nanoparticle with differences in their physical and chemical properties relevant to interactions with the enzyme molecules. The development of a cost-effective method for preparation of highly active immobilized lipase is thus a challenge for establishment of a feasible eco-friendly biocatalytic biodiesel production process.

Bioethanol from lignocellulosic biomass is another potent renewable biofuel that could help reducing ethanol production from sugar and starch, which competes with the food supply chain. This provides a potential approach for production of bioethanol with near-zero greenhouse gas emission based on life-cycle assessment [7]. Lignocellulosic biomass e.g. forestry residue, agriculture residue, and wood products is a renewable resource composed of cellulose, hemicelluloses and lignin as the primary constitution. Typically, bioethanol production requires several steps involving pretreatment of substrates, followed by saccharification of the biomass to release fermentable sugars from polysaccharides, and fermentation of sugars prior to subsequent downstream distillation step. Apart from the conventional fermentation of glucose to ethanol by *Saccharomyces cerevisiae*, other sugars, such as xylose, mannose, and arabinose, can also be converted to

ethanol [8, 9]. This can be performed by genetically modified *S. cerevisiae* and other pentose-fermentative ethanologenic microorganisms. A thermophilic bacterium of *Geobacillus thermoglucosidasius* TM242 has been reported to utilize both hexose and pentose as well as the short-chain oligosaccharides e.g. cellobiose, and mannobiose as substrates for ethanol fermentation and hence considered a potent alternative ethanologen for production of ethanol from lignocellulose [8, 10].

In order to develop efficient processes for biocatalytic biodiesel and bioethanol production from palm feedstock, this study focus on (i) the development of high-performance immobilized lipase in microcrystalline form and optimization of the process conditions for both esterification and transesterification, as well as the study of reaction kinetics in a laboratory-scale process using the developed biocatalyst; (ii) modification of lipase immobilization on magnetic nanoparticle to develop a highly efficient biocatalyst for biodiesel synthesis; (iii) construction of cell-surface and secreted lipase expression system in *Pichia pastoris* for trial in whole-cell biocatalyst production of biodiesel; (iv) utilization of palm kernel cake as an alternative feedstock for bioethanol using a new ethanologenic bacteria *G. thermoglucosidasius* compared to the conventional yeast. These findings would lead to the further development of the cost-efficient biocatalytic processes for biofuel production from palm feedstocks.

## 1.2 Objectives

The aim of this research was targeted on the development of biocatalysts for a biodiesel synthesis process using new immobilized lipase designs focusing on microcrystalline lipase and magnetic nanoparticle lipase. The biocatalytic processes were optimized for transesterification and esterification of palm oil feedstocks. The reaction kinetics of the biocatalytic biodiesel synthesis process using the developed biocatalyst was studied. Another focus is on conversion of lignocellulosic palm oil waste to ethanol using the novel *G. thermoglucosidasius* strain in which the work involved optimization of pretreatment and enzymatic hydrolysis of the substrate for subsequent ethanol fermentation by the recombinant. *G. thermoglucosidasius* strain. The research provides a basis for conversion of oil palm and its by-products to biofuels using efficient and eco-friendly biotechnological processes for further application in biofuel industry.

1. To study the effects of buffered or non-buffered core matrix components on the catalytic performance and operational stability of microcrystalline lipase (CL-PCMC: cross-linked protein coated microcrystalline enzyme) on esterification and transesterification of palm oil products.
2. To investigate the kinetic parameters of the CL-PCMC lipase catalyzed on esterification of palmitic acid.
3. To develop high-performance immobilized lipase on magnetic nanoparticle supports using different covalent modification designs and to optimize the biocatalytic transesterification reaction using response surface methodology (RSM) based on a central composite design (CCD) for maximizing product yields.
4. To construct the recombinant *P. pastoris* expressing *Thermomyces lanuginosus* (lipase TL) and *Candida antarctica* (lipase CA) in cell surface display forms and in secreted forms and to evaluate the lipase activity of the whole-cell biocatalyst.
5. To study the conversion of palm kernel cake to ethanol by evaluating the effects of hydrothermal pretreatment by steam explosion, optimizing enzymatic hydrolysis process, and comparing ethanol fermentation by the recombinant *G. thermoglucosidasius* strain and the conventional yeast *Saccharomyces cerevisiae*.

# CHAPTER 2
# LITERATURE REVIEW

Renewable biofuels, particularly biodiesel and bioethanol, are thus promising sustainable alternatives to conventional fossil fuels, such as diesel and gasoline, in the transportation sector. The alkali catalyzed process is conventionally used in biodiesel industry. However, the alkaline catalyzed reaction is energy intensive and suffers from difficulties in recovery of glycerol and catalyst, interfered saponification reactions and waste water treatment [11]. The biocatalytic process can overcome these drawbacks and is environmentally friendly and has receiving increasing attention for production of eco-biodiesel from crude vegetable oil with high free fatty acid content e.g. crude palm oil and palm fatty acid distillate Along with palm oil and biodiesel production, a large amount of cellulose and hemicellulose is generated as by-products from palm oil refining. These palm waste provide alternative lignocellulosic feedstocks for conversion to ethanol production which can alleviate the controversy between “food v.s. fuel” utilization. Development of bio-technological processes based on enzyme catalysis and fermentation with novel biocatalyst designs and microbes for production of biodiesel and bioethanol from oil palm is thus an interesting approach for establishment of near-zero waste process and lead to valorization of products and by-products from palm oil industry.

This chapter reviews the conversion of oil palm feedstock into liquid biofuels, especially biodiesel and bioethanol. A general overview of these alternative fuels is introduced for providing the general knowledge on this work. In biodiesel part, this review covers methods on lipase immobilization for biodiesel synthesis with the focus on different potent biocatalyst designs particularly protein-coated microcrystals (PCMCs), cross linked protein-coated microcrystals (CL-PCMCs), magnetic nanoparticle, and whole cell biocatalyst. Another part of the review is focused on technology review on enzymatic hydrolysis of lignocellulosic biomass and conversion of sugars to bioethanol using various processes e.g. separated hydrolysis fermentation (SHF), simultaneous saccharification and co-fermentation processes (SSCF), and consolidated bioprocessing process (CBP).

## 2.1 Oil palm

Typically, biodiesel is derived from a variety of feedstocks in a reaction with an excess of short chain alcohols. There are five categories of raw materials, including vegetable oils, animal fats, waste oil, non-edible oils and algae oils [12]. The use of different feedstocks to produce biodiesel in each country depends on specific plant variety, cultivation practices, and weather and soil conditions. For example, rapeseed oil, including sunflower oil is the dominant feedstock used to make biodiesel in Europe. In the US, biodiesel has generally been made from soybean oil, because of its large domestic production. Oil palm is currently the largest supply of feedstock many tropical and subtropical countries such as Thailand, Malaysia and Indonesia. This feedstock is superior to other crops in terms of higher annual yield, leading to the greater biodiesel production yield as shown in Table 2.1.

**Table 2.1** Potential of oil crops for biodiesel production [13].

| Oil crop | Annual yield/(tonnes/ha) | Oil extraction rate/ (%) | Annual biodiesel yield/ (l/Ha) |
|---|---|---|---|
| **Oil palm** | 17,544 | 18.6 | 3527 |
| **Soy bean** | 1438 | 22.9 | 350 |
| **Peanut** | 1575 | 20.3 | 346 |
| **Sesame** | 619 | 24.2 | 162 |
| **Castor bean** | 688 | 40.7 | 302 |
| **Jatropha** | 5000-1875 | 25 | 1355 |

In general, oil palm (*Elaeis guineensis*) is native to West and Central Africa. The oil palm fruit is firstly harvested after 3 years from planting that has an economic life span with 25–30 years. Its maximum production yield is in the 12th or 13th year and declines afterward until the end of life time [14]. Normally, the properties of palm oil biodiesel are typically associated with high cloud point and pour point which limit its usage in cooler climates. However, winterization, additives and blending with other oils can solve these problems by changing the cold flow properties [15]. Apart from palm oil, other possible raw materials for biodiesel productions in Thailand are jatropha oil, coconut oil, and soybean oil [13].

### 2.1.1 Palm oil processing

In general, fresh fruit bunches after oil palm processing demonstrated a variety of products is composed of 21% palm oil, whereas the 79% remaining were lignocellulosic wastes comprised of 6–7% palm kernel, 14–15% fiber, 6–7% shell, and 20-23% empty palm fruit bunch (EPFB) as illustrated in Figure 2.1 [16, 17]. Utilization of oil palm wastes as renewable sources for biofuel and other bio-based products is a great challenge for valorization of by-products from palm oil industry.

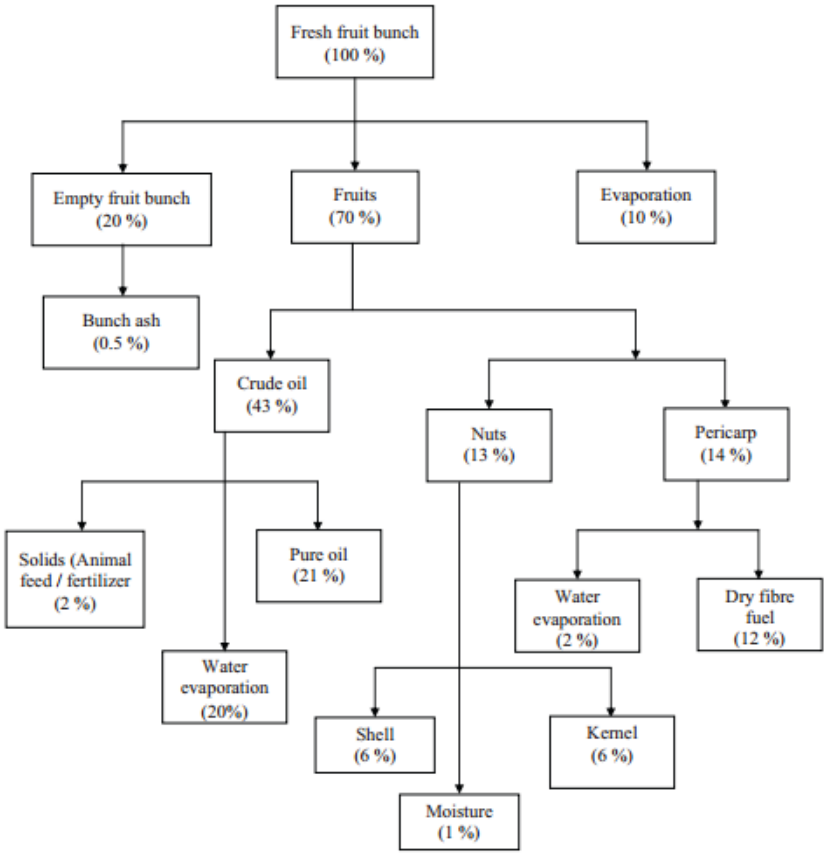


**Figure 2.1** Products from oil palm processing [16].

Crude palm oil is mostly refined in to refined palm olein (RPO) by physical or chemical processes for food consumption, while the remaining 10% is used for biodiesel production employing alkali-catalysed transesterification reactions (Figure 2.2) [18]. Free fatty acid and impurities and by-product are separated to palm fatty acid distillate (PFAD) which is currently used in the production of low grade soap.

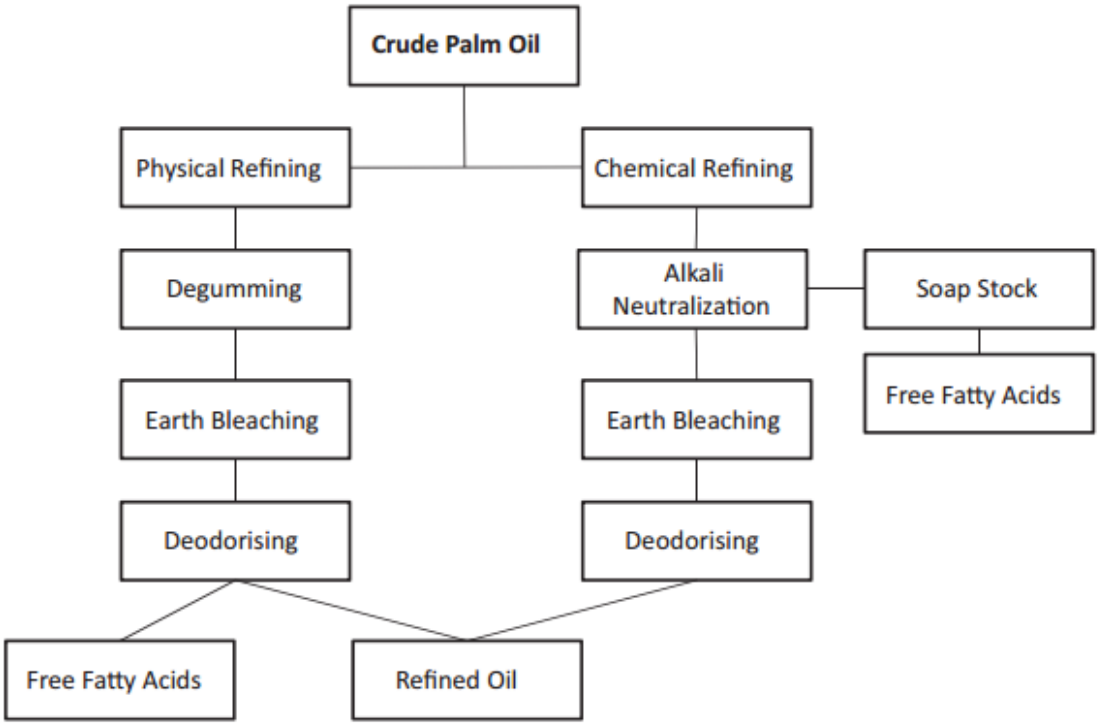


**Figure 2.2** Palm oil refining process [19].

The composition of different feedstocks from the palm oil industry is illustrated in Table 2.2 [4]. It was found that the RPO mainly contains 39.8% of palmitic (16:0), 42.5% of oleic (18:1), and 11.2% of linoleic acids, with other fatty acids as minor constituents. CPO contained mostly the same composition as RPO but with higher impurities and free fatty acids up to 4%. PFAD is the fatty acid rich fraction from palm oil refining and contained 93.2% fatty acid as the major composition. Interests on using crude palm oil (CPO) and palm fatty acid distillate (PFAD) have been increasing in order to reduce the feedstock cost of biodiesel production. Conversion of feedstocks with high fatty acid to alkyl esters is generally performed by an acid-catalyzed process. However, this process suffers from difficulties in recovery of the catalyst, the cost of wastewater treatment, and corrosion of the processing equipment [18]. Therefore, the use of enzymatic process for conversion of high free fatty acid feedstocks to biodiesel is thus of great interest. [4, 5].

**Table 2.2** Composition of different feedstocks from palm oil industry for biodiesel production [4].

| Feedstock | Free fatty acid content (%) | Composition of fatty acid (%) | | | | |
|---|---|---|---|---|---|---|
| | | Palmitic | Oleic | Linoleic | Stearic | Others |
| **Refined palm olein (RPO)** | 0 | 39.8 | 42.5 | 11.2 | 4.4 | 2.1 |
| **Crude palm oil (CPO)** | 7 | 43.5 | 39.8 | 10.2 | 4.3 | 2.2 |
| **Palm fatty acid distillate (PFAD)** | 93.2 | 47.1 | 35.7 | 9.3 | 4.5 | 3.4 |

Regarding the oil palm wastes, palm kernel cake (PKC) is derived from the pressing and extraction of oil from palm kernels. A large amount of PKC obtained from palm oil processing is used for producing feed supplement for animals due to its high protein contents of around 15%. Nevertheless, the high fiber content of carbohydrate, including the low amount of nutritional value protein restricts the efficiency of PKC feed. Utilization on carbohydrates in this fiber residues for conversion to biofuels and other valorized products is thus of great interest. After ethanol production, the final product enriched in protein and also with reduced the fiber content can then be used as a, more attractive feed supplement compared with traditional PKC. The PKC components mainly consist of approximated 50% of carbohydrates, providing the major sugars of hexose (mannose and glucose) and a trace amount of pentose (xylose and arabinose). The main carbohydrate in PKC is mannan or galactomannan that compose of a linear (1→4) linked β-D-mannopyranose backbone with (1→6) linked α-D-galactopyranose side groups (minor quantity) [20]. Although the intrinsic crystalline structure of mannan is much similar to cellulose, this crystalline attributes of galactomannan in mannan is easier to digest by endomannanases compared to cellulose. Based dry basis, mannose is the principal carbohydrate in PKC with content in the range of 35–45%, while the glucose content is also 7–12% glucose [21]. The large proportion of polysaccharides in PKC containing the favorable fermentable sugars is a promising source of sugars for bioethanol production from oil palm waste.

## 2.2 Biodiesel

Biodiesel, namely fatty acid alkyl esters, is an environmentally friendly alternative fuel for replacing conventional diesel fuel. It can be directly used in diesel engine without engine modification and has lower emission of pollutants, including oxides of nitrogen, oxides of sulfur, oxides of carbon, lead, unburned hydrocarbons, and particulate matters [22]. Normally, its physical characteristic is a clear amber-yellow liquid with a viscosity similar to that of diesel, and insoluble in water. Several processes for biodiesel synthesis such as pyrolysis, microemulsification, transesterification and esterification have been reported by many researchers [12]. Chemical transesterification has received high attention due to its simple and high efficient process for conversion of triglycerides with short chain alcohols (methanol and ethanol) into alkyl esters. Biodiesel can also be produced by esterification of free fatty acids (FFAs) and alcohols. For example, palm fatty acid distillate (PFAD) with methanol could be converted to methyl ester with 95% conversion using the commercially immobilized lipase, Novozyme 435 by esterification reaction [23]. The reactions for transesterification and esterification are illustrated in Figure 2.3.

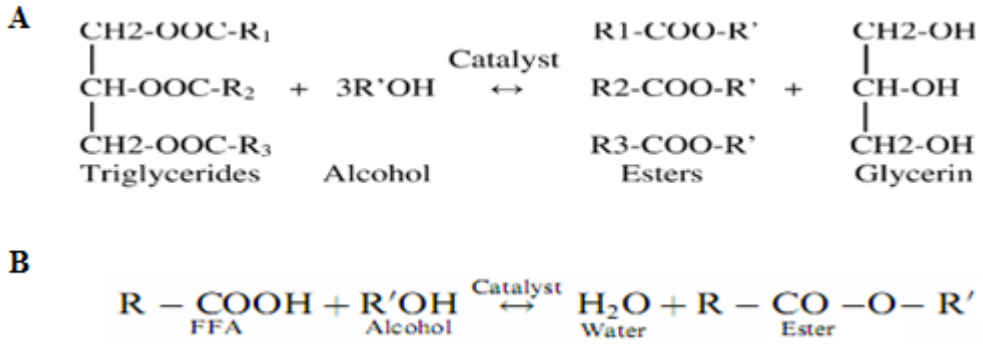


**Figure 2.3** Different reactions for biodiesel production: (A) transesterification and (B) esterification [24].

A wide range of feedstocks, such as vegetable oils, animal fats, waste oil, and algae has been used for biodiesel synthesis [12]. Particularly, the use of various vegetable oils, such as soybean oil [25], rice bran oil [26], sunflower oil [27], and palm oil [4] as main feedstocks for catalytic production of biodiesel has been extensively studied and commercialized. With regard to short chain alcohols, methanol is the most commonly used alcohol in the industrial production of biodiesel due to its relatively low cost and availability [11]. However, the deactivation of lipase and the difficulty of glycerol

separation have been found for reactions with methanol. Ethanol has relatively higher costs for producing biodiesel at present, although it is more eco-friendly as it can be produced from renewable resources. There are different types of catalysts for biodiesel synthesis including alkaline catalysts, such as sodium or potassium hydroxides, acid catalysts, such as sulfuric acid, and enzymes, i.e. lipases, as well as heterogeneous solid catalysts, such as zeolites, and hydrotalcites. Conversion of triglycerides to alkyl esters by thermal processes using supercritical and subcritical methanol processes has also been reported. The comparison of different catalytic technologies in biodiesel synthesis is presented in Table 2.3. These catalysts have different advantages and disadvantages on biodiesel production.

**Table 2.3** Comparison of the different technologies for biodiesel production [28].

| Variable | Base catalyst | Acid catalyst | Lipase catalyst | Supercritical alcohol | Heterogeneous catalyst |
|---|---|---|---|---|---|
| **Reaction temperature (°C)** | 60-70 | 55-80 | 30-40 | 239-385 | 180-220 |
| **Free fatty acid in raw materials** | Saponified products | Esters | Methyl esters | Esters | Not sensitive |
| **Water in raw materials** | Interfere with reaction | Interfere with reaction | No influence | | Not sensitive |
| **Yields of methyl esters** | Normal | Normal | Higher | Good | Normal |
| **Recovery of glycerol** | Difficult | Difficult | Easy | | Easy |
| **Purification of methyl esters** | Repeated washing | Repeated washing | None | | Easy |
| **Production cost of catalyst** | Cheap | Cheap | Relatively expensive | Medium | Potentially cheaper |

The transesterification reaction is conventionally catalyzed by strong bases, such as sodium hydroxide, strong acids, such as sulfuric acid, or enzymes. Strong acids and enzymes are also used for esterification reaction as alkali catalysts cause saponification when used with feedstocks with high free fatty acid content. Enzymatic biodiesel synthesis processes using lipase have been reported as a promising alternative to the conventional chemical methods. This process also has many advantages, including being less energy intensive, simple purification and downstream processing, and environmentally friendly [29]. Lipases from various microorganisms, such as *Candida antarctica* [30],

*Pseudomonas cepacia* [31] and *Thermomyces lanuginosus* [32] have been employed as biocatalysts, either in soluble and immobilized forms.

Several researchers have reported that soluble lipases can be used as effective catalysts for the production of biodiesel. However, the use of free lipases in an industrial scale is restricted by high cost of the enzymes. The problem can be overcome by enzyme immobilization which allows recycling of the biocatalysts and thus reducing the cost of the enzymatic process. This enzyme has been so far immobilized on various types of carriers by different methods, such as adsorption [33], covalent bonding [34], entrapment [35], and carrier-free immobilization e.g. cross-linking including cross-linked enzyme aggregates (CLEAs), cross-linked enzyme crystals (CLECs) [36] and using precipitation in microcrystalline forms such as protein-coated microcrystals (PCMCs) [4] and cross-linked protein-coated microcrystals (CL-PCMC) [5].

To increase the immobilization efficiency, new solid supports have been introduced e.g. polyvinylidene fluoride (PVDF) membrane and magnetic nanoparticle [37, 38]. In addition, the use of whole cell biocatalyst expressing lipase intracellularly or on cell surface is also attractive for biodiesel synthesis [39, 40]. Effects of reaction parameters for catalysis in non-aqueous reaction for examples, temperature, time, types of alcohols and molar ratio of alcohol to oil and water activity on biocatalytic biodiesel synthesis has been studied. This leads to the typical biodiesel yield of >90% from the biocatalytic reactions under mild reaction conditions from different vegetable oils.

### 2.2.1 Biodiesel production processes

#### 2.2.1.1 Dilution (Blending)

Dilution is a common method that provides crude vegetable oils blended directly with diesel fuel for the improvement of viscosity and engine performance, including increasing carbon deposits. However, dilution is not suitable for long term use in a direct injection engine, so the other techniques have been explored further [12].

#### 2.2.1.2 Pyrolysis

Pyrolysis, or thermal cracking process, can be used to reduce viscosity and improve the cetane number of vegetable oils, leading to products such as alkanes, alkenes, alkadienes, cycloalkanes, alkylbenzenes, carboxylic acids, aromatics and small amounts of gaseous products. For example, soy bean oil, and rapeseed oil are successfully cracked with appropriate catalysts to generate biodiesel [22]. However, the process is restricted by high cost of equipment and also suffers from the presence of sulfur in the final products which can interfere with its use in combustion.

#### 2.2.1.3 Microemulsification

Microemulsification is another approach to reduce the viscosity of vegetable oils. This process specially requires surfactants, such as methanol, ethanol and propanol, for emulsifying the oil and water, as well as cetane improvers such as alkyl nitrates. The process can lead to viscosity reduction, increase in cetane number and good spray characters of the biodiesel product. However, its long term usage might probably cause the problem of injector needle blockage, carbon deposit formation and incomplete combustion [22].

#### 2.2.1.4 Transesterification

Transesterification is the most popular method for biodiesel synthesis from vegetable oils with alcohols. This could be due to the fact that the physical characteristics of fatty acid esters are very close to those of diesel fuel, allowing alkyl esters produced from transesterification to be used without engine modifications [41]. An illustration of the reaction shows that triglycerides reacted with alcohols, such as methanol and ethanol, to form diglyceride and subsequently, monoglyceride, and finally, methyl esters with glycerol as a by-product (Figure 2.4).

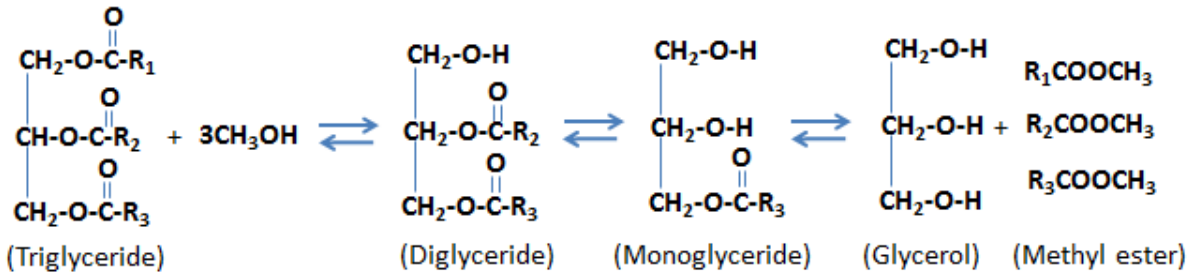


**Figure 2.4** Transesterification process [42].

### 2.2.2 Catalytic transesterification/esterification processes

#### 2.2.2.1 Alkali-catalyzed process

Alkali catalysts are most commonly used in the biodiesel industry. The process is fast and the reaction conditions are moderate. Sodium hydroxide (NaOH) or potassium hydroxide (KOH) are used as catalysts along with methanol or ethanol, as illustrated in Figure 2.5. Initially, during the process, alcoxy is formed by reaction of the catalyst with alcohol and the alcoxy is then reacted with vegetable oil to form a mixture of alkyl ester and by-product as glycerol. Removal of glycerol is required as it can be converted to formaldehyde or acetaldehyde in combustion which can cause to toxicity effect to health. Alkaline metal alkoxides e.g. sodium methoxide ($CH_3ONa$) and potassium methoxide ($CH_3OK$) are more active alkali catalysts since they give very high biodiesel yields (>98%) in short reaction times [28]. The reaction using sodium methoxide in methanol and a vegetable oil is very rapid. It has been shown that triglycerides on transesterification can be completely converted to product within 2–5 mins at room temperature. The alkali-catalyzed reaction provides an efficient and less corrosive process with high product yield compared to the acid-catalyzed process. However, it is sensitive to the presence of free fatty acod in the feedstock which can cause saponification, leading to a lower product yield and difficulty in the separation process [12, 43].

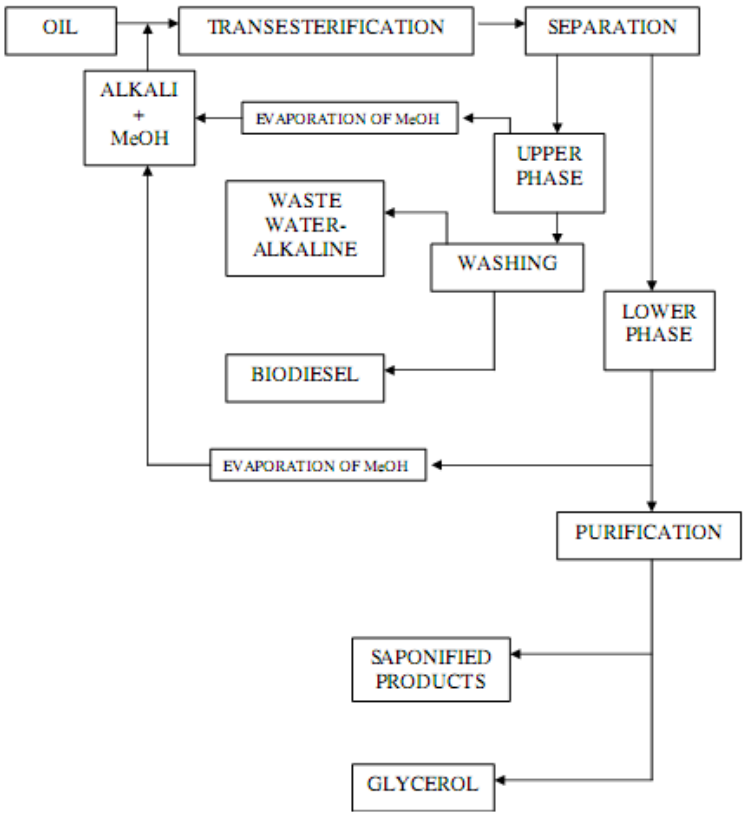


**Figure 2.5** Alkali-catalyzed biodiesel synthesis process [18].

#### 2.2.2.2 Acid-catalyzed process

The acid-catalyzed reaction is an alternative for biodiesel production from feedstock, containing high free fatty acid content by esterification and transesterification. The most commonly used acids are sulfuric acid and sulfonic acid [12]. The acid-catalyzed process on production synthesis from grease with methanol in the presence of sulfuric acid is presented in Figure 2.6. The mechanism of the acid-catalyzed esterification of fatty acids is illustrated in Figure 2.7. The initial step is on protonation of the acid to give an oxonium ion (1), which can undergo an exchange reaction with an alcohol to give the intermediate (2), and this in turn can lose a proton to become an ester (3) [12]. However, the drawbacks of the acid-catalyzed process include corrosion of equipment, low reaction rate, and the need for more extreme temperatures and pressure conditions [41].

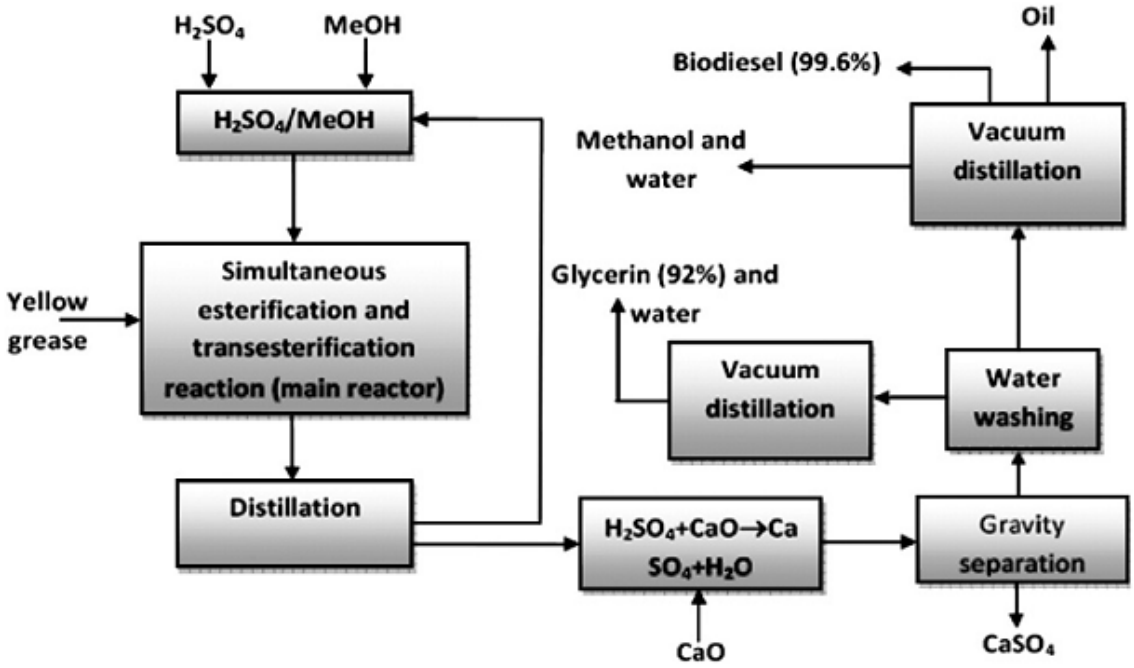


**Figure 2.6** Simplified blockflow diagram of the acid-catalyzed process for the production of biodiesel [28].

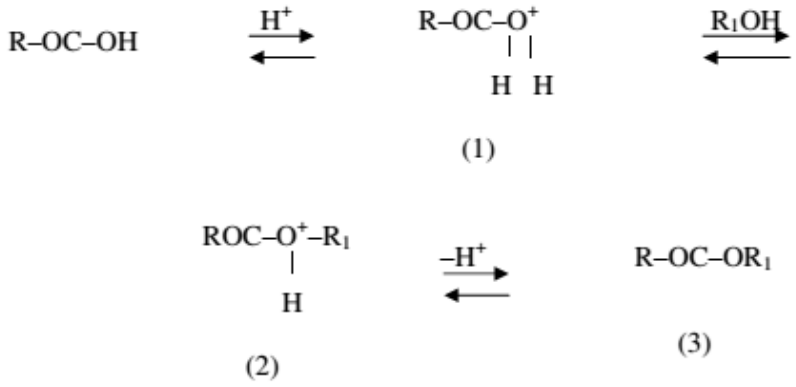


**Figure 2.7** Mechanism of acid-catalyzed esterification of fatty acids [12].

### 2.2.2.3 Enzyme-catalyzed process

The use of lipases in soluble and immobilized forms can be used for catalyzing both transesterification and esterification reactions (Figure 2.8). The processes are operated under mild conditions and generate no chemical wastes [43, 44]. However, lipases are generally sensitive to excess methanol in the reaction. Heterogeneous immobilized lipases can be recycling and is superior to the soluble form with its improved operational stability which lead to improvement of the process efficiency with lower cost [18].

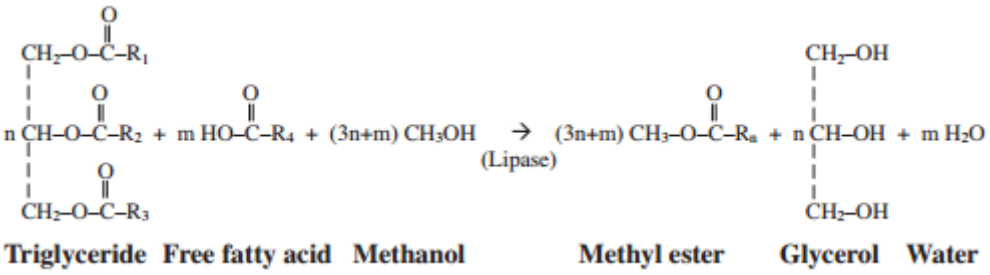


**Figure 2.8** Combined esterification and transesterification reactions using lipase [44].

### 2.2.2.4 Heterogenous chemical catalyzed process

In addition to immobilized enzymes, heterogenous catalysts such as amorphous zirconia, zeolites, hydrotalcites, oxides, and γ-alumina, are becoming more attractive for catalyzing the transesterification/esterification of vegetable oils due to their relatively lower costs than the costs of lipase [45]. Most of these catalysts are alkali or alkaline oxides on solid support with large surface area. Normally, solid basic catalysts are more active than solid acid catalysts. For example, the use of calcium oxide (CaO) provides several advantages such as long catalyst lifetimes, higher activity, and mild reaction conditions; however, the reaction rate on biodiesel synthesis was slow. Among the industrial processes, solid acid catalysts, such as Nafion-NR50, sulfated zirconia and tungstated zirconia were chosen to catalyze on transesterification due to the presence of sufficient acid site strength and higher selectivity [28]. However, the use of heterogenous chemical catalysts consumes more energy and obtain lower alkyl ester product compared to the enzymatic process.

#### 2.2.2.5 Supercritical fluid process

Supercritical fluid processes are a novel approach for biodiesel production with no external catalysts. At the supercritical stage, methanol can solve the problems associated with the two-phase nature of normal methanol/oil mixtures by forming a single phase reaction as a result of the lower value of the dielectric constant of methanol in the supercritical state. Figure 2.9 shows two-stage continuous biodiesel production processes with subcritical water and supercritical methanol. The triglyceride is rapidly hydrolyzed to free fatty acids under the supercritical conditions with the pressure of 10 MPa at 445 K. Then, the pressure is reduced and the mixture promptly separates into two phases. The water phase can be separated to recover glycerol [46].

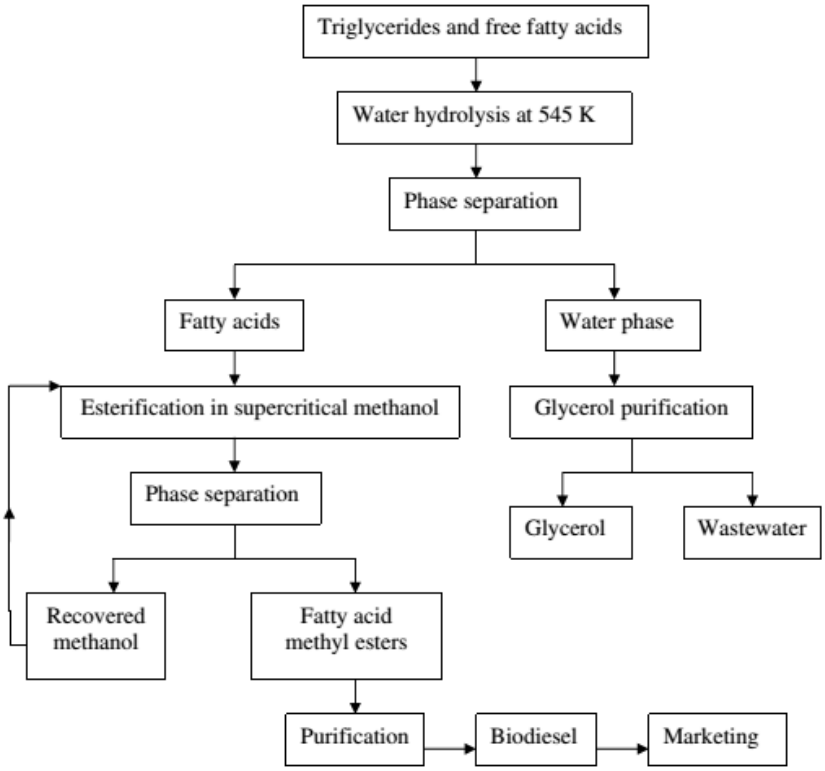


**Figure 2.9** Continuous biodiesel production process with subcritical water and supercritical methanol stages [46].

This process has several advantages in comparison to chemical-catalyzed reactions using alkali and acid catalysts, such as no need for catalysts, simple purification of products, no saponification as a side reaction, no requirement of waste treatment, no effect of water content and free fatty acids in the reaction, and lower reaction time [28, 47]. The comparison of catalytic methanol (MeOH) process and supercritical methanol (SCM) method on transesterification is shown in in Table 2.4. However, the supercritical process requires intensive energy consumption with high temperature and pressure which limits its application in industry.

**Table 2.4.** Comparisons between catalytic methanol (MeOH) process and supercritical methanol (SCM) method for biodiesel from vegetable oils by transesterification [46].

| | **Catalytic MeOH process** | **SCM method** |
|---|---|---|
| **Methylating agent** | Methanol | Methanol |
| **Catalyst** | Alkali | None |
| **Reaction temperature (K)** | 303-338 | 523-573 |
| **Reaction pressure (MPa)** | 0.1 | 10-25 |
| **Reaction time (min)** | 60-360 | 7-15 |
| **Methyl ester yield (wt%)** | 96 | 98 |
| **Removal for purification** | Methanol, catalyst, glycerol, soaps | Methanol |
| **Free fatty acids** | Saponified products | Methyl esters, water |
| **Continuity easiness** | Discontinue | Easy continuity |

## 2.3 Lipase for biodiesel production

Enzymes are derived from living organisms, such as plants, animals and microorganisms, and are widely used to catalyze various reactions of industrial importance. However, the drawbacks of enzymes in industrial application are the lack of long term operational stability and shelf-storage life, the complex recovery process, and the relative high price. Immobilization of enzymes has been introduced aimed for improving operational stability, facilitating separation and reusability. Various enzymes for example, penicillin G, acylase, lipases, proteases etc. have been immobilized in different forms for a range of industrial applications [18].

Normally, lipase can be catalyzed various reactions in aqueous systems and in non-aqueous systems, including hydrolysis, alcoholysis and acidolysis, and also transesterification and esterification in biodiesel production. Either soluble enzymes or immobilized forms can be used in these reactions. Lipases from various microbial origins, including *Rhizopus oryzae* [48], *Thermomyces lanuginosus* [4], and *Pseudomonas cepacia* [49] have been employed as biocatalysts for biodiesel synthesis. The list of lipases from different sources is reported in Table 2.5. The advantages of lipase-catalysed biodiesel synthesis are mild operating conditions, ability to convert free fatty acids present in the feedstock to alkyl esters, no requirement for waste water treatment, ease on glycerol separation, and environmentally-friendly. However, the industrial application of the enzymatic processes is still limited by the high cost and low stability of the enzymes. Therefore, the immobilized enzymes have been developed for cost reduction and improvement of the enzyme's operational time and reusability.

**Table 2.5** Lipase-catalyzed processes for production of biodiesel from different feedstocks [50].

| Alcohol | Fat | Lipase | System | Time [h] | Yield [%] |
|---|---|---|---|---|---|
| Methanol | Tallow | *Mucor miehei* IM60 | Solvent-free | 5 | 19.4 |
| | | | hexane | 5 | 73.8 |
| | | | hexane | 8 | 94.8 |
| | Sunflower oil | *Pseudomonas fluorescens* | Solvent-free | 24 | 3.0 |
| | | | Petroleum ether | 24 | 79.0 |
| | Cotton oil | *Candida antarctica (Novozym 435)* | Solvent-free | 7 | 91.5 |
| | | | *tert*-butanol | 10 | 90.0 |
| | Soybean oil | *Pseudomonas cepacia* | Solvent-free | 48 | 93.8 |
| | Palm oil | | Solvent-free | 8 | 15.0 |
| | Coconut oil | | | 8 | *traces* |
| Ethanol | Tallow | *Mucor miehei* IM60 | Solvent-free | 5 | 65.5 |
| | | | hexane | 5 | 98.0 |
| | | | Solvent-free | 5 | 83.0 |
| | Sunflower oil | *Pseudomonas fluorescens* | Solvent-free | 24 | 82.0 |
| | Palm oil | *Pseudomonas cepacia* | Solvent-free | 8 | 72.0 |
| | Coconut oil | | | 8 | 35.0 |
| Isopropanol | Tallow | *Candida antarctica* SP435 | Solvent-free | 16 | 90.3 |
| | | | hexane | 16 | 51.7 |
| | Palm oil | *Pseudomonas cepacia* | Solvent-free | 8 | 24.0 |
| | Coconut oil | | | 8 | 16.0 |
| Isobutanol | Tallow | *Mucor miehei* IM60 | Solvent-free | 5 | 97.4 |
| | | | hexane | 5 | 98.5 |
| | Palm oil | *Pseudomonas cepacia* | Solvent-free | 8 | 42.0 |
| | Coconut oil | | | 8 | 40.0 |
| 2-butanol | Tallow | *Candida antarctica* SP435 | Solvent-free | 16 | 96.4 |
| | | | hexane | 16 | 83.8 |
| 1-butanol | Palm oil | *Pseudomonas cepacia* | Solvent-free | 8 | 42.0 |
| | Coconut oil | | | 8 | 40.0 |

### 2.3.1 Types of enzyme immobilization

Immobilization of lipase is a cost-effective approach and allows recycling of biocatalysts in consecutive or continuous processes. Several methods for lipase immobilization, such as adsorption, covalent bonding, entrapment, and cross-linking, have previously studied [3]. The diagram of various immobilized enzymes is illustrated in Figure 2.10. Advantages and limitations of immobilized lipases are also summarized in Table 2.6.

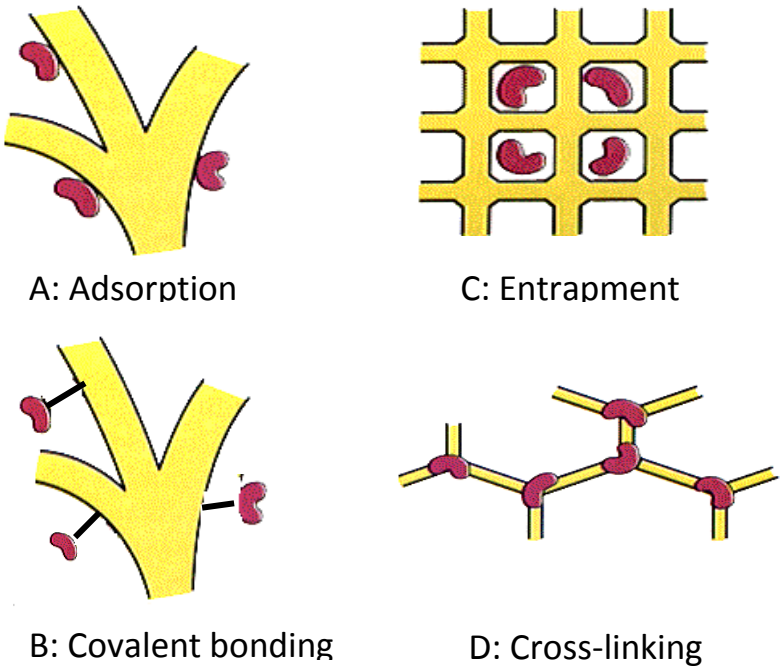


**Figure 2.10** The traditional methods of enzyme immobilization.

Adsorption is the attachment of lipases on the surface of the support (carrier) by weak forces, such as van der walls, hydrophobic interactions or dispersion forces. This technique has several advantages including simple immobilization process under mild condition, easy recovery of the immobilized support, and low cost. However, it possesses several drawbacks from sensitivity of the immobilized enzymes to pH, ionic strength and temperature due to weak forces between the enzymes and the support materials as well as the small adsorption capacity of the enzymes on the support matrix. Immobilization of enzymes by covalent bonding is rather more stable than the adsorption technique as a result of the strong interaction between the enzyme and the support, but the preparation condition of covalent bonding can cause the loss of activity during the immobilized process while some coupling reagents are toxic.

Entrapment is the capture of enzymes within a matrix of a polymer, such as hydrophobic sol-gel. This method has been employed using a wide range of carriers and enzymes as it is fast, cheap, easy, and can be prepared using mild condition. The disadvantage of entrapment is the mass transfer limitation during the catalytic process. Enzyme immobilization by the cross-linking method has many advantages over other immobilization methods, including a low mass-transfer limitation, high catalytic performance, improved stability and reusability, and low preparation cost [4]. There are several forms of cross-linked biocatalysts with potential for biodiesel synthesis such as cross-linked enzyme aggregates (CLEAs), cross-linked enzyme crystals (CLECs), and microcrystal enzymes which are protein-coated microcrystals (PCMCs) and cross-linked protein coated microcrystals (CL-PCMCs).

Apart from various immobilization methods, several solid supports, especially magnetic nanoparticle have been increasingly interesting due to its intrinsic property with regard to the catalytic function of biocatalyst [51]. Currently, magnetic nanoparticle lipase is well known as biocatalyst for enzymatic biodiesel reaction process due to ease of separation under a magnetic field without the separated contamination using chemical reagent, the lower mass transfer limitation and fouling in reaction, the high specific surface area for immobilization, and the high catalytic efficiency and stability [52].

**Table 2.6** Comparison of the advantageous and disadvantageous lipase immobilized techniques [3].

| Methods | Advantages | Disadvantages |
|---|---|---|
| **Adsorption** | Preparing conditions are mild and easy with low cost. The carrier can be regenerated for repeated use. | The interaction between the lipase and the carrier is weak, so the immobilized lipase was sensitive to pH, ionic strength, temperature, etc. The adsorption capacity is small and the protein might be stripped off from the carrier. |
| **Covalent bond** | The immobilized lipase is rather stable because of the strong forces between the protein and the carrier. | The preparation conditions are rigorous, so the lipase might lose its activity during the immobilized process. Some coupling reagents are toxic. |
| **Cross-linking** | The interaction between the lipase and the carrier is strong and the immobilized lipase is stable. | The cross-linking conditions are intense and the mechanical strength of the immobilized lipase is low. |
| **Entrapment** | The entrapment conditions are moderate, and the immobilized method is applicable to a wide range of carrier and lipase. | This immobilized lipase always has the mass transfer restriction during the catalytic process, so the lipase is only effective for low molecular weight substrates. |

Typically, immobilized enzymes consist of two components: the non-catalytic structural component (carrier or support), which is designed to aid separation and reuse of the catalyst as well as facilitating control of the process, and the catalytic function component (enzyme), which is designed to convert the substrates of interest into the desired products. The non-catalytic parameters are related to the physical and chemical nature of the non-catalytic part, especially the geometric parameters such as shape, size and length, whereas the catalytic parameters are linked to the catalytic functions, such as activity, selectivity and stability. Therefore, the requirements of efficient non-catalytic function depend on the design of reactor configurations (batch, stirred-tank, column and plug-flow), the type of reaction medium (aqueous, organic solvent or two-phase system), the reaction system (slurry, liquid-to-liquid, liquid-to-solid or solid-to-solid), and the process conditions (pH, temperature and pressure), aimed for achieving easy separation of the immobilized enzymes from the reaction mixture, flexibility of reactor design and broad applicability in various reaction media and reaction systems. Also, the achievements of catalytic function have focused on fewer side reactions, high tolerance to structural variation of the substrates, high productivity and space-time yield, including high durability of the catalyst [53].

According to many research works, immobilized enzymes in various forms have effectively been used for the synthesis of biodiesel from various oils and alcohols. However, the costs of conventional immobilized lipase is still expensive and the activity of enzyme is lost during the biocatalyst preparation step and biodiesel synthesis as shown in Figure 2.11A. Therefore, the whole cell catalyst has been studied as an alternative for biodiesel production to overcome the drawbacks of traditional immobilized lipases (Figure 2.11B).

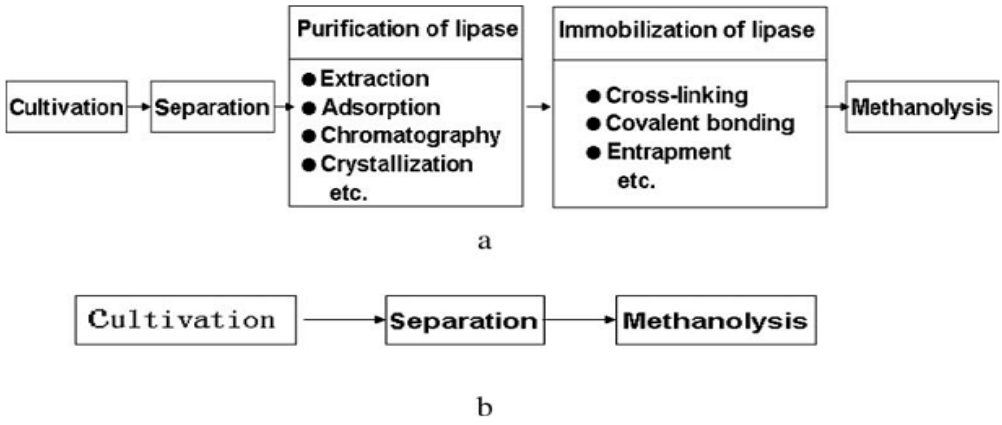


**Figure 2.11** Different processes of biodiesel production: (A) conventional immobilized lipase and (B) whole cell biocatalyst [11].

### 2.3.2 Technology of immobilization lipase

Immobilization of lipases in the forms of microcrystalline enzymes represents a cost- effective approach for the preparation of high-performance biocatalysts for catalysis in non-aqueous reactions. Several forms of carrier-free microcrystalline enzymes, such as cross linked enzyme crystals (CLECs), cross-linked enzyme aggregates (CLEAs) and carrier-based microcrystalline biocatalysts, such as protein coated microcrystals (PCMCs), and cross-linked protein coated microcrystals (CL-PCMCs) have been reported.

#### 2.3.2.1 Cross-linked enzyme crystals (CLECs)

The use of cross-linked enzyme crystals (CLECs) as industrial biocatalysts was introduced in the early 1990s [36]. The CLEC synthesis process consists of two major steps that are the crystallization of enzymes and the chemical crosslinking of crystals. Moreover, CLEC formulations can overcome the other immobilized forms, because they are highly active, easy to handle, recyclable, possible to incorporate into fabrics and indifferent to shear and foaming [54]. However, highly purified enzyme and extensive protein purification are needed for CLEC preparation [53]. These several disadvantages can be overcome by using CLEAs.

#### 2.3.2.2 Cross-linked enzyme aggregates (CLEAs)

Crosslinked enzyme aggregates (CLEAs) have been recently proposed as an alternative to conventional immobilization on solid supports and to cross-linked enzyme crystals [55]. The preparation of CLEAs depends on the precipitating of enzymes and subsequently cross-linking of formed aggregates (Figure 2.12). CLEAs preparation usually uses the precipitation of the enzyme and chemical cross-linking of the protein with ammonium sulfate and glutaraldehyde, respectively [36]. Cross-linking prevents the solubilization and possible loss of the aggregates after removing the precipitating agent. Some additives have been proposed for the stabilization of CLEAs, such as bovine serum albumin (BSA) and polyionic polymers [56, 57]. In general, proteins can be precipitated by organic agents without undergoing denaturation. Consequently, cross-linking of performed physical aggregates of enzymes constitute a simple method for the preparation of CLEAs. This technique was successfully applied in the preparation of cross-linking enzyme immobilization of aminoacylase [58], tyrosinase [55] and lipases [59], using pure enzyme preparations.

The advantages of CLEAs are highly concentrated enzyme activity in the catalyst, high stability and low production cost due to the exclusion of an additional carrier [60]. Moreover, the CLEA methodology is applicable to essentially any enzyme including crude preparations. This method leads to the preparation of stable and recyclable catalysts with high retention of activity [61]. Importantly, it does not require highly purified enzymes. Remarkably, the productivity of the CLEAs was even higher than that of the free enzyme, because the free enzyme has limited thermal stability and a low tolerance to organic solvents [36].

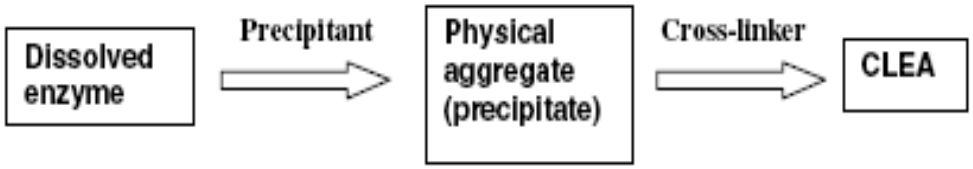


**Figure 2.12** Protocol for preparing CLEA [56].

#### 2.3.2.3 Protein coated microcrystals (PCMCs)

Protein coated microcrystals (PCMCs) have been reported to be a new technology for the immobilization of protein molecules as a uniform layer on the surfaces of salt crystals [62]. The formation of PCMC consists of water-soluble micron-sized particles, which are coated on the salt crystal. The general procedure of PCMCs preparation is illustrated in Figure 2.13.

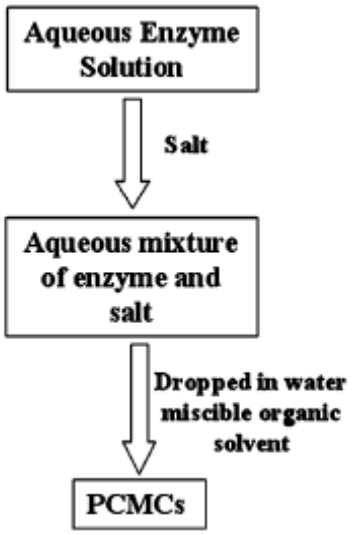


**Figure 2.13** General protocol for PCMCs preparation [63].

Kumari et al. 2006 [64] produced biodiesel from *Madhuca indica* oil containing a high free fatty acid content using *Pseudomonas cepacia* lipase immobilized in different forms, of which PCMCs and CLEAs were shown to be highly active in biodiesel production by esterification. This paper showed that the substrate is easily accessible to the enzyme in PCMCs. Hence, PCMCs as heterogeneous catalysts are believed to have less mass-transfer limitations, as compared to lyophilized powders. Also, even in CLEAs, the active site would not be on the biocatalyst surface, and this design is expected to have somewhat of a higher mass-transfer limitation as compared to PCMCs. Figure 2.14 shows that the use of CLEAs and PCMCs, prepared from *P. cepacia* lipase and Mahua oil. The use of PCMCs led to a higher conversion yields than those using CLEAs at different amount of lipase [64].

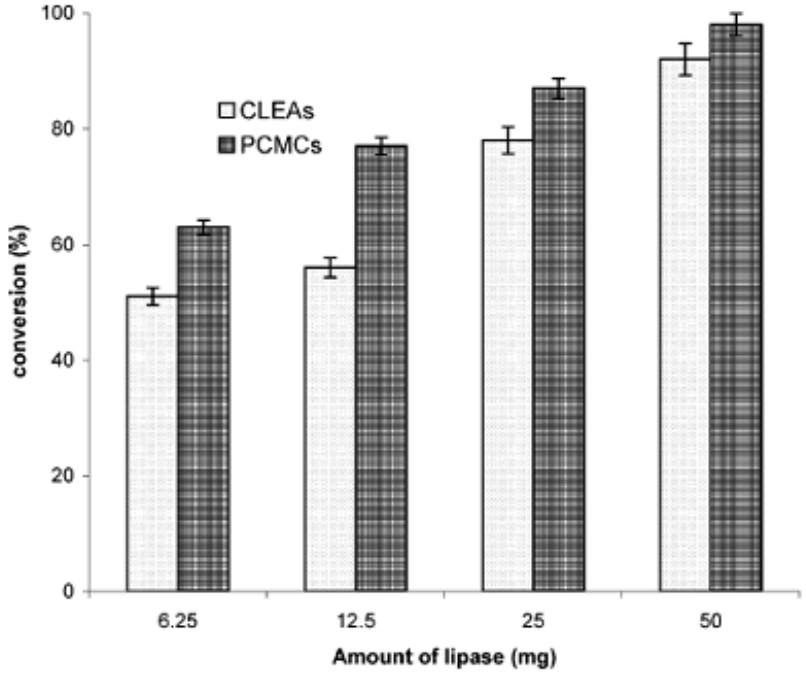


**Figure 2.14** Biodiesel production from Mahua oil catalyzed from CLEAs and PCMCs of *Pseudomonas cepacia* lipase [64]. The reactions were conducted at a reaction temperature at 40°C for 2.5 h with constant shaking at 200 rpm.

Atomic force microscopy (AFM) analysis showed that PCMCs prepared from lipase of *Pseudomonas cepacia* are in the size range of 500-1000 nm. These enzyme coated micro-crystals showed enhanced transesterification rates as compared to the soluble enzyme in biodiesel production. Also, the PCMCs showed higher thermo stability, as they were stable at 60 °C, whereas the free enzyme lost all activity [65]. Recently, synthesis of

biodiesel from palm oil with ethanol using PCMC prepared from *Thermomyces lanuginosus* lipase in *tert*-butanol system has been reported by Raita et al, 2010. This research found that PCMC lipase gave the high product yields compared to commercial immobilized enzymes (Novozyme®435 and Lipolase 100T) under the same enzyme loading (20%) and reaction conditions at 45 °C for 24 h, as illustrated in Figure 2.15. In addition, PCMC lipase can be reused in consecutive batches under the optimized reactions with high stability with treatment of the biocatalytst by tert-butanol (Figure 2.16).

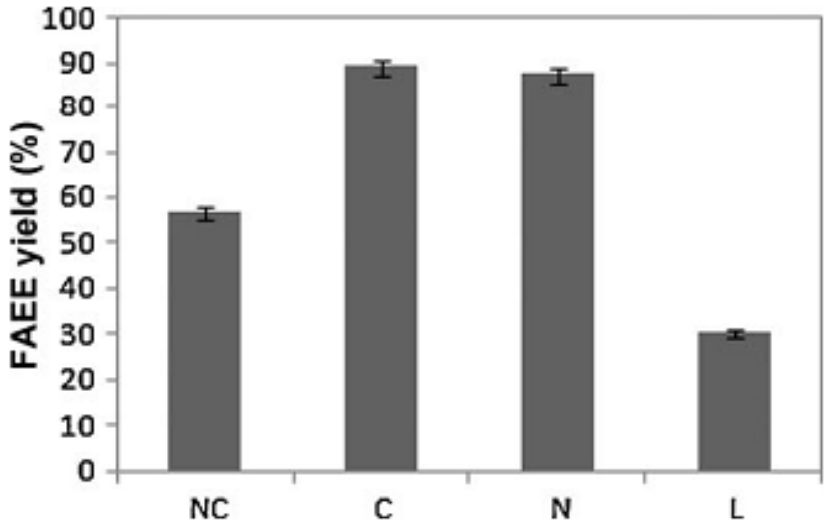


**Figure 2.15** Comparison of FAEE synthesis using different immobilized lipases [4]. NC: PCMC prepared from nonconcentrated DELIP 50L; C: PCMC prepared from concentrated DELIP 50L; N:Novozyme®435; L: Lipolase 100T. The reactions were incubated at 45 °C for 24 h.

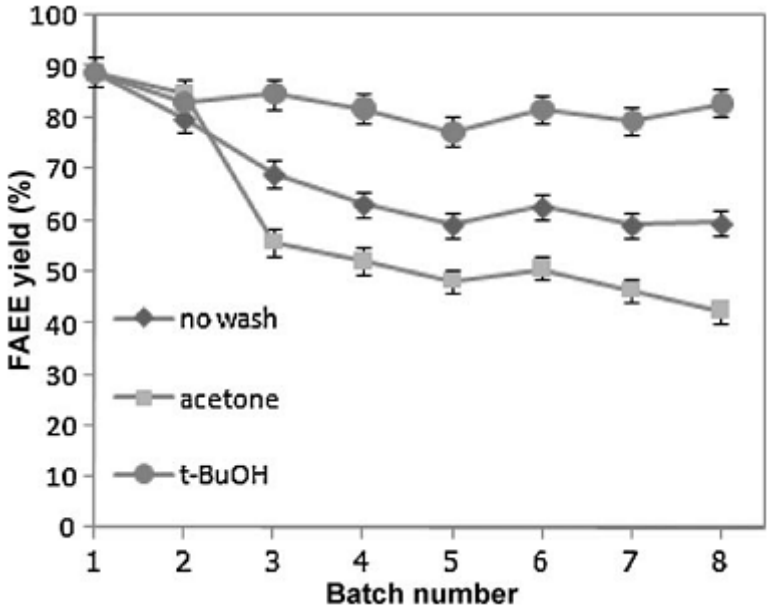


**Figure 2.16** Stability of PCMC-lipase in consecutive batch reactions [4]. The reactions were incubated at 45 °C for 24 h.

#### 2.3.2.4 Cross-linked protein coated microcrystals (CL-PCMCs)

An alternative potential immobilization design, which is called cross-linked protein-coat microcrystals (CL-PCMCs), were introduced as an improvement of conventional PCMCs [6]. The formation of CL-PCMCs is characterized as a cross-linked enzyme layer on the surface of micron-sized inner inorganic matrix, which can be prepared by co-precipitation of the enzyme and the matrix component in an organic solvent as for conventional PCMC preparation with an extra step on enzyme covalent crosslinking. The procedure of CL-PCMC preparation has been shown in Figure 2.17. In general, glutaraldehyde is used as a crosslinking agent for CL-PCMC preparation [66]. Various matrix components, including potassium sulphate, amino-acids, and sugars have been employed as the core matrix by co-precipitating with enzymes in different organic solvents such as acetone, ethanol, or *tert*-butanol [5].

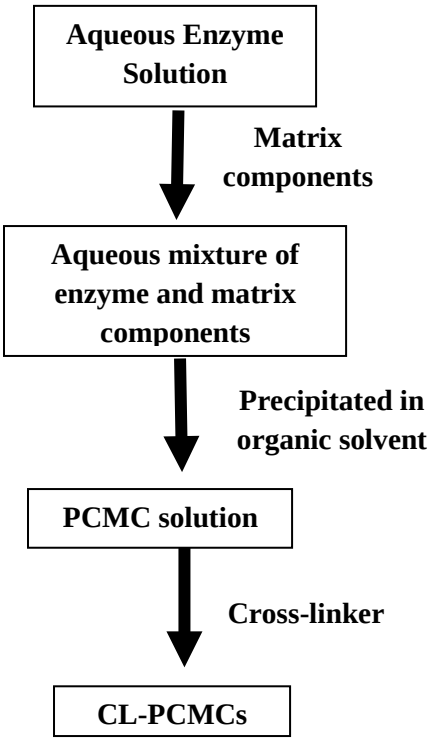


**Figure 2.17** General protocol for the preparation of CL-PCMCs [6].

Shah et al. (2008) [6] reported that CL-PCMCs showed enhanced reaction rates for transesterification in organic solvents. especially *Subtilisin Carlsberg* gave 98% conversion at 80 °C in 6 hours while PCMCs presented only 58% conversion in 8 hours, as shown in Figure 2.18. The advantages of CL-PCMC over the conventional immobilized method are less mass-transfer limitation and higher enzymatic performance efficiency including improvement of stability and reusability in aqueous/non-aqueous system.

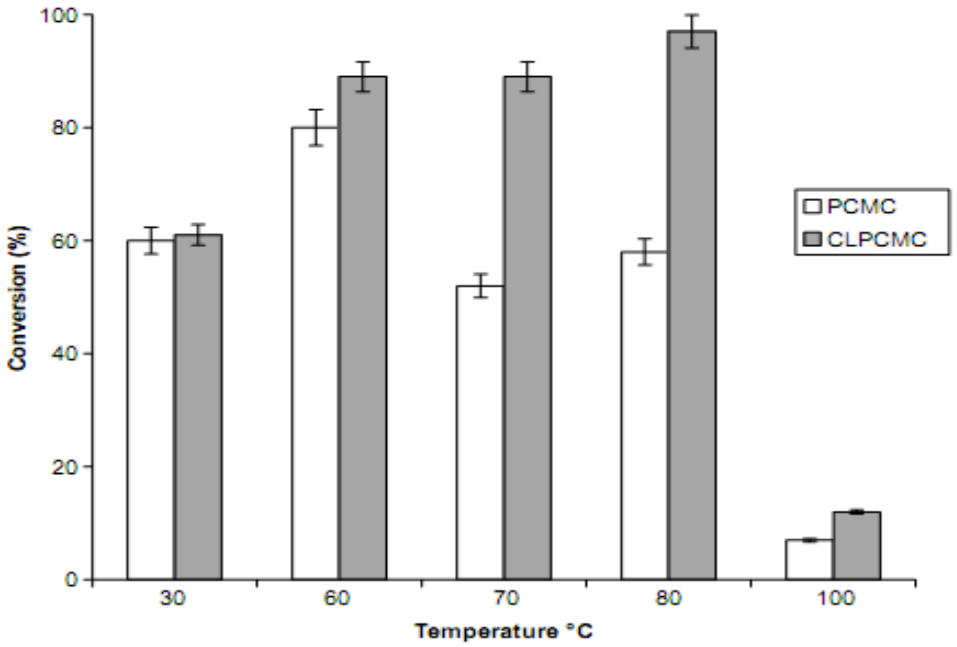


**Figure 2.18** Effect of temperature on transesterification reaction catalysed by PCMCs and CL-PCMCs of *Subtilisin Carlsbreg* in anhydrous octane [6]. The reaction was maintained for 24 h with constant shaking at 200 rpm

#### 2.3.2.5 Magnetic nanoparticle lipase

Currently, the novel nano-sized solid supports have been receiving increased interest for use as the carrier matrix in enzyme immobilization with potential applications in biotechnology, biofuel, immunesensing, and biomedical areas. This nano-sized support provides not only a biocompatible and inert environment with the native structure of the protein, but also high specific surface area, mass transfer resistance, and effective enzyme loading (Table 2.7).

**Table 2.7** Advantages and disadvantages of using nano immobilization [67].

| Advantages | Disadvantages |
|---|---|
| Mass transfer resistance | Cost of the fabrication |
| Effective enzyme loading | Large scale application |
| High surface area | Separation of the reaction medium |
| High mechanical strength | |
| Diffusional problems minimization | |

Several types of nanomaterials e.g. nanoporous, nanofiber, and nanoparticle have been studied for enzyme immobilization. Magnetic nanoparticle has been reported as one potent carrier matrix. The advantages of magnetic nanoparticle enzyme include its has high catalytic efficiency and operational stability due to its high reactive surface area and low mass transfer limitation. The simple separation process by magnetic field also leads to cost reduction in downstream process. The uses of magnetic nanoparticles for enzyme immobilization in several biotechnological applications are listed in Table 2.8.

**Table 2.8** Enzymes immobilized on magnetic nanoparticles and their biotechnological applications [68].

| Enzyme | Nanoparticle utilized | Applications |
|---|---|---|
| **Cholesterol oxidase** | $Fe_3O_4$ nanoparticles | Analysis of total cholesterol in serum |
| **Haloalkane dehalogenase** | Silica coated iron oxide nanoparticles | Production of fusion proteins containing dehalogenase sequence |
| **Laccase** | Chitosan-magnetic nanoparticles | Bioremediation of environmental pollutants |
| **Keratinase** | $Fe_3O_4$ nanoparticles | Synthesis of keratin |
| **a-Amylase** | Cellulose-coated magnetite nanoparticles | Starch degradation |
| **b-Galactosidase** | Con A layered ZnO nanoparticles | Lactose hydrolysis |
| **Lipase** | $Fe_3O_4$ nanoparticles | Hydrolysis of pNPP |

Utilization of magnetic nanoparticle support for the immobilization of lipase in renewable biofuel application has been reported by several studies. The high performance of the magnetic nanoparticle in biodiesel synthesis is reported with different designs of immobilized lipase on the magnetic carriers.

Xie et al. (2009) [38] stated that the use of magnetic nanoparticles ($Fe_3O_4$) treated with aminopropyl trimethoxysilane (APTES) by cross-liked glutaraldehyde provided the highest FAME yield of 94% from the transesterification of soybean oil with a three-step addition of methanol after 30 h of incubation at 50 °C using 60% immobilized lipase loading (Figure 2.19). Similarly, Xie et al. (2010) reported the conversion of soybean oil by lipase immobilized on $Fe_3O_4$ support via 1-ethyl-3-(3-dimethylaminopropyl) carbodiimide solution (EDC) as the activating agent. The product yield achieved reach over 90% using 40% immobilized lipase loading after incubation at 45 °C for 25 h with

three stepwise addition of methanol. The formation of covalently bound proteins on the biocatalysts was confirmed by FT-IR analysis (Figure 2.20). In Figure 2.20a, the FT-IR spectra of pure lipase from *Thermomyces lanuginosus* showed the signature peaks at 1657 $cm^{-1}$ of the carbonyl amide groups and 1542 $cm^{-1}$ of amide groups from N-H bending vibration, while the absorption peaks at 578 $cm^{-1}$ and 3441 $cm^{-1}$ of Fe-O stretching and hydroxyl group vibrations respectively were shown in Figure 2.20b. In addition, the signature absorption peaks of both free lipase and the magnetic support were obviously observed in Figure 2.20c, indicating binding of lipase molecules onto the magnetic support.

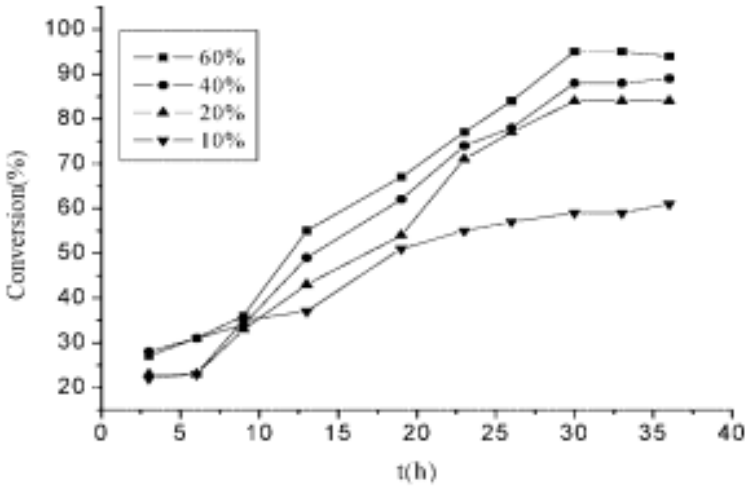


**Figure 2.19** Effect of various amounts of lipase on methanolysis of soybean oil [38]. The reactions were conducted at 50 °C.

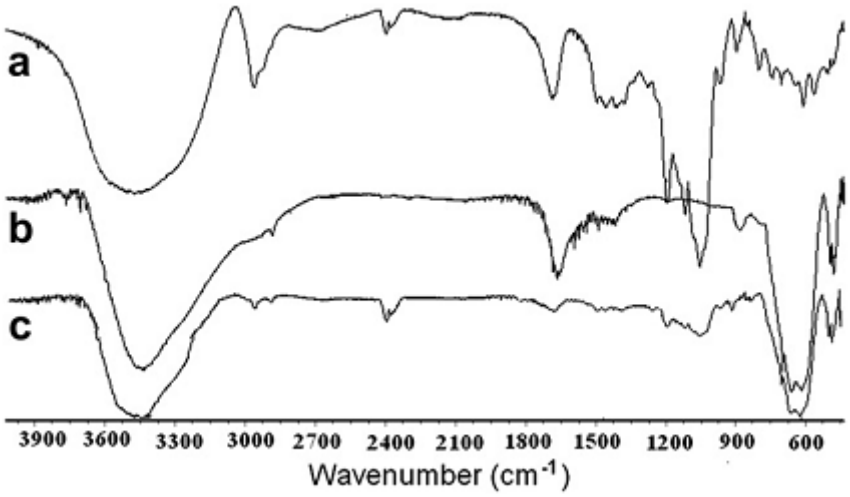


**Figure 2.20** FT-IR spectrum of the magnetic nano-particles: (a) free lipase, (b) protein-free $Fe_3O_4$; and (c) lipase-bound magnetic particles [51].

Tran et al. (2012) studied the immobilization of lipase from *Burkholderia* sp. on ferric silica nanocomposites ($Fe_3O_4$–$SiO_2$) for biodiesel production [69]. Core–shell nanoparticles were synthesized by coating $Fe_3O_4$ core with silica shell and treating with dimethyl octadecyl [3-(trimethoxysilyl) propyl] ammonium chloride used for immobilization supports. This immobilized lipase was used to catalyze transesterification of olive oil with methanol to produce methyl ester, providing the FAME yield of over 90% within 30 h using 11 %(w/w) enzyme loading.

Ngo et al. (2010) reported that novel magnetic nanobiocatalyst aggregates (MNA) prepared from covalently immobilized *Thermomyces lanuginosus* lipase on core–shell structured iron oxide magnetic nanoparticle could improve the recycling of the enzymes and retain 88% productivity in the $11^{th}$ cycle on the methanolysis of grease [70]. Likewise, Kuo et al. (2012) [71] reported that the $Fe_3O_4$ nanoparticle lipase coated by chitosan provided the high operational stability with 83% residual activity after twenty repeated uses (Figure 2.21). The comparison of methanolysis catalyzed by several immobilized lipase was listed in Table 2.9. The great potential of magnetic nanoparticle lipase was observed from the high FAME yield and repeated uses in several cycles compared to the conventional immobilized lipase.

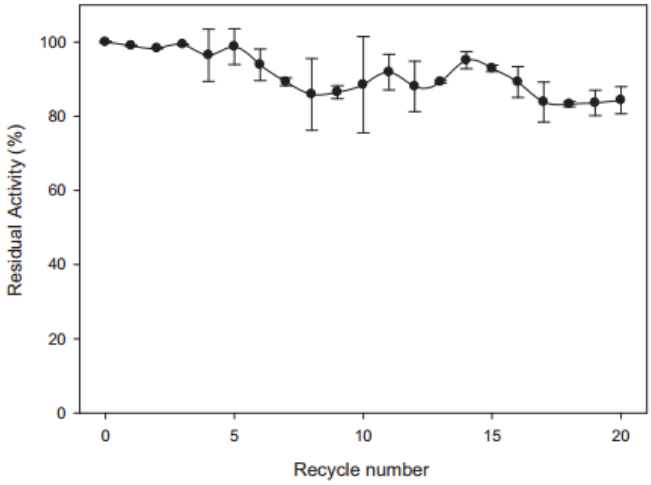


**Figure 2.21** Improvement on operational stability using chitosan-coated $Fe_3O_4$ nanoparticles on lipase assay [71]. The reaction was performed under the optimum immobilization conditions with enzyme/support ratio 0.73 (w/w) at pH 6.37 for 2.14 h.

**Table 2.9** Comparison of biodiesel synthesis performance using immobilized lipases [69].

| Strain | Carrier | Immobilization method | Substrate | Condition | FAME conversion (%) | Reusability (cycle) |
|---|---|---|---|---|---|---|
| *Candida Antarctica* (Novozym 435) | Acrylic resin | NA | Mixture of soybean and rapeseed oils | Temp., 30°C MeOH/oil, 3:1 Stepwise adding Solvent-free Water, <1% pH,not controlled Catalyst, 4.2% | 98.4%, 72 h | NA |
| *Pseudomonas fluorescens Pseudomonas cepocia* | Macroporous polypropylene | Physical adsorption | Soybean oil | Temp., 40°C MeOH/oil, 8:1 Solvent-free Water, 0% pH, not controlled Catalyst, 6.25% | 58% 22 h 37% 51.5 h | NA |
| Novozym 435 (immobilized *Candida antarctica* lipase B) | Acrylic resin | NA | Refined palm oil | Temp., 40°C MeoOH/oil, 3:1 t-butanol, 78.09% Water, 0.35-0.45% pH, not controlled Catalyst, 4% | 85%, 30 h | 5 |
| Lipazyme-TL of *Thermomyces lanuginose*, Novozymes | $Fe_3O_4$ | Covalent bonding | Soybean oil | Temp., 45°C Stepwise MeOH addition; (MeOH/oil, 1:1 each step) pH 7.0 Catalyst, 40% | 90%, 35 h | 5 |
| *Burkholderia* sp. C20 | Alkyl-$Fe_3O_4$-$SiO_2$ | Adsorption on hydrophobic surface | Olive oil | Temp., 40°C MeOH/oil, 4:1 pH 9.0 Water, 10% Catalyst, 11% | 92%, 30 h | 10 |

#### 2.3.2.6 Whole cell biocatalyst

Regarding the conventional enzyme immobilizations, the high cost of immobilized enzyme preparation and complicated immobilization process could limit the use of immobilized enzymes for industrial-scale process development. The use of whole cell biocatalysts is thus a promising approach to overcome these problems of conventional immobilization. There are several microorganisms for the preparation of whole cell biocatalysts, such as bacteria, yeasts, and filamentous fungi, specifically *Rhizopus* species that have been extensively studied in laboratory-scale research for efficient catalytic biodiesel production [48, 72]. The use of whole cell biocatalyst for fatty acid methyl ester synthesis has been firstly presented by Ban et al, 2001 [73]. Later, the transesterification processes of different whole cell biocatalysts expressing *Rhizopus* lipase immobilized on either biomass support particles (BSPs) made from polyurethane or the surface of yeast cells have been reviewed by Fukuda et al, 2008 (Table 2.10). Improvement of whole cell biocatalysts in tert-butanol system using glutaraldehyde cross-linking treatment led to an increase on operation stability and an enhanced reaction rate of lipase [74, 75].

**Table 2.10** Comparison of biodiesel production methods using different whole-cell biocatalysts [76].

| Whole-cell Biocatalyst | Oil | Alcohol | Solvent | ME (%) | Time (h) | Temp (°C) |
|---|---|---|---|---|---|---|
| **BSPs with *R.oryzae*** | Soybean | Methanol | None | 80-90 | 72 | 32 |
| **BSPs with *R.oryzae*** | Soybean | Methanol | None | 90 | 48 | 35 |
| **BSPs with *R.oryzae*** | Soybean | Methanol | *t*-butanol | 72 | NA | 35 |
| **BSPs with *R.oryzae*** | Jatropha | Methanol | None | 89 | 60 | 30 |
| **BSPs with *R.oryzae*** | Rapeseed (refined) | Methanol | *t*-butanol | 60 | 24 | 35 |
| **BSPs with *R.oryzae*** | Rapeseed (crude) | Methanol | *t*-butanol | 60 | 24 | 35 |
| **BSPs with *R.oryzae*** | Rapeseed (acidified) | Methanol | *t*-butanol | 70 | 24 | 35 |
| **Mycelium of *R. chinensis*** | Soybean | Methanol | None | 86 | 72 | NA |
| ***S. Cerevisiae* (Intracellular ROL)** | Soybean | Methanol | None | 71 | 165 | 37 |
| ***S. Cerevisiae* (Cell surface ROL)** | Soybean | Methanol | None | 78 | 72 | 37 |

The further developments of these technologies have been carried out on the study of potentially enzymatic application in industrial-scale biodiesel production process. Cell surface technology has been purposed for modification of traditional whole cell biocatalysts for reducing the mass transfer limitation [76]. The construction of cell-surface engineered yeasts overproducing *Rhizopus oryzae* lipase has been reported by Matsumoto et al (2001) [77]. It found that the use of yeast cells that displayed recombinant lipase for biodiesel synthesis led to a methyl ester content of 78.6% after 72 hours after a three-step addition of methanol whereas that of a yeast whole cell biocatalyst expressing intracellular produced 71% methyl ester yield after 165 hours of reaction [77]. According to these results, cell surface display is thus a promising technology for economical synthesis of biodiesel on industrial-scale enzymatic process.

Cell surface engineering is an alternative method for biocatalyst design by expressing a heterologous peptide or protein of interest as a fusion protein with various anchoring motifs (carrier proteins) on the cell surface. Several microorganisms have been used as host cells for the surface display of heterologous proteins, such as bacteria and yeasts, especially *S. cerevisiae*. Many carrier proteins on the yeast cell surface, including agglutinin (Agα1 and Aga1) and Flocculin Flo1, Sed1, Cwp1, Cwp2, Tip1, and Tir1/Srp1 have been employed as the anchor proteins for surface display of target heterologous proteins. Glycosylphosphatidylinositol (GPI) anchors play an important role in the expression of cell surface proteins. The advantages of cell surface display system are the unnecessary to permeabilize the cell membrane to increase substrate access ability removal of the enzyme purification step and low biocatalyst preparation cost. Cell surface display has many potential industrial applications, including live vaccine development, peptide library screening, and bioconversion using whole cell biocatalysts for biodiesel production, as shown in Figure 2.22. The development of cell-surface displayed whole-cell biocatalysts is of great potential of application in a range of industries.

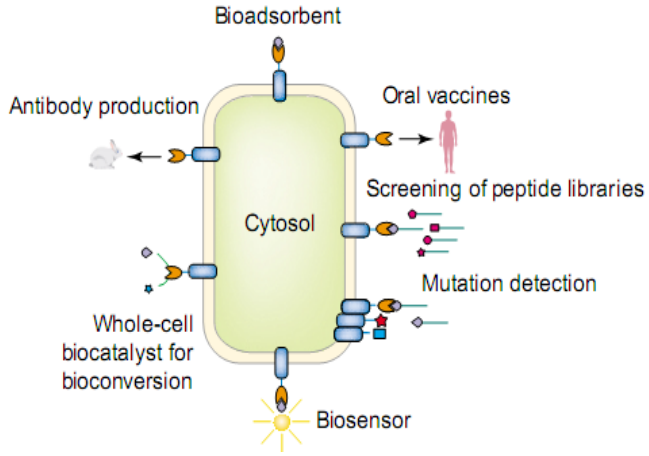


**Figure 2.22** Applications of cell surface display [78].

## 2.4 Effect of reaction parameters on enzymatic biodiesel synthesis process

Reaction parameters, such as type of alcohol, methanol/oil molar ratio, co-solvent in reaction, enzyme amount, temperature, and water content show strong influences on the yield of biodiesel and the rate of the reaction. Effects of key reaction parameters on biodiesel synthesis using free and immobilized lipases are reviewed as below.

### 2.4.1 Effect of alcohols

Alcohols are employed as nuclophiles in transesterification and esterification with vegetable oils, especially methanol and ethanol. Methanol is extensively used in the biodiesel industry due to its availability and lower cost. However, ethanol is a more eco-friendly alternative in biocatalytic biodiesel synthesis to the conventionally used methanol and is less toxic to lipases [79]. Tamalampudi et al. (2008) [80] reported the use of different alcohols on transesterification of jatropha oil catalyzed by immobilized *C. Antarctica* lipase (Novozyme 435) and whole cell R. *oryzae* immobilized onto biomass support particles (BSPs) as shown in Figure 2.23. It was found that the highest catalytic activity of both lipases was observed with methanol in comparison to other alcohols (ethanol, n-propanol, and n-butanol) under reaction temperature 30°C for 60 min. This could be due to the fact that methanol has low molecular weight and higher polarity, as a result, it might easily access into the intracellular lipase localized in the cell membrane of *R. oryzae* or the immobilized lipase on acrylic resin of Novozyme 435, which thus led to the higher reaction rate while increasing the length of the alcohols resulted in less reaction efficiency.

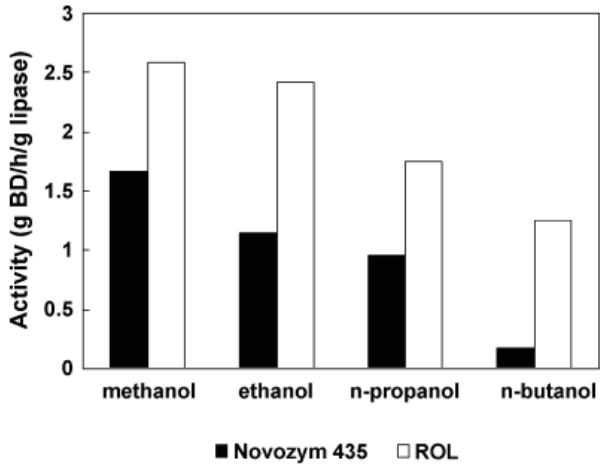


**Figure 2.23** Effect of different alcohols on lipase activities [80]. Reactions contained with 0.2 g of lipases loading at 30 °C for 60 min.

### 2.4.2 Effect of methanol/oil molar ratio

The molar ratio of alcohol and oil is one of the most important factors that need to be optimized in biodiesel synthesis by transesterification and esterification. Increasing the molar ratio of methanol in transesterification generally results in high conversions at lower ratio, but excess of methanol in enzymatic process can lead to lower alkyl ester product. Li et al. (2006) [81] described the effects of the methanol/oil in methanolysis of rapeseed oil were investigated using the molar ratio range of 2:1 to 6:1 with a reaction temperature of 35 °C for 24 h and 5% (w/w) loading of Lipozyme TL IM (Figure 2.24). The result showed that increasing FAME yield was obtained with increasing methanol/oil molar ratio from 2:1 to 6:1 (mol/mol). Further increase in the ratio can lead to lower FAME yield due to inactivation of lipases by the immiscible methanol in the reaction.

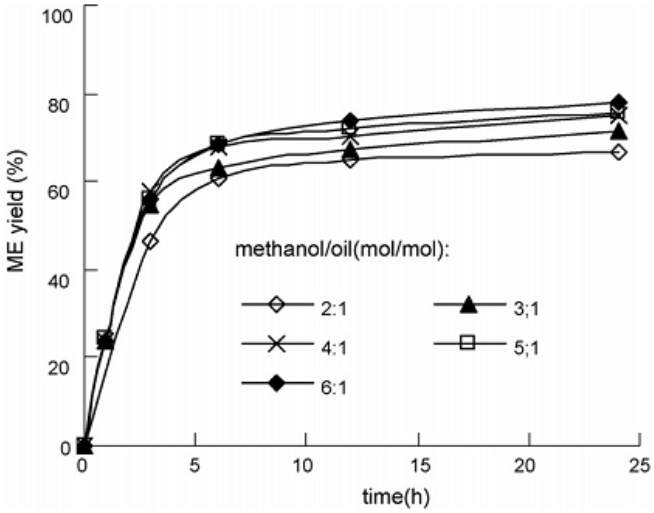


**Figure 2.24** Effect of methanol/oil molar ratio on the methanolysis of rapeseed oil [81]. Reactions were incubated at 35 °C at 1:1 [tert-butanol]/[oil] volume ratio with 5% Lipozyme TL IM based on oil weight.

### 2.4.3 Effect of co-solvent in reaction

Various organic solvents have been proposed as the reaction medium for lipase-mediated methanolysis of vegetable oils in biodiesel production. Du et al. (2007) [82] studied the operational stability of biocatalyst in consecutive batch cycles using several hydrophobic organic solvents, such as n-hexane, petroleum ether and tert-butanol, as illustrated in Figure 2.25. It was observed that lipase activity dropped obviously in the hexane and petroleum ether during repeated uses, whereas no significant loss of activity was found after 100 batches in the tert-butanol system.

Tert-butanol has been demonstrated as an ideal co-solvent for biodiesel production as it can improve the operational stability of the lipase by preventing enzyme inactivation by the immiscible methanol. It also eliminates the adsorption of glycerol on the biocatalyst surface. With its advantages, tert-butanol has been then used as a co-solvent in many reports on biocatalytic biodiesel synthesis using lipases from different sources.

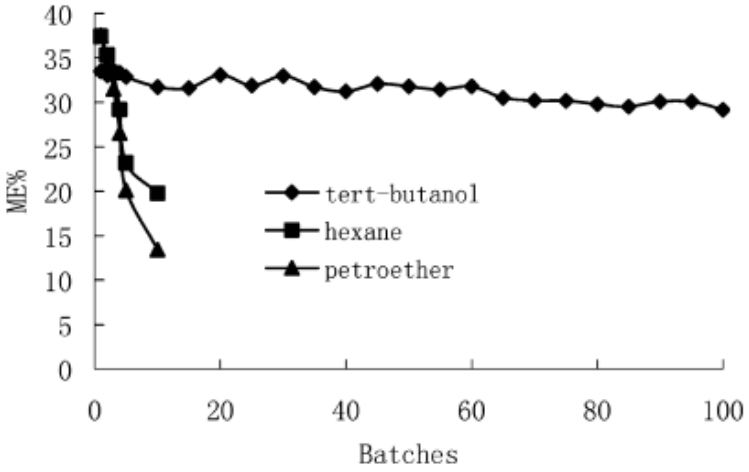


**Figure 2.25** Reusability of lipase in different organic solvents [82]. Reactions contained at 10 g of rapeseed oils with 5% Lipozyme TL based on oil weight at 35°C for 4 h.

Li et al. (2007) [74] studied the stability of whole cell biocatalyst from *R. oryzae* in solvent-free and tert-butanol system as shown in Figure 2.26. In the solvent-free system, the relative activity of *R. oryzae* whole cell dropped quickly during repeated uses until all activity loss in batch 4 while high stability of the biocatalyst was retained with 90% of the initial activity after 10 batch cycles in the tert-butanol system. Accumulation of glycerol and methyl ester was detected inside the whole cell in solvent-free system during the repeated uses, unlike in the tert-butanol system, which could lead to inactivation of the whole cell biocatalysts.

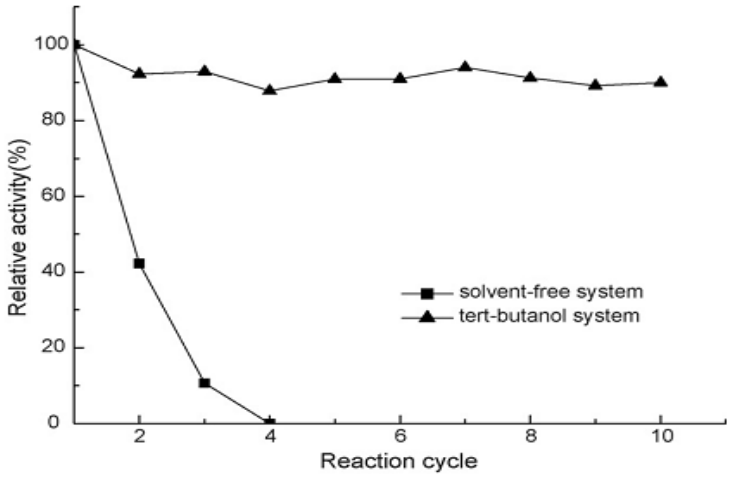


**Figure 2.26** Comparison of whole cell lipase stability in solvent-free and tert-butanol systems [74]. Reactions were incubated at 35 °C with constant shaking at 130 rpm for 24 h.

### 2.4.4 Effect of enzyme loading

Huang et al. (2007) [83] studied the effects of enzyme loading on the transesterification of lard with methanol using two immobilized lipases (Novozym 435 and Lipozyme TLIM) for (Figure 2.27). Increasing methyl ester is initially consistent to gradually increase the enzyme amount, but no significant effect was observed with further increase in enzyme loading over the optimal point. The highest product with 90.5% and 72.8% was reached using enzyme loading at 3 % (w/w) of Novozyme 435 and 8 % (w/w) of Lipozyme TLIM. This reflected the increase in active sites at the initial increasing in biocatalyst loading which resulted in higher conversion rate while its further led to limited availability of the substrate in excessive active sites and thus no significant increase in the product yield.

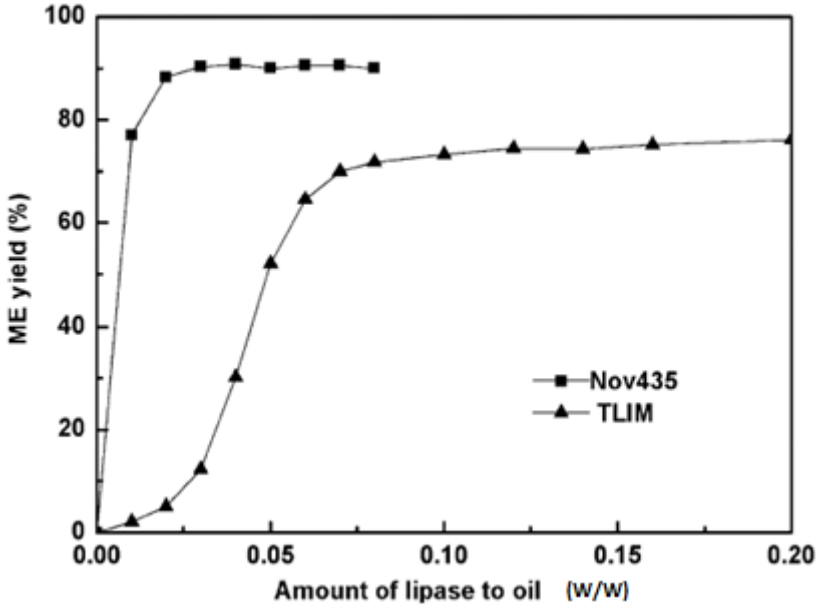


**Figure 2.27** Effect of enzyme loading on transesterification [83]. Reaction was conducted at reaction temperature of 50°C for 24 h.

### 2.4.5 Effect of reaction temperature

Temperature is one key parameter in enzyme catalysed reactions. In biodiesel synthesis reactions, temperature has an influence on the enzyme catalytic activity and the solubility of the reactants. Normally, the enzymatic biodiesel synthesis processes are operated under mild reaction temperature in range of 30 to 50 °C. Jeong et al. (2008) [84] reported that the effect of temperature on rapeseed oil methanolysis was assessed in a temperature range of 25 to 55 °C for 2 h using 5% (w/w) Novozyme 435 in presence of methanol at 3:1 to oil molar ratio. Figure 2.28 showed that increasing conversion was

found with increasing reaction temperatures up to 40 °C, and then obviously declined at 55 °C. The highest product of 45.3% was obtained from reaction temperature at 40 °C. However, the influence of temperature on the enzymatic biodiesel synthesis needed to be optimized with the individual enzymes and substrates.

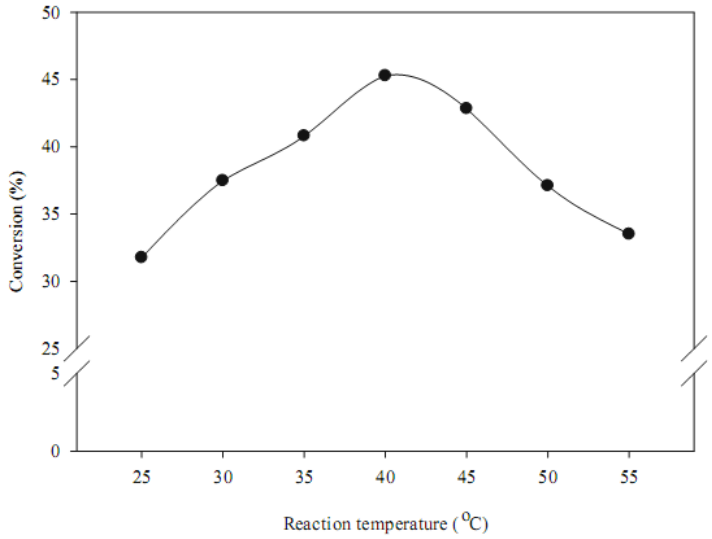


**Figure 2.28** Effect of reaction temperature on rapeseed oil methanolysis [84]. Reactions contained 5% (w/w) Novozyme 435 based on oil weight at 3:1 [methanol]/[oil] molar ratio for 2 h.

### 2.4.6 Effect of water content

Water content is an important factor in the conventional catalytic transesterification of vegetable oil. The presence of water is important for enzyme performance; however, it also leads to hydrolysis of the ester product, which is the unwanted side reaction. Jeong et al. (2008) [84] studied the effects of the water content on the enzyme-catalyzed methanolysis of rapeseed oil using Novozyme 435 by adding different amounts of water in the range of 0-10% based on the weight of oil (Figure 2.29). It was found that the highest conversion was approximately 76.1% at a water content of 1% (w/w) after 24 h incubation at 40 °C. Increasing the conversion in linear fashion was consistent to the increase of water content within a range of below 1% (w/w), while the excess of water higher than 1% (w/w) resulted in continual reduction in product yield.

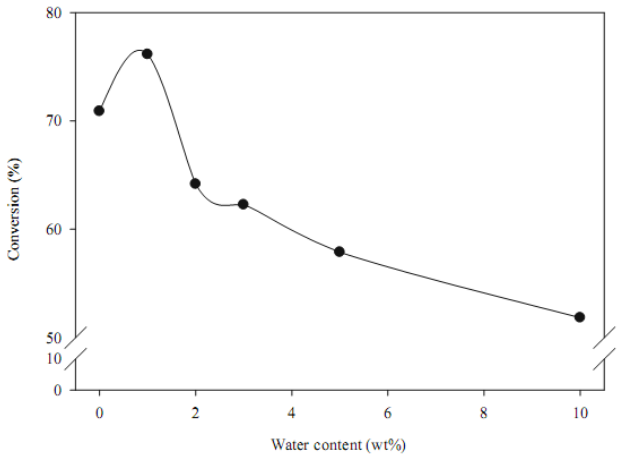


**Figure 2.29** Effect of water content on rapeseed oil methanolysis [84]. Reactions contained 5% (w/w) Novozyme 435 based on oil weight at 3:1 [methanol]/[oil] molar ratio at 40 °C.

## 2.5 Bioethanol

Bioethanol is a widely used biofuel which is produced from renewable resources, such as sugar, starch and biomass. Ethanol can be blended with gasoline or burned in its pure form for using modified spark-ignition engines. The mixture of ethanol and gasoline for transportation has higher combustion performance in vehicles due to the higher octane level from ethanol. This also reduces emission of carbon monoxide, unburned hydrocarbons, carcinogens, and sulphur in comparison to gasoline. In order to avoid competition between “food v.s. feed”, production of second generation bioethanol from lignocellulosic biomass has received increasing attention. This provides the basis for establishment of sustainable and environmentally friendly biofuel and biorefinery industry which produce biofuels and biochemical from lignocellulosic components in an integrated biorefineries complex.

Conversion of lignocellulose to valorized products can be performed using thermochemical (e.g. pyrolysis, gasification, or catalytic) routes or by the multidisciplinary sugar platform approach. Each method has advantages and limitations which need to be considered which is related to choices of the starting materials and the target products. Due to energy intentive requirement of the thermochemical route, most of current biorefineries focus on sugar platform process which operates under mild conditions. Basically, the sugar platform process for bioethanol and biochemical production involves three main steps: pretreatment, hydrolysis, and fermentation or catalytic conversion which produce sugar as

the key intermediate before further the conversion to target products. Utilization of the hemicellulose and lignin fractions for production of value-added products has also received great interest in order to maximize economic feasibility with the zero waste concepts.

### 2.5.1 Composition of lignocellulosic materials

The three main components of lignocellulosic materials are cellulose, hemicelluloses and lignin, which are fabricated into a highly ordered complex structure. In addition to minor components e.g. extractives, triglycerides, wax, and ash. Its general structure is demonstrated in Figure 2.30. Different biomass e.g. hardwood, softwood, and agricultural residues contained different relative composition of lignocellulosic constituents and also has variation in their detailed physicochemical and chemical characteristics of the components. The content of lignocellulosic materials from various sources is shown in Table 2.11.

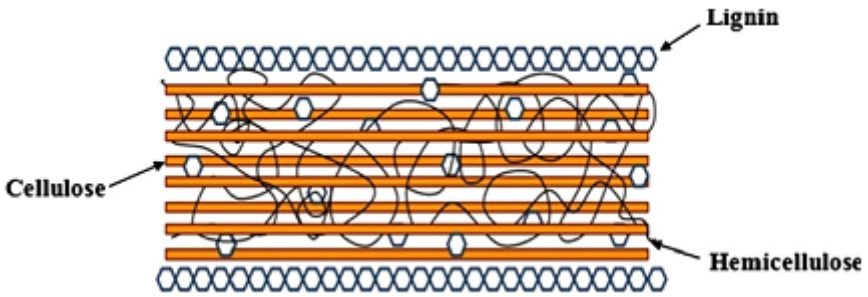


**Figure 2.30** Schematic structure of lignocellulosic materials [85].

**Table 2.11** Content of lignocellulosic material [85].

| Lignocellulosic biomass | Cellulose glucan | Hemicellulose | | | | Lignin | |
|---|---|---|---|---|---|---|---|
| | | Xylan | Arabinan | Galactan | Mannan | Acid-insoluble lignin | Acid-soluble lignin |
| **Barley hall** | 33.6 | 30.5 | 6.1 | 0.6 | Trace | 19.3 | ND |
| **Barley straw** | 33.8 | 21.9 | - | - | - | 13.8 | - |
| **Corn cobs** | 33.7 | 31.9 | - | - | - | 6.1 | - |
| **Corn stover** | 38.3 | 21 | 2.7 | 2.1 | ND | 17.4 | - |
| **Cotton straw** | 14.4 | - | 14.4 | - | - | 21.5 | - |
| **Wheat straw** | 30.2 | 18.7 | 2.8 | 0.8 | ND | 17 | - |
| **Rice straw** | 31.1 | 18.7 | 3.6 | ND | ND | 13.3 | - |
| **Rye straw** | 30.9 | 21.5 | ND | ND | ND | 22.1 | 3.2 |
| **Oat straw** | 39.4 | 27.1 | - | - | - | 17.5 | - |
| **Soya stalks** | 34.5 | 24.8 | - | - | - | 9.8 | - |
| **Sunflower stalks** | 42.1 | 29.7 | - | - | - | 13.4 | - |
| **Switchgrass** | 39.5 | 20.3 | 2.1 | 2.6 | ND | 17.8 | 4 |
| **Sugarcane bagasse** | 43.1 | 31.1 | - | - | - | 11.4 | - |
| **Sweet sorghum bagasse** | 27.3 | 13.1 | 1.4 | ND | ND | 14.3 | - |
| **Forage sorghum** | 35.6 | 18.4 | 1.8 | ND | ND | 18.2 | - |
| **Olive tree pruning** | 25 | 11.1 | 2.4 | 1.5 | 0.8 | 16.2 | 2.2 |
| **Poplar** | 43.8 | 14.8 | ND | ND | ND | 29.1 | - |
| **Spruce** | 43.8 | 6.3 | ND | ND | 14.5 | 28.3 | 0.53 |
| **Oak** | 45.2 | 20.3 | ND | ND | 4.2 | 21 | 3.3 |

#### 2.5.1.1 Cellulose

Cellulose is the most abundant organic carbon in nature. It is a long chain of D-glucose linear homopolymers linked by β-1,4 glycosidic bonds [86]. The whole fraction of cellulose in lignocellulosic materials consists of the highly crystalline part and amorphous fraction with an average molecular weight of around 100,000. The cellulose chains are ‘bundled’ together and form the so called cellulose fibrils or cellulose bundles. These cellulose fibrils are mostly independent and weakly bound through hydrogen bonding. The hydrogen bonds in structure can maintain and support the linear conformation of the cellulose fibers. The ends of cellulose chains are hydrophobic while the sides of the cellulose chains are hydrophilic [87]. The highly ordered and crystalline structure of cellulose makes it resistant to enzymatic degradation.

#### 2.5.1.2 Hemicellulose

Hemicellulose is a branched heteropolymer of pentose (e.g. xylose and arabinose), hexoses (e.g. glucose, mannose, and galactose) and sugar acids. The dominant component of hemicellulose from hardwood and agricultural plants, such as grasses and straw, is xylan, while this is glucomannan for softwood. Hemicellulose has amorphous structure and has a lower molecular weight than cellulose, and branch with short lateral chains that consist of different sugars, which are easily hydrolysable. Hemicellulose serves as a connection between the lignin and the cellulose fibers and gives the whole cellulose–hemicellulose–lignin network more rigidity.

#### 2.5.1.3 Lignin

Lignin is an amorphous heteropolymer consisting of three different phenylpropane units (p-coumaryl, coniferyl and sinapyl alcohol) that are held together by different kinds of linkages [88]. The main function of lignin is to give the plant structural support, impermeability, and resistance against microbial attack and oxidative stress. It is also non-water soluble and optically inactive, making it highly recalcitrant to degradation. Removal of lignin by chemical or thermochemical methods is the pre-requisite to increasing enzymatic digestibility of biomass to give a feasible level of sugars. Mostly the lignin fraction is used for low value energy production by combustion; however, increasing interest on the valorization of lignin to composite materials, such as phenolic resins and aromatics, has gained the more interest which is expected to significantly contribute to the overall value of the integrated biorefinery process.

### 2.5.2 Pretreatment of lignocellulosic materials

Hydrolysis of lignocellulosic biomass into sugars consists of two steps: the pretreatment of biomass and the enzymatic saccharification of the pretreated biomass into sugars for further conversion. The factors that have been identified to affect the hydrolysis of cellulose include porosity (accessible surface area) of the materials, cellulose fiber crystallinity, lignin and cellulose content and degree of polymerisation [89]. The presence of lignin and hemicellulose makes the access of cellulase enzymes to cellulose difficult, thus reducing the efficiency of hydrolysis. Lignin can also interfere with the hydrolysis by irreversibly binding to hydrolytic enzymes. The purpose of the pretreatment step is thus to remove lignin and hemicellulose, reduce crystallinity and increase the porosity of the materials.

In general, the pretreatment must meet the following requirements: (1) improve the formation of sugars or the ability to subsequently form sugars by the downstream enzymatic hydrolysis; (2) avoid the degradation or loss of carbohydrate; (3) avoid the formation of by-products inhibitory to the subsequent enzymatic or conversion processes; and (4) be cost-effective to make the process viable [90]. Implementation of optimal pretreatment step will result in improved total yield of monomeric sugars in the hydrolysis step and the production of target fermentation products. Due to their differences in chemical composition (Table 2.12), the pretreatment step for each biomass needs optimization in order to determine the optimal conditions and reaction parameters with the balance of saccharification efficiency, cost and energy consumption.

**Table 2.12** Chemical composition of potential lignocellulosic agricultural biomass

| Biomass | % composition | | | Reference |
|---|---|---|---|---|
| | Cellulose | Hemicellulose | Lignin | |
| Sugarcane bagasse | 50 | 25 | 25 | Pandey et al, 2000 |
| Rice straw | 36.5 | 25.6 | 12.8 | Lin & Chen 2006 |
| Empty palm fruit brunch | 44.2 | 33.5 | 20.4 | Aziz et al, 2002 |
| Corn stover | 36.1 (glucan) | 29.2 | 17.2 | Wyman 2005 |
| Eucalyptus | 45 | 19.2 | 31.3 | Sjostrom, 1993 |

Physical, chemical, thermal, and biological approaches have been studied for the efficient pretreatment of lignocellulosic biomass. Each pretreatment technology has different advantages and disadvantages in terms of efficiency and economics, and is suitable for different biomass. They also possess different effects on the cellulose, hemicelluloses and lignin, the three main components of lignocellulosic biomass. Physical pretreatment e.g. milling leads to the reduction of size and crystallinity. The increase in specific surface area, including reduction of degree of polymerization and shearing results in the increase of the total hydrolysis yield of the cellulose. Although the milling method does not result in generation of inhibitors, like furfural and HMF, this method requires high energy and does not economically feasible for pretreatment of biomass in large-scale [91]. Physical pretreatment by radiation (e.g. gamma ray and electron beam) has also been recently reported; however, its feasibility in up-scaled process needs further study.

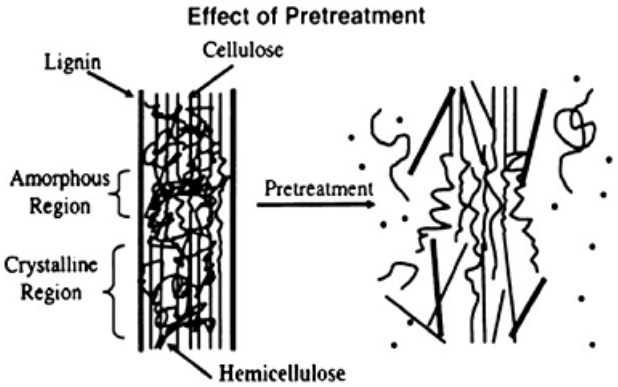


**Figure 2.31** Schematic representation of the matrix of polymers in which cellulose exists [92].

Chemical pretreatments were originally developed and have been extensively used in the paper industry for the delignification of cellulosic materials to produce high quality paper products. A wide range of chemical and thermochemical processes have been developed including (steam explosion, ammonia fiber explosion, etc.), alkali treatment, acid treatment, etc. Chemical pretreatments are generally highly efficient method and possess different effects to the lignocellulosic biomass components. For acid pretreatment, the main effects are on hydrolysis and removal of the hemicellulose fraction which leads to increasing accessibility to the cellulose fiber. However, there is a risk on the formation of

volatile degradation products. The condensation and precipitation of lignin components is also an unwanted reaction, resulting in decreased digestibility of the pretreated biomass. Alkaline pretreatment causes hemicelluloses and part of lignin to solubilise. This leads to the loss of fermentable sugars and production of inhibitory compounds.

It can be concluded that pretreatments such as concentrated acids, wet oxidation, solvents and metal complexes, are effective but too expensive compared to the value of glucose [93]. Among various of pretreatment technologies, steam pretreatment, lime pretreatment, liquid hot water and ammonia based pretreatments are the promising ones according to the economic effectiveness and the effects of the pretreatments [94]. Biological pretreatment is based on selective decomposition of lignin by microorganisms mainly white rot fungi [95]. Lignin degradation occurs through the action of lignin degrading enzymes secreted by the fungi. Even though biological pretreatments involve mild conditions and are of low cost, the disadvantages are the low rates of hydrolysis and long pretreatment times required compared to other technologies. The effects on the structure of lignocellulose as well as the advantages and limitation of different pretreatment methods are shown in Tables 2.13 and 2.14.

**Table 2.13** Effects of different pretreatment technologies on the structure of lignocellulose [95].

| | Milling | Steam explosion | LHW | Acid | Alkaline | Oxidative | AFEX | ARP | Lime | $CO_2$ explosion |
|---|---|---|---|---|---|---|---|---|---|---|
| **Increases accessible surface area** | H | H | H | H | H | H | H | H | H | H |
| **Cellulose decrystallization** | H | - | n.d | - | - | n.d. | H | H | n.d. | - |
| **Hemicellulose solubilization** | - | H | H | H | L | - | M | M | M | H |
| **Lignin removal** | - | M | L | M | M | M | H | H | H | - |
| **Generation of toxic compounds** | - | H | L | H | L | L | M | M | M | - |
| **lignin structure alteration** | - | H | M | H | H | H | H | H | H | - |

H=High effect; M=Moderate effect; L= Low effect; n.d. =Not determined

**Table 2.14** Summary of the advantages and disadvantages of different methods for pretreating lignocellulosic biomass [95].

| Pretreatment method | Advantages | Disadvantages |
|---|---|---|
| **Biological** | -Degrades lignin and hemicellulose<br>-Low energy consumption | -Low rate of hydrolysis |
| **Milling** | -Reduces cellulose crystallinity | -High power and energy consumption |
| **Steam explosion** | -Causes lignin transformation and hemicellulose solubilization<br>-Cost-effective<br>-Higher yield of glucose and hemicellulose in the two-step method | -Generation of toxic compounds<br>-Partial hemicellulose degradation |
| **AFEX** | -Increase accessible surface area<br>-Low formation of inhibitor | -Not efficient for raw materias with high lignin content<br>-High cost of large amount of ammonia |
| **$CO_2$ explosion** | -Increase accessible surface area<br>-Cost-effective<br>-Do not imply generation of toxic compounds | -Does not affect lignin and hemicellulose<br>-Very high pressure requirements |
| **Wet oxidation** | -Efficiency removal of lignin<br>-Low formation of inhibitors<br>-Minimizes the energy demand (exothermic) | -High cost of oxygen and alkaline catalyst |
| **Ozonolysis** | -Reduces lignin content<br>-Do not imply generation of toxic compounds | -High cost of large amount of ozone needed |
| **Organosolv** | -Causes lignin and hemicellulose hydrolysis | -High cost<br>-Solvents need to be drained and recycled |
| **Concentrated acid** | -High glucose yield<br>-Ambient temperature | -High cost of acid and need to be recovered<br>-Reactor corrosion problems<br>-Formation of inhibitors |
| **Diluted acid** | -Less corrosion problems than concentrated acid<br>-Less formation of inhibitors | -Generation of degradation products<br>-Low sugar concentration in exit stream |

Among the pretreatment methods, steam explosion pretreatment or autohydrolysis, is the most commonly used method for the pretreatment of lignocellulosic materials. Increasing to biomass digestibility can be achieved by hydrolysis of the hemicellulose fraction while the lignin transformation leads to partial removal of lignin from the lignocellulosic structure which in overall lead to increasing accessibility to the cellulose fibers and thus enhancing its enzymatic digestibility.

Steam explosion is generally highly efficient for a variety of biomass leading to markedly improvement in sugar yield obtained from enzymatic hydrolysis. It also has several technical advantages over other pretreatment methods include potential for lower capital investment, significantly lower environmental impact, high energy efficiency, and less generation of hazardous process chemicals. [92]. Steam explosion starts with treatment of biomass with high-pressure saturated steam under high temperature (160-220 °C) and pressurized conditions from several seconds to minutes before swift reduction of pressure which lead to explosive decomposition of the material. Particle size, temperature, residence time, and the combined effect of both temperature and time are key factors to affect the pretreatment efficiency. However, the main drawbacks of steam explosion pretreatment are partially hemicellulose degradation and the generation of some toxic compounds that could affect the following hydrolysis and fermentation steps [96].

In general, the toxic compounds generated depend on the type and amount of raw material, and harshness of the pretreatment conditions. The major inhibitors are furan derivatives, weak acids and phenolic compounds. Two main furan derivatives are furfural and 5-hydroxymethyl furfural derived from pentoses and hexoses degradation, respectively. These inhibitors impact with prolongation of the lag phase during batch fermentation [97]. The weak acids generated during steam explosion are mostly acetic acid, formed from the acetic groups present in the hemicellulosic fraction, including formic and levulinic acids derived from further degradation of furfural and HMF [98]. The lignin degradation also generates the wide range of phenolic compounds. This thus results in the requirement for subsequent delignification of the pretreated biomass. However, this additional step leads to increasing cost of overall process.

Steam explosion pretreatment has been extensively studied with a variety of biomass. Negro et al. (2003) [99] studied steam explosion and liquid hot water methods for pretreatment of *Populus nigra* biomass. The best results were obtained in steam explosion pretreatment at 210 °C and 4 min, providing cellulose recovery approximated at 95%, enzymatic hydrolysis yield around 60%, and 41% xylose recovery in the liquid fraction.

Later, the addition of acid promoters (e.g.$H_2SO_4$ or $SO_2$) in steam explosion can decrease time and temperature, effectively improve hydrolysis, decrease the production of inhibitory compounds, and lead to the complete removal of hemicellulose. Ballesteros et al. (2006) [100] applied acid-catalyzed steam explosion pretreatment of wheat straw for bioethanol production by varying the temperature (160–200 °C), the residence time (5, 10 or 20 min) and the acid concentration [$H_2SO_4$ 0.9% (w/w)]. It was found that the best pretreatment conditions provided 80% ethanol yield from wheat straw conversion after steam explosion at 190 °C and 10 min or 200 °C and 5 min (Figure 2.32)

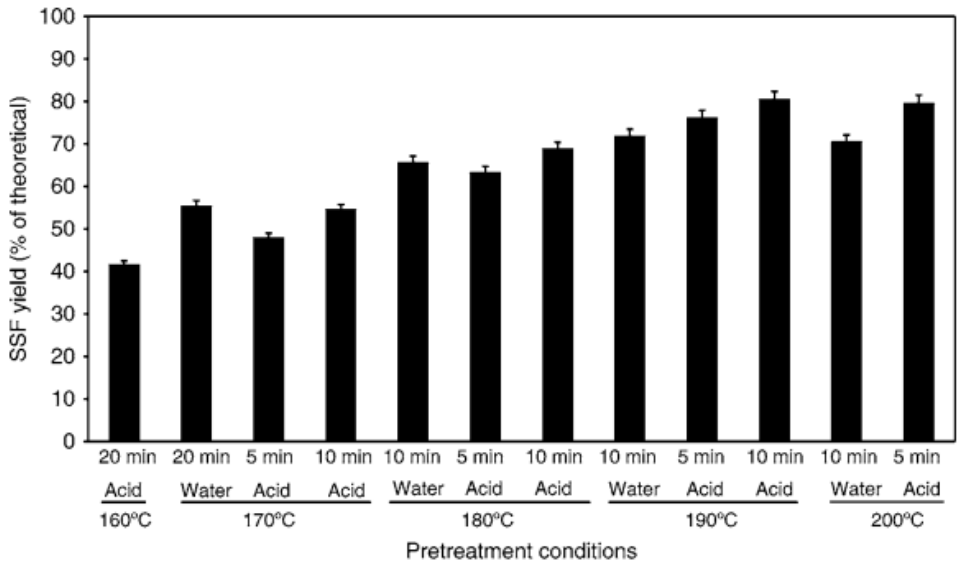


**Figure 2.32** Ethanol yield of steam-exploded wheat straw at different pretreatment conditions [100].

### 2.5.3 Enzymatic hydrolysis

Hydrolysis is a subsequent step for the conversion of pretreated biomass into sugars. Unlike chemical hydrolysis using strong acids (e.g. $H_2SO_4$ at high temperature), enzymatic hydrolysis is achieved under mild reaction conditions (pH and temperature), and thus requires less energy and has no corrosion problem. The main factors that influence the enzymatic hydrolysis of cellulose in lignocellulosic biomass can be divided in two groups: enzyme-related and substrate-related factors, though many of them are interrelated during the hydrolysis process. Three classes of enzymes act synergistically to hydrolyse cellulose to glucose: endo-β-1,4-glucanases (EG, EC 3.1.2.4) attack the endogenous part of cellulose chain, cellobiohydrolases (CBH, EC 3.2.1.91) attack the ends of the polymer, releasing cellobiose that is ultimately cleaved into two glucose molecules by β-glucosidases (BG, EC 3.2.1.21) [86]. The heterogenous hemicellulose is hydrolyzed by a variety of hemicellulase to release its composite sugars, including xylose, arabinose, galactose, glucose and/or mannose. Hexoses such as glucose, galactose, and mannose are readily fermented to ethanol by many naturally occurring organisms, but the pentoses including xylose and arabinose are fermented to ethanol by few native strains, and usually at relatively low yields. However, development a feasible enzymatic hydrolysis process is limited by the high costs of enzyme production, long residence time of hydrolysis, and the excessive enzymatic dosages necessary to hydrolyse the pretreated biomass. Developing a highly active enzyme with high performance under the hydrolysis conditions is thus a key for producing cost competitive sugar for further conversion.

The optimization of enzyme mixtures and hydrolysis conditions for the hydrolysis of different lignoellulosic biomass has been studied. Zhao et al. (2011) [101] described the enzymatic digestibility of alkali/peracetic acid (PAA)-pretreated bagasse. For testing the enzymatic digestibility of the substrate cellulose, the pulp was digested by cellulase loading of 5–20 FPU/g solid with 0–40 CBU/g solid of supplemental β-glucosidase at pH 4.8 in 0.1M sodium acetate buffer incubated at 50 ± 0.5 °C in an air-bath with shaking at 130 rpm for 5 days. The initial solid consistency was 2.5–10%. It found that enzymatic glycan conversion could reach about 80% after 24 h incubation when enzyme loading was 10 FPU/g solid. Additionally, Zhong et al. (2009) [102] showed that the hydrolysis efficiency of lignocellulosic biomass increased with the combination of enzymes such as cellulase, xylanases and pectinases. It was found that the addition of Multifect® xylanase at 2.67 mg protein/g glucan and Multifect® pectinase at 3.65 mg protein/g glucan to CP

cellulose and Novozyme$^{TM}$ 188 was optimal for sugar conversion of AFEX-treated rice straw. Glucan and xylan conversions to monomeric sugars reached 81.7% and 75.8%, whereas cellulase dosage 15 FPU/g glucan loading about 80.6% of glucan conversions and 89.6% of xylan conversions (including monomeric oligomeric sugars) were achieved.

Palm kernel cake (PKC) represents one of the most potent under-used types of biomass from the palm oil refinery industry. PKC contained approximately 50% polysaccharide content which can be hydrolyzed to sugars. Its main polymers are mannan and galactomannan that can be hydrolyzed by the multiple enzymes comprising endo-1,4-β-mannanase, β-mannosidases, and β-galactosidases in the enzymatic hydrolysis step. Cerveró et al. (2010) [20] described that a binary mixture of enzyme at 1:1 of Mannaway 25L (mono enzyme of mannanase) and Gammanase 1.0L (multiple enzymes of mannanase, β-mannosidase, α-glactosidase, and β-glucosidase) is effective for enzymatic hydrolysis of PKC treated in an autoclave at 126 °C for 11 min. This gave the maximal total of released sugars of 13.9 g/L, including 71.7% and 15% of mannan and glucan conversions, respectively (Table 2.15).

**Table 2.15** Effect of pretreatment conditions on enzymatic hydrolysis of PKC [20].

| | **Pretreatment temperature (°C)** | **Pretreatment time (min)** | **Mannose (%)[a]** | **Glucose (%)[a]** | **Total (g/L)[b]** |
|---|---|---|---|---|---|
| **Condition A** | - | - | 66.0±0.4 | 13.8±0.4 | 12.9±0.1 |
| **Condition B** | 126 | 11 | 71.7±0.7 | 15.0±0.1 | 13.9±0.1 |
| **Condition C** | 180 | 10 | 58.4±6.4 | 13.6±1.4 | 11.4±1.2 |

All reactions carried out at 5% (w/w) of PKC. Enzymatic hydrolysis was for 24 h with a 1:1 mixture of Mannaway and Gammanase with total 10% (v/w) enzyme loading.

[a]Relative to maximum theoretical based on PKC composition

[b]Sum of released sugars (mannose and glucose)

Jørgensen et al. (2010) [21] reported that high PKC digestibility was achieved by an enzyme mixture comprising 30:10:1 of endomannanase/β-mannosidase/cellulase on PKC prehydrolysed at 50 °C. This led to the maximal final ethanol product of 70.1 g/kg after fermentation with *S. cerevisiae* at 30 °C for 216 h using simultaneous saccharification and fermentation process (SSF). This final ethanol yield was equivalent to 70% theoretical yield or 200 g ethanol/kg PKC. This finding suggested that the presence of cellulase in the enzyme mixtures resulted in significant improvement of ethanol yield.

**Table 2.16** Ethanol product after SSF of PKC at 35% DM [21].

| **Prehydrolysis time[a] (h)** | **Total time[a] (h)** | **Enzyme loading[b] (ml/kg PKC)** | **Final ethanol concentration (g/kg)** | **Ethanol yield (g/kg PKC)** |
|---|---|---|---|---|
| 24 | 192 | 61.5 | 57.6±0.5 | 164±2 |
| 48 | 216 | 61.5 | 59.3±1.1 | 169±3 |
| 24 | 192 | 123 | 65.5±1.2 | 190±3 |
| 48 | 216 | 123 | 70.1±0.6 | 200±2 |

[a]Prehydrolysis was performed at 50°C, and total time includes time for prehydrolysis and SSF

[b]Total enzyme loading using a 30:10:1 mixture of endomannanase/β-mannosidase/cellulase

### 2.5.4 Ethanol fermentation

Fermentation of lignocellulose hydrolysates into bioethanol requires efficient microorganisms for utilizing all hexose and pentose sugars in the presence of inhibitory compounds, including weak acids, furaldehydes and phenolics. In general, several microorganisms, such as yeast (*Saccharomyces cerevisiae)*, bacteria (*Zymomonas mobilis*, and *Escherichia coli*), and fungi (*Fusarium oxysporum* and *Neurospora crassa*), can be used for fermentation [87]. The baker's yeast *S. cerevisiae* is the most commonly used microorganism for fermentation of alcoholic beverages from sugar sources e.g. rice, wheat, barley, and corn due to relatively high tolerance with the inhibitory compounds. However, the wild-type *S. cerevisiae* lacks the ability to utilize the pentose sugars (xylose and arabinose) leading to the low ethanol yield for lignocellulosic conversion. Besides, the most promising yeast species e.g. *Candida shehatae*, *Pichia stipitis* and *Pachysolen tannopilus* can be ferment xylose with relatively high yield of ethanol. The co-fermentation of glucose and pentoses to ethanol is a key target for efficient conversion of all sugars to ethanol. The potential of different fermentable microorganisms for conversion of lignocellulose into ethanol is compared in Table 2.17. According to the fermentable reaction, the theoretical maximum yield is 0.51 kg ethanol and 0.49 kg $CO_2$ per kg of xylose and glucose.

$$3C_5H_{10}O_5 \rightarrow 5C_2H_5OH + 5CO_2$$
$$C_6H_{12}O_6 \rightarrow 2C_2H_5OH + 2CO_2$$

**Table 2.17** The potential of microorganisms in lignocellulosic-based bioethanol fermentation [87].

| Species | Characteristics | Advantages | Drawbacks |
|---|---|---|---|
| *Saccharomyces cerevisiae* | Facultative anaerobic yeast | • Naturally adapted to ethanol fermentation.<br>• High alcohol yield (90%).<br>• High tolerance to ethanol (up to 10% v/v) and chemical inhibitors.<br>• Amenability to genetic modifications | • Not able to ferment xylose and arabinose sugars.<br>• Not able to survive high temperature of enzyme hydrolysis. |
| *Candida shehatae* | Micro-aerophilic yeast | • Ferment xylose | • Low tolerance to ethanol<br>• Low yield of ethanol<br>• Require micro-aerophilic conditions<br>• Dose not ferment xylose at low pH |
| *Zymomonas mobilis* | Ethanologenic Gram-negative bacteria | • Ethanol yield surpasses S. cerevesiae (97% of the theoretical).<br>• High ethanol tolerance (up to 14% v/v)<br>• High ethanol productivity (five-fold more than S. cerevisiae volumetric productivity)<br>• Amenability to genetic modification<br>• Does not require additional oxygen | • Not able to ferment xylose sugars<br>• Low tolerance to inhibitors<br>• Neutral pH range |
| *Pichia stipitis* | Facultative anaerobic yeast | • Best performance xylose fermentation<br>• Ethanol yield (82%)<br>• Able to ferment most of cellulosic-material sugars including glucose, galactose and cellobiose<br>• Possess cellulose enzymes favorable to SSF process | • Intolerant to a high concentration of ethanol above 40 g/L<br>• Dose not ferment xylose at low pH<br>• Sensitive to chemical inhibitors<br>• Requires micro-aerophilic conditions to reach peak performance<br>• Re-assimilates formed ethanol |
| *Pachysolen tannophilus* | Aerobic fungus | • Ferment xylose | • Low yield ethanol<br>• Required micro-aerophilic conditions<br>• Dose not ferment xylose at low pH |
| *Esherichia coli* | Mesophilic Gram-negative bacteria | • Ability to use both pentose and hexose sugars<br>• Amenability for genetic modifications | • Repression catabolism interfere to co-fermentation<br>• Limited ethanol tolerance<br>• Narrow pH and temperature growth range<br>• Production of organic acids<br>• Genetic stability not proven yet<br>• Low tolerance to inhibitors and ethanol |
| *Kluveromyces marxianus* | Thermophilic yeast | • Able to grow at a high temperature above 52°C<br>• Suitable for SSF/CBP process<br>• Reduces cooling cost<br>• Reduces contamination<br>• Ferments a board spectrum of sugars<br>• Amenability to genetic modifications | • Excess of sugars affect its alcohol yield<br>• Low ethanol tolerance<br>• Fermentation of xylose is poor and leads mainly to the formation of xylitol |
| Thermophilic bacteria:<br>**Thermoanaerobacterium saccharolyticum*<br>**Thermoanaerobacter ethanolicus*<br>**Clostridium thermocellum* | Extreme anaerobic bacteria | • Resistance to an extremely high temperature of 70°C<br>• Suitable for SSCombF/CBP Processing<br>• Ferment a variety of sugars<br>• Display cellulolytic activity<br>• Amenability to genetic modification | • Low tolerance to ethanol |

Fermentation can be operated in a batch, fed-batch, or continuous process. The most suitable choice depends on the kinetic properties of the microorganism in addition to aspects of process economics. The improvement on immobilization and recirculation of cells are to increase the cell mass concentration in the fermenter which leads to a higher productivity. The typical goals of fermentation process are the higher the productivity, and the smaller the fermenter required, leading to the lower capital cost.

The process configurations are divided into four strategies. The four biologically mediated events occur in the step of producing ethanol from cellulosic biomass using enzymatic hydrolysis: enzyme production, enzymatic hydrolysis, hexose fermentation, and pentose fermentation [103, 104]. A variety of bioprocessing options for the conversion of lignocellulosic biomass is illustrated in Figure 2.33. It was found that the separate hydrolysis and fermentation (SHF) involves four bioreactors. The integrated step of enzymatic hydrolysis and hexose fermentation is namely simultaneous saccharification and fermentation (SSF). In this process, the sugars released by enzymatic hydrolysis are fermented by microorganisms simultaneously, so the compromise of reaction parameters in both processes is necessary for the optimized ethanol production. The SSF process focuses on reducing the inhibition of cellulases caused by high concentration of end products (glucose and oligo-glucose) from hydrolysis. The combination of pentose fermentation with SSF is defined as simultaneous saccharification and co-fermentation (SSCF) process.

The SSCF approach can increase the final ethanol concentration and overall yield derived from pentose conversion, especially xylose. This can be achieved by several strategies including fermentation with naturally pentose utilizing ethanologens and engineered *Saccharomyces cereviciae* for xylose utilising capability. The SSCF method has several advantages including high ethanol productivity, shorter process time, and reduced contamination risk. The last bioprocessing is consolidated bioprocessing (CBP) that accomplishes to integrate the whole steps of enzyme production, hydrolysis, and fermentation simultaneously in a single bioreactor. CBP is the ideal case in development of biomass conversion technology. Unlike the other bioprocessing strategies, CBP is defined as the use of single microbial community for enzyme production and fermentation. This can be achieved from the modified pathways of the ethanologenic organisms for expressing lignocellulose degrading enzymes combined with fermentation by using genetic engineering techniques. The superiors of CBP are no capital or operating costs for dedicated enzyme production, greatly reduced diversion of substrate for enzyme

production, and compatible enzyme and fermentation systems [105]. This technology is idealistic for economic possibility of industrial ethanol production if limitations of current techniques can be overcome.

Several bioprocessing technologies for ethanol production from lignocelluloses have been previously reported. For instance, Abedenifar et al. (2009) [106] studied rice straw conversion to ethanol by separated enzymatic hydrolysis and fermentation by *Mucor indicus*, *Rhizopus oryzae*, and *S. cerevisiae*. The *M. indicus* was able to grow on the hydrolysate, and produced ethanol as the major product and glycerol as the main by-product. The glucose was completely assimilated in less than 25 h and the ethanol yield of 0.43 g/g was obtained. Similar to *M. indicus*, *R. oryzae* was able to grow on the hydrolysate and produce ethanol. On the other hand, complete consumption of hexoses by *R. oryzae* required two days of fermentation, and formation of 0.05–0.09 g/g lactic acid in fermentation by *R. oryzae* was observed. *S. cerevisiae* produced the maximum of ethanol yield of 0.45 g/g and glycerol yields from different hydrolysate were 0.01–0.02 g/g which was more than that obtained from *M. indicus*.

Yadav et al. (2011) [107] studied the bioethanol fermentation of concentrated rice straw hydrolysate using a co-culture of *Saccharomyces cerevisiae* and *Pichia stipitis*. In this work, the concentrated and detoxified hydrolysate prepared from rice straw was fermented with co-culture of *S. cerevisiae* OVB11 and *P. stipitis* NCIM3498. Batch fermentation of ethanol using *S. cerevesiae* with 30 g/L of total sugars produced the maximum ethanol of 7.5 g/L at 36 h of incubation with a yield 0.3 g/g and productivity of 0.20 g /l/h. On the other hand batch fermentation of ethanol using co-culture of *S. cerevesiae* and *P. stipitis* produced the maximum ethanol of 12 g/L at 36 h of incubation with an efficiency of 95%.

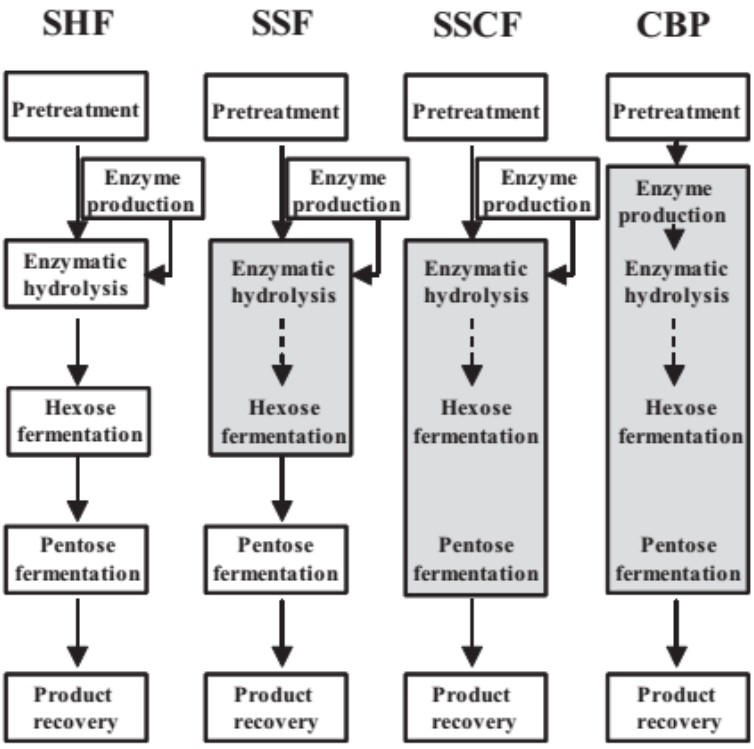


**Figure 2.33** Bioprocessing technologies of lignocellulosic conversion [103].

Oloffson et al. (2010) [108] described the simultaneous saccharification and co-fermentation SSCF using genetically modified yeast strains. The work demonstrated a new approach for controlling the glucose release rate from the enzymatic hydrolysis of spruce by controlling the addition of enzymes in SSCF. Enzyme kinetics and yeast sugar uptake rates for a recombinant xylose utilizing strain *S. cerevisiae* TMB3400 were studied. It found that glucose release rate of 2.0 g $L^{-1}$ $h^{-1}$ resulted in the highest total xylose uptake of 69% and the corresponding highest ethanol yield of 0.39 g/g of total sugars (i.e. glucose, xylose, mannose, galactose, glucan and mannan). This corresponded to 77% of the maximum theoretical yield.

Khuong et al. (2014) [109] studied consolidated bioprocessing fermentation by the cellulose-fermenting fungus *Phlebia* sp. MG-60 using sugarcane bagasse pretreated by alkaline pretreatment. This fungus produced cellulase and xylanase rapidly over 120 h. After *Phlebia* sp. MG-60 was cultured with 20 g/L of sugarcane bagasse pretreated by NaOH, the highest ethanol product was obtained up to 4.5 g/L with ethanol yields at 65.7% of the theoretical maximum under incubation at 28 °C for 10 days.

Recently, the ethanologenic thermophilic bacterium, *Geobacillus thermoglucosidasius* TM242 bacteria strain, was introduced for efficient ethanol production as compared to the conventional yeast. The TM242 strain is a thermophilic

bacterium with the optimal growth temperature of 60 °C and is naturally capable of fermenting glucose and xylose and can assimilate short-chain oligosaccharides e.g cellobiose and mannobiose. It was genetically modified for enhancing ethanol production ability by elimination of lactate dehydrogenase and pyruvate formate lyase pathways, and upregulation of pyruvate dehydrogenase expression, leading to its high performance for ethanol fermentation from biomass hydrolysate [9, 10]. Cripps et al (2009) [8] reported that the achievement of TM242 strain showed the efficient conversion of cellobiose and sugar mixture (hexose and pentose) to ethanol with high productivity. This finding demonstrated the maximal conversion of cellobiose using TM242 with 0.47 g ethanol/g of cellobiose (92% of the maximum theoretical yield).

**Table 2.18** Metabolite profiles and ethanol productivity of engineered strains of *G. thermoglucosidasius* 11955 [8].

| Strain | Substrate | Max. ethanol level (h)[a] | Metabolite concentrations (mM) | | | | | | | Ethanol yield (g/g substrate used) |
|---|---|---|---|---|---|---|---|---|---|---|
| | | | Initial substrate | Residual substrate | Ethanol | Lactate | Acetate | Formate | Pyruvate | |
| Wild type | Glucose | 6.5 | 175 | 0 | 69 | 210 | 30 | 26 | 0 | 0.1 |
| TM89 ($Idh^-$) | Glucose | 12 | 178 | 3 | 167 | 15 | 5 | 33 | 60 | 0.24 |
| TM180 ($Idh^-$,pdh up) | Glucose | 6.5 | 188 | 0 | 286 | 9 | 15 | 19 | 3 | 0.39 |
| TM236 ($Idh^-$,$pfl^-$) | Glucose | 7.5 | 182 | 66 | 127 | 10 | 4 | 0 | 37 | 0.28 |
| TM242 ($Idh^-$,pdh up,$pfl^-$) | Glucose | 7.5 | 192 | 0 | 314 | 10 | 13 | 0 | 1 | 0.42 |
| TM242 ($Idh^-$,pdh up,$pfl^-$) | Cellobiose | 6.1 | 90 | 0 | 322 | 4 | 12 | 0 | 0 | 0.47 |
| TM242 ($Idh^-$,pdh up,$pfl^-$) | Xylose | 12.8 | 193 | 11 | 208 | 7 | 47 | 0 | 2 | 0.35 |

[a]Time post inoculation that peak ethanol concentration achieved

$Idh^-$ = Inactivation of lactate dehydrogenase (IDH)

pdh up = Upregulation of pyruvate dehydrogenase (PDH)

$pfl^-$ = Inactivation of pyruvate formate lyase (PFL)

# CHAPTER 3

# BIOCATALYTIC ESTERIFICATION OF PALM OIL FATTY ACID FOR BIODIESEL PRODUCTION USING GLYCINE-BASED CROSS-LINKED PROTEIN COATED MICROCRYSTALLINE LIPASE*


## Abstract

The conversion of feedstocks containing high free fatty acid contents to alkyl esters is limited by the currently used alkali-catalyzed biodiesel synthesis process. In this study, esterification of palm fatty acids to ethyl esters was studied using heterogeneous cross-linked protein coated microcrystalline (CL-PCMC) lipase. Optimization of biocatalyst synthesis by variation of matrix components and organic solvents showed that highly active CL-PCMCs could be prepared from *Thermomyces lanuginosus* lipase with glycine as the core matrix in acetone. The optimized reaction contained 20% (w/w) glycine-based CL-PCMC-lipase, a 1:4 fatty acid molar equivalence to ethanol in the presence of an equimolar amount of *tert*-butanol which led to production of 87.2% and 81.4% (mol/mol) of ethyl ester from palmitic acid and industrial palm fatty acid distillate (PFAD), respectively after incubation at 50$^{o}$C for 6 h. CL-PCMC-lipase is more catalytically efficient than protein coated microcrystalline (PCMC) lipase, Novozyme®435 and Lipolase 100T for both free fatty acids and palm fatty acid distillate. The CL-PCMC-lipase showed high operational stability with no significant loss in product yield after 8 consecutive batch cycles. The glycine-based microcrystalline lipase is thus a promising alternative economical biocatalyst for biodiesel production from inexpensive feedstocks with high free fatty acid contents.



* This chapter has been published in:

Raita M, Laothanachareon T, Champreda V, Laosiripojana N. Biocatalytic esterification of palm oil fatty acids for biodiesel production using glycine-based cross-linked protein coated microcrystalline lipase. Journal of Molecular Catalysis B: Enzymatic. 2011; 73:74-9.

### 3.1 Backgrounds

Biodiesel is an alternative fuel for diesel engines produced mainly by the transesterification of vegetable oils or animal fats with short chain alcohols. In Thailand and Southeast Asian countries, the main local feedstock for biodiesel production is purified palm oil (PPO), which is derived from refinery crude palm oil (CPO), a product of the palm oil processing industry. Typically, an alkali-catalyzed transesterification reaction is used for the conversion of triacylglycerol in the feedstock to fatty acid alkyl esters. However, this process is sensitive to free fatty acids (FFAs), which cause undesirable saponification, leading to low product yields and complication in the subsequent separation steps [110]. Due to increasing demand of palm oil for biodiesel and food industry, the price of crude palm oil has been increasing in the past few years (1,100 US$/ton in 2011). Conversion of cheaper alternative feedstocks to biodiesel is thus of interest in order to economically compete with petroleum-based fuel. Palm fatty acid distillate (PFAD) is a by-product from the refinement of CPO to PPO which has a high free fatty acid content. Typically, 3-10% of PFAD is obtained from crude palm oil, which is produced at 800,000 tons/year in Thailand, making it an economically promising feedstock for biodiesel production. The development of an efficient process to convert PFAD and feedstocks containing high FFAs to biodiesel is thus needed for improving the economics of the biodiesel industry.

Typically, the conversion of FFAs to biodiesel can be carried out by acid-catalyzed esterification processes using strong acids, mostly $H_2SO_4$. However, a major limitation of the homogeneous acid catalyzed process is the difficulty in catalyst recovery and waste treatment, as well as corrosion of the equipment, which thus increase the overall cost of the process. Several alternative approaches for biodiesel production from feedstocks containing high FFA content have been reported, including heterogeneous acid catalyzed processes [111] and the non-catalytic or catalytic near- and super-critical methanol processes [112, 113]. However, these approaches still have drawbacks due to high cost of the heterogeneous catalysts and the high energy consumption of the thermal processes. Research on a less energy-intensive and environmentally-friendly alternative process for biodiesel synthesis from PFAD or other feedstocks containing high FFA contents is thus of great interest.

Biocatalytic processes employing lipase biocatalysts have gained increasing interest for industrial biodiesel production [114] which allows high conversion efficiency of feedstocks containing glycerides with high FFA contents under mild operational conditions with no requirement for subsequent wastewater treatment [115]. The development on enzymatic processes for biodiesel production has been focused on the cost reduction for lipases and improvement of the enzyme's operational time and reusability, which would benefit the commercialization of the biocatalytic process. Immobilization is a potential approach for optimizing the operational performance of enzymes and cost of biocatalysts in industrial processes, especially for non-aqueous systems. Enzyme immobilization by precipitation is a cost efficient approach for biocatalyst preparation for use in organic media. This alternative immobilization method involves several forms of biocatalysts including cross-linked enzyme aggregates (CLEAs) [56], cross-linked enzyme crystals (CLECs) [116], and protein-coated microcrystals (PCMCs) [4, 62, 64, 65].

Recently, cross-linked PCMCs (CL-PCMCs) have been reported as an improved biocatalyst design based on conventional PCMCs [13]. CL-PCMCs are characterized as a cross-linked enzyme layer on the surface of micron-sized inner core matrix, which can be prepared by rapid dehydration and co-precipitation of enzyme and the matrix component in an organic solvent, the same as for conventional PCMC preparation, with an extra step on enzyme covalent crosslinking. CL-PCMCs possess several advantages over existing carrier-based or carrier-free immobilization methods, including a low mass-transfer limitation and high catalytic performance, with improved stability and reusability.

In this study, the synthesis of CL-PCMC lipase biocatalysts has been optimized using various core matrices and precipitating organic solvents for efficient esterification of FFAs, used as model reactants and PFAD from palm oil industry. The effects of reaction parameters have been investigated based on the biocatalyst's reactivity on ethyl ester synthesis. The results of this study could be applied for synthesis of biodiesel from feedstocks with high fatty acid content, thus providing an economically and environmentally attractive approach for biodiesel production.

## 3.2 Materials and methods

### 3.2.1 Materials

Refined edible grade palm oil (palm olein; RPO containing ≥ 99% triacylglycerol (TAG)) was obtained from a local market. Crude palm oil (CPO) and palm fatty acid distillate (PFAD) were obtained from the Pathum Vegetable Oil, Co. Ltd. (Pathumthani, Thailand). The CPO sample contained ≥ 95% (w/w) TAG, 4% (w/w) free fatty acid (mainly palmitic acid), and 0.2 % (w/w) of moisture and impurities e.g. trace metals (iron, copper, and nickel) phosphorus and sulphur. The PFAD sample contained 93% (w/w) free fatty acid (45.6% palmitic, 33.3% oleic, 7.7% linoleic as the major FFA) and the rest comprising triglycerides, diglycerides, monoglycerides and trace impurities. Free fatty acids (palmitic, oleic and linoleic acids) and fatty acid ester standards were obtained from Sigma-Aldrich. Liquid *Thermomyces lanuginosus* lipases, from genetically modified *Aspergillus* sp., DELIP 50L (50 KLU/g) was supplied by Flexo Research, Pathumthani, Thailand (1 KLU is defined as the amount of enzyme liberating 1 mmol of titratable butyric acid from tributyrin in 1 min). Liquid *Thermomyces lanuginosus* lipase (Lipolase 100T) and Novozymes® 435 (immobilized *Candida antarctica* lipase B) were purchased from Novozymes (Bagsvaerd, Denmark). All chemicals and reagents were analytical grade and obtained from major suppliers (Sigma-Aldrich, Merck, and Fluka). Solvents and soluble palm oils (RPO, CPO, and PFAD) were dehydrated with a 3Å molecular sieve (Fluka) before use.

### 3.2.2 Cross-linked protein coated microcrystal lipase (CL-PCMC-lipase)

CL-PCMC-lipase was prepared based on the method reported by Shah et al. (2008) [6] with modification on synthesis conditions and variation in core matrices and solvents. The *T. lanuginosus* lipase (500 mL) was clarified by centrifugation (12,000 xg, 10 min) and pre-concentrated (10x, to 50 mL) using ultrafiltration on a Minimate tangential flow filtration system using a Minimate TFF capsule with 10 kDa MWCO membrane (Pall, Easthills, NY). For the optimization of CL-PCMC-lipase synthesis, 1.5 volume of a saturated solution of the matrix components (potassium sulphate ($K_2SO_4$), glycine, MOPS and glucose) were added to 1 volume of the concentrated lipase solution (1000 mg/mL). This combined mixture was then added drop-wise to a stirring vial (150 rpm) containing 20 volume of acetone. The precipitate was obtained by centrifugation at 2,200 x g for 5 min and then washed thrice with 0.5 volume of acetone. The enzyme precipitate (i.e. PCMCs)

was resuspended in 2.5 volume of acetone, followed by addition of 0.05 volume of glutaraldehyde (25% v/v in water). The mixture was incubated at 4$^{o}$C with stirring at 300 rpm for 1 h and then washed thrice with acetone. The air dried precipitate was used as the biocatalyst in this study. The protocol for preparation of the optimal glycine-based CL-PCMC-lipase is shown in Figure 3.1. Protein content was determined at the PCMC stage with Bio-Rad protein assay reagent based on Bradford's method using bovine serum albumin as the standard.

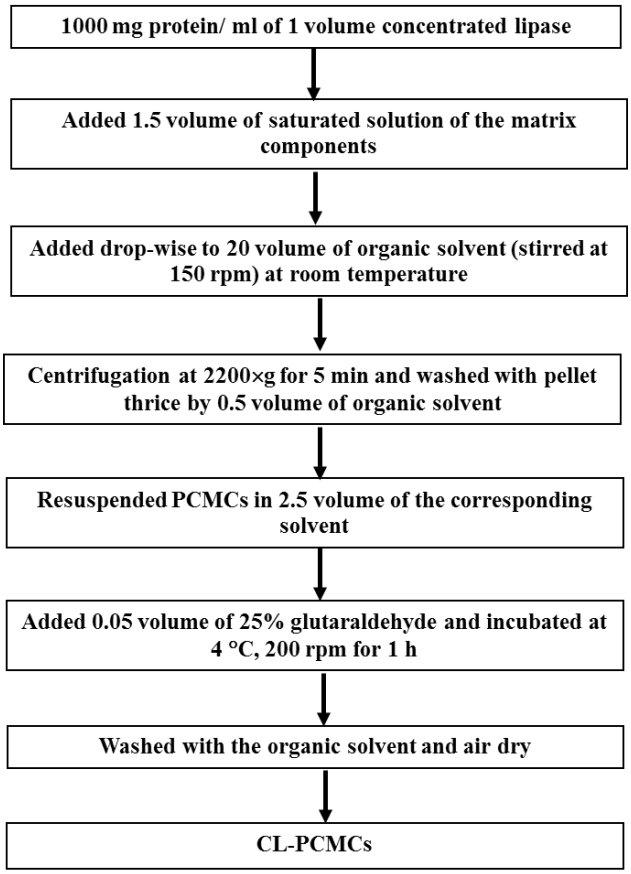


**Figure 3.1** Preparation of CL-PCMC-lipase from commercial lipase.

### 3.2.3 Lipase catalyzed esterification

For the optimized reaction, 250 mg of FFA or PFAD and ethanol was reacted in a molar ratio of 4:1 ([EtOH]/[FFA]) in the presence of tert-butanol at a 1:1 molar ratio ([t-BuOH]/[FFA]). The optimal CLPCMC-lipase prepared with glycine and acetone was added at 20% (w/w based on FFA or PFAD) in the reaction and incubated at 50 °C on a vertical rotator. Samples were withdrawn at time intervals. The samples (2 µl) were diluted with hexane (10 µl) and mixed with lauric acid methyl ester (5 µl) as an internal standard. The amount of esters formed was then determined by gas chromatography according to Raita et al. The FAEE production yield (%) is the amount of fatty acid ethyl esters converted from available fatty acid equivalence (as FFAs and glycerides) on a molar basis. For reusability study, the biocatalyst was recovered by centrifugation, washed with 1 ml of the organic solvent twice (if indicated), and air-dried before use in the next batch. The reactions were done in triplicate and standard deviations were reported for all experimental results.

### 3.2.4 Lipase activity assay

Lipase hydrolysis activity was assayed based on the hydrolysis of *p*-nitrophenyl palmitate [Gilham and Lehner, 2005] [117]. The standard reaction (200 µl) contained 20 mM sodium phosphate buffer, pH 8, 1 mM of *p*-nitrophenyl palmitate and an appropriate dilution of the enzyme or immobilized enzyme. The reaction was incubated at 45°C for 30 min and then terminated by addition of 100 µl of 0.2 M $Na_2CO_3$. The formation of *p*-nitrophenolate was determined by measuring the absorbance at 405 nm. One unit of the enzyme activity was defined as the amount of enzyme catalyzing the release of 1 µmole *p*-nitrophenolate/min under the standard experimental conditions used.

### 3.2.5 Gas chromatography analysis

Biodiesel yields were analyzed by gas chromatography on a Shimadzu 2010, equipped with a flame ionization detector (Shimadzu, Kyoto, Japan) and a polyethylene glycol capillary column (Carbowax 20 M, 30 m x 0.32 mm, Agilent Technologies, Santa Clara, CA). The column oven temperature was at 200$^{o}$C with injector and detector temperatures at 250 and 260$^{o}$C, respectively. Helium was used as the carrier gas at a constant pressure of 64.1 kPa with linear velocity at 25 cm/s. The amount of fatty acid ethyl ester (FAEE) was determined based on standard curves using the corresponding

esters. The product yield (%) is the amount of FAEE converted from the available fatty acid equivalence (as FFAs and glycerides) on a molar basis.

### 3.2.6 Physical analysis techniques

#### 3.2.6.1 Scanning electron microscope (SEM)

The structure and morphology of the CL-PCMC-lipase was analyzed by a scanning electron microscope (SEM) using a JSM-6301F Scanning Electron Microscope (JEOL, Tokyo, Japan). The samples were dried and coated with gold for analysis. An electron beam energy of 5 kV was used for analysis.

#### 3.2.6.2 X-ray diffraction (XRD)

X-ray diffraction (XRD) data were collected at room temperature on a Rigaku TTRAX III X-ray diffractometer using Cu Kα radiation (λ = 1.5418 Å) (Rigaku, Tokyo, Japan). The sample was scanned in the 2θ value of 10-45$^{o}$ at a rate of 2$^{o}$/min.

### 3.2.7 Reaction kinetic analysis

The kinetic study on the esterification and transesterification reactions was demonstrated by the Ping Pong Bi Bi mechanism [118, 119]. In this study, the expression of Ping Pong Bi Bi mechanism with alcohol inhibition was depicted as follows in Cleland's notation as illustrated in Figure 3.2. The reaction rate on enzymatic process of esterification from palmitic acid with methanol was fitted to Equation 3.1.

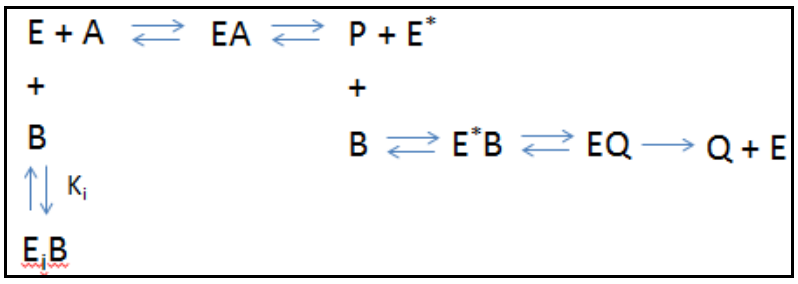


**Figure 3.2** Ping Pong Bi Bi mechanism model with alcohol inhibition [119].

Details of this mechanism are described as follows. Firstly, the free fatty acid (A) binds to the free enzyme (E) and forms a noncovalent enzyme-acid complex (EA), which releases the first product, water (P) and E* modified enzyme. Next, the second substrate as alcohol (B) reacts with E* to give the complex E*B, follow to the complex EQ, and then provide the final products as ester (Q) and free enzyme (E). At the same time, B also forms to the complex [$E_iB$] by binding with free enzyme [E].

$$v = \frac{v_m[A][B]}{K_{mB}[A] + K_{mA}[B]\left(1 + \frac{[B]}{K_i}\right) + [A][B]} \quad (3.1)$$

Where $V$ is the reaction rate; $V_m$ is the maximum reaction rate; $K_{mA}$ and $K_{mB}$ are the Michaelis constant for palmitic acid and methanol, respectively; $K_i$ is the inhibition constant for methanol; and [A] and [B] are the concentrations of palmitic acid and methanol.

Proper manipulation of Eq. (3.2) leads to

$$\frac{1}{v} = \left(1 + \frac{[B]}{K_i}\right)\frac{K_{mA}}{v_m}\frac{1}{[A]} + \frac{1}{v_m}\left(\frac{K_{mB}}{[B]} + 1\right) \quad (3.2)$$

This is an equation of a straight line, which is called the primary plot:

$$\text{Slope}_1 = \frac{K_{mA}}{v_m K_i}[B] + \frac{K_{mA}}{v_m} \quad (3.3)$$

$$\text{Intercept}_1 = \frac{K_{mB}}{v_m}\frac{1}{[B]} + \frac{1}{v_m} \quad (3.4)$$

$\text{Intercept}_1$ can be plotted against 1/[B] to get the following:

$$\text{Intercept}_2 = \frac{1}{v_m} \quad (3.5)$$

$$\text{Slope}_2 = \frac{K_{mB}}{v_m} \quad (3.6)$$

The kinetic study was performed using under the optimized parameter for esterification in the presence of 15% enzyme loading at 50 °C with shaking 40 rpm using varying concentrations of methanol (2.0 to 8.96 mol/L) at different concentration of palmitic acid (0.74 to 2.24 mol/L).

## 3.3 Results and discussions

### 3.3.1 Optimization of CL-PCMC synthesis

In the first stage, the synthesis conditions for the CL-PCMC-lipase biocatalyst were optimized based on their reactivity towards the production of ethyl palmitate from palmitic acid used as a model reactant. *Thermomyces* (*Humicola*) *lanuginosus* lipase was used for its high reactivity on biodiesel production from palm oil feedstock [4]. The 3x pre-concentrated enzyme in solution showed high hydrolysis activity towards *p*-nitrophenyl palmitate with the specific activity of 6.93 $x10^{-3}$ IU/mg equivalent to the volumetric activity of 0.27 IU/ml, and was used for preparation of CL-PCMC conjugate. Two key factors for CL-PCMC synthesis were investigated, namely (i) the matrix components, which were selected to represent inorganic and organic matrices ($K_2SO_4$, glucose, 3-morpholinepropanesulfonic acid (MOPS), and glycine), and (ii) the precipitating organic solvents (ethanol, *tert*-butanol, and acetone). The reactions were optimized based on ethanolysis due to the *T. lanuginosus* lipase's higher stability in ethanol in comparison to methanol, which showed inactivation effect to the lipase from *T. lanuginosus* [4]. The use of ethanol as nucleophile is also advantageous for the development of green biodiesel, where all the reactants are from renewable biological sources.

The highest reactivity of the lipase biocatalyst was obtained using glycine as the matrix component with acetone as the precipitating organic solvent (Table 3.1). The glycine-based CL-PCMCs formed fine crystalline particles and had the protein content of 155 µg/mg of CL-PCMCs. This optimized combination led to FAEE synthesis at 85.0% yield after 6 h in the presence of *tert*-butanol under the optimal synthesis conditions while the control reaction with no biocatalyst led to no detectable products under the same conditions. Lower FAEE yields were obtained with glycine-based CL-PCMCs using ethanol and *tert*-butanol as the precipitating solvents or CL-PCMCs prepared using other matrix components. $K_2SO_4$ is the most commonly used matrix for synthesis of several forms of biocatalyst *e.g.* PCMCs and CL-PCMCs of various enzymes [6]. However, lower FAEE yields were obtained for the $K_2SO_4$-based CL-PCMC-lipase prepared using different solvents (range: 69.9-74.7%).

Glucose and MOPS were found to be unsuitable matrix for CL-PCMC-lipase preparation due to their lower catalytic efficiency per weight basis and the low amount of biocatalysts obtained after precipitation. Different core matrices including salts, sugars, amino acids, and inorganic/organic buffer substances with protic or aprotic solvents were previously used for optimization of PCMC synthesis from various enzymes [120, 121]. Amino acids, including L-glutamine and DL-valine were previously used for preparation of PCMCs for biocatalysts and for vaccine formulation [122]. The effects of core matrix components in microcrystalline biocatalyst preparation are generally dependent on manipulation of the micro-environment of the enzyme and the physical properties and morphology of the carrier, which are the result of the intrinsic properties of the carrier, coupled with the choice of precipitating solvent.

Matrix components prepared from the solid-state buffer substances as the core matrix were reported to give biocatalysts with improved reactivity and stability as demonstrated for PCMCs of subtilisin prepared with organic or inorganic buffer carriers (either as a mixture of the $Na^+$ salt and the zwitterionic form or as a one-component solid state buffer *e.g.* Na-AMPSO, $NaCO_3$, and $NaHCO_3$) in comparison to that prepared using the non-buffered inert $K_2SO_4$ [120]. In PCMCs, the intimate association of the enzyme and solid-state buffer compound would allow efficient equilibration of the ionization state of the biocatalyst.

So far as is known, this study is the first report on the use of zwitterionic glycine as the core matrix for biocatalyst synthesis applied in water immiscible organic solvent systems. Addition of external glycine/$Na^+$ salt was previously used for ionization state control for biocatalysis in organic media [123]. However, due to the use of only the zwitterioinic form of glycine and its $pK_a$ in aqueous system, the mechanism of improved catalytic performance of the optimized glycine-based CL-PCMC lipase may not be clearly understood based on the hypothesis on ionization state control of the enzyme by solid-state buffer. The finding thus suggested further detailed study on the roles of core matrix component and its interaction with the enzyme in CL-PCMC preparation. Acetone was used as the precipitating solvent for the preparation of various forms of lipase biocatalyst *e.g.* PCMCs, CL-PCMCs, and acetone rinsed enzyme preparation (AREP). The preference of acetone as the precipitating solvent to a series of alcohols with different polarities was different to that reported for preparation of different biocatalyst designs *e.g. n*-propanol for PCMCs of subtilisin [62] and 1,2-dimethoxyethane for enzymes prepared and rinsed with

organic solvent (EPROS) of lipases [124]. The result thus suggests the prerequisite to screen the best combination of the core matrix and precipitating solvent for obtaining a high performance biocatalyst for a specific process in organic media.

**Table 3.1** Optimization of CL-PCMC synthesis. CL-PCMC-lipases were prepared with different matrix components in different organic solvents.

| **matrix component** | **FAEE yield (%)** mol/mol | | |
|---|---|---|---|
| | acetone | ethanol | *tert*-butanol |
| $K_2SO_4$ | 69.9 ± 3.3 | 74.7 ± 3.3 | 73.6 ± 2.2 |
| Glucose | 67.2 ± 2.5 | 49.8 ± 1.2 | NA |
| MOPS | 45.9 ± 1.5 | NA | NA |
| Glycine | 85.0 ± 2.3 | 17.5 ± 0.2 | 27.0 ± 0.7 |

The reactions contained 250 mg of palmitic acid, 4:1 [EtOH]/[FFA] molar ratio in the presence of 1:1 [*t*-BuOH]/[FFA] molar ratio with 20% (w/w) CL-PCMC-lipase. The reactions were incubated at 50$^{o}$C for 6 h.

NA: not analyzed due to no or low amounts of CL-PCMCs obtained

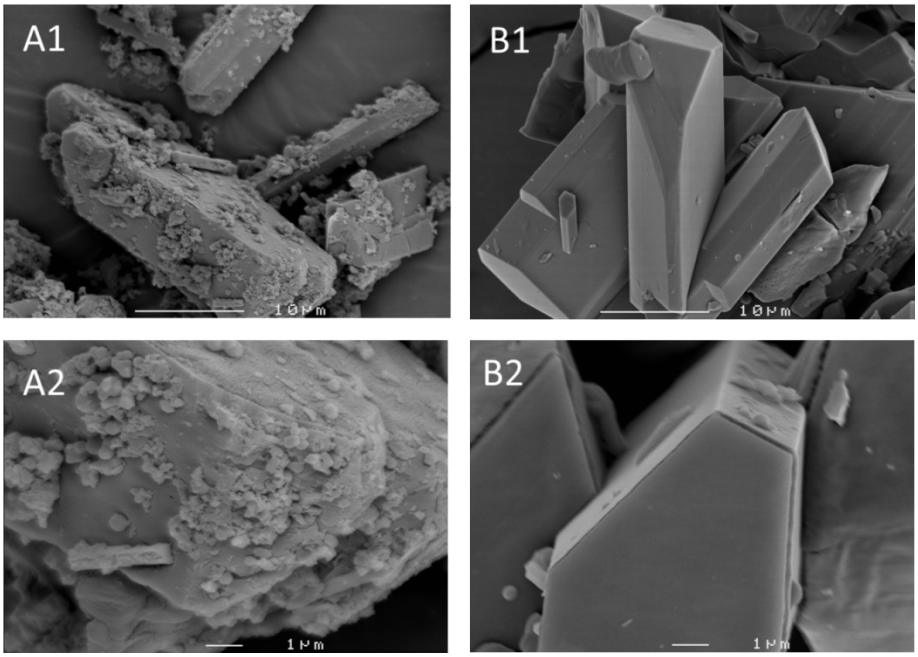


**Figure 3.3** SEM analysis of CL-PCMC-lipase. (A) CL-PCMC-lipase prepared from glycine in acetone; (B) glycine crystals control, no lipase added.

The physical characteristics of CL-PCMC-lipase were examined using SEM (Figure 3.3). The biocatalysts had a variable size distribution in the micron size range of 10-20 μm. The overall surface of CL-PCMC-lipase was different to the glycine salt control, which showed a homogeneous monoclinic crystal structure. The biocatalysts were formed as protein aggregates on the glycine crystal surface, which is suggestive of enzyme molecule aggregation on the amino acid crystals. XRD analysis showed that the glycine-based CL-PCMCs were highly crystalline (Figure 3.4). Signature peaks of α-glycine were identified (JCPDS number 32-1702), reflecting crystal structure of the core matrix. The formation of enzyme layer on the salt crystals in CL-PCMCs results in higher exposed reactive surface area of the biocatalyst (based on the same enzyme content on weight basis) and lower mass transfer limitation to the lipase active site in comparison to CLEAs or CLECs [56, 116]. However, characterization of the biocatalyst surface area using BET surface area analysis was limited by the low melting temperature of glycine.

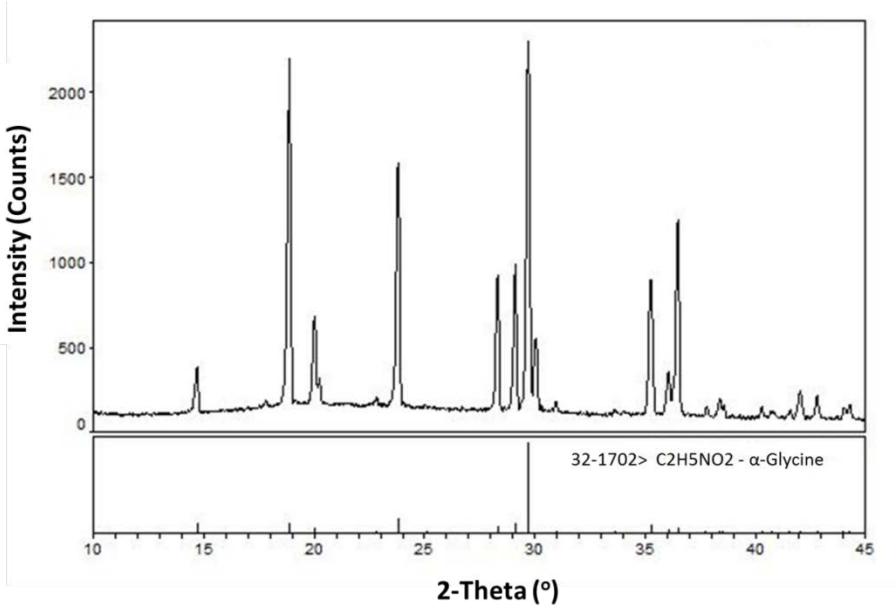


**Figure 3.4** X-ray diffraction analysis of glycine-based CL-PCMC-lipase. Reference XRD pattern of α-glycine (JCPDS number 32-1702) is shown in the lower panel.

### 3.3.2 Effects of reaction parameters using ethanol on esterification

Initial trials on optimization of the operational conditions for biodiesel synthesis were focused on the effects of nucleophile and co-solvent ratios to free fatty acids based on the esterification of palmitic acid (Figure 3.5). Systematic optimization of ethanol and *tert*-butanol contents was investigated for all combinations. The reaction temperature in this study was set at 50$^{o}$C to allow complete solubilization of FFAs. In most cases, increasing the ethanol:FFAs ratio led to increased FAEE yields at all *tert*-butanol ratios. The optimal [EtOH]/[FFA] ratio of 4:1 is comparable to previous reports on biocatalytic transesterification of different vegetable oils [4, 64]. The presence of *tert*-butanol at a 1:1 molar ratio ([*t*-BuOH]/[FFA]) in the reaction led to an increase in FAEE yield from 78.1% in the solvent-free system to 84.4% at the optimal [EtOH]/[FFA] ratio. However, further increase of *tert*-butanol led to lower FAEE yields when compared at the same ethanol content. A sharp increase in FAEE yield was observed during the early phase of incubation, leading to >95% of the maximized conversion yields after 6 h incubation at 50$^{o}$C (Figure 3.6). CL-PCMC-lipase loading at 20% (w/w) based on FFA was found to be optimal (data not shown).

The biocatalyst loading in this study was in the same range (4-50%) as those previously reported using different forms of immobilized lipase on transesterification [65, 125, 126]. The optimal reaction conditions for CL-PCMC-lipase catalyzed reactions were thus at 4:1 [EtOH]/[FFA] in the presence of 1:1 [*t*-BuOH]/[FFA] as the co-solvent with CL-PCMC-lipase loading at 20% (w/w) and incubation at 50$^{o}$C for 6 h. The optimal conditions were used for subsequent experiments in this study.

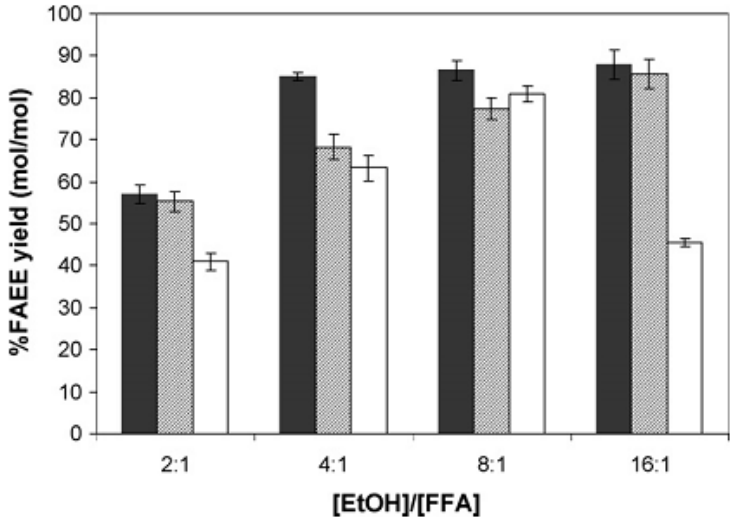


**Figure 3.5** Effects of nucleophile and co-solvent concentrations on FAEE synthesis. The reactions contained 250 mg of palmitic acid as the substrate with 20% (w/w) CL-PCMC-lipase with varying ethanol and tert-butanol ratios to FFA. The reactions were incubated at 50$^{o}$C for 6 h. [*t*-BuOH]/[FFA] = 1:1 (black); 2:1 (shaded); and 4:1 (white).

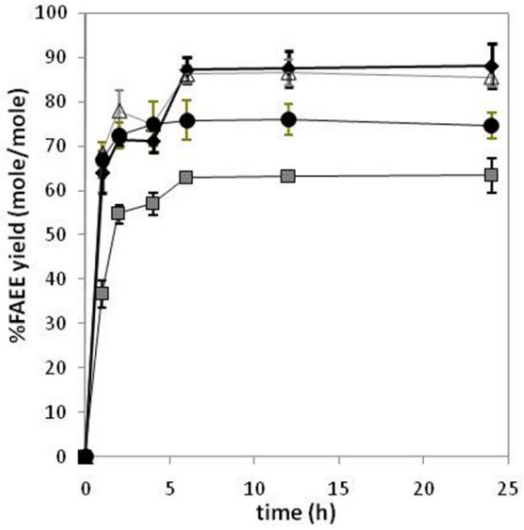


**Figure 3.6** Reactivity of CL-PCMC-lipase on biodiesel synthesis from FFAs and PFAD. The reactions contained 250 mg of FFAs or PFAD, 4:1 [EtOH]/[FFA] molar ratio in the presence of 1:1 [*t*-BuOH]/[FFA] molar ratio with 20% (w/w) CL-PCMC-lipase. The reactions were incubated at 50$^{o}$C. Substrate: Palmitic acid (diamond), Oleic acid (square), Linoleic (triangle), and PFAD (circle).

The observed trend of increasing FAEE yield with increasing nucleophile concentration is the opposite to that previously reported for the transesterification of refined palm olein using PCMC-lipase [4]. This can be explained by different sensitivity of the biocatalysts to the nucleophile (ethanol) in the reaction, involving deactivation effect on the biocatalyst contact of the lipases with the immiscible polar organic phase [125]. Although a decrease in FAEE yield might be observed at a very high nucleophile and co-solvent ratio, the results shown here suggest an improved ethanol tolerance of CL-PCMC for esterification reactions compared to the conventional PCMCs. The enhancing effect of *tert*-butanol in the reaction medium has been reported for different forms of immobilized lipases *e.g.* PCMCs and whole-cell biocatalysts for transesterification of triacylglyceride based feedstocks [74, 81, 82].

The optimal equimolar ratio of *tert*-butanol and FFA is similar to the previous studies using PCMC-lipase [4] and lower than that for the commercial immobilized lipases and whole-cell biocatalysts in which 1-1.5:1 volume ratio of the co-solvent to oil feedstock was used [74]. Addition of *tert*-butanol to the reaction mixture was shown to increase catalytic activity and operational stability of lipases, resulting in increasing conversion

yields [127]. The activation and stabilization of lipases in esterification could be due to the effects of *tert*-butanol on lipase stabilization from the nucleophile inactivation by linear low molecular weight alcohols [82]. To our knowledge, although the catalysis and stability enhancing effects of *tert*-butanol have been shown for lipase-catalyzed transesterification and whole-cell catalyzed esterification of FFAs [48], this study is the first to demonstrate these effects on precipitation-based immobilized lipases in esterification of FFAs on the biodiesel synthesis reaction.

The potential of CL-PCMC-lipase on the esterification of FFAs and PFAD was compared with other types of immobilized lipases under the same enzyme loading (20%) and reaction conditions (Figure 3.7). CL-PCMC-lipase led to high FAEE yields from palimitic acid (87.1%) and PFAD (81.4%). Ethyl palmitate shared the highest fraction in the esterification product from PFAD in comparison with ethyl oleate and ethyl linoleate, reflecting the FFA composition in PFAD and the biocatalyst reactivity towards different FFAs. The FAEE yields from CL-PCMC-lipase were higher than those using PCMC-lipase prepared on glycine in acetone (75.7% and 67.5% for palmitic and PFAD, respectively), suggesting the additional effects of crosslinking in higher performance of CL-PCMCs and also the widely used immobilized *Candida antarctica* lipase (Novozyme®435) (79.5% and 63.3% for palmitic acid and PFAD, respectively).

In contrast, Lipolase 100T led to low FAEE yields from both substrates. PCMC-lipase prepared on $K_2SO_4$ showed the optimal operational temperature at 45$^{o}$C [4] suggesting partial inactivation of PCMC-lipase at 50$^{o}$C. The higher product yields from CL-PCMCs could thus be partially due to the improved thermostability of the biocatalyst in comparison with PCMCs by the effect of enzyme molecule crosslinking [6]. Addition of molecular sieve for continuous removal of water from the reaction led to no significant increase in FAEE yields from FFAs and PFAD, which was in contrast to some previous reports in which simultaneous dehydration resulted in significant improved product yields [48, 128]. This would suggest the less sensitivity of CL-PCMC-lipase on water activity in esterification of FFAs.

In overall, the reactivity of the glycine-based CL-PCMC-lipase in this study was comparable to that of various forms of immobilized lipases for esterification of feedstock containing high FFA content *e.g.* soybean oil deodorizer distillate [129] and used palm oil [130], although this cannot be directly compared due to the sensitivity of biocatalysts to the feedstock (*i.e.* type of substrates and contaminants) and reaction conditions. The high conversion yields thus demonstrated the potential of the glycine-based CL-PCMC-lipase as an economical heterogeneous biocatalyst for biodiesel production by the esterification of FFAs in feedstocks.

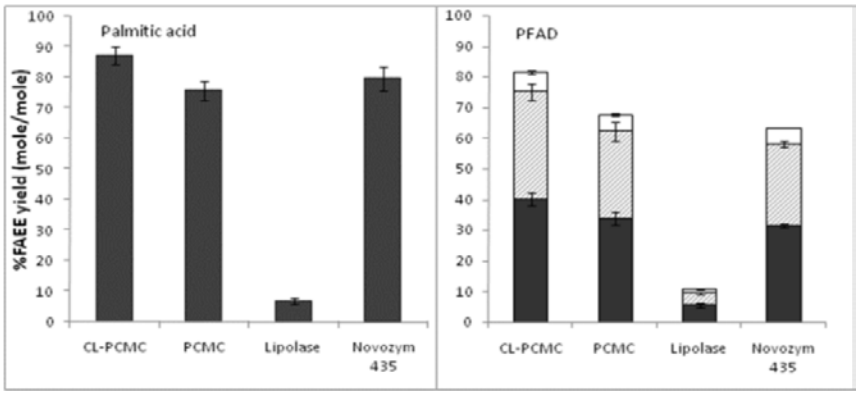


**Figure 3.7** Comparison of FAEE synthesis using different immobilized lipases. The reactions contained 250 mg of palmitic acid or PFAD, 4:1 [EtOH]/[FFA] molar ratio in the presence of 1:1 [*t*-BuOH]/[FFA] molar ratio with 20% (w/w) CL-PCMC-lipase. The reactions were incubated at 50$^{o}$C for 6 h. CL-PCMC: CL-PCMC-lipase prepared from glycine in acetone; PCMC: PCMC-lipase prepared from glycine in acetone. FAEE products: ethyl palmitate (black); ethyl oleate (shaded); and ethyl linoleate (white).

### 3.3.3 Reusability of CL-PCMC-lipase

The reusability of CL-PCMC-lipase was studied by analyzing the conversion efficiency after consecutive batch cycles under the optimal reaction conditions (Figure 3.8). CL-PCMC-lipase showed high stability in the esterification of palmitic acid with no siginificant alteration in FAEE yield for at least 8 consecutive batch processes with the average product yields of 84.8 ± 5.0%. Treatment by organic solvents with different polarities (ethanol, *n*-propanol and *tert*-butanol) led to no improvement on FAEE yields, leading to 62.7, 55.3, and 73.0% FAEE yield in batch 8. The effect of *tert*-butanol on the biocatalyst stability was different to the $K_2SO_4$-based PCMC-lipase, in which *tert*-butanol treatment led to improved stability of the biocatalyst in consecutive batches of palm olein

transesterification [4]. This could be due to the nucleophilic deactivation effect of short chain alcohols, particularly ethanol and propanol on the biocatalyst stability. The result thus suggested the potential of recycling CL-PCMC-lipase in further consecutive batch process development with no additional organic solvent treatment.

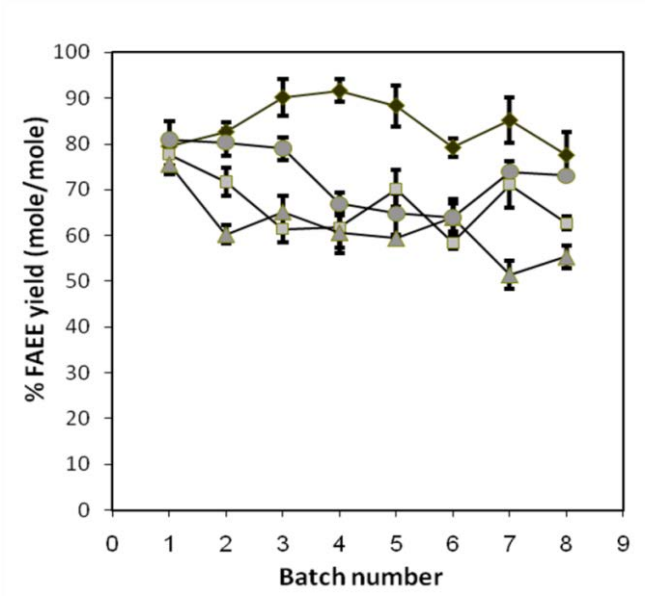


**Figure 3.8** Stability of CL-PCMC-lipase in consecutive batch reactions. CL-PCMC-lipase was reused in consecutive batch reactions with or without organic solvent treatment. The reactions contained 250 mg of palmitic acid, 4:1 [EtOH]/[FFA] molar ratio, in the presence of 1:1 [*t*-BuOH]/[FFA] molar ratio with 20% (w/w) CL-PCMC-lipase. The reactions were incubated at 50$^{o}$C for 6 h. CL-PCMC-lipase was treated by washing with 1 ml of the solvent twice before being used in the consecutive batch. No solvent wash treatment (diamond: ♦); ethanol (square: ■ ); *n*-propanol (triangle: ▲), and *tert*-butanol (circle: ●)

### 3.3.4 Kinetic analysis of CL-PCMC-lipase catalyzed reaction

Reaction kinetics on the esterification of palmitic acid in the presence of a CL-PCMC-lipase/Gly was studied using methanol as a nucleophile. The kinetics of the reaction was studied at varying agitation speed, enzyme loading, reaction temperature, and molar ratio of methanol to palmitic acid. The kinetic parameters were analyzed based on the Ping-Pong bi-bi mechanism with methanol inhibition [119, 131].

### 3.3.4.1 Effect of agitation speed

Firstly, the effect of mass transfer on the reaction kinetics was studied by varying the agitation speed from 40-200 rpm while the other reaction parameters were fixed at the 4:1 [MeOH]/[FFA] molar ratio and 10 (%w/w) of enzyme dosage at 50°C for 6 h. A sharp rising in FAME yield was observed during the first 50 min, which accounted for 47.7-74.8% of the maximal product yield at the end of the reaction. The result showed that the agitation speed at 40 rpm gave the maximum FAME yield of 88.5% ± 5.9 from the reactions containing 10 (%w/w) of CL-PCMC-Lipase/Gly loading at 50°C for 6 h with the [MeOH]/[FFA] ratio of 4:1 (Figure 3.9). Increasing the agitation speed resulted in a slightly lower in the FAME yield. The decrease in FAME yield at the high agitation rates could be due to shearing and inactivation of the biocatalyst caused from foam formation under vigorous mixing condition as reported by Halim and Kamaruddin (2008) [131] which could also be observed in our study.

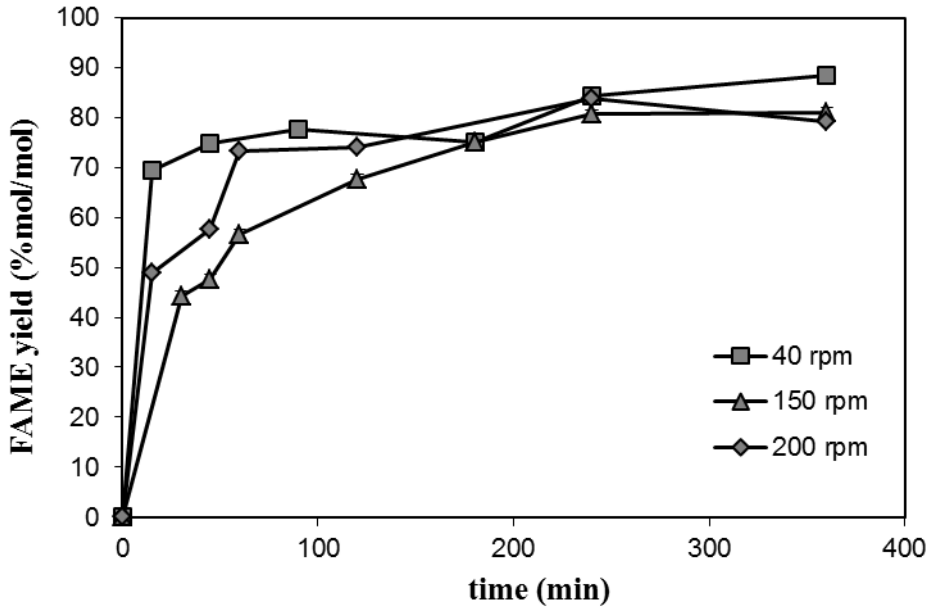


**Figure 3.9** Effects of agitation on the esterification of palmitic acid. The reaction contained 4:1 [MeOH]/[FFA] in the presence of 1:1 mol/mol [*t*-BuOH]/[FFA] with 10% of CL-PCMC-lipase/Gly dosage incubated at 50$^{o}$C.

### 3.3.4.2 Effect of enzyme loading

Kinetics of the esterification reaction at various enzyme loadings between 5% and 20% were studied based on feedstock weight. The concentrated *T. lanuginosus* lipase solution showed a catalytic activity at 2.1 IU/mL (specific activity at 3.7 x $10^{-3}$ IU/mg protein) on hydrolysis of *p*-nitrophenyl palmitate. The result showed that a sharp increase in FAME yield was found in the early phase of the reaction, particularly at the high enzyme loadings where more than 85% of the final product yield was achieved in the first 10 min. The final product yield was in the range of 81.4-97.2% at the end of the 60 min reaction. The results indicate that the enzyme loading of 15% was optimal for the esterification reaction as a sufficient amount of active sites of the biocatalyst fitted to the substrate loading. The highest FAME yield was achieved with 15 % enzyme loading after incubation at 50 °C for 1 h in the reaction containing [MeOH]/[FFA] ratio at 4:1 (mol/mol) with *tert*-butanol as a co-solvent with an agitation speed at 40 rpm (Figure 3.10A). However, the initial rate of reaction was found to increase linearly related to the catalyst loading up to 20% loading ($R^2$ = 0.98) (Figure 3.10B). The optimal enzyme loading basically depended on the catalytic rate and stability of the enzyme under the operating conditions in relation to the amount of available substrates and mass transfer in the reaction. The excessive amount of enzyme was also found to result in higher solid content and viscosity in the reaction which caused difficulties in mixing and mass transfer in the reaction [131].

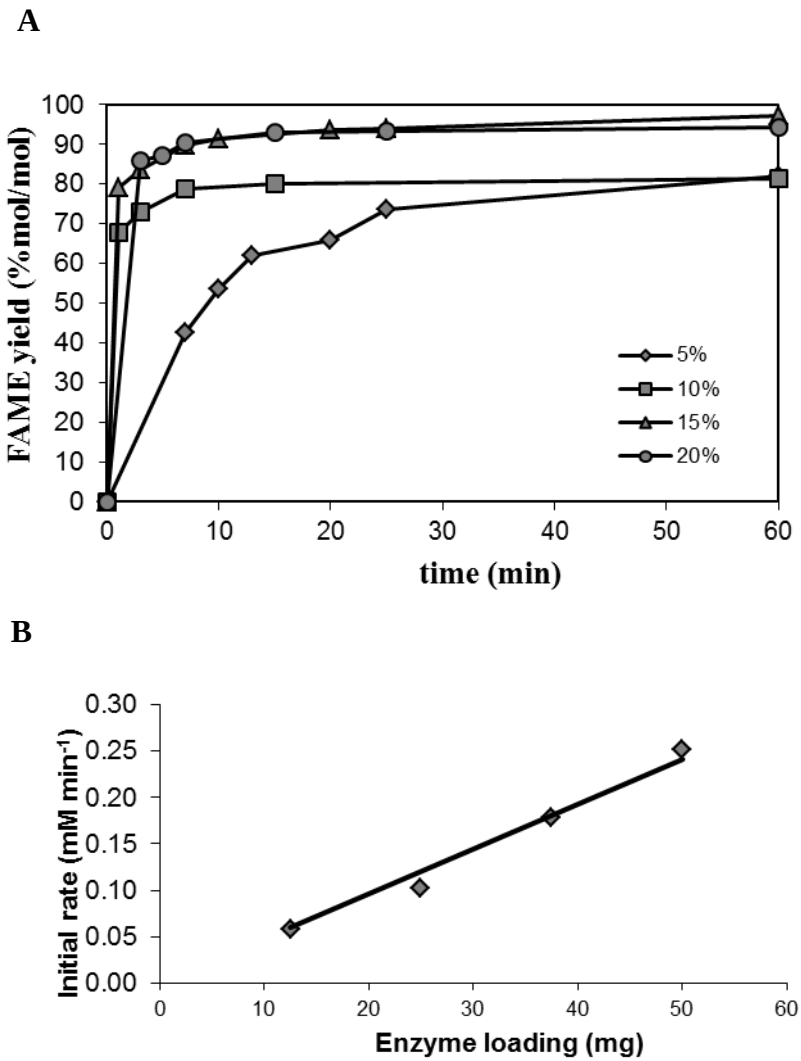


**Figure 3.10** Effects of enzyme loading on the esterification of palmitic acid. The reaction contained 4:1 [MeOH]/[FFA] in the presence of 1:1 mol/mol [*t*-BuOH]/[FFA] with varying loading of CL-PCMC-lipase/Gly. The reactions were incubated at 50$^{o}$C. A: Time-curve of the reaction; (B) Initial velocity.

### 3.3.4.3 Effect of reaction temperature

Temperature is one of the key parameters in enzymatic reactions and has an influence on the enzyme catalytic activity and the solubility of the reactants. The effect of reaction temperature on the esterification of palmitic acid was examined in the range of 30-60°C. It was observed that increasing temperature from 30-50°C led to a respective increase in the FAME yield particularly at the early phase of the reaction. The highest FAME yield of 96.6% was obtained at 50$^{o}$C after incubation for 1 h for the reaction containing 4:1 [MeOH]/[FFA] with 15% enzyme loading at the agitation rate of 40 rpm (Figure 3.11A). The Arrhenius plot showed a linear relationship ($R^2$ = 0.96). The activation energy (*E*a) was calculated to be 12.6 kcal/mol (Figure 3.11B), which are typical in biocatalytic reaction determining by reaction-limited regime. The *E*a obtained with the CL-PCMC-lipase/Gly catalyzed reaction was in the same range compared to the previous works where the *E*a of 1.6-17.4 kcal/mol was reported for the pseudo second order reaction for transesterification of corn oil with methanol using immobilized *C. antarctica* lipase and esterification of levulinic acid with n-butanol using Novozyme 435 [119, 132].

Liu et al (2009) reported that the pseudo first-order reaction for the transesterification of waste cooking oil with methanol using the combined lipases (Novozyme 435 and Lipozyme TL IM) showed the activation energy of 12.4 kcal/mol [133]. In another study, Liu et al (2010) reported the pseudo third-order reaction on transesterification of waste baked duck oil using the same combined lipases and methanol with the activation energy of 7.6 kcal/mol [134]. Maury et al (2005) described that esterification of lauric acid with 1-octanol catalyzed by the free lipase from *Burkohlderia cepacia* and the encapsulated lipase in silica aerogel presented the *E*a of 2.5 and 3.4 kcal/mol, respectively [135].

**A**

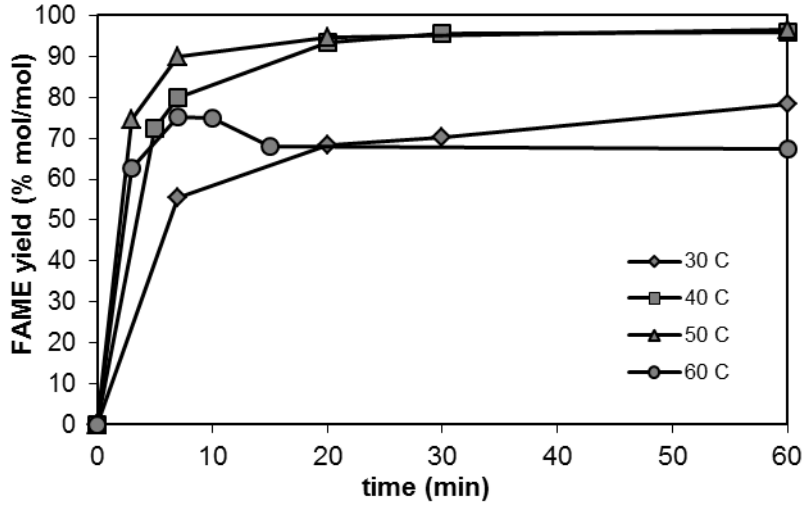


**B**

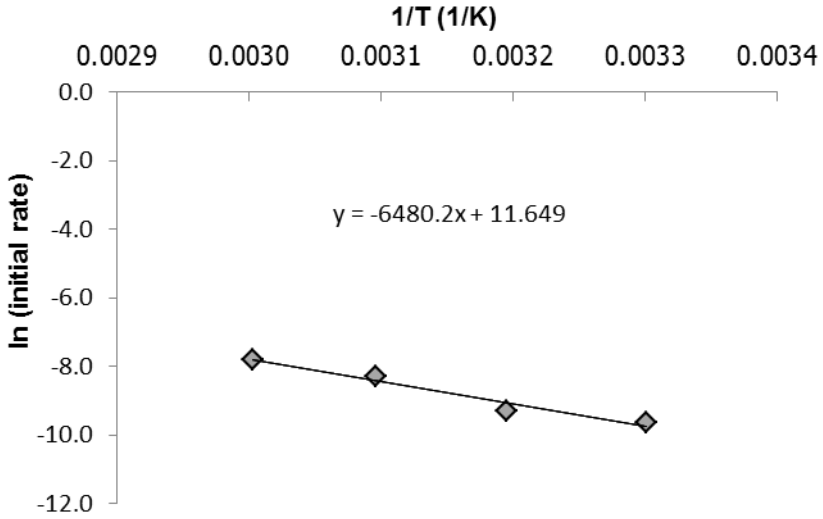


**Figure 3.11** Effects of reaction temperature on esterification of palmitic acid. The reaction contained 4:1 [MeOH]/[FFA] in the presence of 1:1 mol/mol [*t*-BuOH]/[FFA] with 15% (w/w) CL-PCMC-lipase/Gly. The reactions were incubated at varying temperatures, A: time-curve of the reaction, and B: Initial velocity.

### 3.3.4.4 Effect of molar ratio of methanol to fatty acid

Next, the effect on methanol content in the reaction was studied by varying the [MeOH]/[PA] ratio with a constant mole of palmitic acid (Figure 3.12). Increasing the [MeOH]/[PA] ratio from 2:1-4:1 led to a respective increase in the FAME yield. The ratio of [MeOH]/[PA] at 4:1 (mol/mol) resulted in confirmation of the maximum FAME yield from the reaction containing 15 % w/w CL-PCMC-lipase/Gly after incubation at 50°C for 1 h. Further increase in [MeOH]/[FFA] ratio to 6:1 and 8:1 led to the lower FAME yield of 94.1% and 86.5%, respectively. The decrease in product yield at high methanol content was due to the inhibitory effect of the immiscible methanol on the catalytic site of the enzyme, leading to enzyme deactivation [136]. Shimada et al. [137] reported that the immobilized *C. antarctic* lipase was inactivated in a reaction mixture containing greater than 1.5 molar equivalents of methanol to waste edible oil. The effects of methanol on enzyme inactivation could be alleviated by the use of *tert*-butanol as a co-solvent in the reaction, which can improve the enzyme performance in esterification and transesterification by increase solubility of methanol in the mixture and preventing formation of the immiscible methanol phase in the reaction [131].

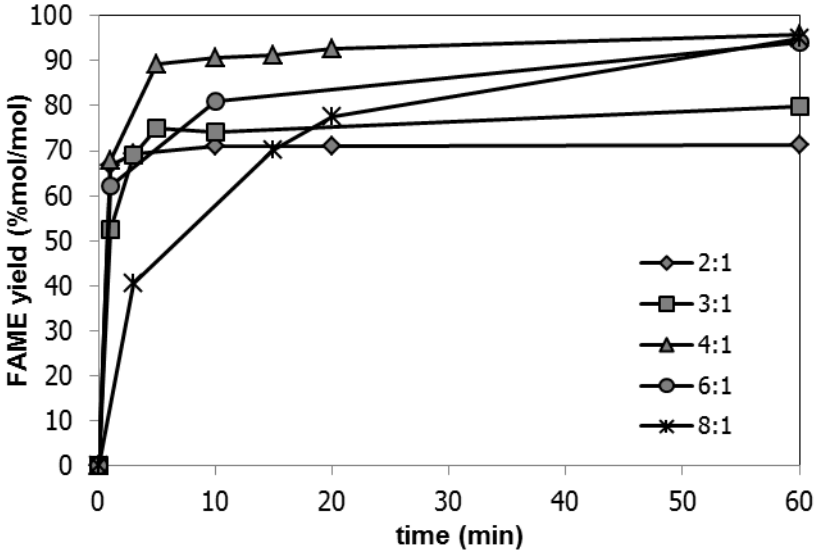


**Figure 3.12** Effects of mole ratio on esterification of palmitic acid. The reaction contained 1:1 mol/mol [*t*-BuOH]/[FFA] with 15% (w/w) CL-PCMC-lipase/Gly after incubation at 50°C.

### 3.3.4.5 Determination of kinetic parameters

The influence of substrate concentrations at different levels of palmitic acid (0.74, 1, 1.49, and 2.235 M) and methanol (2, 2.98, 5.98, and 8.96 M) was plotted to determine the kinetic constants according to Eq. 3.1 (Figure 3.13). This esterification reaction was performed using the optimized reaction conditions i.e. 15 % (w/w) CL-PCMC-lipase/Gly and incubated at 50°C for 6 h with agitation at 40 rpm. The kinetic equation on enzymatic esterification of palmitic acid was fitted based on Ping-Pong bi-bi mechanism model with methanol inhibition. The kinetic parameters obtained are shown in Table 3.2. It was found that the maximal rate of reaction ($V_m$) achieved 0.7 M/min, while the Michaelis constant for palmitic acid ($K_{mA}$) and methanol ($K_{mB}$) was 3669.4 and 1076.3 M, respectively. The inhibition constant of methanol of methanol ($K_i$) was 31.2 M. The turnover number ($k_{cat}$) of CL-PCMC-lipase/Gly was 388.0 $min^{-1}$ that represented the number of palmitic acid molecule converted to FAME per unit of time based on the total enzyme catalytic site.

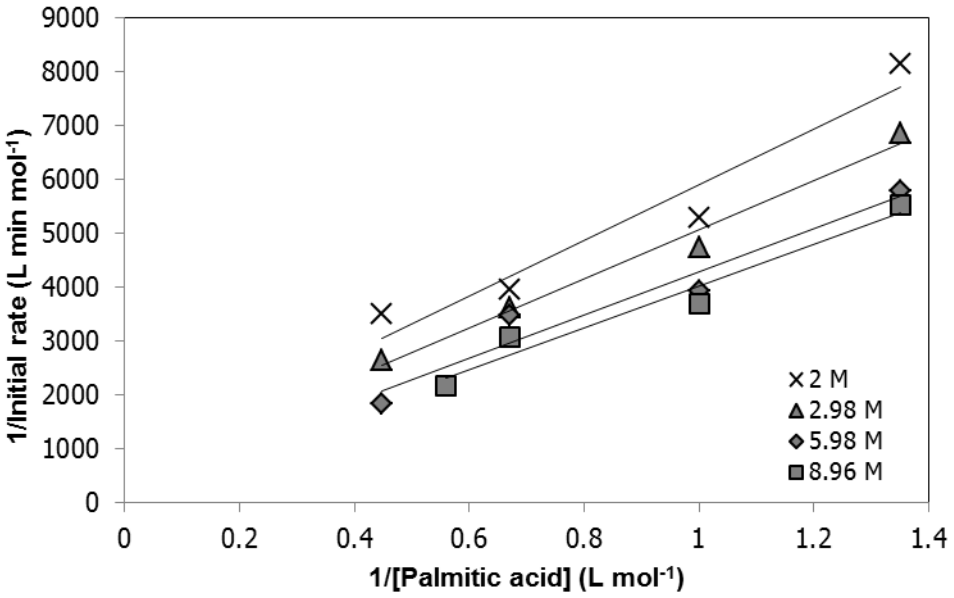


**Figure 3.13** Linewear-Burk plot on reciprocal rate of palmitic acid and methanol concentrations.

**Table 3.2** Kinetic parameters on esterification of palmitic acid with methanol using CL-PCMC-lipase/Gly.

| **Kinetic constant** | |
|---|---|
| $V_m$ (M/min) | **0.7** |
| $K_{mA}$ (M) | **3669.4** |
| $K_{mB}$ (M) | **1076.3** |
| $K_i$ (M) | **31.2** |
| $k_{cat}$ ($min^{-1}$) | **388** |

## 3.4 Conclusion

Biocatalytic synthesis by CL-PCMC-lipase is considered a promising approach for biodiesel production from feedstocks containing high FFA contents. The optimized process led to high product yields comparable to those previously reported for acid-catalyzed [138], thermocatalytic [113] and whole-cell biocatalytic methods [82]; however, with its key advantages over the existing methods, including mild operating conditions and low catalyst preparation costs. The use of glycine as the core matrix for precipitation-based immobilized enzyme was reported, suggesting the potential on using glycine as the core matrix component for preparation of high performance CL-PCMCs for catalysis in non-aqueous systems. The reaction kinetics was studied in the Ping-Pong Bi-Bi mechanism model with n-butanol substrate inhibition. The biocatalytic process developed in this study thus provides a promising approach for production of biodiesel from inexpensive feedstocks with high FFA contents. Further development of the CL-PCMC-lipase based processes would lead to an improvement on the process economics of the biodiesel industry.

.

# CHAPTER 4

# BIOCATALYTIC METHANOLYSIS ACTIVITIES OF CROSS-LINKED PROTEIN-COAT MICROCRYSTALLINE LIPASE TOWARD ESTERIFICATION/TRANSESTERIFICATION OF RELEVANT PALM PRODUCTS*


## Abstract

Biocatalysis by immobilized lipase is an efficient alternative process for the conversion of crude vegetable oil with high free fatty acid content to biodiesel, which is the limit of the conventional alkaline-catalyzed reaction. This studyexamines influences of solid-state organic and inorganic buffer core matrices with different $pK_a$ on catalytic performance of cross-linked protein coated microcrystalline biocatalysts prepared from *Thermomyces lanuginosus* lipase (CL-PCMC-lipase) toward esterification of palmitic acid (PA), transesterification of refined palm oil (RPO), and co-ester/transesterification of crude palm oil (CPO) to fatty acid methyl ester (FAME). Glycine, CAPSO, and TAPS were shown to be potent core matrices for these reactions. The optimal reaction contained 4:1 [methanol]/[fatty acid] molar equivalence ratio with 20% (w/w) CL-PCMC-lipase on glycine in the presence of *tert*-butanol as a co-solvent. Deactivation effect of glycerol on the biocatalyst reactive surface was shown by FTIR, which could be alleviated by increasing co-solvent content. The maximal FAME yields from PA, RPO, and CPO reached 97.6, 94.9, and 95.5%, respectively on a molar basis under the optimum conditions after incubation at 50$^{o}$C for 6 h. The biocatalyst retained >80% activity after recycling in five consecutive batches. The work demonstrates the potential of CL-PCMC-lipase on one-step conversion of inexpensive crude fatty acid-rich feedstock to biodiesel.


* This chapter has been submitted for publication.

## 4.1 Backgrounds

Biodiesel is an alternative engine fuel to petroleum diesel. It is produced as fatty acid alkyl esters, which are most often obtained by the refinement of vegetable oils. It possesses several technical advantages over petroleum diesel such as higher cetane rating, less sulfur and carbon monoxide emission, lower unburned hydrocarbons and particulate matter, and can be blended with conventional petrol diesel up to 20% with no engine modification [12]. In Thailand and many tropical countries, palm oil represents the most important and cost-competitive feedstock for the biodiesel industry. Typically, refinery crude palm oil (CPO) is used for biodiesel production by alkaline-catalyzed transesterification of triacylglycerol (TAG). However, this reaction is sensitive to free fatty acids (FFAs) present in the feedstock. This leads to undesirable saponification resulting in low product yields and complication in subsequent separation steps [110].

The conversion of vegetable oil with high FFA is usually performed by a two-step acid/alkaline-catalyzed process where the FFA is first esterified in the acid-catalyzed reaction using strong mineral acids, mainly $H_2SO_4$, before the subsequent transesterification of TAG by the alkaline-catalyzed reaction. However, this sequential process has key drawbacks on difficulty in recovery of homogeneous catalysts, waste treatment, and corrosion of the equipment by the strong acid. These drawbacks increase the overall cost of the process. Several alternative methods have been reported for production of biodiesel from feedstocks containing high FFA, including acid-catalysis using solid acid catalysts [111], and non-catalytic or catalytic near- and super-critical methanol processes [112, 113]. However, these approaches still suffer from high cost and stability of the catalysts as well as intensive energy requirement.

Biocatalytic biodiesel synthesis using microbial lipases has received increasing interest as an efficient and eco-friendly approach for the conversion of glyceride feedstocks containing high FFA to biodiesel under mild operational conditions with simple downstream purification steps [115]. Several immobilization methods have been studied for the preparation of heterogeneous biocatalysts for biodiesel production involving carrier-based methods, such as adsorption [139], covalent immobilization [140], and entrapment [141], as well as carrier-free methods, such as cross-linked enzyme aggregates (CLEAs) [56, 142] and cross-linked enzyme crystals (CLECs) [116, 143]. Protein-coated microcrystals (PCMCs) are alternative biocatalysts with the potential for catalysis in non-

aqueous systems [4, 62]. Cross-linked PCMCs (CL-PCMCs), a more recent development, are superior microcrystalline biocatalysts [64, 65]. CL-PCMCs are fabricated as enzyme layered on the surface of a micron-sized inner core matrix, which can be prepared by rapid dehydration and co-precipitation of enzyme and the matrix component in an organic solvent, followed by crosslinking of enzyme molecules [6]. CL-PCMCs possess several advantages over existing carrier-based and carrier-free immobilization methods, including a low mass transfer limitation and increased stability, leading to its high catalytic performance. The use of CL-PCMC lipase on synthesis of biodiesel has been recently reported for esterification of palm fatty acid distillate [5] and biodiesel production from waste cooking oil [144]. CL-PCMCs are thus an attractive design for cost efficient preparation of biocatalysts with improved performance in organic media systems.

The inner core matrix has a great influence on the performance of CL-PCMC biocatalysts. It has been shown that various organic and inorganic solid-state buffer compounds enhance the catalysis and stability of PCMCs made from serine proteases and lipase as compared with the use of conventional inert inorganic salts [120]. In this study, different biological and inorganic buffer core matrices were explored for the fabrication of CL-PCMC lipase. The performances of the biocatalysts produced were tested for esterification and transesterification of palm oil feedstocks with varying FFA content to FAME. The optimized biocatalysts showed high performance on co-ester/transesterification of CPO in consecutive batch process. The work provides an attractive approach for development of highly active biocatalyst for production of biodiesel from inexpensive crude vegetable oils with high FFA content for establishment of a sustainable biofuel industry.

## 4.2 Materials and methods

### 4.2.1 Materials

Refined edible grade palm oil (palm olein; RPO containing ≥ 99% TAG) was obtained from a local market. Crude palm oil (CPO) was obtained from the Pathum Vegetable Oil Co. Ltd. (Pathumthani, Thailand). The CPO sample contained ≥ 95% (w/w) TAG, 4% (w/w) free fatty acid (mainly palmitic acid), and 0.2 % (w/w) of moisture and impurities e.g. trace metals (iron, copper, and nickel) phosphorus and sulphur. Palmitic acid (PA) and other free fatty acids (oleic and linoleic acids) and fatty acid ester standards were obtained from Sigma-Aldrich. Liquid *Thermomyces lanuginosus* lipase (Lipolase 100T) and Novozymes® 435 (immobilized *Candida antarctica* lipase B) were purchased from Novozymes (Bagsvaerd, Denmark). Amano Lipase PS from *Burkholderia cepacia* was obtained from Sigma-Aldrich. Organic buffers MES (2-morpholinoethanesulfonic acid), MOPS (3-morpholinepropanesulfonic acid), TAPS ([(2-hydroxy-1,1-bis(hydroxymethyl)ethyl)amino]-1-propanesulfonic acid), HEPES (4-(2-hydroxyethyl)piperazine-1-ethanesulfonic acid), CAPSO (3-(cyclohexylamino)-2-hydroxy-1-propanesulfonic acid) and amino acids (Glutamic acid and Glycine) were obtained from Sigma-Aldrich. All solvents were dehydrated with a 3Å molecular sieve (Fluka, Buchs, Switzerland) before use.

### 4.2.2 Crosslinked protein coated microcrystal lipase (CL-PCMC-lipase)

CL-PCMC-lipase was prepared based on the method reported by Shah et al. (2008) [6] with modification of the synthesis conditions and variation in core matrices and solvents. The *T. lanuginosus* lipase (500 mL) was clarified by centrifugation (12,000 xg, 10 min) and pre-concentrated (10x, to 50 mL) using ultrafiltration on a Minimate tangential flow filtration system using a Minimate TFF capsule with 10 kDa MWCO membrane (Pall, Easthills, NY). For optimization of CL-PCMC-lipase synthesis, 1.5 volume of a saturated solution of the matrix components as organic (Glutamic acid, MES, MOPS, TAPS, HEPES, CAPSO, and Glycine) or inorganic ($NaH_2PO_4$, $Na_2HPO_4$, $NaHCO_3$, and $Na_2CO_3$) buffer components either as an acid (H) or a sodium salt (Na) form (Table 4.1) were added to 1 volume of the concentrated lipase solution (1000 mg/mL). This combined mixture was then added drop-wise to a stirring vial (150 rpm) containing 20 volume of acetone. The precipitate was obtained by centrifugation at 2,200 x g for 5 min and then washed thrice with 0.5 volume of acetone. The enzyme precipitate (i.e. PCMCs)

was resuspended in 2.5 volume of acetone, followed by the addition of 0.05 volume of glutaraldehyde (25% v/v in water). The mixture was incubated at 4$^{o}$C with stirring at 300 rpm for 1 h and then washed thrice with acetone. The air dried precipitate was used as the biocatalyst in this study. Protein content was determined at the PCMC stage with Bio-Rad protein assay reagent based on Bradford's method using bovine serum albumin as the standard.

**Table 4.1** Matrix components used for CL-PCMC-lipase preparation.

| Matrix components | pKa |
|---|---|
| Glycine/Glycine-Na | 2.35 and 9.6 |
| L-Glutamic acid/L-Glutamic acid Na | 4.3 |
| MES/MES-Na | 6.1 |
| MOPs/MOPs-Na | 7.2 |
| HEPES/HEPES-Na | 7.5 |
| TAPs/TAPs Na | 8.4 |
| CAPSO/CAPSO-Na | 9.6 |
| $NaHCO_3$ / $Na_2CO_3$ | 6.4 and 10.3 |
| $NaH_2PO_4$ / $Na_2HPO_4$ | 6.86 and 12.4 |

### 4.2.3 Lipase catalyzed esterification and transesterification

For the optimized reaction, 250 mg of PA (esterification)/ RPO (transesterification)/ or CPO (co-ester/ transesterification), and methanol was reacted in a molar ratio of 4:1 [MeOH]/[FFA] in the presence of 0.3:1 (v/v) *t*-BuOH to PA or 1:1 (v/v) *t*-BuOH to RPO or CPO. The CL-PCMC-lipase was added at 20% (w/w based on PA/RPO/or CPO) in the reaction and incubated at 50$^{o}$C for 6 h with mixing on a vertical rotator at 40 rpm. The amount of esters formed was determined by gas chromatography according to Raita et al. [4]. For reusability study, the biocatalyst was recovered by centrifugation, washed with 0.5 mL of *t*-BuOH, and air-dried before use in the next batch. The reactions were done in triplicate and standard deviations were reported for all experimental results.

### 4.2.4 Lipase activity assay

Lipase hydrolysis activity was assayed based on the hydrolysis of *p*-nitrophenyl palmitate [Gilham and Lehner, 2005] [117]. The standard reaction (200 µl) contained 20 mM sodium phosphate buffer, pH 8, 1 mM of *p*-nitrophenyl palmitate and an appropriate dilution of the enzyme or immobilized enzyme. The reaction was incubated at 45°C for 30 min and then terminated by addition of 100 µl of 0.2 M $Na_2CO_3$. The formation of *p*-nitrophenolate was determined by measuring the absorbance at 405 nm. One unit of the enzyme activity was defined as the amount of enzyme catalyzing the release of 1 µmole *p*-nitrophenolate/min under the standard experimental conditions used.

### 4.2.5 Gas chromatography analysis of FAME

Fatty acid methyl ester (FAME) yields were analyzed by gas chromatography on a Shimadzu 2010, equipped with a flame ionization detector (Shimadzu, Kyoto, Japan) and a polyethylene glycol capillary column (Carbowax 20 M, 30 m x 0.32 mm, Agilent Technologies, Santa Clara, CA). The column oven temperature was at 200$^{o}$C with injector and detector temperatures at 250 and 260$^{o}$C, respectively. Helium was used as the carrier gas at a constant pressure of 64.1 kPa with linear velocity at 25 cm/s. The amount of FAME was determined based on standard curves using the corresponding esters. The product yield (%) is the amount of FAME converted from available fatty acid equivalence (as FFAs and glycerides) on a molar basis.

### 4.2.6 Physical analysis techniques

#### 4.2.6.1 Scanning electron microscope (SEM)

The structure and morphology of the CL-PCMC-lipase was analyzed by a scanning electron microscope (SEM) using a JSM-6301F Scanning Electron Microscope (JEOL, Tokyo, Japan). The samples were dried and coated with gold for analysis. An electron beam energy of 5 kV was used for analysis.

#### 4.2.6.2 Fourier-Transformed Infrared Spectroscopy (FTIR)

The functional groups on CL-PCMCs were analyzed by Fourier-Transformed Infrared Spectroscopy (FTIR) (Perkin-Elmer System 2000, Waltham, MA) on the infrared spectra at 400-4000 $cm^{-1}$ wavenumber.

## 4.3 Results and discussions

### 4.3.1 Effects of core matrix on CL-PCMC-lipase

CL-PCMC is an immobilized enzyme design which is characterized as a crosslinked enzyme layer on a carrier core matrix. The design offers advantages on high catalytic reactivity and stability due to exposure of the enzyme's catalytic sites to the reaction and chemical crosslinking of enzyme molecules on the biocatalyst surface [6] in comparison to other designs of immobilized enzyme prepared by precipitation method e.g. CLEAs or CLECs [56, 116]. In CL-PCMCs, covalent crosslinking resulted in improvement of the biocatalyst performance in non-aqueous systems due to stronger enzyme conformation and structure. Effects of crosslinking on improvement of thermostability, pH stability, organic solvent tolerance, and operational stability of the microcrystalline biocatalysts on biodiesel production process has been demonstrated, for examples, CL-PCMC lipase prepared from *Geotrichum* sp. on $K_2SO_4$ matrix for biodiesel production from waste cooking oil [144] and CL-PCMC lipase prepared from *T. lanuginosus* lipase on esterification of palm fatty acid distillate [5] The results indicated the advantages of CL-PCMCs design for cost efficient preparation of biocatalysts with improved performance in organic media systems.

Core matrix components play an important role in CL-PCMC performance. Biocatalyst reactivity in CL-PCMC is primarily dependent on its physical properties, morphology, and size distribution of the solid matrix. These properties are determined by the intrinsic properties of the matrix coupled with the properties of precipitating solvent. Moreover, the core matrix exerts its influence on microcrystalline biocatalyst properties by controlling the ionization and hydration states of enzyme by its proximate interaction to the enzyme [120]. Salts, sugars, amino acids, and buffer substances were previously used as the core matrix with protic or aprotic precipitating solvents for synthesis of PCMCs from various enzymes [120, 121] of these core matrix substances. Among them, organic or inorganic solid-state buffers were superior for conferring improved reactivity and stability of biocatalyst [120].

In the first step, a series of organic and inorganic solid-state buffer components was studied for their effects on the reactivity of the biocatalysts towards the esterification of PA and the transesterification of RPO using methanol as a nucleophile. The pre-concentrated *T. lanuginosus* lipase solution showed a specific activity of 1.29 x $10^{-2}$ IU/mg (0.328

IU/mL) on hydrolysis of *p*-nitrophenyl palmitate and was used for preparation of CL-PCMC conjugate. A range of biological buffer compounds either as the acid (H) or Na salt (S) counterpart were selected for testing as potential solid-state buffers: L-Glutamic acid ($pK_a$ = 4.3), MES ($pK_a$ = 6.1), MOPS ($pK_a$ = 7.2), HEPES ($pK_a$ = 7.5), TAPS ($pK_a$ = 8.4), CAPSO ($pK_a$ = 9.6), and Glycine ($pK_a$ = 9.6). In addition, the following organic and inorganic buffer salts were used: $NaH_2PO_4$ ($pK_a$ = 6.86), $Na_2HPO_4$ ($pK_a$ = 12.4), $NaHCO_3$ ($pK_a$ = 6.4), and $Na_2CO_3$ ($pK_a$ = 10.3). The biocatalyst was obtained by rapid co-precipitation in acetone. CL-PCMCs prepared using Gly (H), CAPSO (H/Na), Glu (Na), MES (H/Na), TAPS (H), MOPS (H/Na), $Na_2HPO_4$, $NaHCO_3$, and $Na_2CO_3$ formed fine homogenous particles. For Gly(Na), Glu(H), TAPS(Na), HEPES(H/Na), and $NaH_2PO_4$ buffers, core matrix was not precipitated in acetone or formed a gel-like substance, which could not be easily separated for subsequent use.

The reactivity of the biocatalysts was initially studied under the initial standard conditions containing 4:1 [MeOH]/[FFA] with 20% CL-PCMCs in the presence 0.3:1 v/v of *t*-BuOH/PA or RPO. Varying FAME yields were obtained using CL-PCMCs prepared on different core matrices (Table 4.2). Among them, the acid form of Gly, CAPSO, and TAPS were good candidates for core matrix components for *T. lanuginosus* lipase, as high FAME yields were obtained from both esterification of PA (85.8-97.2%) and transesterification of RPO (79.1-85.0%). Some showed higher reactivity towards either transesterification (L-Glu(Na) and $Na_2HPO_4$) or esterification (MOPS(H)), while the rest showed low catalytic performance on both reactions and were not studied further.

**Table 4.2** Reactivity of CL-PCMC-lipase prepared on different core matrix components on esterification and transesterification.

| Matrix component | FAME yield (% mol/mol) | |
|---|---|---|
| | **Palmitic acid (Esterification)** | **Refined palm olein (Transesterification)** |
| **Glycine** | 97.20 ± 2.9 | 85.01 ± 3.6 |
| **Glycine-Na** | N.P | N.P |
| **CAPSO** | 92.47 ± 2.5 | 83.50 ± 1.1 |
| **CAPSO-Na** | N.A | 7.26 ± 0.5 |
| **L-Glutamic acid** | N.P | N.P |
| **L-Glutamic acid Na** | 77.42 ± 3.1 | 46.36 ± 3.5 |
| **MES** | 75.52 ± 2.2 | 70.85 ± 3.2 |
| **MES-Na** | N.A | 9.55 ± 0.4 |
| **TAPS** | 85.82 ± 6.0 | 79.13 ± 2.4 |
| **TAPs Na** | N.P | N.P |
| **HEPES** | N.P | N.P |
| **HEPES-Na** | N.P | N.P |
| **MOP**S | N.A | 40.43 ± 1.5 |
| **MOPS-Na** | N.A | 4.93 ± 0.6 |
| **$NaH_2PO_4$** | N.P | N.P |
| **$Na_2HPO_4$** | 71.02 ± 3.4 | 13.14 ± 3.7 |
| **$NaHCO_3$** | N.A | 2.01 ± 0.7 |
| **$Na_2CO_3$** | N.A | 13.71 ± 3.0 |

The reactions contained 250 mg of PA or RPO, 4:1 [MeOH]/[FFA] molar ratio in the presence of 0.3:1 v/v t-BuOH/FFA with 20% w/w CL-PCMCs and incubated at 50°C for 6 h.

N.A.: not analyzed due to no or low amount of CL-PCMCs obtained

N.P.: not precipitated or formed gel-like substances

Solid state buffer matrices comprise a zwitterion/Na-salt pair that is present as a solid or crystalline form in a non-aqueous system. Stabilization of enzymes by solid-state buffer matrix can be explained by the control of ionization state of the enzyme in an organic solvent, which is determined by the pH of the aqueous storage solution of the enzyme before CL-PCMC fabrication [120]. This "pH memory" effect allows the protein to retain its structural integrity following lyophilization or immobilization in organic solvents. In contrast to an aqueous medium where the ionization state of an enzyme is dependent to pH ($H^+$) of the solution alone, counterions (i.e. $Na^+$ and $Cl^-$) also play an important role in controlling ionizable groups on the enzyme in a non-aqueous system of low dielectric constant. The ionization state of an enzyme in organic media is described by the two equilibria model involving the exchange of $H^+$ and a cation with acidic groups of the protein ($a_{H+}/a_{Na+}$) and transfer of $H^+$ and an anion onto basic groups of the protein ($a_{H+}/a_{Cl-}$) [145, 146]. Any change of these charges on the biocatalyst directly affects catalytic activity, solubility, and stability of the enzyme.

The use of solid state buffers can result in stabilization of ionization state of an enzyme by its buffering property on controlling the acid-base condition by exchange of protons and counterions on the enzyme [146]. The efficiency on controlling the proton and counterion exchanges is affected by the $pK_a$ of the solid-state buffer compounds [120]. Solid-state acid–base buffers have been successfully utilized for the stabilization of enzymes in polar and nonpolar organic solvents [120, 147, 148]. Zacharis et al. (1997) reported that Lys and Lys-HCl solid buffers could control the $a_{H+}/a_{Cl-}$ parameter on immobilized subtilisin protease in hexane and toluene [146]. The control of ionization state of subtilisin CLECs by $a_{H+}/a_{Na+}$ exchange was also studied using various solid state buffers in supercritical ethane [149]. The amount of the acid and salt counterpart for solid-state buffer capacity has been shown to be theoretically irrelevant [123]. The demonstration that PCMCs of subtilisin prepared from only Na-AMPSO have comparable activity to PCMCs prepared with a mixture of Na-AMPSO and its zwitterionic form led to the proposal that single compound solid-state buffers are advantageous, as biocatalyst morphology can be controlled to be more homogeneous [120].

In CL-PCMCs, the intimate association of the enzyme and solid-state buffer compounds would allow the efficient equilibration of the ionization state of the microcrystalline biocatalysts. Glycine has $pK_{a1}$ and $pK_{a2}$ of 2.4 and 9.6, respectively. Its saturated aqueous solution is approximately pH 7 in which it exists as a zwitterion. This

pH is close to the optimal pH of *T. lanuginosus* lipase (pH 7-8) [150]. The use of zwitterionic glycine as the core matrix for biocatalyst synthesis for preparation of CL-PCMC-lipase biocatalyst was previously reported for esterification of PA and palm fatty acid distillate using ethanol as the nucleophile [5]. The superior catalytic performance of the optimized CL-PCMC-lipase/Gly could be related to the controlled thermodynamic activities, $a_{H+}/a_{Na+}$ (or pH-pNa) and $a_{H+}/a_{Cl-}$ (or pH+pCl) exchanges of ionizable groups on enzyme by the solid-state buffer and the structural morphology of the core matrix.

### 4.3.2 The physical characterization of CL-PCMCs by SEM analysis

The physical characteristics of the CL-PCMCs prepared from Gly, CAPSO, and TAPS were examined by SEM and compared with the protein-free salt matrices (Figure 4.1). Protein aggregates were clearly observed on the surface of carrier matrices of biocatalysts, which showed a different morphology to the protein-free control matrices. The CL-PCMC-lipase on glycine (CL-PCMC-lipase/Gly) showed a well-defined homogeneous monoclinic crystal structure with a variable size distribution in the micron size range of 5x10-20 μm. An overall similar structure and morphology was observed for CL-PCMC-lipase/TAPS. However, CL-PCMCs/CAPSO existed as aggregates with a less defined crystal structure, while its control protein-free carrier exhibited a micron-sized flake morphology. This could be related to the intrinsic property of CAPSO and its interaction to the precipitating solvent.

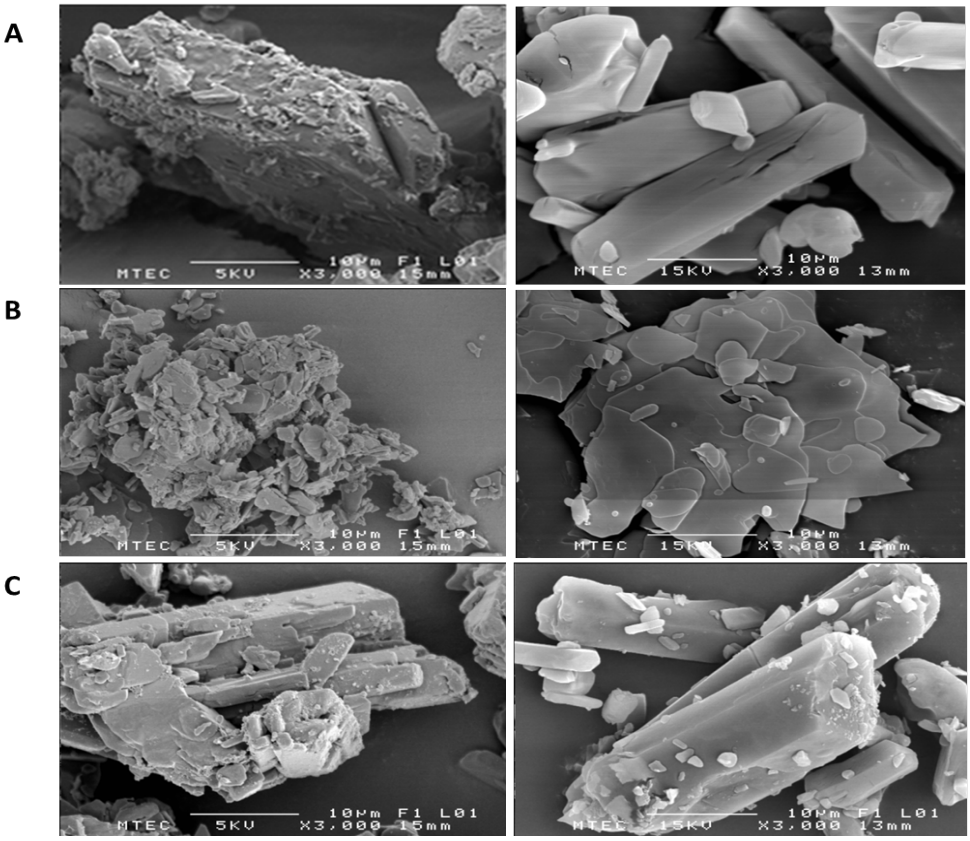


**Figure 4.1** SEM analysis of CL-PCMC-lipase prepared on different core matrices (left) and their crystals controls with no lipase added (right). (A) Glycine; (B) CAPSO; (C) TAPS.

### 4.3.3 CL-PCMCs performance on co-ester/transesterification

The catalytic performance of CL-PCMC-lipase containing the optimal protein content on the simultaneous esterification/transesterification of CPO was studied with catalyst loading varying from 1-40% under similar reaction conditions with 0.3:1 v/v of *t*-BuOH/CPO. CL-PCMCs prepared on different core matrices showed varying reactivity and resulted in different FAME yields (Figure 4.2). A rise in FAME yield was found with increasing enzyme dosage with the maximal product yield at 20% CL-PCMC dosage. Catalytic performance of the biocatalysts varied for CL-PCMCs prepared on different core matrices in the order of Gly > TAPS > CAPSO. The highest FAME yield of 85.3% was achieved using CL-PLMCs-lipase/Gly. Conversion of CPO to FAME showed a sharp increase in the first 6 h of the reaction, which plateaued afterwards (Figure 4.3). Glycine was thus selected as the optimal core matrix for both esterification and transesterification

and their simultaneous reaction. The glycine-based biocatalyst (CL-PCMC-lipase/Gly) had a protein content of 170.6 mg/g catalyst using the optimal initial protein content.

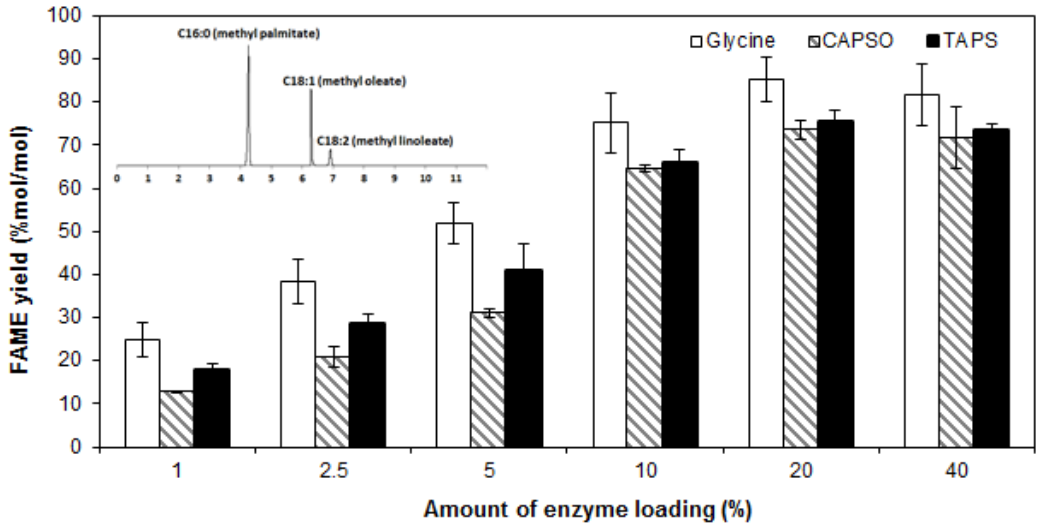


**Figure 4.2** Effects of CL-PCMC-lipase loading on co-ester/transesterification of CPO. The reactions contained 250 mg of CPO, 4:1 [MeOH]/[FFA] molar ratio, in the presence of 0.3:1 v/v *t*-BuOH/CPO and incubated at 50$^{o}$C for 6 h.

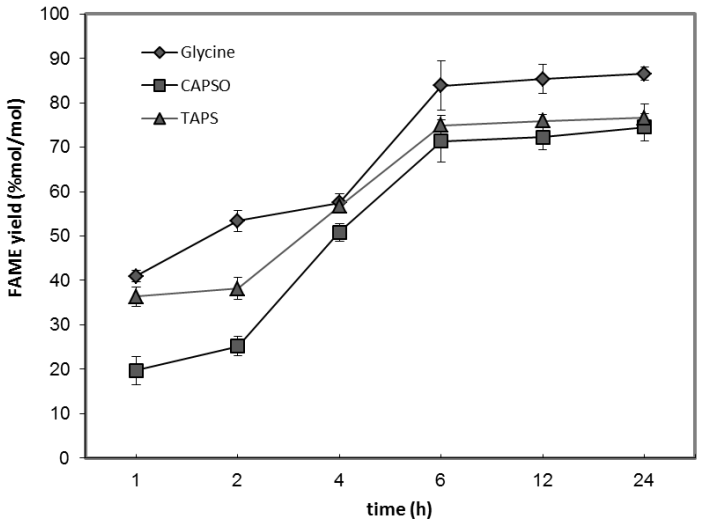


**Figure 4.3** Effects of reaction time using CL-PCMC-lipase prepared by different core matrixes on co-ester/transesterification of CPO. The reactions contained 250 mg of CPO, 4:1 [MeOH]/[FFA] molar ratio, in the presence of 0.3:1 v/v *t*-BuOH/CPO with 20% w/w CL-PCMCs and incubated at 50$^{o}$C.

The catalytic performance of CL-PCMC-lipase/Gly on esterification and transesterification of different palm oil feedstocks was compared with other types of immobilized lipases under the same enzyme loading (20%) and reaction conditions (Figure 4.4). All enzymes showed higher reactivity towards esterification than transesterification resulting in higher FAME yields in the order of PA > CPO > RPO, respectively. CL-PCMC-lipase/Gly catalysis gave the highest FAME yield from esterification of PA (97.4%), transesterification of RPO (82.2%) and co-ester/transesterification of CPO (85.1%). Lower FAME yields were obtained using commercial immobilized *C. antarctica* lipase (Novozyme® 435) and immobilized *B. cepacia* lipase (Amano lipase PS) under the experimental conditions.

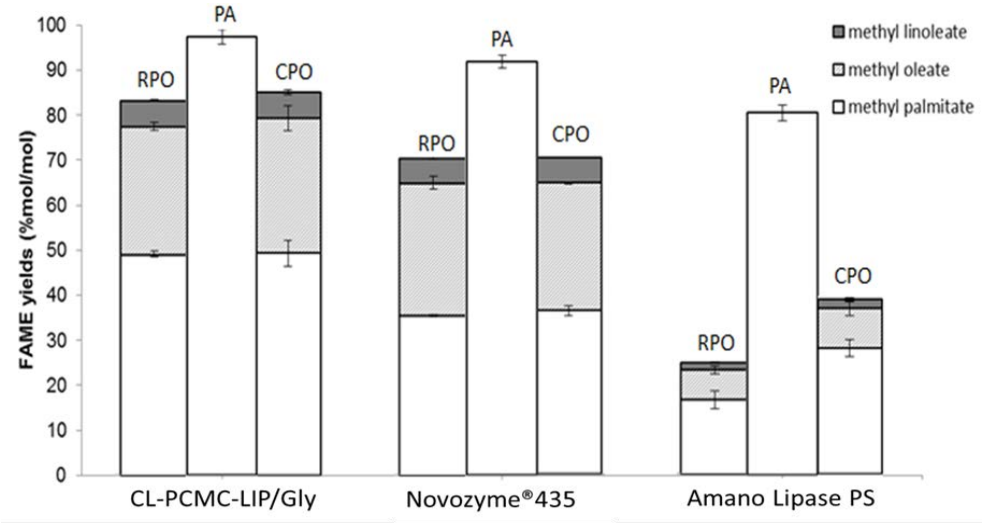


**Figure 4.4** Comparison of reactivity of CL-PCMC-lipase/Gly with commercial immobilized lipases on biodiesel production from different palm oil feedstocks. The reactions contained 250 mg of PA/RPO/CPO, 4:1 [MeOH]/[FFA] molar ratio, in the presence of 0.3:1 v/v of *t*-BuOH to PA, RPO, or CPO with 20% w/w enzyme and incubated at 50$^{o}$C for 6 h. N: Novozyme® 435; B: Amano lipase PS.

The biocatalytic reaction using CL-PCMC-lipase/Gly in this study achieved >95% FAME yield under the optimized conditions with high stability in consecutive batch recycling. *T. lanuginosus* lipase is a 1, 3-specific lipase and has been used for its high reactivity on biodiesel production from palm oil feedstock [4, 5]. This enzyme shows alkyl group translocation under specific conditions, which can give high biodiesel yield from various feedstocks [29]. The microcrystalline lipase showed high catalytic performance

and stability on both esterification and transesterification compared with immobilized lipases from different microbial origins, such as *Candida antarctica* and *Burkhoderia cepacia*, in various immobilization designs, such as covalent crossinking, adsorption, and entrapment from which 70-98% FAME yield was reported [3, 151]. The high yield achieved by methanolysis in this study was also higher than that obtained by ethanolysis using the same catalyst design recently reported, indicating stability of CL-PCMC-lipase/Gly in reactions containing methanol, which usually poisons lipase. The superior performance of CL-PCMC-lipase/Gly could be due to its higher reactive surface and low mass transfer limitation of the biocatalyst. The higher FAME yield from CL-PCMC catalyzed reactions could also be related to the improved stability of the biocatalyst by the effect of enzyme molecule crosslinking [5, 6].

The biocatalyst showed relatively higher efficiency on esterification than on transesterification under the same experimental conditions. The lower yield from transesterification could be due to its more complicated chemistry compared with esterification. Mechanistically, transesterification of TAG to FAME is a three-step reversible reaction. Each step starts with an attack on the carbonyl carbon atom of the triglyceride, diglyceride or monoglyceride by the methoxide ion ($CH_3O^-$) generated from methanol, while esterification is a one-step reaction where methoxide directly attacks the carbonyl group of free fatty acid [12]. In addition, the formation of glycerol as the by-product and the residual diglycerides and monoglycerides in the reaction can also lead to reduced product yield [42]. According to the cost of immobilized lipase in Table 4.3, the CL-PCMC-lipase/Gly showed higher catalytic performance compared to the commercial immobilized lipases (Novozyme® 435 and Amano lipase PS) as suggested by the higher FAME yield obtained. (Figure 4.4). Although the cost of CL-PCMC is relatively high due to the high cost of commercial soluble lipase and acetone, this is still cheaper than Novozymes® 435, which is the conventionally used immobilized biocatalyst in biocatalytic biodiesel synthesis study. The cost of CL-PCMC-lipase can be substantially reduced by in-house preparation of active microbial lipases by development of recombinant expression systems for lipase production in *Escherichia coli* or *Pichia pastoris* and optimization of fermentation media and conditions as well as by using industrial grade reagents. The cost of 990 THB/kg is targeted based on our preliminary estimation, as well as the reusability of acetone for CL-PCMC preparation. Recycling the enzyme more than 100 times is expected to achieve 10% enzyme cost of the total costs for biodiesel production.

**Table 4.3** Capital cost of immobilized enzyme preparation.

| Chemical reagents | Immobilized lipase cost (baht/kg enzyme) | | |
|---|---|---|---|
| | Novozyme® 435[1] | Amano lipase PS[2] | CL-PCMC-lipase/Gly (this study) |
| Liquid lipaseTL | - | - | 23,076.9 |
| Glycine | - | - | 50.0 |
| Acetone | - | - | 3769.2 |
| Glutaraldehyde | - | - | 9.2 |
| Total | 90,000 | 146,900 | 26,905.3 |

[1,2] Commercial immobilized enzymes supplied from Sigma-Aldrich.

Next, the effect of the co-solvent on product yields from esterification and transesterification of palm oil feedstocks was studied. Increases in *t*-BuOH to 1:1 volume ratio to the palm oil substrates led to a marked increase in FAME yield from the transesterification of RPO to 95.4%, while there was no significant difference on esterification production from PA (Table 4.4). The result indicated the positive effects of *t*-BuOH on catalytic efficiency of CL-PCMC-lipase/Gly for the transesterification reaction. This increase in transesterification efficiency led to a substantial rise of the overall FAME yield from the co-ester/transesterification of CPO to 96.0%. The result suggested partial inactivation of the biocatalyst by glycerol, a co-product from transesterification reaction. *t*-BuOH has been used for alleviating the inhibitory effects of glycerol and enzyme inactivation by methanol in biocatalytic biodiesel synthesis [18]. It is non-reactive in enzymatic methanolysis due to the sterically hindered butyl group. In order to achieve high FAME yields from transesterification, higher *t*-BuOH was required than for esterification. This was probably due to the solubilizing properties of *t*-BuOH which alleviate blockages of the biocatalyst active sites by glycerol formed as a by-product in transesterification, and reduced enzyme inactivation from the presence of immiscible methanol in the system [84, 131]. Further system design for co-solvent recovery is needed for improving economic feasibility of the overall process.

**Table 4.4** Effects of *t*-BuOH on FAME yield. The reactions contained 250 mg of PA/RPO/CPO and 4:1 [MeOH]/[FFA] molar ratio in the presence of different t-BuOH to substrate volume ratios with 20% w/w CL-PCMCs and incubated at 50 °C for 6 h.

| **Substrate** | **FAME yield (% mol/mol)** | |
|---|---|---|
| | **0.3:1 (v/v) *t*-BuOH/substrate** | **1:1 (v/v) *t*-BuOH/substrate** |
| **PA** | 98.5 ± 2.5 | 90 ± 0.8 |
| **RPO** | 80.8 ± 3.6 | 95.4 ± 2.7 |
| **CPO** | 85.8 ± 4.6 | 96.0 ± 3.1 |

Adsorption of glycerol on CL-PCMCs was demonstrated by FT-IR. (Figure 4.5) The esterification reaction using PA as the substrate was spiked with 5.2% glycerol to simulate the formation of glycerol in the transesterification reaction. The reference glycerol standard showed the signature peaks of the O-H stretching at 3371 $cm^{-1}$, C-H stretching from 2939-2885 $cm^{-1}$, C-O-H bending from 1456-1416 $cm^{-1}$, C-O stretching at 1110 $cm^{-1}$ as primary alcohol, and $H_2O$ bending at 1645 $cm^{-1}$, which are similar to those reported by Hidawati and Sakinah (2011) [152]. The CL-PCMC-lipase reaction product showed signature protein peaks at 2917-2849 $cm^{-1}$ for C-H, 1443-1411 $cm^{-1}$ for C-O-H bending, 1618 $cm^{-1}$ for O=C stretching and 1513 $cm^{-1}$ for N-H bending. The FTIR spectra of the CL-PCMC reaction spiked with glycerol showed the signature peaks of the main functional groups of both glycerol and CL-PCMC-lipase. This finding suggested that glycerol can be absorbed onto the CL-PCMC surface, leading to inactivation of the biocatalyst.

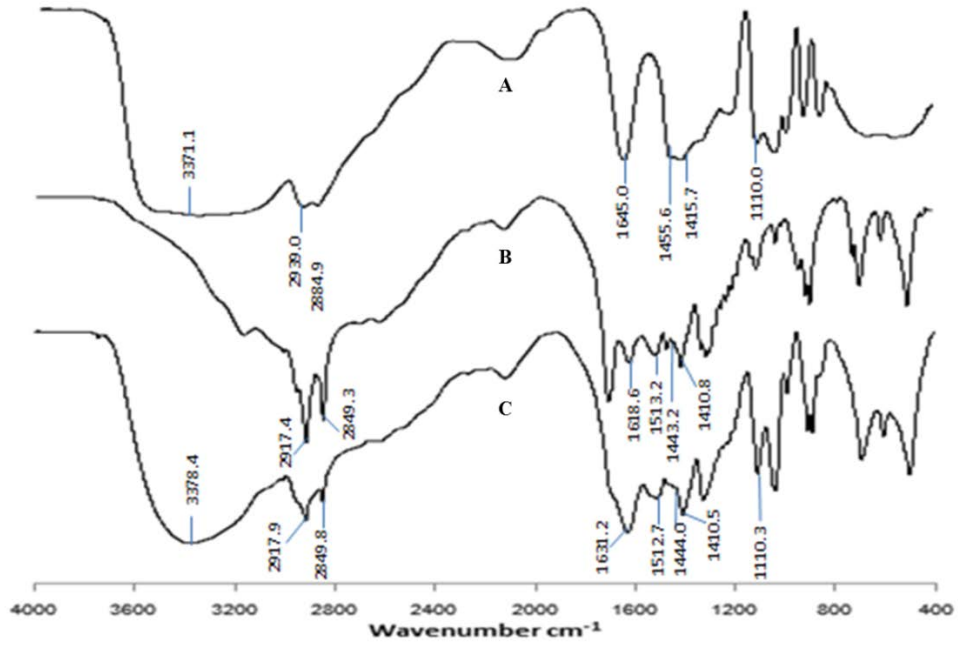


**Figure 4.5** FT-IR analysis on the adsorption of glycerol on CL-PCMC-lipase. (A) glycerol; (B) CL-PCMC-lipase; (C) CL-PCMC-lipase in esterification reaction spiked with 5.2% glycerol. The biocatalyst was recovered by centrifugation and used for analysis.

### 4.3.4 Reusability of the biocatalysts

The reusability of CL-PCMC-lipase/Gly was studied by analyzing the conversion efficiency after consecutive batch cycles under the optimal reaction conditions (Figure 4.6). CL-PCMC-lipase/Gly showed high stability in the esterification and transesterification of various palm oil feedstocks and retained >80% activity after 5 consecutive batch cycles with the average product yields of 84.7%, 91.3% and 92.8% for PA, RPO, and CPO, respectively under the optimal reaction conditions. Treatment with *t*-BuOH after each batch reaction was found to maintain the stability of the biocatalyst in the subsequent batch process by reducing glycerol absorption on the enzyme's surface. The result thus shows the potential of recycling CL-PCMC-lipase for the consecutive batch process or continuous process development, which could lead to significant cost saving on the developed enzyme-catalyzed biodiesel production process.

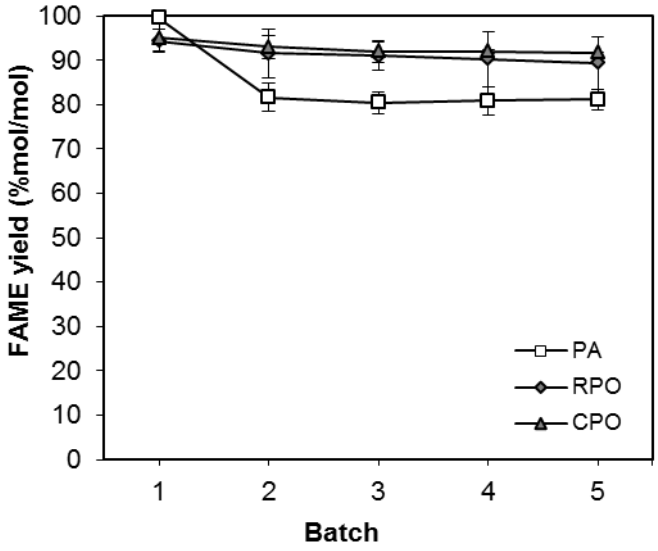


**Figure 4.6** Stability of CL-PCMC-lipase/Gly on esterification, transesterification, and co-ester/transesterification. The reactions contained 250 mg of PA/RPO/CPO, 4:1 [MeOH]/[FFA] molar ratio, in the presence of 0.3:1 v/v *t*-BuOH/PA or 1:1 (v/v) *t*-BuOH to RPO or CPO with 20% w/w enzyme and incubated at 50$^{o}$C for 6 h.

## 4.4 Conclusion

Investigation on the effects of core matrix components on the catalytic performance of CL-PCMC-lipase was demonstrated in this study. The buffer matrix carrier was shown to influence the microenvironment and the physical characteristics of the biocatalysts. The optimized process led to higher FAME yields than those previously reported using a solid acid catalyst [153], a heterogeneous alkaline catalyst [154] and the whole-cell biocatalytic method [39]. Furthermore, CL-PCMC-lipase has other advantages including low catalyst preparation cost, stability after repeated use and high catalytic performance under mild operating conditions. The biocatalytic process developed in this study provides a promising approach for production of biodiesel from CPO and other inexpensive crude feedstocks with high FFA content.

# CHAPTER 5
# MODIFICATION OF IMMOBILIZED LIPASE ON MAGNETIC NANOPARTICLE FOR BIODIESEL PRODUCTION FROM PALM OIL*


## Abstract

Biocatalytic conversion of vegetable oil by immobilized lipase to fatty acid alkyl esters is an efficient alternative to the conventional alkaline-catalyzed biodiesel synthesis process. In this work, the immobilization of *Thermomyces lanuginosus* lipase on $Fe_3O_4$ was studied using different designs on covalent linkages and protein crosslinking. Immobilized lipase on the magnetic supports was shown by Fourier-Transformed infrared microscopy and scanning electron microscopy. Immobilized lipase prepared on the $Fe_3O_4$ carrier modified by 3-aminopropyl triethyoxysilane and covalently linked by 1-ethyl-3-(3-dimethylaminopropyl) carbodiimide and N-hydroxysuccinimide ($Fe_3O_4$-AP-EN-lipase) showed the highest catalytic activity on the hydrolysis of *p*-nitrophenyl palmitate and the transesterification of refined palm oil. Reaction variables were optimized by central composite design, which identified 23.2% w/w enzyme loading and 4.7:1 methanol to fatty acid molar ratio with 3.4% water content in the presence of 1:1 (v/v) *tert*-butanol to oil as optimal conditions. A 97.2% experimental yield of fatty acid methyl ester (FAME) was obtained after incubation at 50$^{o}$C for 24 h under these conditions. The biocatalyst showed high operation stability and could be recycled for at least 5 consecutive batches with >80% activity remaining. The magnetic nanoparticle lipase and optimal conditions for its use are superior to previous reports, and thus are advantageous for eco-friendly biodiesel production with high performance and simple separation.


* This chapter has been submitted for publication.

## 5.1 Backgrounds

Biodiesel is an alternative renewable fuel to petroleum diesel. It is produced as fatty acid alkyl esters, which are mostly obtained by the transesterification or the esterification of glycerides and fatty acids in vegetable oils with short chain alcohols. At present, biodiesel accounts for around 10% of the world's diesel usage, and its share is expected to increase owning to fluctuation in petroleum price and environmental concerns. It possesses several technical and environmental advantages over conventional diesel such as higher cetane rating, less sulfur and carbon monoxide emission, lower unburned hydrocarbons and particulate matter, and can be blended with conventional petrol diesel up to 20% with no engine modification [18].

Several chemocatalytic, thermocatalytic, and biocatalytic approaches have been explored for increasing the efficiency of biodiesel production, and for overcoming the drawbacks of the currently used alkaline-catalyzed process, which is sensitive to free fatty acid in crude feedstock and requires high chemical usage with costly downstream processing [151, 155]. The synthesis of biodiesel by biocatalysis has generated interest in the biodiesel industry due to its mild operational conditions and simple downstream processing steps [29]. The lipase-catalyzed enzymatic process has many advantages for the synthesis of alkyl esters over the alkaline-catalyzed reaction, including easy recovery of glycerol, ability to convert free fatty acids to esters (which allows for complete conversion of glycerides with high free fatty acid content), and no requirement for subsequent wastewater treatment [130].

Immobilization offers a promising approach for improving enzyme operational stability and performance in non-aqueous systems, and allows for reusability of the biocatalyst. Various techniques have been used for lipase immobilization, such as adsorption [156], covalent bonding [157], entrapment [158, 159], and microcrystalline enzymes, including protein-coated microcrystals (PCMCs) [4] and cross-linked PCMCs (CL-PCMCs) [5]. Solid carriers play an important role on preparation of immobilized lipase with influences on catalytic performance of the biocatalysts. A range of solid supports have been explored for lipase immobilization e.g. acrylic resin [160], hydrophobic sol gel [31], textile membrane [161], polyvinylidene fluoride (PVDF) membrane [162] and magnetic nanoparticle [52] with differences in their physical characteristics (shape, size

distribution, and reactive surface area) and chemical properties related to interactions with the enzyme molecules.

Recently, several types of nano-structure supports have been extensively studied as solid matrices for enzyme immobilization [68]. Among them, magnetic nanoparticles have become a highly potent support material owing to its advantages on fast and facile separation under a magnetic field without the separated contamination using a chemical reagent. Various enzymes e.g. laccase, α-amylase, β-galactosidase, and lipase have been studied for immobilization on magnetic nanoparticle [68]. This immobilized enzymes exhibit properties of high-performance biocatalysts with high reactive surface area and low mass transfer limitation and fouling in reaction for immobilization, and the high catalytic efficiency and stability [163]. Various covalent modification techniques have been explored for linking the active group on the solid matrices to the enzyme molecules with different activating agents e.g. glutaraldehyde (GA) [164], 1-ethyl-3-(3-dimethylaminopropyl) carbodiimide solution (EDC) [51], and N-hydroxysuccinimide (NHS) [165]. High performance lipase biocatalyst on $Fe_3O_4$ nanoparticle treated with (3-aminopropyl) triethoxysilane (APTES) using glutaraldehyde as a coupling reagent was reported on transesterification of soybean oil [38]. The high operational stability of chitosan-coated $Fe_3O_4$ nanoparticle lipase via EDC and NHS in consecutive batch cycles has also been demonstrated [71].

In this study, molecular designs of magnetic nanoparticle lipase for biodiesel synthesis were explored using different covalent modification methods. Their physicochemical characteristics were analyzed and the catalytic performance on the transesterification of refined palm oil (RPO) was evaluated. Key reaction factors were optimized for the best nanoparticle-lipase using the central composite design for maximizing product yield. The work shows the approach for development of a highly active biocatalyst for eco-biodiesel industry.

## 5.2 Materials and methods

### 5.2.1 Materials

Refined edible grade palm oil (palm olein; RPO containing > 99% TAG) was obtained from a local market. Fatty acid ester standards were obtained from Sigma-Aldrich. Liquid *Thermomyces (Humicola) lanuginosus* lipase (Lipolase 100T) was purchased from Novozymes (Bagsvaerd, Denmark). Lipase hydrolysis activity was assayed based on hydrolysis of *p*-nitrophenyl palmitate [4]. Chemical and reagents for immobilized lipase preparation (3-aminopropyl triethoxysilane (APTES), 1-ethyl-3-(3-dimethylaminopropyl) carbodiimide (EDC), and N-hydroxysuccinimide) were purchased from Sigma-Aldrich. Chemicals were of analytical grade and obtained from major chemical suppliers (Sigma-Aldrich, Merck, and Fluka). All reagents on transesterification were dehydrated with 3 Å molecular sieves (Fluka, Buchs, Switzerland) before use.

### 5.2.2 Magnetic nanoparticle lipase ($Fe_3O_4$ nanoparticle lipase)

The preparation of magnetic nanoparticle support ($Fe_3O_4$ nanoparticle) was performed using the method modified from Xie and Ma 2010 [51]. $Fe_2SO_4 \cdot 7H_2O$ (2.78 g) and $FeCl_3 \cdot 6H_2O$ (5.4 g), equivalent to a molar ratio of 1:2, were dissolved in 100 mL distilled water at a final concentration of 0.3 mol/L $Fe^{2+}/Fe^{3+}$ combined ions. Iron nanoparticles were co-precipitated by drop-wise addition of 75 ml of 25 % ammonia hydroxide solution at 25$^{o}$C in a stirring vial. The suspension was incubated at 80°C for 30 min and then cooled down to room temperature. The precipitate was separated by centrifugation at 5,000×g and washed thrice with distilled water. The $Fe_3O_4$ nanoparticle was then dried in a dry oven at 60°C. The magnetic-APTES nanoparticle ($Fe_3O_4$-APTES nanoparticle) was prepared by treating the $Fe_3O_4$ nanoparticle (0.25 g) with 0.15 ml (3-aminopropyl) triethoxysilane (APTES) in 4.85 ml ethanol based on the method modified from Xie and Ma 2009 [38]. The mixture was sonicated at a frequency of 35 kHz with shaking overnight at room temperature. The product was separated by magnetic separation, washed thrice with 5% ethanol and dried in a dry oven at 60°C.

#### 5.2.2.1 Type I: $Fe_3O_4$ nanoparticle lipase via EDC ($Fe_3O_4$-E lipase)

The $Fe_3O_4$ nanoparticles (0.2 g) were dispersed in 2 ml of 3 mM potassium phosphate buffer (PPB), pH 6 containing 100 mM NaCl. The suspension was added to 0.5 ml of 2.5 mg/ml solution of 1-ethyl-3-(3-dimethylaminopropyl) carbodiimide solution (EDC) and then sonicated at a frequency of 35 kHz for 15 min. The lipase solution (2.5 ml) was added to the suspension and sonicated at 30 kHz for 30 min. The biocatalyst was separated by magnetic decantation and then washed with PPB for several times until no free lipase was detected in the supernatant as shown by Bio-Rad Bradford's assay reagent using bovine serum albumin (BSA) as a standard. The biocatalyst ($Fe_3O_4$-E lipase) was air dried and stored at $4^oC$ for subsequent use.

#### 5.2.2.2 Type II: $Fe_3O_4$ nanoparticle lipase via EDC and cross-linked by GA ($Fe_3O_4$ –E/G lipase)

The $Fe_3O_4$-E lipase (0.2 g) was treated with 0.2 ml of 0.5% v/v glutaraldehyde (GA) and 0.5 ml of 25 mM potassium phosphate buffer, pH 7 in the total reaction volume of 10 ml. The suspension was incubated at room temperature with shaking at 100 rpm for 2 h. The resulting nanoparticle lipase was separated by magnetization and washed thrice with distilled water to remove excessive GA. The biocatalyst was air-dried and stored at $4^oC$ for subsequent study.

#### 5.2.2.3 Type III: $Fe_3O_4$-APTES nanoparticle lipase via EDC and NHS ($Fe_3O_4$ -AP-EN lipase)

The lipase solution (2.5 ml) was mixed with 0.5 ml of 2.5 mg/ml 1-ethyl-3-(3-dimethylaminopropyl) carbodiimide solution (EDC) and incubated at room temperature for 2 h with shaking at 200 rpm. The mixture was added to 3 mg of N-hydroxysuccinimide (NHS) and further incubated under the same conditions for 2 h. The solution was then added to 0.25 g of $Fe_3O_4$-APTES nanoparticle and further incubated for 2 h. The nanoparticle lipase was separated by magnetization and then washed with distilled water for several times until no free lipase was detected in the supernatant. The biocatalyst was air-dried and stored at $4^oC$ for subsequent study.

#### 5.2.2.4 Type IV: $Fe_3O_4$-APTES nanoparticle lipase via EDC and NHS and cross-linked by GA ($Fe_3O_4$ –AP-EN/G lipase)

The $Fe_3O_4$–AP-EN lipase (0.25 g) was crosslinked with 0.2 ml of 0.5% v/v glutaraldehyde (GA) and 0.5 ml of 25 mM phosphate buffer (PPB), pH 7 in a total reaction volume of 10 ml. The suspension was incubated at room temperature for 2 h with shaking at 100 rom. The nanoparticle lipase was removed by magnetic separation and washed thrice with distilled water for removing excess GA. The biocatalyst was air-dried and stored at 4$^{o}$C for subsequent study. The immobilization efficiency of lipase was determined according to Equation (5.1).

$$\text{Immobilization efficiency (\%)} = \frac{(C_i - C_f)\times V_1}{C_i \times V_2} \times 100 \qquad (5.1)$$

$C_i$ and $C_f$ represent the initial concentrations of protein in the lipase solution before immobilization and the final concentration of protein in the supernatant after immobilization, respectively (mg/ml). $V_1$ and $V_2$ are the volumes of the starting lipase solution and the final supernatant, respectively (ml).

### 5.2.3 Lipase catalyzed biodiesel synthesis

For the standard reaction, 250 mg of refined palm oil (RPO) and methanol was reacted in a molar ratio of 4:1 [MeOH]/[FFAs] in the presence of 1:1 (v/v) *t*-BuOH to RPO. The magnetic nanoparticle lipase was added at 20% (w/w based on RPO) in the reaction and incubated at 50$^{o}$C for 6 h with mixing on a vertical rotator at 40 rpm. The amount of esters formed was determined by gas chromatography according to Raita et al. (2011) [5]. For the reusability study, the biocatalyst was recovered by magnetization, washed with 0.5 mL of *t*-BuOH, and air-dried before use in the next batch. The reactions were done in triplicate and standard deviations were reported for all experimental results.

### 5.2.4 Lipase activity assay

Lipase hydrolysis activity was assayed based on the hydrolysis of *p*-nitrophenyl palmitate [Gilham and Lehner, 2005] [117]. The standard reaction (200 µl) contained 20 mM sodium phosphate buffer, pH 8, 1 mM of *p*-nitrophenyl palmitate and an appropriate dilution of the enzyme or immobilized enzyme. The reaction was incubated at 45°C for 30 min and then terminated by addition of 100 µl of 0.2 M $Na_2CO_3$. The formation of *p*-nitrophenolate was determined by measuring the absorbance at 405 nm. One unit of the

enzyme activity was defined as the amount of enzyme catalyzing the release of 1 μmole *p*-nitrophenolate/min under the standard experimental conditions used.

### 5.2.5 Gas chromatography analysis of FAME

Fatty acid methyl ester (FAME) yields were analyzed by gas chromatography on a Shimadzu 2010, equipped with a flame ionization detector (Shimadzu, Kyoto, Japan) and a polyethylene glycol capillary column (Carbowax 20 M, 30 m x 0.32 mm, Agilent Technologies, Santa Clara, CA). The column oven temperature was at 200$^{o}$C, with injector and detector temperatures at 250 and 260$^{o}$C, respectively. Helium was used as the carrier gas at a constant pressure of 64.1 kPa with linear velocity at 25 cm/s. The amount of FAME was determined based on standard curves using the corresponding esters. The product yield (%) is the amount of FAME converted from available fatty acid equivalence (as FFAs and glycerides) on a molar basis.

### 5.2.6 Physical analysis techniques

#### 5.2.6.1 Scanning electron microscope (SEM)

The structure and morphology of the CL-PCMC-lipase was analyzed by scanning electron microscope (SEM) using a JSM-6301F Scanning Electron Microscope (JEOL, Tokyo, Japan). The samples were dried and coated with gold for analysis. An electron beam energy of 5 kV was used for analysis.

#### 5.2.6.2 Fourier-Transformed Infrared Spectroscopy (FTIR)

The functional groups on CL-PCMCs were analyzed by Fourier-Transformed Infrared Spectroscopy (FTIR) (Perkin-Elmer System 2000, Waltham, MA) on the infrared spectra at 400-4000 cm$^{-1}$ wavenumber.

### 5.2.7 Experimental design

The FAME synthesis reaction using magnetic nanoparticle lipase was optimized by response surface methodology (RSM) using central composite design (CCD) with three factors and five code levels, including six replicates at the center points. The reaction variables were enzyme loading ($X_1$), molar ratio of [MeOH]/[FFAs] ($X_2$), and water content ($X_3$) as illustrated in Table 5.1. The experimental range and levels of independent variables involved 20 experimental runs. The variables $X_i$ (the real value of an independent variable) were coded as $x_i$ according to equation 5.2:

$$x_i=(X_i-X_0)/\Delta X_i, \quad (5.2)$$

Where $x_i$ is the dimensionless coded value of the variable $X_i$; $X_o$ is the value of $X_i$ at the center point; and $\Delta X_i$ is the step change.

The prediction of FAME yield taken as the response of the design experiments was analyzed by response surface regression and fit to the second-order polynomial multiple regression equation (equation 5.3) [166]. Data were analyzed using Design Expert software (Version 9, Stat-Ease, Inc., Minneapolis, USA).

$$Y = b_o + \sum_{i=1}^{n} b_i x_i + \sum_{i=1}^{n} b_{ii} x_i^2 + \sum_{i=1}^{n-1} \sum_{j=i+1}^{n} b_{ij} x_i x_j + e_i, \qquad (5.3)$$

Where Y is the predicted response; n is the number of factors; $x_i$ and $x_j$ are the coded variables; $b_o$ is the offset term; $b_i$, $b_{ii}$, and $b_{ij}$ are the first-order, quadratic, and interaction effects, respectively; i and j are the index numbers for factor; and $e_i$ is the residual error.

**Table 5.1** Experimental range and levels of the independent variables

| Variables | Factor | Range and code level | | | | |
|---|---|---|---|---|---|---|
| | | -1.682 | -1 | 0 | 1 | 1.682 |
| **Enzyme loading %(w/w)** | $X_1$ | 3.18 | 10 | 20 | 30 | 36.82 |
| **Molar ratio of [MeOH]/[FFAs] (mol/mol)** | $X_2$ | 0.636:1 | 2:1 | 4:1 | 6:1 | 7.364:1 |
| **Water content %(w/w)** | $X_3$ | 0 | 2 | 5 | 8 | 10 |

## 5.3 Results and discussion

### 5.3.1 Preparation of magnetic nanoparticle lipases

In the first stage, the immobilized lipases were synthesized in four different forms with variation in covalent linkages and protein crosslinking. The pre-concentrated lipase had an initial protein content of 574.8 mg/ml and a specific activity of 3.7 x $10^{-3}$ IU/mg protein. $Fe_3O_4$ or $Fe_3O_4$-APTES nanoparticles were covalently coupled with lipase via EDC and/or NHS as activating agent with or without protein cross-linking by glutaraldehyde, which is a bi-functional protein crosslinker. The schematic diagrams of the magnetic nanoparticle enzymes in different forms are shown in Figure 5.1. In $Fe_3O_4$-E lipase, the hydroxyl groups of $Fe_3O_4$ nanoparticles were activated by EDC and subsequently reacted with the carboxyl groups of the lipase, and the enzyme molecules on the biocatalyst's surface were further crosslinked by GA to obtain $Fe_3O_4$-E/G. The $Fe_3O_4$-AP-EN lipase was prepared by linking the carboxy groups of lipase to the amino groups of $Fe_3O_4$-APTES activated by EDC and NHS and then further crosslinked to obtain $Fe_3O_4$-AP-EN/G lipase.

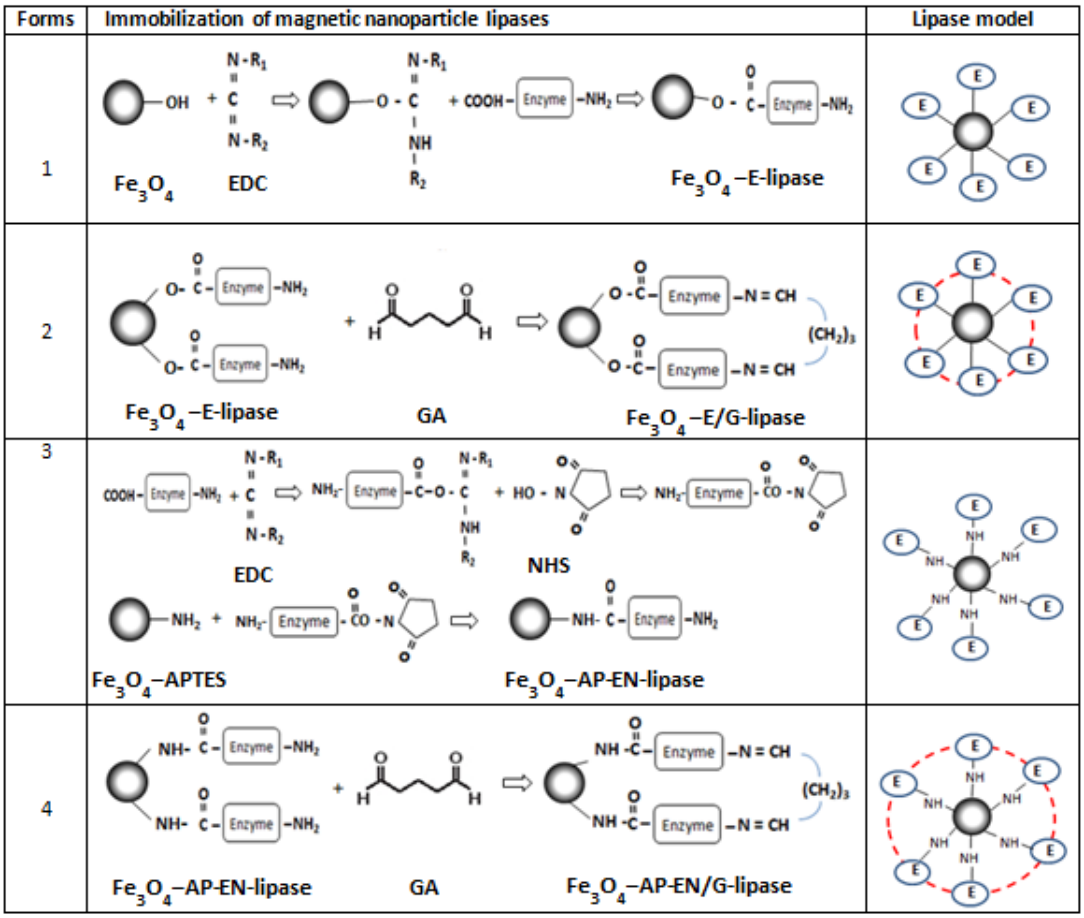


**Figure 5.1** Schematic diagram of magnetic nanoparticle lipase immobilization methods.

### 5.3.2 Physical characterization of magnetic nanoparticle lipase

The physical characteristics of magnetic nanoparticle lipases were examined by SEM (Figure 5.2). The protein-free nanoparticle supports ($Fe_3O_4$and $Fe_3O_4$-APTES) showed well-defined structures with variable size distribution in the micron size range of 50-100 μm and smooth, clear surfaces (Figure 5.2A, B). Protein aggregates were clearly present on the carrier matrix in all forms of the magnetic nanoparticle lipase (Figure 5.2C-F). The protein layer of all lipase conjugated nanoparticles showed a rough surface with nano-sized pores. This structure provides a highly reactive surface area of the immobilized enzymes.

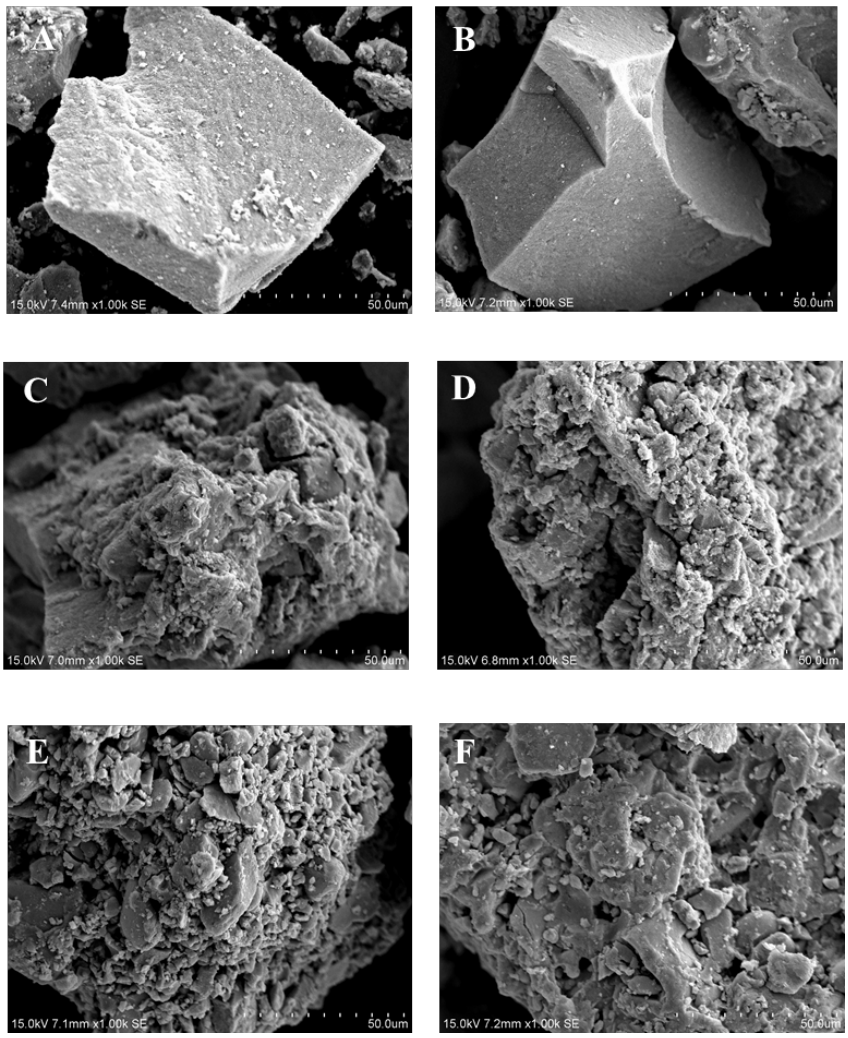


**Figure 5.2** SEM analysis of magnetic nanoparticle lipases and the protein-free nanoparticle supports. (A) $Fe_3O_4$ nanoparticle; (B) $Fe_3O_4$-APTES nanoparticle; (C) $Fe_3O_4$ –E lipase; (D) $Fe_3O_4$ –E/G lipase; (E) $Fe_3O_4$ -AP-EN lipase; (F) $Fe_3O_4$-AP-EN/G lipase.

The formation of covalently bound proteins on the biocatalysts was demonstrated by FT-IR (Figure 5.3). The FT-IR spectra of *T. lanuginosus* lipase showed signature peaks at 1643.99 $cm^{-1}$ for the carbonyl amide group (O=C stretching vibration) and 1557.26 $cm^{-1}$ for the amide group from N-H bending vibration. The absorption peaks at 579.64 $cm^{-1}$ and 568.25 $cm^{-1}$ of Fe-O stretching vibrations were identified for the $Fe_3O_4$ and $Fe_3O_4$-APTES, respectively. The hydroxyl absorption peak (O-H stretching vibration) of $Fe_3O_4$ nanoparticle support was observed at 3375.54 $cm^{-1}$, while the $Fe_3O_4$- APTES support showed both the hydroxyl group and amine group as N-H stretching vibration at 3391.01 $cm^{-1}$. These spectral patterns corresponded well with the spectra of magnetic nanoparticle support previously reported by Xie & Ma 2009, 2010 [38, 51]. The immobilized lipase in all forms showed signature peaks of both the lipase and the magnetic particle. This indicated the formation of bound enzyme molecules on the nanoparticle. Nevertheless, the absorption peak of imine group (C=N stretching vibration) at 1690-1640 $cm^{-1}$ on cross-linked enzyme molecule by glutaraldehyde was not identified in $Fe_3O_4$-E/G and $Fe_3O_4$-AP-EN/G, as its position is overlapped by the broad peak of carbonyl amide group at 1680-1630 $cm^{-1}$ [167].

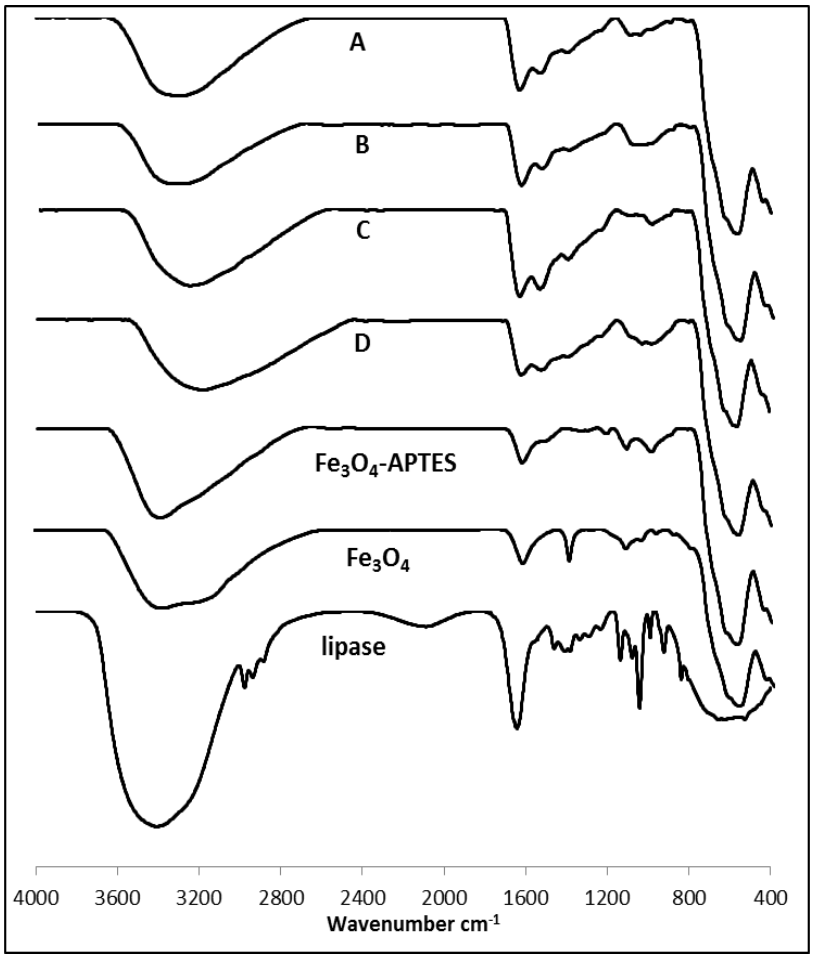


**Figure 5.3** FT-IR spectra of immobilized lipase on magnetic nanoparticles in different forms.

### 5.3.3 Catalytic activity of magnetic nanoparticle lipases

Catalytic efficiencies of the immobilized enzymes on the hydrolysis of *p*-nitrophenyl palmitate and transesterification of RPO were evaluated. The highest hydrolysis activity of 32.0 nmole/min/g was observed for the $Fe_3O_4$-AP-EN lipase, while lower activity was found for the immobilized lipases prepared in other forms (Table 5.2). The highest FAME yield of 85.0% was also obtained under the initial standard conditions for transesterification using methanol as a nucleophile in the absence of water. The $Fe_3O_4$-AP-EN/G cross-linked lipase form showed markedly lower activity on both hydrolysis (3.3 nmole/min/g) and transesterification (34.76%). The $Fe_3O_4$-lipase conjugates immobilized via the carboxyl groups of the enzyme ($Fe_3O_4$-E and $Fe_3O_4$-E/G) showed correspondingly lower activities on both hydrolysis and transesterification compared with those prepared on

$Fe_3O_4$-APTES linked by EDC/NHS. The immobilization efficiency of $Fe_3O_4$-AP-EN lipase was 86.5%.

**Table 5.2** Catalytic activity of magnetic nanoparticle lipases on hydrolysis and transesterification

| | Type | Activity (nmole/min/g) | FAME yield from RPO (%mol/mol) |
|---|---|---|---|
| 1 | $Fe_3O_4$-E-lipase | 2.2 | 10.28 |
| 2 | $Fe_3O_4$-E/G-lipase | 1.3 | 13.63 |
| 3 | $Fe_3O_4$-AP-EN-lipase | 32.0 | 85.04 |
| 4 | $Fe_3O_4$-AP-EN/G-lipase | 3.3 | 34.76 |

Reaction conditions: The reactions contained 250 mg of refined palm oil (RPO), 4:1 [MeOH]/[FFAs] molar ratio in the presence of 1:1 (v/v) [t-BuOH]/[TGA] with 20% (w/w) magnetic nanoparticle lipase in the reaction and incubated at 50 °C for 6 h with mixing on a vertical rotator at 40 rpm.

The higher catalytic performance of the biocatalysts prepared on $Fe_3O_4$-APTES matrix could be related to the silane coating, i.e. APTES on the surface of the magnetic support, which provides a high density of surface functional groups for coupling [168]. Silane coatings enhance enzyme binding to the support and improve enzyme stability [169]. The addition of NHS to EDC is also known to decrease the hydrolysis of active ester (o-acylisourea) from EDC activating formation in aqueous solution, leading to increased efficiency of the EDC-mediated coupling reaction [170] together with the improvement of solubility and stability of active intermediate groups [171].

The superior performance of the $Fe_3O_4$-AP-EN lipase under the experimental conditions is thus consistent with literature on nanoparticle coupling conditions. The lower performance of crosslinked $Fe_3O_4$-E/G and $Fe_3O_4$-E/G enzymes in this study was in contrast to those previously reported for the enhancement of biocatalyst's operational stability by crosslinking of bound enzyme molecules, e.g. microcrystalline lipase [5] and glutaryl acylase on aminated sepabeads supports [172]. The lower catalytic performance of cross-linked enzymes in this study could be due to the formation of excess intramolecular and intermolecular interactions within or between the enzyme molecules bound on the biocatalyst's surface [173]. These covalent bridges could lead to increased enzyme rigidity

and loss of structural flexibility required in catalysis [174]. In addition, cross-linking could also lead to partial distortion of the enzyme's overall structure, which could affect the active site conformation, and thus, the catalytic efficiency of the immobilized enzymes [175].

### 5.3.4 Optimization of transesterification reaction

In order to maximize the FAME yield from the $Fe_3O_4$-AP-EN lipase catalyzed transesterification of RPO, the key factors for biodiesel synthesis i.e. the amount of enzyme, [MeOH]/[FFAs] ratio, and water content were optimized using the central composite design (CCD) approach. The experimental design involved 20 experimental runs. The actual FAME yields are shown in Table 5.3. The highest experimental FAME yield of 95.4% was obtained from the reactions at the center point using 20% w/w enzyme loading to RPO with 4:1 [methanol]/[FFAs] in the presence of 5% w/w water content. The FAME yield obtained was within ±1 % SD of the predicted value.

The linear terms of the enzyme dosage ($X_1$), the molar ratio of MeOH and FFAs ($X_2$), and the water content ($X_3$), as well as the quadratic terms ($X_1^2$, $X_2^2$, and $X_3^2$) were significant effects on the FAME yield (ANOVA $P < 0.05$) (Table 5.4). The coefficient of determination ($R^2$) in this regression model was 0.97, indicating validity of the model. The deduced polynomial model showing relationship of significant independent variables to the FAME yield is described by Equation 4.

$$Y = 95.19+8.52X_1 +11.73X_2 -10.46X_3 – 2.47X_1X_2 -0.11X_1X_3 +0.01\ X_2X_3 -12.75X_1^2 - 14.26X_2^2 -10.19X_3^2 \quad (4)$$

Where Y is the FAME yield (% mol/mol); $X_1$, $X_2$, and $X_3$ represent enzyme loading, molar ratio of methanol to TAG, and water content, respectively.

**Table 5.3** Central composite design with three independent variables for predicted and experimental results.

| Experimental number | Coded variables | | | Experimental plan | | | % FAME yield (mol/mol) | |
|---|---|---|---|---|---|---|---|---|
| | ENZ loading (%w/w) | [MeOH]/[FFAs] (mol/mol) | Water content (%w/w) | $X_1$ | $X_2$ | $X_3$ | Observed | Responded |
| 1 | −1 | -1 | -1 | 10 | 2 | 2 | 47.80 | 45.66 |
| 2 | 1 | -1 | -1 | 30 | 2 | 2 | 70.99 | 67.86 |
| 3 | −1 | 1 | -1 | 10 | 6 | 2 | 78.06 | 74.04 |
| 4 | 1 | 1 | -1 | 30 | 6 | 2 | 85.76 | 86.36 |
| 5 | -1 | -1 | 1 | 10 | 2 | 8 | 30.39 | 24.94 |
| 6 | 1 | -1 | 1 | 30 | 2 | 8 | 47.54 | 46.70 |
| 7 | -1 | 1 | 1 | 10 | 6 | 8 | 55.09 | 53.36 |
| 8 | 1 | 1 | 1 | 30 | 6 | 8 | 67.97 | 65.24 |
| 9 | −1.682 | 0 | 0 | 3.18 | 4 | 5 | 39.19 | 44.78 |
| 10 | 1.682 | 0 | 0 | 36.8 | 4 | 5 | 72.14 | 73.44 |
| 11 | 0 | −1.682 | 0 | 20 | 0.64 | 5 | 30.68 | 35.22 |
| 12 | 0 | 1.682 | 0 | 20 | 7.36 | 5 | 72.32 | 74.68 |
| 13 | 0 | 0 | −1.682 | 20 | 4 | 0 | 81.11 | 83.95 |
| 14 | 0 | 0 | 1.682 | 20 | 4 | 10 | 44.71 | 48.76 |
| 15 | 0 | 0 | 0 | 20 | 4 | 5 | 95.62 | 95.19 |
| 16 | 0 | 0 | 0 | 20 | 4 | 5 | 95.50 | 95.19 |
| 17 | 0 | 0 | 0 | 20 | 4 | 5 | 95.66 | 95.19 |
| 18 | 0 | 0 | 0 | 20 | 4 | 5 | 94.65 | 95.19 |
| 19 | 0 | 0 | 0 | 20 | 4 | 5 | 95.59 | 95.19 |
| 20 | 0 | 0 | 0 | 20 | 4 | 5 | 95.26 | 95.19 |

The optimum conditions for the transesterification of RPO were then refined by numerical optimization. The regression model response surface and contour plots are shown in Figure 5.4. Increasing enzyme loading and methanol ratio to FFAs at a fixed water content led to increased FAME yield (Figure 5.4A). However, further increases in the enzyme loading led to decreased FAME yield, which is explained by lower mixing efficiency and enzyme aggregation [176]. Excess methanol reduces yield (Figure 5.4A, C) since enzyme is deactivated in the immiscible polar organic phase of methanol [125]. Water content also showed significant influence on FAME yield (Figure 5.4B, C). The

effects of water on control of enzyme activity in transesterification were previously reported [110, 177]. In the optimum amount of water, the enzyme possesses a flexible structure and undergoes conformational change as required for catalysis. Moreover, the interfacial phase of the reaction between the oil and aqueous phases is available to the enzyme in optimum water content [178]. In contrast, high water content can lead to undesirable triglyceride hydrolysis reaction as well as hydrolysis of the ester products, which reduce FAME yield [178].

The optimal reaction conditions for the maximal FAME yield were determined by polynomial regression. The optimized reaction parameters were 23.2 %w/w of enzyme loading in the presence of a [MeOH]/[FFAs] ratio of 4.7:1 and a water content of 3.4 %w/w. A FAME yield of 97.2% was obtained experimentally under the predicted optimal conditions after incubation at 50$^{o}$C for 24 h which was only slightly lower than the predicted yield (100%).

**Table 5.4** Analysis of variance (ANOVA) for response surface quadratic model.

| **Source** | **Coefficient Estimate** | **Degrees of freedom** | **Sum of squares** | **F value** | **P value** |
|---|---|---|---|---|---|
| Model | 95.19 | 9 | 10083.41 | 71.75 | < 0.0001 |
| $X_1$ | 14.31 | 1 | 990.84 | 63.45 | < 0.0001 |
| $X_2$ | 11.73 | 1 | 1878.57 | 120.31 | < 0.0001 |
| $X_3$ | -10.46 | 1 | 1493.39 | 95.64 | < 0.0001 |
| $X_1X_2$ | -4.15 | 1 | 48.87 | 3.13 | 0.1073 |
| $X_1X_3$ | -0.18 | 1 | 0.095 | 6.066E-003 | 0.9395 |
| $X_2X_3$ | 0.012 | 1 | 1.142E-003 | 7.313E-005 | 0.9933 |
| $X_1^2$ | -35.99 | 1 | 2344.51 | 150.14 | < 0.0001 |
| $X_2^2$ | -14.23 | 1 | 2917.22 | 186.82 | < 0.0001 |
| $X_3^2$ | -10.19 | 1 | 1497.76 | 95.92 | < 0.0001 |

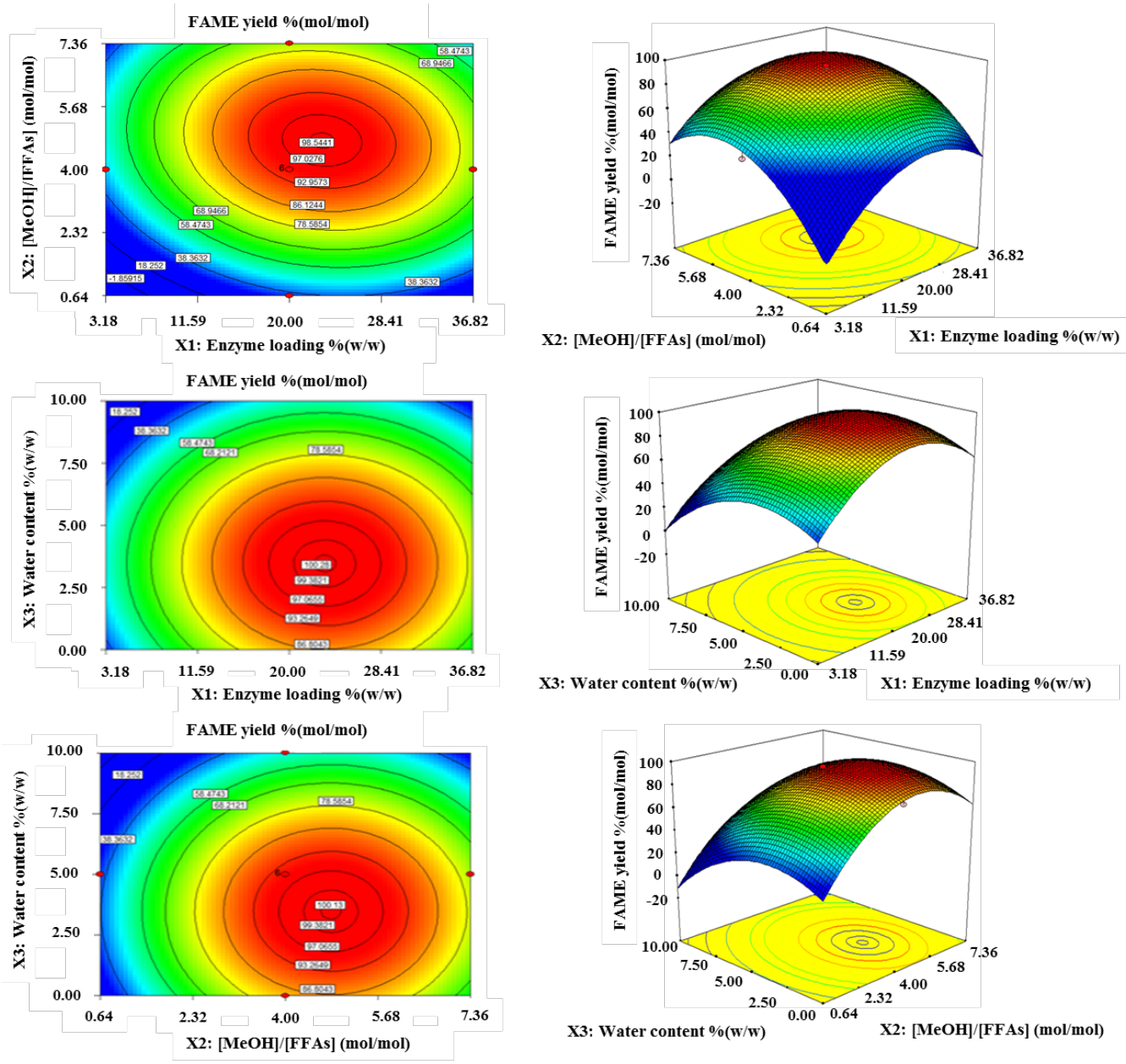


**Figure 5.4** Contour plots and response surfaces showing the effects of reaction parameters on FAME yield on the transesterification of RPO using $Fe_3O_4$-AP-EN lipase. The reactions were incubated at 50°C for 24 h in the presence of 1:1 (v/v) *t*-BuOH/RPO. (A) Effects of enzyme dosage and [MeOH]/[FFAs] at a fixed water content (5 %w/w); (B) Effects of enzyme loading and water content at a fixed [MeOH]/[FFAs] (4:1); (C) Effects of [MeOH]/[FFAs] and water content at a fixed enzyme dosage (20 %w/w).

### 5.3.5 Reusability of $Fe_3O_4$ –AP-EN lipase for transesterification

The reusability of $Fe_3O_4$-AP-EN nanoparticle lipase was studied by analyzing the conversion efficiency after consecutive batch cycles under the optimal reaction conditions (Figure 5.5). The biocatalyst retained operational stability after repeated use with >80% of the original activity remaining after 5 consecutive batch cycles. No treatment of the immobilized lipase with organic solvent was needed. This result thus demonstrates the potential of $Fe_3O_4$-AP-EN lipase in consecutive batch or continuous process development.

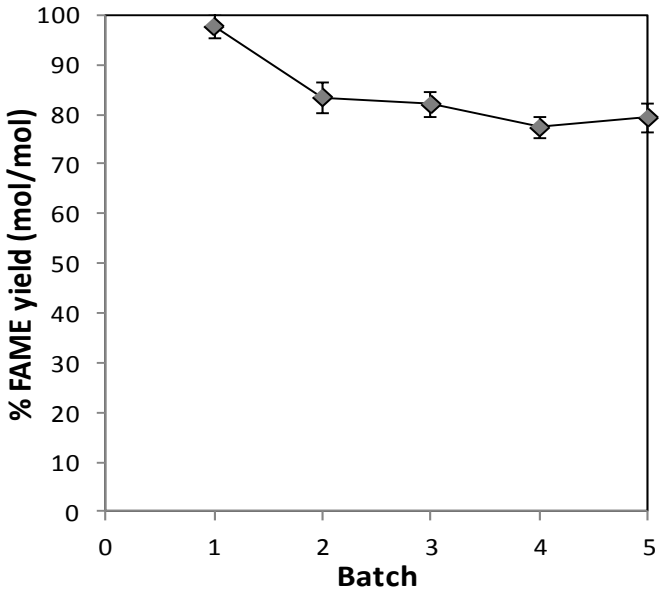


**Figure 5.5** Reusability of the magnetic nanoparticle lipase in consecutive batch process. The reaction contained 23.2% $Fe_3O_4$-AP-EN lipase, 5.4:1 [MeOH]/[FFAs], 3.4% water content and incubated at 50 °C for 24 h in the presence of 1:1 (v/v) *t*-BuOH/RPO.

Variation in biodiesel yields (70-98%) has been previously reported for the conversion of vegetable oils of different origins to FAME using lipase immobilized by different methods, such as absorption, covalent bond, and cross-linking [3, 179]. The FAME yield of >90% was determined using magnetic nanoparticle lipase with different designs to the optimized form in this studied. Conversion of soybean oil using immobilized lipase on $Fe_3O_4$-nanoparticle lipase by EDC (equivalent to $Fe_3O_4$-E-lipase) and $Fe_3O_4$-APTES by glutaraldehyde showed a high FAME yield of 94%; however with the caveats that high enzyme loading (40 - 60 %w/w) and three-stepwise addition of methanol were required [38, 51]. Functionalization of nanoparticle was studied to increase the efficiency of functional groups on covalent immobilization using different modification methods e.g. chitosan [71] and silica layer [69]. This led to the preparation of biocatalysts with high

operational stability in different designs, such as $Fe_3O_4$-chitosan nanoparticles via EDC and NHS coupling agents, and alkyl-grafted $Fe_3O_4$-$SiO_2$ nanoparticles.

The $Fe_3O_4$-AP-EN nanoparticle lipase developed in this study by functionalization of the iron matrix by APTES and linked to the lipase via EDC and NHS yielded higher FAME compared with most previously reported biocatalysts [69, 180]. The superior catalytic performance and operational stability of our biocatalyst could be related to the improved enzyme's binding and stability with the modified covalent linkages and reflected in its lower enzyme loading and reaction time to achieve the maximal FAME yield under the CCD-optimized conditions. The high operational stability of the biocatalyst with no need for the regeneration step by organic solvent also allows cost saving in the consecutive batch process. The FAME yield obtained in this study using the biocatalytic process was relatively high compared to biodiesel synthesis using the conventional alkaline-catalyzed reaction and other methods under development, such as acid catalysis by heterogenous catalysts [181], thermal process using sub-critical or critical methanol [182], and whole-cell biocatalytic process using wild-type and recombinant microbial cells [183].

## 5.4 Conclusion

Magnetic nanoparticle lipase represents a promising biocatalyst for biodiesel production with advantages on high reactive surface area, low mass transfer resistance, and simple separation by magnetization. The optimized biocatalyst design showed high performance on both catalytic efficiency and operational stability. This could lead to the development of an efficient biocatalytic process for the green biodiesel industry.

# CHAPTER 6
# DEVELOPMENT OF WHOLE CELL BIOCATALYST EXPRESSING LIPASE FOR BIODIESEL SYNTHESIS

Whole cell biocatalysts expressing lipase represent a simple and inexpensive approach for converting vegetable oil to fatty acid methyl ester. The development of arming yeast with cell-surface display of enzymes is an approach for preparing biocatalysts with low mass transfer limitation on catalysis. In this study, recombinant *P. pastoris* systems for expression of *Thermomyces lanuginosus* and *Candida antarctica* lipases in cell-surface display and secreted forms were developed. The cell-surface display lipase was aimed for using as a whole cell biocatalyst for conversion of palm oil to biodiesel. Production of enzyme in the secreted form was considered as a control for cell surface expression and as a platform for local lipase production for preparation of immobilized enzyme.

## 6.1 Materials and methods

### 6.1.1 Materials

Genes encoding *Thermomyces lanuginosus* lipase (lipase TL) and *Candida antarctica* lipase (lipase CA) were obtained from GenScript (USA) based on the sequence in GenBank (Genbank accession number AF054513 and Z30645, respectively) with codon optimization for expression in *Pichia pastoris*. Restriction enzymes and DNA modifying enzymes were from MBI Fermentas (St. Leon-Rot, Germany). *P. pastoris* KM71 and the expression vector pPICZαA were purchased from Invitrogen (Invitrogen, Carlsbad, CA, USA). *E. coli* DH5α was used as the recipient strain for vector propagation. PCR primers were synthesized by BioDesign (Bangkok, Thailand).

### 6.1.2 Construction of recombinant yeast strain for cell surface expression of lipase

Amplification of the target sequences were performed using *Pfu* DNA polymerase (Thermo Scientific, Waltham, MA) according to the manufacture's protocol. The primers used are listed in Table 6.1. The reactions contained 4 mM $MgSO_4$, 0.2 mM dNTPs, 20 ng template DNA, 0.8 μM of each primer, and 2.5 unit *Pfu* DNA polymerase. The mature lipase genes

(without the leader sequence) of *T. lanuginosus* (lipase TL) and *C. antarctica* lipase (lipase CA) were amplified from the full-length synthesized lipase gene using primers LipTL_F and LipTL_R for lipase TL, and LipCA_F and LipCA_R for lipase CA and using the amplification conditions as follows: pre-denaturation at 94°C for 5 min, followed by 30 cycles of denaturation at 94°C for 10 sec, annealing at 55°C for 30 sec, extension at 72°C for 3 min, and a prolonged final extension at 72°C for 10 min. The sequence encoding C-terminal fusion of agglutinin was amplified from pMUC [184] using primers LipTL_agg_F and LipTL_agg_R for lipase TL, and LipCA_agg_F and LipCA_agg_R for lipase CA the amplification conditions as follows: pre-denaturation at 94°C for 5 min, followed by 30 cycles of denaturation at 94°C for 10 sec, annealing at 55°C for 30 sec, extension at 72°C for 3 min, and a prolonged final extension at 72°C for 10 min. Overlap extension PCR was performed using primers LipTL_F and LipTL_agg_R for lipase TL, and LipCA_F and LipCA_agg_R for lipase CA with the following PCR conditions: one cycle of pre-denaturation at 94 °C for 5 min; 30 cycles of denaturation using at 94 °C for 1 min, annealing at 55 °C for 1 min, and extension at 72 °C for 5 min; and one cycle of prolonged extension at 72 °C for 10 min. The final PCR product contained the lipase gene fused to the 3′-half of the α-agglutinin was named LipaseTL_agg and LipaseCA_agg. The amplicons (LipaseTL_agg: 2.3 kb and LipaseCA_agg: 2.4 kb) were purified (APPENDIX B: Figure B1) and cloned into pJET1.2 vector (Fermentas, Thermo Fisher Scientific Inc., Waltham, USA). The recombinant plasmids were then digested with *Xho*I and *Xba*I and ligated to a similarly digested pPICZαA vector (Figure 6.1), placing the LipaseTL_agg and LipaseCA_agg constructs under the AOX1 promoter and directly downstream of an α-factor secretion signal. Corrected insertion of the PCR fragments was verified by DNA sequencing. The resulting recombinant plasmid was designated pLipaseTL_agg and pLipaseCA_agg.

These plasmids were linearized with *Pme*I, which resulted in 5.8 kb and 6.0 kb fragments for pLipaseTL_agg and pLipaseCA_agg, respectively (APPENDIX B: Figure B2). The linearized plasmids were transferred into *P. pastoris* KM71 by electroporation as described in the instruction manual (Invitrogen, Carlsbad, CA, USA). Transformants were allowed to grow on YPD agar plates containing 100 μg/ml zeocin at 30 °C for 2–3 days. The transformant cells were verified for the integration of pLipaseTL_agg and pLipaseCA_agg

into *P. pastoris* genome by PCR using 5'AOX and 3'AOX primers. The construction of recombinant plasmids for the cell surface display of lipase was shown in Figure 6.2.

**Table 6.1** Primers used for construction of recombinant plasmids for cell-surface display of lipase

| Lipase | Primer name | Gene (5′ → 3′) |
|---|---|---|
| *T. lanuginosus* | LipTL_F | *Xho* I — Lipase TL gene<br>GCGCCTCGAGAAAAGATCCCCTATTAGAAGAGAGGT<br>Kex2 signal cleavage |
| | LipTL_R | Lipase TL complementary<br>GAGATAAAAGAGCTTTTGGCCAAGCAAGTACCAATAAGTC |
| | LipTL_agg_F | Agglutinin gene<br>GACTTATTGGTACTTGCTTGGCCAAAAGCTCTTTTATCTC |
| | LipTL_agg_R | *Xba* I<br>CCGCGCTCTAGATTTGATTATGTTCTTTCTAT |
| *C. antarctica* | LipCA_F | *Xho* I — Lipase CA gene<br>ATCACTCGAGAAAAGAACCCCTTTGGTTAAGAGATT<br>Kex2 signal cleavage |
| | LipCA_R | Lipase CA complementary<br>GAGATAAAAGAGCTTTTGGCTGGTGTGACGATTCCT |
| | LipCA_agg_F | Agglutinin gene<br>CTCAGGAATCGTCACACCAGCCAAAAGCTCTTTTAT |
| | LipCA_agg_R | *Xba* I<br>CCGCGCTCTAGATTTGATTATGTTCTTTCTAT |

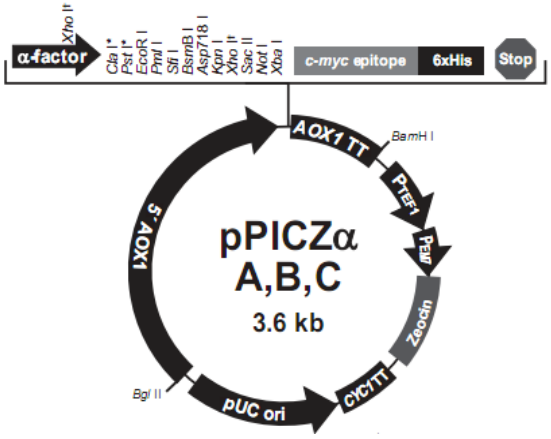


**Figure 6.1** Physical map of pPICZαA, B, C (Invitrogen, Carlsbad, CA, USA).

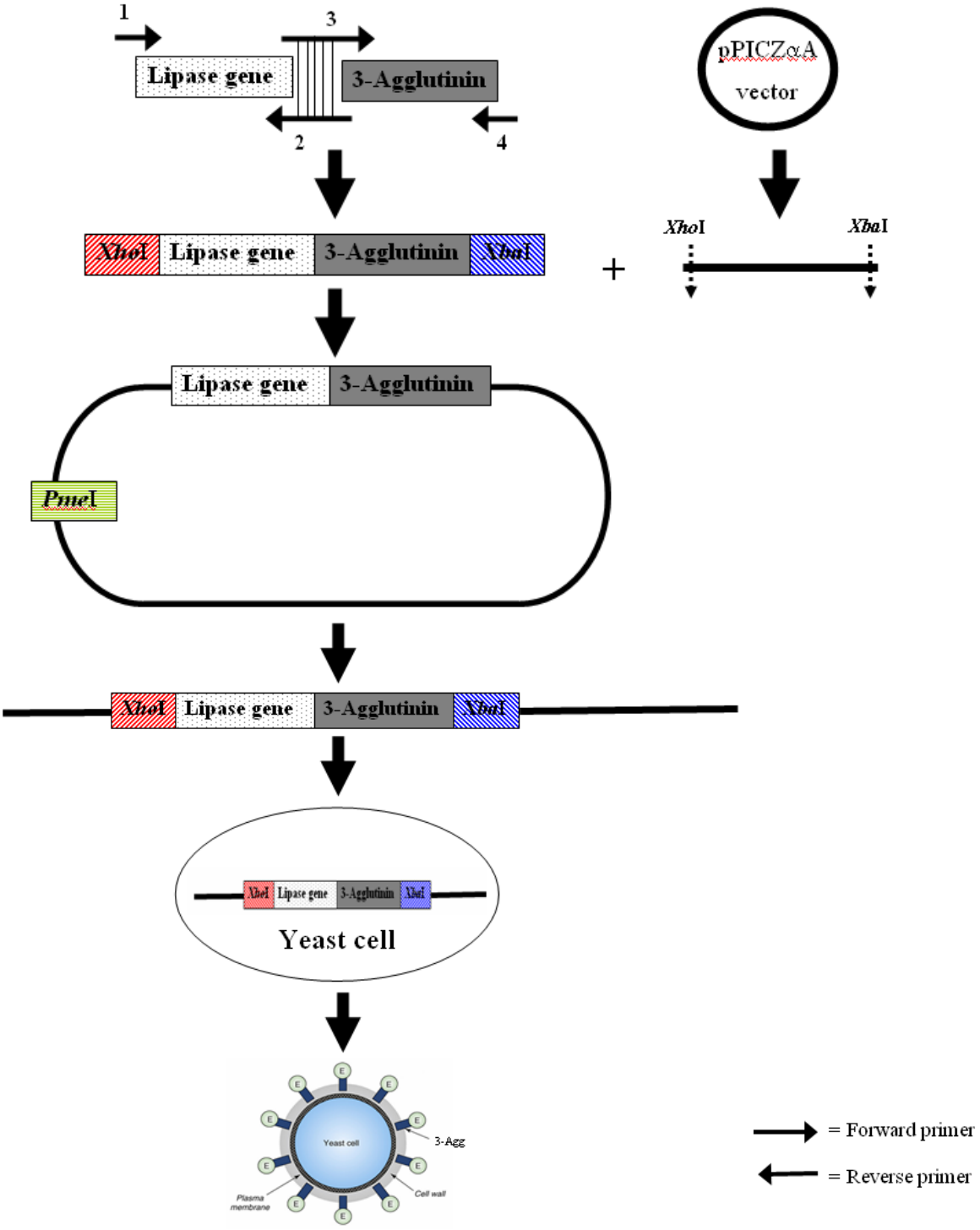


**Figure 6.2** Construction of recombinant plasmids for cell surface expression of lipase**.**

### 6.1.3 Construction of recombinant *P. pastoris* for extracellular expression of lipase

For expression of extracellular lipase in *P. pastoris*, the mature genes of lipase from *T. lanuginosus* (lipase TL) and *C. antarctica* lipase (lipase CA) (876 bp for lipaseTL and 1029 bp for lipaseCA) were amplified from the full-length synthesized lipase gene using LipTL_sec_F and LipTL_sec_R for lipase TL, and LipCA_sec_F and LipCA_sec_R for lipase CA (Table 6.2) with the amplification conditions for the cell surface expression of lipase. The PCR products contained the lipase gene was named LipaseTL_sec and LipaseCA_sec. The amplicons were purified (APPENDIX B: Figure B3) and cloned into pJET1.2 vector. An illustration of linearized recombinant plasmids digested with *Pme*I was shown the resulted in 4.5 kb, and 4.6 kb fragments for pLipaseTL_sec and pLipaseCA_sec, respectively (APPENDIX B: Figure B4). Overall, transformation and expression of recombinant *P. pastoris* for extracellular expression of lipase were performed as the same method that used for cell-surfaced expression of lipase.

**Table 6.2** Primers used for construction of extracellular expression of lipase.

| Lipase | Primer name | Gene (5′ ⟶ 3′) |
|---|---|---|
| *T. lanuginosus* | LipTL_sec_F | *Xho* I<br>GCGCCTCGAGAAAAGATCCCCTATTAGAAGA<br>Lipase TL gene<br>Kex2 signal cleavage |
| | LipTL_sec_R | *Xba* I<br>ATCATCTAGAGCCAAGCAAGTACCAATAAGTCC |
| *C. antarctica* | LipCA_sec_F | *Xho* I<br>ATCACTCGAGAAAAGAACCCCTTTGGTTAAGAGATT<br>Lipase CA gene<br>Kex2 signal cleavage |
| | LipCA_sec_R | *Xba* I<br>ATCATCTAGAGCTGGTGTGACGATTCCTGAG |

### 6.1.4 Heterologous expression of lipase from recombinant *P. pastoris*

The transformant cells were grown in 50 ml of buffered glycerol-complex medium (BMGY; Invitrogen) and incubated at 30 °C with shaking until the culture reached an $OD_{600}$ nm of 2–6. Cells were then harvested by centrifugation and resuspended in buffered minimal methanol yeast medium (BMMY) using 1/5 volume of the original buffered minimal glycerol yeast culture (BMGY). The cells were induced by the addition of methanol at 3% (v/v) every 24 h during incubation at 30°C for 5 day. After induction, the cells were harvested by centrifugation, washed three times in ice-cold isolation buffer (20 mM Tris-HCl, pH 8, 150 mM NaCl, 0.01% Triton X-100, and 0.01% gum Arabic), and resuspended in 500 µl of isolation buffer. The harvested cells and supernatants were then analyzed by lipase activity, including the protein analysis by SDS-PAGE electrophoresis.

### 6.1.5 Protein purification by His-Trap affinity columns

The $His_6$ lipase fusion was purified using His-Trap affinity columns containing nickel-nitrilo-triacetic acid matrix according to the manufacturer's protocol (GE-Healthcare Biosciences, Uppsala, Sweden). The soluble fraction from the induced cultures was filtered through a 0.2 µm membrane filter to remove the cell debris. The clarified soluble fraction was applied to the column that pre- equilibrated with 5 column volumes of binding buffer (20 mM sodium phosphate, 0.5 M NaCl, 40 mM imidazole, pH 7.4) at a flow rate of 1 ml/min. The unbound proteins were washed out with 5 column volumes of binding buffer. The $His_6$ tag proteins were eluted with elution buffer by different imidazole concentrations (100 mM, 200 mM, 300 mM, 400 mM, and 500 mM). The purity of the enzyme was estimated on a 12% SDS-PAGE gels and visualized with Coomassie Blue R-250.

### 6.1.6 Western blot analysis

The expression protein from the induced *P. pastoris* was separated on SDS-PAGE and transferred into a nitrocellulose membrane using an electroblotting apparatus as described by the manufactures (Bio-Rad Mini Trans-Blot Electrophoretic Transfer Cell). The protein samples were tested by using the mouse antibody conjugated to anti-His antibody containing alkaline phosphatase (Invitrogent, Carlsbad, CA) and detected the product yield by using BCIP NBT (5-Bromo-4-chloro-3-indolyl phosphate in combination with nitro blue tetrazolium) as the substrate compared with the 12% SDS-PAGE gel and visualized with Coomassie Blue R-250.

### 6.1.7 Lipase activity assay

Lipase activity was assayed based on the hydrolysis of *p*-nitrophenyl palmitate [4, 117]. The standard reaction (200 µl) contained 20 mM sodium phosphate buffer, pH 8, 1 mM of *p*-nitrophenyl palmitate and an appropriate dilution of the enzyme or immobilized enzyme. The reaction was incubated at 45°C for 30 min and then terminated by the addition of 100 µl of 0.2 M $Na_2CO_3$. The formation of *p*-nitrophenolate was determined by measuring the absorbance at 405 nm. One unit of the enzyme activity was defined as the amount of enzyme catalyzing the release of 1 µmole *p*-nitrophenolate/min under the standard experimental conditions. Protein concentration was assayed using a Bradford's method with BioRad Protein Assay Reagent (Biorad, Hercules, CA) according to the manufacture's protocol.

## 6.2 Results and discussion

### 6.2.1 Heterologous expression of recombinant plasmids for cell-surface display and extracellular expression of lipase

The work was focused on the construction of the recombinant plasmids containing a synthesized lipase gene from *T. lanuginosus* and *C. antarctica*. Several recombinant *P. pastoris* clones of cell surface display and secreted forms were constructed for the protein expression of lipase by induction with 3% methanol in BMMY media. The cell surface recombinant *P. pastoris* containing pLipaseTL_agg (*P. pastoris*/pLipaseTL_agg) and pLipaseCA_agg (*P. pastoris*/pLipaseCA_agg) together with the extracellular recombinant *P.*

*pastoris* containing pLipaseTL_sec (*P. pastoris*/pLipaseTL_sec) and pLipaseCA_sec (*P. pastoris*/pLipaseCA_sec) were designated for recombinant expression study. For the extracellular expression of lipase, the expected sizes of the target proteins of LipaseTL_sec (≈35 kDa) and LipaseCA_sec (≈40 kDa) were observed in the supernatant fractions from *P. pastoris*/pLipaseTL_sec clone 6 (T6) and *P. pastoris*/pLipaseCA_sec clone 8 (C8), respectively (Figure 6.3).

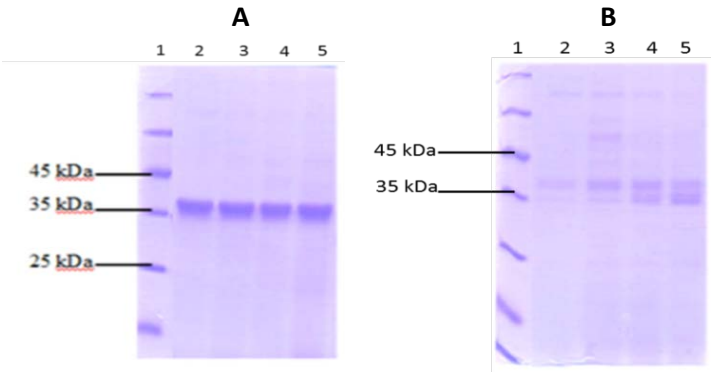


**Figure 6.3** Protein profiles in the supernatant fraction of *P. pastoris* expressed from lipaseTL_sec and lipaseCA_sec gene.
A: Lane 1; protein marker; and Lane 2-5; *P. pastoris*/pLipaseTL_sec clone 6 from Day1-Day4
B: Lane 1; protein marker; and Lane 2-5; *P. pastoris*/pLipaseCA_sec clone 8 from Day1-Day4

The extracellular expression of lipase was confirmed by western blot analysis using an antibody against the $His_6$ tag (Figure 6.4). A control band of 45 kDa was detected. However, a positive band with the corresponding size was observed only for lipaseCA_sec while no band was detected for LipaseTL_sec. The cell surface protein lipases could be not detected by SDS-PAGE method, so these lipases were analyzed by lipase activity.

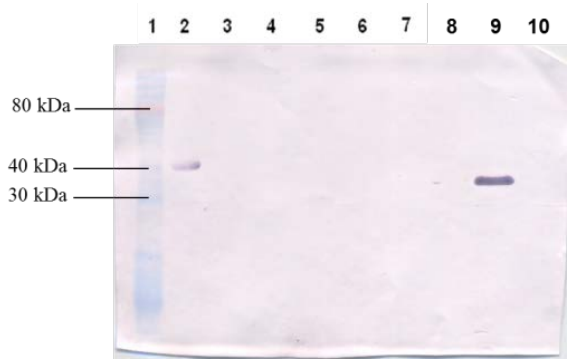


**Figure 6.4** Western blot analysis of protein profiles from recombinant *P. pastoris* clones expressing lipaseTL_sec and lipaseCA_sec gene. Lane 1: pre-stained protein marker, Lane 2: positive control (Uridine-cytidine kinase 1, UCK1), Lane 3: negative control (*P. pastoris*/pPICZαA), Lane 4: *P. pastoris/* pLipaseTL_sec clone T5**,** Lane 5: *P. pastoris*/pLipase TL_sec clone T6**,** Lane 6: *P. pastoris/* pLipaseTL_sec clone T7**,** Lane 7: *P. pastoris*/pLipaseTL_sec clone T9, Lane 8: *P. pastoris*/pLipaseCA_sec clone C6**,** Lane 9: *P. pastoris*/pLipaseCA_sec clone C8**,** Lane 10: *P. pastoris*/pLipaseCA_sec clone C12**.**

### 6.2.2 Lipase activity analysis of cell-surface display lipase

Lipase activity of the cell-surface display yeasts were analyzed by assaying the hydrolysis activity on *p*-nitrophenyl palmitate. The recombinant *P. pastoris*/pLipaseTL_agg showed a higher lipase activity in the cell pellet fraction in comparison to the supernatant fraction while no significant lipase activity was found for the control yeast, suggesting the potential expression of the lipase on the yeast cell-surface (Table 6.3). The highest lipase activity in the cell pellet fraction of $21.8\times10^{-3}$ IU/ml was observed at day 4 for *P. pastoris*/pLipaseTL_agg clone number 2.

**Table 6.3** Analysis of lipase activity in the cell and supernatant fractions of the recombinant *P. pastoris* for lipase TL.

| Date | Activity (IU/ml)×$10^{-3}$ | | | | | |
|---|---|---|---|---|---|---|
| | *P. pastoris*/pLipaseTL_agg clone 2 | | *P. pastoris*/pLipaseTL_agg clone 15 | | *P. pastoris* control | |
| | cell pellet | medium | cell pellet | medium | cell pellet | medium |
| 0 | 0 | 0 | 0 | 0 | 0 | 0 |
| 1 | 10.5 | 6.4 | 0.1 | 0 | 0 | 0 |
| 2 | 12 | 4.8 | 0.1 | 0 | 0 | 0 |
| 3 | 13.1 | 3 | 0.5 | 0 | 0 | 0 |
| 4 | 21.8 | 6.8 | 0.6 | 1.2 | 0.4 | 0 |
| 5 | 14.7 | 4.7 | 0.6 | 1.2 | 0.6 | 0 |

The recombinant *P. pastoris*/pLipaseCA_agg showed a higher lipase activity in the cell pellet fraction in comparison to the supernatant fraction while no significant lipase activity was found for the control yeast, suggesting potential expression of the lipase on the yeast cell-surface (Table 6.4). The highest lipase activity in the cell pellet fraction of 71.2 ×$10^{-3}$ IU/ml was observed at day 5 for *P. pastoris*/pLipaseCA_agg clone number 4.

**Table 6.4** Analysis of lipase activity in the cell and supernatant fractions of the recombinant *P. pastoris* for lipase CA.

| Date | Activity (IU/ml)×$10^{-3}$ | | | | | |
|---|---|---|---|---|---|---|
| | *P. pastoris*/pLipaseCA_agg clone 1 | | *P. pastoris*/pLipaseCA_agg clone 4 | | *P. pastoris* control | |
| | cell pellet | medium | cell pellet | medium | cell pellet | medium |
| 1 | 0.1 | 0 | 2.8 | 0.2 | 0 | 0 |
| 2 | 1.7 | 0.1 | 11.1 | 2.8 | 0 | 0 |
| 3 | 6.1 | 1.2 | 22.2 | 3.6 | 1.0 | 0 |
| 4 | 20.7 | 3.4 | 39.6 | 4.2 | 1.1 | 0 |
| 5 | 39.5 | 4.5 | 71.2 | 7.8 | 1.1 | 0 |

Preliminary study on conversion of RPO and palmitic acid using whole cell *P. pastoris*/pLipaseTL_agg and *P. pastoris*/pLipaseCA_agg were performed under the standard biodiesel synthesis reaction. The reaction contained 10% of the whole cell biocatalyst, and incubated at 50 °C for 24 h in presence of tert-butanol. However, no FAME was detected under the experimental conditions. This could be due to the relatively low lipase

activity of the recombinant cell surface lipase display yeasts as compared with that of cell surface lipase expressed on *S. cerevisiae* cells using Flo1p protein at N-terminal fusion which presented the lipase activity with $145\times10^{-3}$ IU/ml [185]. This finding can be related to several factors, including the effect of the fusion sequence to gene expression and folding, and the intrinsic properties of the target lipase.

### 6.2.3 Lipase activity analysis and enzyme purification of secreted lipase

Lipase activity of the secreted lipase was analyzed by the hydrolysis activity on *p*-nitrophenyl palmitate. The recombinant *P. pastoris*/pLipaseTL_sec and *P. pastoris*/pLipaseCA_sec showed a high lipase activity in supernatant fraction while no significant lipase activity was found for the control yeast, suggesting potential expression of the secreted lipase (Table 6.5). The highest lipase activity in the supernatant fraction of $0.3\times10^{-3}$ IU/ml was observed at day 2 for *P. pastoris*/pLipaseTL_sec clone number 6, and $1.4\times10^{-3}$ IU/ml at day 3 for *P. pastoris*/pLipaseCA_agg clone number 8.

**Table 6.5** Analysis of lipase activity in the supernatant fractions of the recombinant *P. pastoris.*

| Date | Activity (IU/ml)×$10^{-3}$ | | |
|---|---|---|---|
| | *P. pastoris*/pLipaseCA_sec clone 8 | *P. pastoris*/pLipaseTL_sec clone 6 | *P. pastoris* control |
| 1 | 0.8 | 0.1 | 0.0 |
| 2 | 1.1 | 0.3 | 0.0 |
| 3 | 1.4 | 0.2 | 0.0 |
| 4 | 1.3 | 0.2 | 0.0 |

The recombinant $His_6$-tagged lipases (LipaseTL_sec and LipaseCA_sec) were purified from the crude supernatant of the corresponding recombinant *P. pastoris* at day 4. The crude supernatant showed lipase activity of $0.2\times10^{-3}$ IU/ml and $1.3\times10^{-3}$ IU/ml, respectively for LipaseTL_sec and LipaseCA_sec (Table 6.6). This was equivalent to the specific activity of $1.2\times10^{-3}$ IU/mg and $12.5\times10^{-3}$ IU/mg, respectively. The target proteins were then purified on a His-Trap column according to the manufacturer's protocol. The protein bands of ≈35-45 kDa were observed in the eluted fraction using 100-200 mM imidazole and 200 mM imidazole concentration for LipaseTL_sec and LipaseCA_sec, respectively. The purified proteins were

obtained with >95% homogeneity according to SDS-PAGE (Figures 6.5-6.6). The flow through fraction of LipaseTL_sec had found no expressed protein and that of LipaseCA_sec showed another size of the unknown protein.

**Table 6.6** Analysis of catalytic lipase efficiency in the supernatant fractions of the recombinant *P. pastoris* using LipaseTL_sec (T6), and LipaseCA_sec (C8)

| Expression clone | Conditions | Day | Enzyme Assay | | | | | |
|---|---|---|---|---|---|---|---|---|
| | | | Activity (IU/ml)×$10^{-3}$ | Total volume (ml) | Total activity (IU)×$10^{-3}$ | Yield (%) | Protein (mg/ml) | Specific activity (IU/mg)×$10^{-3}$ |
| T6 | Crude | 4 | 0.2 | 5 | 1.0 | 100 | 0.173 | 1.2 |
| | Purification | 4 | 0.15 | 3.8 | 0.57 | 57.0 | 0.077 | 1.9 |
| C8 | Crude | 4 | 1.3 | 5 | 6.5 | 100 | 0.106 | 12.5 |
| | Purification | 4 | 0.4 | 2.5 | 1.0 | 15.4 | 0.027 | 13.1 |

The purified LipaseTL_sec showed a slightly higher specific activity of $1.9\times10^{-3}$ IU/mg compared to the crude supernatant. A higher specific activity of $13.1\times10^{-3}$ IU/mg was also observed with the purified LipaseCA_sec. The specific lipase activities observed with the recombinant lipases in this study was dramatically lower than the previous works, which were 8571 and 372 IU/mg of specific activity from recombinant *P. pastoris* of extracellular *Rhizopus oryzae* and *Geotrichum candidum* lipase, respectively [186, 187]. This could be due to effect of folding and intrinsic properties of the target lipase. However, these finding suggested that the specific activity of purified His-tagged protein was higher than that of crude protein prior to purification step due to the removal of endogenous protein by His-trap affinity column. Therefore, the purified proteins of *P. pastoris*/pLipaseTL_sec clone T6 and *P. pastoris*/pLipaseCA_sec clone C8 will be further done on production of lipase, leading to immobilized lipase for application in biodiesel production process.

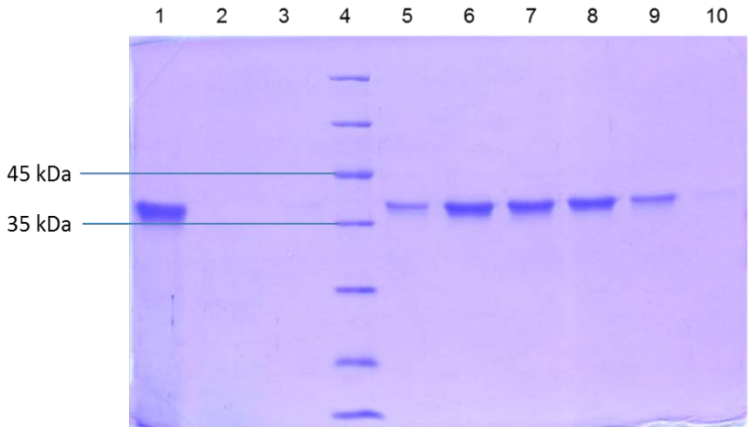


**Figure 6.5** SDS-PAGE analysis of protein profile from recombinant *P. pastoris*/pLipaseTL_sec clone T6 purified on a HisTrap HP affinity column. Lane 1: the supernatant of T6, Lane 2: flow through fraction, Lane 3: washing fraction, Lane 4: protein marker, Lane 5-7: eluted fraction with 100 mM imidazole at 1, 2, and 3 ml**,** respectively Lane 8-10: eluted fraction with 200 mM imidazole at 1, 2, and 3 ml, respectively.

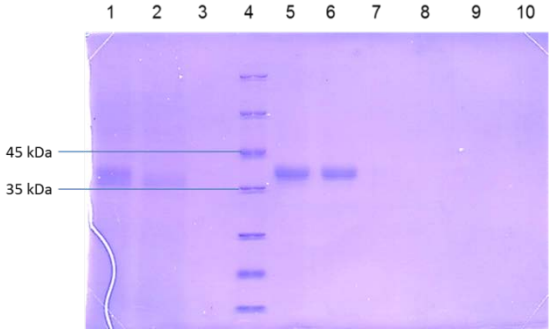


**Figure 6.6** SDS-PAGE analysis of protein profile from recombinant *P. pastoris*/pLipaseCA_sec clone C8 purified on a HisTrap HP affinity column. Lane 1: the supernatant of C8, Lane 2: flow through fraction, Lane 3: washing fraction, Lane 4: protein marker, Lane 5-7: eluted fraction with 200 mM imidazole at 1, 2, and 3 ml**,** respectively Lane 8-10: eluted fraction with 300 mM imidazole at 1, 2, and 3 ml, respectively.

## 6.3 Conclusion

Expression systems for the cell-surface display and the extracellular expression of lipase in *P. pastoris* were constructed in this study. Lipase activity was detected for all constructed; however, with a very low level compared to the previous works [185, 187-190]. This could be due to effect of folding and intrinsic properties of the target lipase, including the deactivation of target proteins and *P. pastoris* cells by high concentration of inducible methanol. Therefore, these problems could be improved by further optimization of the induction conditions; for example, by varying the proportion of methanol additions (0.5%, 1%, 2% (v/v)) in BMMY media, including selection more transformant cells from corrected insertion of PCR fragments for cell-surface display and extracellular expression of lipase.

Several alternative promoters in *P. pastoris* expression system such as pFLD1, pEPEX8, pYPT1, pTEF and pGAP have been reported for replacing the AOX1 promoter [191]. Especially, the glyceraldehyde-3-phosphate dehydrogenase promoter (pGAP) has been mostly used for constitutive expression of heterologous recombinant proteins due to removal of methanol induction and requirement single carbon source for cell growth and protein expression, leading to cost-effective approach for non-methanol inducible *P. pastoris* expression system [191, 192]. The recombinant *P. pastoris* can then apply to product lipase for preparation of immobilized enzymes using the techniques developed in this thesis.

# CHAPTER 7
# BIOETHANOL PRODUCTION FROM PALM KERNEL CAKE

Bioethanol is a renewable fuel conventionally produced from sugar and starch-based feedstock with the potential for production from lignocellulosic biomass. The conversion of lignocelluloses to ethanol involves three main steps: pretreatment, enzymatic hydrolysis, and fermentation process. In Thailand, oil palm wastes, including palm kernel cake (PKC) from palm oil processing represent potent underused lignocellulosic biomass for valorization. This study focused on the conversion of PKC to bioethanol by engineered *Geobacillus thermoglucosidasius* in comparison to *Saccharomyces cerevisia* yeast. The effects of steam explosion pretreatment on enzymatic hydrolysis of PKC were studied for subsequent conversion to ethanol using the novel ethanologen.

## 7.1 Materials and methods

### 7.1.1 Materials

Palm kernel cake (97.07% oven dry solids) was obtained from Suksomboon Palm Oil Industry, Thailand. The PKC was milled to reduce the size after sorting out some stone-hard kernel shells (5% of the total PKC). Enzyme, Driselase from *Basidiomycetes* sp was purchased from Sigma Aldrich, while Advanced Enzymes Technology mannanase (AET Mannanase) was obtained from Advanced Enzymes Technology, India and, Cellic CTec2 cellulase (CTec2) was supplied by Novozymes (Bagsvaerd, Denmark). *A thermophilic* bacterium, *Geobacillus thermoglucosidasius* TM242 strain was provided by TMO Renewables Limited (through Prof. David Leak, University of Bath). Two other yeast strains, Vodka Turbo Yeast (*Saccharomyces cerevisiae*) and a *Saccharomyces cerevisiae* strain S228C were obtained from Hambleton Bard, Chesterfield, UK (hambletonbard.com) and Allen Wheals collection, University of Bath, respectively and used in comparing ethanol production from enzyme hydrolyzed PKC. All chemical reagents and standard sugars e.g. mannose, glucose, xylose, arabinose, and galactose were analytical grade (>99% purity) and purchased from Sigma Aldrich. For the growth of the bacteria, the Tryptone Soya Agar (TSA) plate was composed of 15 g casein peptone, 5 g soy peptone, 5 g sodium chlorides, and 15 g agars per liter. Inoculum production was on Salt Peptone Yeast extract (SPY) containing 16 g peptone, 8 g yeast extract, and 5 g

sodium chloride per liter. For the growth of yeast, Yeast Peptone Dextrose (YPD) medium or agar plates were used for the the yeast culture, which contained 10 g yeast extract, 20 g peptone, 20 g glucose, and 15 g agar (for plates) per liter.

### 7.1.2 Steam explosion pretreatment of PKC

PKC was milled by a grinder and separated through a 2-mm diameter sieve. A 20% w/w of PKC in distilled water was pre-treated using steam explosion in a 1 L volume of Parr 4531 floor stand pressure reactor (Parr Instruments, USA) with a steam generator (Priorclave Ltd, London, Ik). Various pre-treatment conditions of pressure (4.5 – 6.5 bar), temperatures (148-163 °C), and incubation times (5-20 min) were applied. High pressure steam supplied by the steam generator was injected into the reactor chamber together with extra heating from a heat jacket until it reached the target experimental temperature. The biomass was exploded by immediately releasing the pressure out of reaction chamber, leading to further size reduction of PKC, and the pretreated biomass was collected from the pressure release pipe into a collecting vessel on ice. The reactor was also cooled with an ice pack during the explosion, and the pretreated contents were mixed with the initial collection from the pressure release pipe. The PKC samples were pretreated by steam explosion compared to the standard sterilization condition in an autoclave (121°C and 15 minutes) which was used as a benchmark method. All corresponding samples after pretreatment were sterilized by autoclave treatment and kept in 500 ml of plastic bottles at 4 °C in refrigerator before use in enzyme hydrolysis and fermentation step.

### 7.1.3 Enzymatic hydrolysis (EH)

A cellulase from Novozymes (Cellic CTEC2) at 10.38 FPU/g glucan was used as a basic enzyme for cellulose hydrolysis in PKC. The enzyme was supplemented with mannanase (Driselase (≥800 U/g), AET Mannanase (25,678 U/g), or a 1:1 mixture of them) at different levels (1.67%, 5%, and 10% mannanase/g mannan) using 5%w/w pretreated PKC at 4.5 bar at 5 min. The pretreated PKC was adjusted to 5%w/w dry matter in screw-capped tubes and was adjusted to pH 5 using 5 M phosphoric acid ($H_3PO_4$) and 5 M potassium hydroxide (KOH) prior to enzyme addition, and subsequently incubated at 50 °C for 72 h with shaking at 250 rpm in a Centrifuge 5810R (Eppendorff AG, Hamburg, Germany). The enzyme reaction was terminated by boiling at 100 °C for 5 min and kept at 4 °C in refrigerator before use for fermentation or analysis. All other enzymatic hydrolysis (EH) of 5% w/w of PKC at various pretreatment conditions were performed by using the determined optimal enzyme loading under the same reaction conditions in triplicate.

After the enzymatic hydrolysis, some of the samples were fermented to ethanol, while some of the corresponding samples was centrifuged at 4,000 x g for 15 min, and then filtered through 0.22 μm of nylon syringe filters for sugar analysis. The 5% PKC samples before enzyme hydrolysis were also filtered and analyzed for monomeric and oligomeric sugars (by acid hydrolysis of filtered samples). All chemicals, reagents and equipment in this step were sterilized before use.

**7.1.4 Inoculum production and PKC fermentation/ethanol production**

The *G. thermoglucosidadus* TM242 strain stored at -80 °C was spread on Tryptone soya agar plate (TSA plate) and incubated at 60°C overnight. The inoculum production step for bacteria was performed by inoculating a colony of bacteria into 50 ml of SPY medium of pH 7 in 250 ml sterile baffled flasks and incubated aerobically at 60°C and 250 rpm in a Innova 44 incubator shaker (New Brunswick Scientific Ltd, city, UK) until the absorbance at 600 nm reached between 7 and 8. The 5 %w/w of PKC hydrolysate was adjusted to pH 7 using the same chemical reagents as in EH step, and subsequently 1.2 ml of 1 M organic buffer mix (MOPS, HEPES, and Bis-Tris), and some drops of antifoam (0.44 ml) to minimize foaming were added to 10 ml of hydrolyzed biomass in a sterile plastic screw-cap tube. The tubes were warmed up to 60°C and inoculated with 1 ml of TM242 in SPY medium ($OD_{600}$ at 7-8) and fermented at 60 °C for 48 h with shaking at 250 rpm with the lids tightly closed. The *S. cerevisiae* strains were separately pre-cultured in YPD plate incubated at 30°C overnight. Then, the yeasts were grown in 50 ml of YPD medium at pH 5.5. After 24 h, 1 ml of yeast cell (diluted to OD 8) in YPD medium was added to the 5 % w/w of hydrolyzed PKC (adjusted to pH 5.5) containing the same buffer and antifoam. Fermentation of PKC by yeasts was done at 250 rpm, 30°C and 48- 72 h with/without the additional step of puncturing the screw-cap with the needle (the top of needle was filled with sterile cotton wool) to let out excess $CO_2$ in tubes. After fermentation, the fermented samples were centrifuged at 4,000 x g for 15 min and then filtered through 0.22 μm of a syringe nylon filter. The amounts of sugars, ethanol, and by-products were determined by HPLC analysis based on the standard curves of the corresponding products (monosaccharides, ethanol, and metabolic products e.g. citrate, pyruvate, acetate, and lactate). The theoretical ethanol yield (%) is the amount of ethanol converted from available total sugars in 5% PKC based on the maximal theoretical yield of 0.51 g ethanol/g glucose. The residue sugars in the forms of monosaccharides and oligosaccharides were analyzed by ion chromatography with/without acid hydrolysis step

based on standard curves of the corresponding monosaccharides (glucose, mannose, xylose, galactose, and arabinose).

### 7.1.5 Acid hydrolysis and total sugar compositional analysis in samples and PKC biomass

All samples were analyzed for monomeric sugars, and an additional step for analyzing soluble oligomeric sugars were performed through acid hydrolysis, which cleaved off glycosidic bonds from oligosaccharides to produce monosaccharides, which could then be determined by the sugar ion chromatogram. The difference between the sugars post acid hydrolysis and pre-acid hydrolysis was assumed to be oligomeric sugars after correction for sugar recovery under acid hydrolysis. The samples were filtered and 0.035 ml of 72% w/w $H_2SO_4$ was added to 1.0 ml of sample in glass vial with lid and then autoclaved at 121 °C for 60 min. The samples were cooled on ice for 10 min before adding calcium carbonate ($CaCO_3$) powder to neutralize the samples to between pH 6 and 7. Then, the neutralized samples were filtrated through a 0.22 μm of nylon syringe filter into a suitable glass vial and kept at -20 °C until further sugar analysis.

The analysis of PKC composition, the crude protein and oil were performed by the micro Kjeldahl nitrogen and hexane extraction methods, respectively. According to sugar composition analysis on the PKC biomass, 3 levels of biomass (0.1g, 0.2g and 0.3g) were individually added to a screw top Duran bottle of 100 ml. Three ml of 72% w/w $H_2SO_4$ was added and the samples were incubated at 30°C for 1 h at 100rpm. Then the samples were diluted with 84 ml of Milli-Q water and autoclaved at 121 °C for 60 min, cooled on ice, neutralized with calcium carbonate ($CaCO_3$) to between pH 6 and 7, and filtered through a 0.22 μm of nylon syringe filter into a suitable glass vial and kept at -20 °C until further sugar analysis. A sugar recovery test was also applied to the samples.

### 7.1.6 Ion chromatography analysis of sugars (monosaccharide and oligosaccharide)

The liquid samples post pretreatment, enzyme hydrolysis and also the samples after acid hydrolysis were all analyzed for sugars. The separation and quantification of arabinose, galactose, glucose, mannose, and xylose were performed using a Dionex ICS-5000 machine (Thermo Scientific, USA) with a Dionex CarboPac SA10 column (4×250 mm) and guard column on 1.5 ml/min of flow rate using pulsed amperometric detection. The separation was performed at 25°C for 10 min using gradient elution with 1 mM sodium hydroxide (NaOH) at 1.5 ml/min and 10 μl injection volume. The samples were

appropriately diluted in Milli-Q water and filtered through a 0.22 μm of syringe filter prior to analysis.

### 7.1.7 High-performance liquid chromatography analysis of ethanol and other acid post-fermentation

The amount of glucose, arabinose, and ethanol after fermentation was done using an Agilent HPLC system with a Phenomenex Rezex RHM Monosaccharide H column (300 m × 7.8 mm, Phenomenex Inc) and (Refractive index and UV) detectors. Separation was performed at 65°C for 30 min with a flow rate of 0.6 ml/min 5 mM $H_2SO_4$. In this column, mannose, galactose, and xylose were all co-eluted, so this was mainly used for ethanol and other metabolic product analysis. All samples were appropriately diluted in Milli-Q water and filtered through a 0.22 μm filter prior to analysis.

## 7.2 Results and discussion

### 7.2.1 Palm kernel cake composition

In the first step, the PKC was milled and sieved to screen for biomass with a homogenous size range. Approximately 90% of milled PKC was recovered while the harsh shell was removed, which accounted for 10% on weight basis. According to component analysis, the PKC contained 52.4 %w/w of carbohydrate, whereas the other compositions comprised 17.1 %w/w of crude protein, 10.2 %w/w of oil/fat, and 20.3 %w/w of other components e.g. lignin, ash, extractives, and minerals on dry weight basis (Table 7.1). The lignin content in PKC was rather low as compared to the other lignocelluloses, such as empty palm fruit bunch, which contained 28.8% lignin [193]. The protein content in PKC was relatively high, suggesting its potential for using as animal feed supplement [194]. The composition of PKC in this study was similar to that previously reported by Jørgensen et al. (2010) which contained 55.2 %w/w of carbohydrate, 10.2 %w/w of lignin, 16.8 %w/w of protein, and 4.4 %w/w of ash [21] .

**Table 7.1** Palm kernel cake composition based on dry weight basis.

| Component | Monosaccharide | Composition (%) |
|---|---|---|
| Cellulose | Glucose | 11.6 |
| Hemicellulose | Mannose | 38.2 |
| | Xylose | 0.9 |
| | Arabinose | 1.2 |
| | Galactose | 0.9 |
| Crude protein | | 17.1 |
| Crude oil | | 10.2 |
| Others (lignin, ash, minerals and extractives) | | 20.3 |

The total sugars in PKC were determined by acid hydrolysis, which cleaves polysaccharide to monosaccharide before analysis by ion chromatography. The results showed that mannose constituted the major sugar in PKC, which accounted for 38.2 %w/w on a dry weight basis, whereas the glucose content was lower with 11.6 %w/w. Other sugars, such as arabinose, xylose, and galactose, was less than 3 %w/w. The sugar profile of PKC in this study was similar to that reported by Cerveró et al [20] which showed that mannose and glucose represented the major sugars in PKC with 35.2% and 8% w/w content, respectively. Regarding to the result, the hemicellulose fraction was accounted for 41.2% in PKC while cellulose constituted 11.6% which resulted in the total carbohydrate content of over 50 %. The main purpose of the study is thus to optimize the pretreatment and enzymatic process to release the maximal sugars from PKC.

### 7.2.2 Effect of steam explosion pretreatment

Steam explosion is an efficient pretreatment method that can increase the digestibility of the cellulose fraction by autohydrolysis of the hemicellulose, and together with the explosive effects of swift pressure release, lead to increasing enzyme accessibility for the cellulose fibers. This pretreatment has been efficiently used with various agricultural residues e.g. corn stover [195] and wheat straw [100]. In this study, the pretreatment of PKC was studied using 20 % w/w dry matter with varying reaction parameters (pressure and temperature) in different residence times. In Table 7.2, the result showed that the severe pretreatment condition at 6.5 bar with 163 °C for 20 min led to the highest total sugar yield of 16.54 g/L (62.7 % of total sugars) compared with the other experimental conditions. High manno-oligosaccharide of 9.42 g/l was found in the liquid phase which accounted for 57% of the total release sugars while the other mono and oligosaccharide (glucose, xylose, arabinose, and galactose) were the minor products.

Increasing sugar yield was found with increasing time from 15 to 20 min under the pressure of 4.5 bar and the temperature at 148 °C which led to the sugar concentration of 13.69 and 13.02 g/L (51.9% and 49.3% of total sugars), respectively. In addition, the more severe temperature and pressure, the higher sugar yields obtained; however the more inhibitors from sugar degradation were also observed. The lowest sugar was obtained with PKC obtained from autoclave pretreatment (121°C and 15 min) due to no explosive effect to the PKC structure. According to the result, the manno-oligosaccharide was observed to the majority of released sugar based on the whole pretreatment conditions.

**Table 7.2** Released sugar from steam explosion pretreatment of palm kernel cake under different conditions.

| Pretreatment conditions | time (min) | sugar (g/L) | | | | | | | | | | | | total sugar (g/L) | % of total sugars |
|---|---|---|---|---|---|---|---|---|---|---|---|---|---|---|---|
| | | Glucan | | Xylan | | Arabinan | | Galactan | | Mannan | | total sugar | | | |
| | | Monos | Oligos | Monos | Oligos | Monos | Oligos | Monos | Oligos | Monos | Oligos | Monos | Oligos | | |
| 4.5 bar | 5 | 0.4 | 0.5 | 0.0 | 0.2 | 0.1 | 0.8 | 0.0 | 1.1 | 0.1 | 3.6 | 0.6 | 6.1 | 6.6 | 25.1 |
| | 10 | 0.6 | 0.7 | 0.0 | 0.5 | 0.2 | 1.1 | 0.0 | 1.7 | 0.1 | 6.1 | 0.9 | 10.1 | 11.0 | 41.6 |
| | 15 | 0.8 | 0.7 | 0.1 | 0.7 | 0.3 | 1.3 | 0.1 | 2.0 | 0.3 | 7.5 | 1.5 | 12.2 | 13.7 | 51.9 |
| | 20 | 0.5 | 0.6 | 0.1 | 0.7 | 0.3 | 1.0 | 0.1 | 1.9 | 0.3 | 7.6 | 1.2 | 11.8 | 13.0 | 49.3 |
| 6.5 bar | 5 | 0.7 | 0.3 | 0.1 | 0.5 | 0.3 | 0.8 | 0.1 | 1.3 | 0.2 | 5.3 | 1.3 | 8.2 | 9.6 | 36.2 |
| | 10 | 0.6 | 0.7 | 0.0 | 0.9 | 0.3 | 1.1 | 0.1 | 2.1 | 0.2 | 6.4 | 1.2 | 11.1 | 12.3 | 46.6 |
| | 15 | 0.5 | 0.9 | 0.0 | 1.2 | 0.3 | 1.1 | 0.1 | 2.4 | 0.2 | 6.1 | 1.2 | 11.7 | 12.8 | 48.6 |
| | 20 | 0.6 | 0.8 | 0.1 | 1.3 | 0.4 | 1.2 | 0.1 | 2.3 | 0.3 | 9.4 | 1.5 | 15.0 | 16.5 | 62.7 |
| Autoclave | 15 | 0.1 | 0.7 | 0.0 | 0.2 | 0.0 | 0.5 | 0.0 | 0.7 | 0.0 | 1.7 | 0.2 | 3.8 | 4.0 | 15.2 |

Harsh pretreatment condition can cause partial hemicellulose and lignin degradation, leading to the loss of soluble sugar and higher degradation of sugar monomers to inhibitory compounds to ethanologens [98, 196]. Several toxic compounds, such as furan derivatives, weak acids, and phenolic compounds, are obtained from the lignin degradation and sugar dehydration during the physicochemical pretreatment process [98, 197]. In this study, the toxic compounds (acetic acid, formic acid, and 5-hydroxymethylfurfural (HMF) were generated by steam explosion pretreatment (Figure 7.1). It was found that the acetic acid was detected as the major by-product generated from the acetyl groups in hemicelluloses together with the small amount of formic acid and HMF. The pretreated condition at 6.5 bar for 20 min led to the highest inhibitor formation which comprised of 0.53 g/L acetic acid and the small proportion of formic acid and HMF at 0.04 and 0.01 g/L, respectively. Lower inhibitor formation was found with pretreatment

under milder conditions. The lowest toxic compounds were observed from autoclave pretreatment.

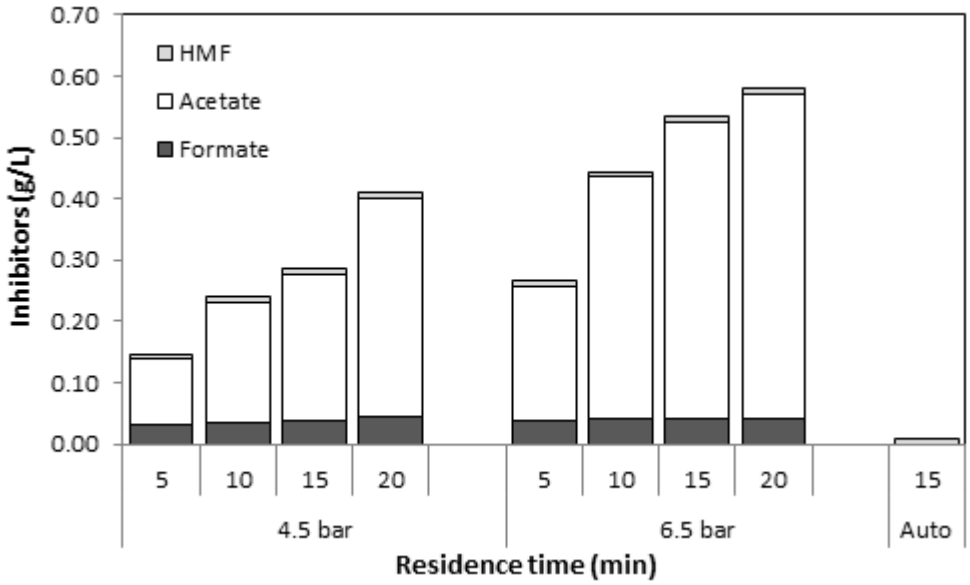


**Figure 7.1** Formation of inhibitory by-products from steam explosion pretreatment of palm kernel cake under different conditions.

According to the results, increasing pressure, temperature, and residence time in the steam explosion pretreatment step of PKC led to the higher sugar yield from enzymatic hydrolysis; however, with increasing toxic compounds under the harsh conditions. The inhibitor profile comprising acetic acid as the major inhibitor from steam explosion was similar to that reported in the pretreatment of spruce, willow, and corn stover [198]. Acetic acid can lead to a drop in the intracellular pH. Acetic acid is dissociated into its anionic form and pass through the cell plasma membrane together with releasing protons into the cytoplasm, which lead to disruption of the cell membrane ATPase efficiency [199]. This damage could affect to metabolism, enzyme activity, and cause higher turgor pressure within the cell, leading to negative effects on biomass and ethanol production [199]. In addition, formic acid can be formed from HMF and furfural degradation under acidic and high temperature conditions. It showed higher toxicity than acetic acid due to its smaller molecular size and its presence in undissociated form which result in its higher membrane permeability [200]. This can lead to inhibition on the synthesis of macromolecule, as well as DNA synthesis and repair [201]. The furan by-product, HMF is derived from hexose degradation, and shows inhibitory effects on glycolytic and fermentative enzymes essential

to metabolic pathways, such as pyruvate dehydrogenases, acetaldehyde dehydrogenases, alcohol dehydrogenases [200], extending lag phase in fermentation [202], as well as protein-protein cross linking and DNA degradation into single strands [203]. These negative effects led to the low growth and fermentation rate, which resulted in reduced ethanol productivity [204]. Furfural is a sugar degradation product from pentoses under harsh pretreatment conditions [205, 206]. It has a similar inhibitory effect to HMF, but with more toxicity [207]. The presence of toxic compounds is a significant obstacle for the development of ethanol production from lignocellulose. In many cases, a detoxification step using biological, physical, and chemical methods might be required for the elimination of these inhibitors; however, this can contribute to higher cost of the overall process [198, 208].

### 7.2.3 Enzymatic hydrolysis

In this step, enzymatic hydrolysis of PKC was initially optimized using the biomass pretreated by steam explosion at 4.5 bar for 5 min in order to reduce the effect of toxic contamination from harsh pretreated conditions. Hydrolysis of the pretreated PKC was studied using a single activity endo-mannanase of Driselase and AET mannanase, or a combination of them (1:1 volume mixture) at 1.67%, 5%, and 10% mannanase/g mannan supplemented with 10.38 FPU/g glucan of Ctec2. As shown in Figure 7.2, it was found that the increase of enzyme loading resulted in the enhancement of released sugar. AET mannanase showed a higher efficiency on hydrolysis of pretreated PKC as compared to Driselase. The increase in total sugar from 27.37 g/L - 29.11 g/L was obtained with increasing AET mannanase dosage after incubation at 50$^{o}$C, pH 5 for 72 h. Approximately 60% of the sugars was in oligomeric form. This was equivalent to the highest total sugar yield of 110.3% from the 5% PKC using 10% AET mannanase loading while >95% of the maximal sugar yield was obtained using 1.67% enzyme. The same trend of increasing sugar with higher enzyme dosage was observed with Driselase but with slightly lower total sugar released and higher relative ratio of oligosaccharides. Combination of both enzyme resulted in lower efficiency on enzymatic hydrolysis of PKC suggesting no activity complementation between the two mannanases. The control reaction with no enzyme led to 9.67 g/L of total sugar indicating partial solubilization of sugars in the pretreated substrate, most of which was in oligomeric form. According to the results, the use of AET mannanase at 1.67% v/w was selected as the optimal dosage for the study based on the

economic aspect. This led to the lowest cost of mannanases with 0.2 baht/kg sugar on enzymatic hydrolysis, as shown in Table 7.3.

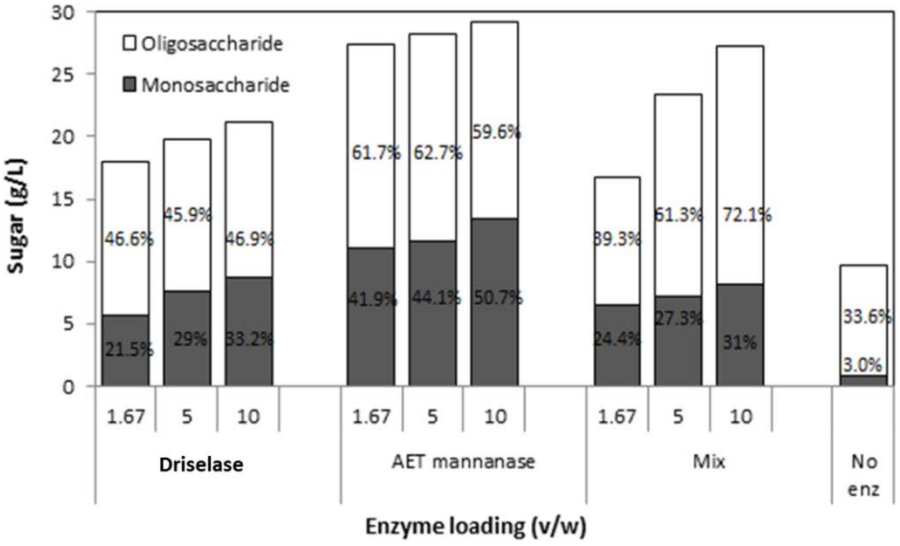


**Figure 7.2** Enzymatic hydrolysis of pretreated palm kernel cake. Reactions contained 5% PKC (pretreated at 4.5 bar for 5 min) at pH 5 with different mannanase (Driselase, AET mannanase or their 1:1 mixture) at varying dosages and incubated at 50 °C for 72 h with shaking at 250 rpm.

**Table 7.3** Cost of mannanases on enzymatic hydrolysis of pretreated palm kernel cake

| Type of mannanase | Enzyme loading (% v/w) | Total sugar (g/L) | Cost (baht/kg sugar) |
|---|---|---|---|
| **Driselase**[1] | 1.67% | 18.0 | 577.2 |
| | 5% | 19.8 | 1572.3 |
| | 10% | 21.1 | 2943.0 |
| **AET mannanase**[2] | 1.67% | 27.4 | 0.2 |
| | 5% | 28.2 | 0.5 |
| | 10% | 29.1 | 1.0 |
| **Mix** | 1.67% | 16.8 | 308.8 |
| | 5% | 23.4 | 665.4 |
| | 10% | 27.2 | 1143.0 |

[1] Driselase cost is 1,554,632 baht/kg (36,238.5 €/kg)

[2] AET mannanase cost is 755.04 baht/kg (17.6 €/kg)

All pretreated samples from different pretreatment conditions were evaluated for their digestibility using the selected conditions for enzymatic hydrolysis (1.67% AET mannanase). Increasing residence time from 5-15 min with a fixed pressure at 4.5 bars led to the increase in total sugar yield from 25.5-28.3 g/L while a slightly decrease in sugar was found at 20 min pretreatment time (Table 7.4). The maximal released sugar (107.2 % of total sugars based on 5% PKC) was achieved from PKC pretreated at 4.5 bar for 15 min. The hydrolysate contained higher monosaccharide (9.1 g/L mannose, 5.1 g/L glucose) than oligosaccharide (9.4 g/L manno-oligo). Increasing pressure to 6.5 bar led to lower sugar product (22.1-24.4 g/L) after enzymatic hydrolysis with a similar trend of residence time. The lower sugar yield have been due to the higher inhibitory by-product formation under the harsher conditions which could in reduce the enzyme activity. The lowest released sugar of 11.4 g/L was observed with PKC pretreated by autoclave, suggesting the marginal effects of the conditions used for conventional sterilization to PKC structure.

The presence of significant oligosaccharide fraction after enzymatic hydrolysis suggested the lack of downstream processing mannanase activity e.g. β-mannosidase in the enzyme mixtures. Normally, β-mannosidase hydrolyzes the β-1,4-manno-oligomers to mannose. Its supplementation to mannanase was reported for hydrolysis of mannan rich substrates. Hydrolysis of PKC on 5% (w/w) dry matter using binary mixtures of mannaway and gammanase (a complex enzyme comprising mannanase, β-mannosidase, α-galactosidase, and β-glucosidase) in 1:1 ratio at 10 %v/w enzyme loading resulted in the total monosaccharide concentration of 13.9 g/L after 24 h reaction at 50$^{o}$C [20]. In addition, the total mannose and glucose of 57 g/L was obtained from hydrolysis of 35% dry matter of PKC incubated at 50 °C for 192 h without pretreatment step using an enzyme mixture at 30:10:1 by volume ratio of endomannanase, β-mannosidase, and cellulase, respectively [21].

In comparison to these previous works, the higher sugar yield with 16.7 g/L using 1.67% AET mannanase was achieved from our work. This would be related to the effects of different pretreatment methods on increasing biomass digestibility. Finding an alternative fermentation strategy using an novel ethanologen which can use oligosaccharide as a substrate for ethanol production is thus a potent approach for reduce cost of the extra β-mannosidase which will contribute to improving economic feasibility of the overall biomass conversion process.

**Table 7.4** Released sugar from enzymatic hydrolysis of pretreated palm kernel cake using AET mannanase.

| Pretreatment conditions | time (min) | Sugar (g/L) | | | | | | | | | | | | Total sugar (g/L) | % of total sugar |
|---|---|---|---|---|---|---|---|---|---|---|---|---|---|---|---|
| | | Glucan | | Xylan | | Arabinan | | Galactan | | Mannan | | Total sugar | | | |
| | | Monos | Oligos | Monos | Oligos | Monos | Oligos | Monos | Oligos | Monos | Oligos | Monos | Oligos | | |
| 4.5 bar | 5 | 5.6 | 0.8 | 0.7 | 0.1 | 0.5 | 0.5 | 0.2 | 1.5 | 6.3 | 9.4 | 13.2 | 12.3 | 25.5 | 96.6 |
| | 10 | 6.4 | 0.3 | 1.0 | 0.0 | 0.7 | 0.5 | 0.4 | 1.7 | 8.0 | 8.3 | 16.4 | 10.8 | 27.1 | 102.7 |
| | 15 | 5.1 | 0.0 | 1.3 | 0.0 | 0.7 | 0.5 | 0.4 | 1.8 | 9.1 | 9.4 | 16.7 | 11.7 | 28.3 | 107.2 |
| | 20 | 6.2 | 0.3 | 1.3 | 0.0 | 0.6 | 0.6 | 0.3 | 1.9 | 6.7 | 9.5 | 15.2 | 12.3 | 27.5 | 104.2 |
| 6.5 bar | 5 | 5.9 | 0.0 | 1.2 | 0.0 | 0.7 | 0.3 | 0.4 | 1.4 | 8.8 | 5.3 | 17.0 | 7.1 | 24.1 | 91.3 |
| | 10 | 5.9 | 0.0 | 1.5 | 0.0 | 0.6 | 0.4 | 0.3 | 1.5 | 5.6 | 6.4 | 13.8 | 8.3 | 22.1 | 83.7 |
| | 15 | 6.4 | 0.0 | 2.2 | 0.0 | 0.7 | 0.3 | 0.5 | 1.6 | 5.2 | 6.4 | 14.9 | 8.3 | 23.2 | 87.9 |
| | 20 | 5.1 | 0.9 | 1.4 | 0.1 | 0.5 | 0.4 | 0.3 | 1.7 | 4.5 | 9.6 | 11.8 | 12.7 | 24.4 | 92.4 |
| Autoclave | 15 | 0.2 | 0.2 | 0.0 | 0.0 | 0.2 | 0.3 | 0.2 | 1.1 | 3.4 | 5.7 | 4.1 | 7.3 | 11.4 | 43.2 |

*The reactions contained 5% PKC (pretreated at 4.5 bar for 15 min) adjusted to pH 5.0 and 1.67% (v/w) AET mannanase and incubated at 50 °C for 72 h with shaking at 250 rpm.

### 7.2.4 Fermentation using different microorganisms

The work in this part is focused on the comparison of the conventional yeast *S. cerevisiae* and the alternative ethanologen *G. thermoglucosidasius* TM242 on fermentation of PKC hydrolysate. *S. cerevisia* is a common ethanologen in ethanol fermentation. Although it is a very robust ethanologen, it does not optimally grow at a temperature higher than 35$^{o}$C and cannot use oligosaccharides for ethanol production. [209, 210]. Recently, an ethanologenic *G. thermoglucosidasius* TM242 has been developed with the capability on thermophilic growth and conversion of oligosaccharide to ethanol. This provides a potent strain appropriate for conversion of the oligosaccharide rich PKC hydrolysate to ethanol. [9].

Figure 7.3 shows that the 5% w/w PKC hydrolysates prepared using different pretreatment conditions were fermented with *G. thermoglucosidasius* TM242 and *S. cerevisiae* S228C. The fermentation mixtures were supplemented with organic buffers and antifoam as described in the method section. *G. thermoglucosidasius* showed high conversion of both mono and oligosaccharides in the hydrolysates compared to the yeast which cannot assimilate oligosaccharides. The highest ethanol concentration of 9.9 g/L was achieved using *G. thermoglucosidasius* with the PKC pretreated under the optimal pretreatment condition (4.5 bar, 15 min) after incubation at 60$^{o}$C for 48 h under anaerobic condition. Lower ethanol yield was found with PKC pretreated at 6.5 bar and with

autoclave. The decrease in ethanol yield with substrates pretreated at 6.5 bar could be related to the higher sugar degradation under conditions with higher severity which led to loss of sugars and formation of inhibitory by-products to enzymes and the fermenting microbe [211]. No accumulation of monosaccharide was observed at the end of fermentation with slight residual concentration of oligosaccharide approximated at 1.1 g/L after fermentation using the thermophilic bacteria under all conditions. The ethanol achieved under the optimal condition was equivalent to 0.47 g/g sugar or 92.4% theoretical (Table 7.5).

Substantially lower ethanol concentration of 2.01 - 4.23 g/L (equivalent to an ethanol yield of 0.10-0.20 g/g) was obtained with the conventional yeast after fermentation at 30$^{o}$C for 72 h using pretreated PKC under different conditions. This was correlated to its lower ethanol yield and sugar utilization efficiency compared to *G. thetmoglucosidasius* under all conditions. The lower ethanol yield from yeast was related to its inability to assimilate oligosaccharide in the hydrolysate as shown by the high residual oligosaccharide that remained after fermentation with slight residual monomeric sugars. The result on ethanol production using *S. cerevisia* S228C was similar to that found with Turbo yeast, which is a commercial yeast strain for wine beverages (data not shown).

**A**

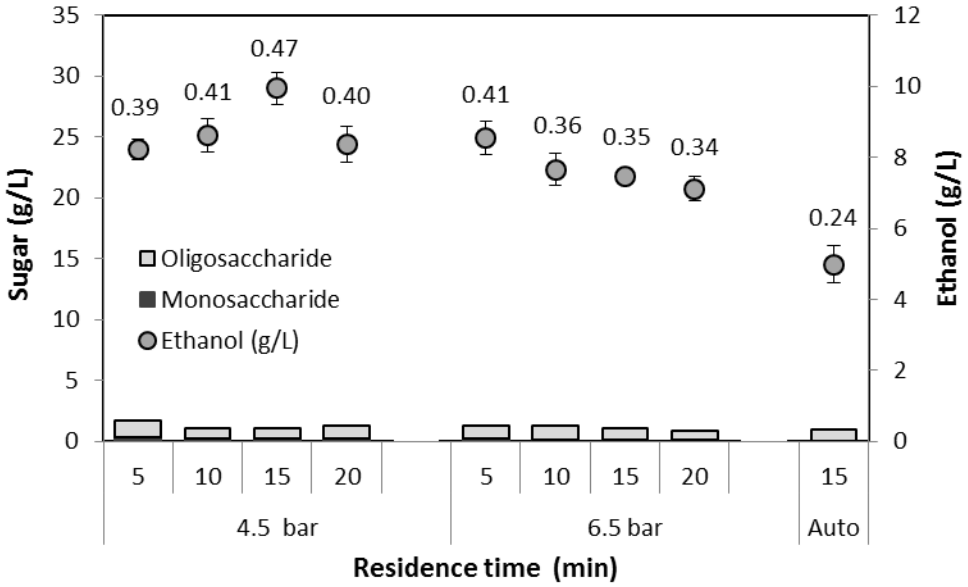


**B**

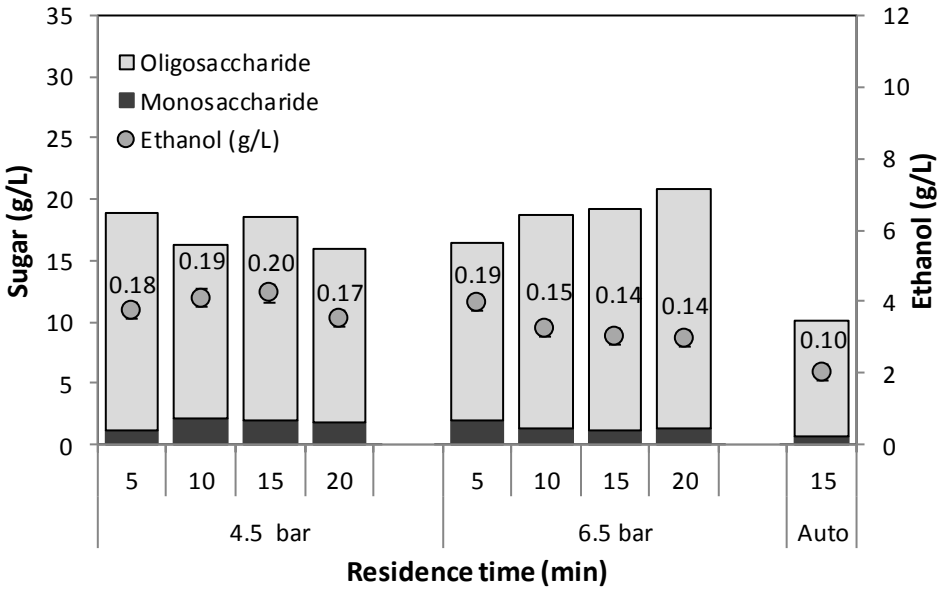


**Figure 7.3** Ethanol productions from pretreated PKC and remaining sugar after fermentation using different microorganisms. The fermentation mixture contained enzymatic hydrolysate of PKC pretreated with steam explosion under different conditions. (A) *G. thermoglucosidasius* TM242 incubated at 60 °C; (B) *S. cerevisiae* S228C incubated at 30 °C.

**Table 7.5** Theoretical ethanol yields

| Sample Name | (%) Theoretical Ethanol Yield (based on total sugars of 5% PKC) | |
|---|---|---|
| | ***Geobacillus sp.* (TM242)** | ***Saccharomyces sp.* (S228C)** |
| **4.5 bar 5 min** | 76.4 | 34.9 |
| **4.5 bar 10 min** | 80.1 | 38.1 |
| **4.5 bar 15 min** | 92.4 | 39.3 |
| **4.5 bar 20 min** | 77.7 | 32.6 |
| **6.5 bar 5 min** | 79.5 | 36.8 |
| **6.5 bar 10 min** | 71.2 | 30.2 |
| **6.5 bar 15 min** | 69.3 | 28.0 |
| **6.5 bar 20 min** | 66.1 | 27.4 |
| **Autoclave** | 46.3 | 18.7 |

Efficiency of the microorganisms in sugar conversion to ethanol was demonstrated by Ion chromatography. The signature peaks of sugar after enzymatic hydrolysis and fermentation by TM242 bacteria and yeast as well as the sugar mixture standard with the corresponding monosaccharides and the main manno-oligosaccharides (mannobiose and mannotriose) were illustrated in Figure 7.4. This sugar mixture standard showed the IC peaks at different retention times including arabinose at 3.4 min, galactose at 3.6 min, glucose at 4.0 min, xylose at 4.3 min, mannose at 4.6 min, fructose at 4.9 min, and main oligosaccharide of mannobiose at 6.5 min and mannotriose at 6.8 min (Figure 7.4A). The corresponding peaks were identified in enzymatic hydrolysate of PKC (Figure 7.4B). Lower monosaccharide peaks were observed in the mixture after fermentation by *S. cerevisiae* S228C while no significant decrease in oligosaccharides was found, suggesting low efficiency of the yeast to assimilate oligosaccharides (Figure 7.4C). Remarkable reduction in both monosaccharide and oligosaccharide peaks was found in the fermentation mixture using TM242 (Figure 7.4D). The result thus indicated the efficiency of the bacterial strain on assimilation of all monosaccharides and oligosaccharides in PKC hydrolysate.

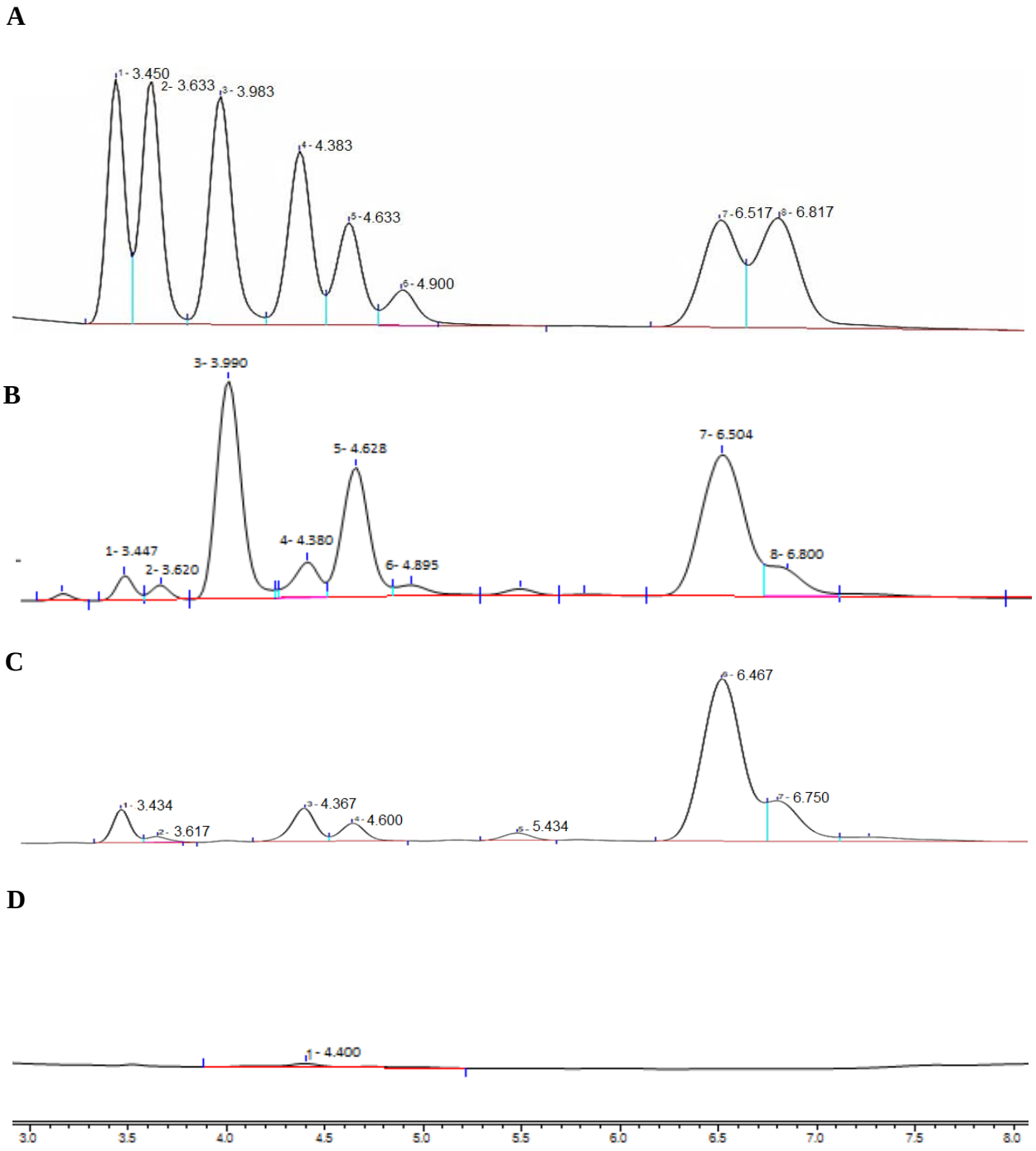


**Figure 7.4**. Sugar profiles in enzymatic hydrolysate of PKC and fermentation products analyzed by Ion Chromatography. (A) Sugar standards (0.3125 mM), (B) Released sugars from enzymatic hydrolysis, (C) *S. cerevisia* S228C efficiency, and (D) *G. thermoglucosidasius* TM242 efficiency.

The *G. thermoglucosidasius* TM242 strain is a thermophilic bacterium genetically modified from G. *thermoglucosidasius* NCIMB 11955 for the ability to consume of both hexose and pentose sugars together with the short-chain oligosaccharides, such as cellobiose and mannobiose, making it a superior strain for ethanol production [8-10]. Cripps et al (2009) [8] reported that the use of TM242 strain for efficient conversion of cellobiose and sugar mixture (hexose and pentose) to ethanol with high yield of 0.47, 0.42, and 0.35 g/g from cellobiose, glucose, and xylose, respectively. [8]. The result in this study thus shows the superior biochemical capability of TM242 on efficient conversion of oligosaccharides to ethanol which is a unique characteristic of this bacterium compared to most conventional ethanologens. This thus allows direct fermentation of the enzymatic hydrolysate with no supplementation of expensive β-mannosidase. The use of oligosaccharide-rich fraction can allow pretreatment under milder conditions which results in less sugar degradation and formation of inhibitors to the subsequent enzymatic hydrolysis and fermentation steps. These advantages altogether can significantly contribute to higher conversion efficiency with and lower cost in ethanol production from PKC and other lignocellulosic substrates.

### 7.3 Conclusion

PKC was shown to be a promising second generation lignocellulosic feedstock for the production of bioethanol with the advantages of its high carbohydrate content and susceptibility to enzymatic hydrolysis. The maximal ethanol over 90% theoretical yields was achieved by the developed process involving steam explosion at 4.5 bar for 15 min, enzymatic hydrolysis by the mannanase and cellulase mixture, and fermentation by *G. thermoglucosidasius* TM242. The thermophilic TM242 bacteria can utilize both hexose and pentose sugars together with the ability to use short-chain oligosaccharide e.g. cellobiose, and mannobiose as the substrate, which are considered advantageous characteristics for bioethanol production. The developed conversion process provides a basis for efficient production of ethanol from PKC.

# CHAPTER 8
# SUMMARY AND FUTURE WORKS

Oil palm is a promising renewable biofuel feedstock for the production of biodiesel and bioethanol production due to its high productivity of oil and availability of the underused lignocellulosic waste from palm oil processing. In this thesis, an efficient biocatalytic process for biodiesel production from the inexpensive CPO and PFAD, the fatty acid rich fraction from palm oil refining has been reported using novel biocatalyst designs i.e. glycine-based crosslinked protein-coated microcrystalline lipase and magnetic nanoparticle lipase with modified covalent linkage. Conversion of palm kernel cake, a mannan-rich by-product from oil palm processing using a novel *G. thermoglucisidasius* TM242 strain was achieved. This provides a potent approach for utilization of the under-utilized lignocellulosic waste for valorization for biofuel production. The results of this study thus provide a promising approach for development of oil palm-based biofuel industry.

The first part of the research focused on the development of highly efficient biocatalytic conversion of different oil palm feedstocks, i.e. CPO, RPO, and PFAD, to biodiesel by transesterification and esterification using microcrystalline lipase. CL-PCMCs is a form of microcrystalline enzyme further developed from PCMCs with covalent crosslinking of the protein molecules on the biocatalyst surface in order to enhance the biocatalyst stability [6]. This microcrystalline design allows inexpensive synthesis of high performance biocatalysts with high operational stability and catalytic reactivity due to low mass transfer limitation. Glycine was found to be a novel component for using core matrix, leading to higher performance of the biocatalyst compared to insert $K_2SO_4$ conventionally used in preparation of microcrystalline enzymes. The high catalytic performance of the biocatalyst could be related to its physical properties (crystalline structure and size) as well as stabilization of the lipase by the glycine, which could act as a solid-state buffer. Reactivity of the CL-PCMC-lipase prepared on glycine using *T. lanuginosus* lipase towards esterification of palm fatty acids (palmitic, oleic, and linoleic acid) using ethanol as nucleophile was studied. The optimal reaction containing 4:1 (mol/mol) ethanol to fatty acid ratio with 1:1 [*t*-BuOH]/[FFA] molar ratio with 20% (w/w) of enzyme loading led to FAEE yield of 87.2% from palmitic acid while a slightly lower FAEE yield of 81.4% was obtained with PFAD. after incubation at 50$^{o}$C for 6 h. The CL-PCMC-lipase showed higher

catalytic performance compared to protein coated microcrystalline (PCMC) lipase and commercial immobilized lipases, such as Novozyme®435 and Lipolase 100T, with high operational stability with no significant loss in product yield after 8 consecutive batch cycles. Reaction kinetics of the CL-PCMC-lipase catalyzed esterification process using methanol as a nucleophile followed the Ping Pong Bi-Bi model. the FAME yield over 95.0 % based on molar basis at 15 %(w/w) enzyme loading with 4:1 [MeOH]/[FFA] molar ratio after incubation at 50 °C with 40 rpm. The key kinetic parameters were obtained including $V$m of 0.7 M/min, $K_{mA}$ of 3669.4 M, $K_{mB}$ of 1076.3 M, $K_i$ of 31.2 M and the $k_{cat}$ of 388 $min^{-1}$. The kinetics result thus provides an important basis for further up-scaling of the process.

Development of the microcrystalline lipase performance was then further investigated on co-ester/transesterification of CPO. The zwitterionic glycine, CAPSO, and TAPS were found to be the superior core matrix from an extensive screening of CL-PLCMC synthesis using a variety of solid-state organic and inorganic buffers with different $pK_a$ on the esterification of palmitic acid and transesterification of RPO. The high performance of the biocatalysts could be due to related to stabilization of the ionization state of the lipase by controlling the exchange of protons and counterions on the enzyme. The maximal FAME product from PA, RPO, and CPO achieved to 97.6, 94.9, and 95.5%, respectively on a molar basis under the optimal conditions containing 4:1 [MeOH]/[FFA] molar ratio with 20% (w/w) glycine-based CL-PCMC-lipase after incubation at 50$^{o}$C for 6 h in the presence of *tert*-butanol as a co-solvent. The adsorption of glycerol on the biocatalyst reactive surface which led to enzyme inactivation was demonstrated by FTIR analysis and could be alleviated by increasing the amount of co-solvent in the reaction. With its high operational stability, the developed CL-PCMC-lipase is considered a promising biocatalyst for one-step conversion of crude palm oil to biodiesel.

Magnetic nanoparticle lipase represents another potent biocatalyst design with high reactive surface area and simple modification by magnetization. Modification of covalent linkages between the iron core matrix and the enzyme in the form of $Fe_3O_4$-AP-EN-lipase showed superior catalytic performance toward the transesterification of RPO. The optimal reaction contained 23.2% w/w enzyme loading and 4.7:1 methanol to oil molar ratio with 3.4% water content in the presence of 1:1 (v/v) *tert*-butanol to oil obtained from experimental design optimization using CCD approach. Under the predicted optimal condition, the maximal FAME yield of 97.2% was achieved after incubation at 50 °C for

24 h, which was slightly lower than the predicted yield. The magnetic nanoparticle lipase developed showed high operational stability and can retained >80% activity after recycling for 3 consecutive batches with no re-generation step by solvent treatment, suggesting its potential for application in consecutive batch or continuous process.

Next, the work is focused on the development of a whole cell biocatalyst expressing lipase on the cell surface, while the construct for the expression of lipase in secreted form was studied as control and a choice for in-house lipase production.

In this study, recombinant *P. pastoris* systems for the expression of lipase in cell-surface display and secreted forms were constructed. Lipase activity was detected for all constructed; however, with a relatively low level. No induced protein bands of cell surface display form were observed from the cell pellet fractions of the recombinant yeasts. However, expression of the secreted form of *T. lanuginosus* and *C. antarctica* lipase in the supernatant showed target protein bands at 45-35 kDa and 40.4 kDa, respectively. The lipase activities in the supernatant were $0.2\times10^{-3}$ and $1.3\times10^{-3}$ IU/ml for the *T. lanuginosus* and *C. antarctica* lipases, respectively. The His6 tagged lipases were purified by affinity chromatography on Ni matrix. The specific activities of the purified enzymes were $1.9\times10^{-3}$ IU/mg and $13.1\times10^{-3}$ IU/mg for the *T. lanuginosus* and *C. antarctica* enzymes, respectively. This thus allows an approach in-house lipase preparation for the preparation of the immobilized enzyme for further study.

The last part of the study focused on the conversion of palm kernel cake (PKC) to ethanol by using genetically engineered thermophilic bacterium *G. thermoglucosidasius* TM242. The effects of the conditions for steam explosion pretreatment and enzyme formulation on the hydrolysis of PKC were studied. The highest fermentable sugars of 28.3 g/L was obtained from 5% PKC pretreated conditions at 4.5 bar for 15 min using 1.67 %v/w of AET mannanase and 10.38 FPU/g glucan of Ctec2 cellulase. Fermentation of the PKC hydrolysate led to the maximal ethanol concentration with 9.9 g/L (92.4% of theoretical yield based on the total sugars in 5% PKC) by TM242 after incubation at 60 °C for 48 h whereas a lower ethanol concentration of 4.23 g/L (39.3% of theoretical yield based on the total sugars in 5% PKC) after 72 h at 30 °C using *S. cerevisiae*. The higher ethanol yield from TM242 was due to the ability of the bacterium on converting both hexose and pentose sugars together with the short-chain oligosaccharide e.g. cellobiose, and mannobiose to ethanol. The *G. thermoglucosidasius* TM242 is thus a promising

alternative microorganism for improvement of bioethanol production from lignocellulosic biomass from PKC and other lignocellulosic biomass.

Overall, the results from this work provide efficient approaches for the improvement of biodiesel and bioethanol production from oil palm both from its crude oil and lignocellulosic wastes. The future research could focus on the study of the biocatalytic biodiesel production process using the developed biocatalysts in batch or flow-through bioreactor in order to optimize the process conditions for further up-scaling study and evaluate of economic feasibility. The recombinant TM 242 can be further modified by metabolic engineering for integration of the ability on enzyme production, saccharification, and fermentation in the single microbe for application in consolidated bioprocessing process. The work in this study thus provides a basis for increasing economic competitiveness of the palm oil based biodiesel industry by improving the technology used for conversion and valorization of the underused by-products.

## REFERENCES


[1]. Gutiérrez LF, Sánchez ÓJ, Cardona CA. Process integration possibilities for biodiesel production from palm oil using ethanol obtained from lignocellulosic residues of oil palm industry. Bioresource Technology. 2009;100:1227-37.

[2]. Mukherjee I, Sovacool BK. Palm oil-based biofuels and sustainability in southeast Asia: A review of Indonesia, Malaysia, and Thailand. Renewable and Sustainable Energy Reviews. 2014;37:1-12.

[3]. Tan T, Lu J, Nie K, Deng L, Wang F. Biodiesel production with immobilized lipase: A review. Biotechnology Advances. 2010;28:628-34.

[4]. Raita M, Champreda V, Laosiripojana N. Biocatalytic ethanolysis of palm oil for biodiesel production using microcrystalline lipase in *tert*-butanol system. Process Biochemistry. 2010;45:829-34.

[5]. Raita M, Laothanachareon T, Champreda V, Laosiripojana N. Biocatalytic esterification of palm oil fatty acids for biodiesel production using glycine-based cross-linked protein coated microcrystalline lipase. Journal of Molecular Catalysis B: Enzymatic. 2011;73:74-9.

[6]. Shah S, Sharma A, Gupta MN. Cross-linked protein-coated microcrystals as biocatalysts in non-aqueous solvents. Biocatalysis and Biotransformation. 2008;26:266-71.

[7]. Goh CS, Tan KT, Lee KT, Bhatia S. Bio-ethanol from lignocellulose: Status, perspectives and challenges in Malaysia. Bioresource Technology. 2010;101:4834-41.

[8]. Cripps RE, Eley K, Leak DJ, Rudd B, Taylor M, Todd M, et al. Metabolic engineering of Geobacillus thermoglucosidasius for high yield ethanol production. Metabolic Engineering. 2009;11:398-408.

[9]. Taylor MP, Eley KL, Martin S, Tuffin MI, Burton SG, Cowan DA. Thermophilic ethanologenesis: future prospects for second-generation bioethanol production. Trends in Biotechnology. 2009;27:398-405.

[10]. Bartosiak-Jentys J, Hussein AH, Lewis CJ, Leak DJ. Modular system for assessment of glycosyl hydrolase secretion in *Geobacillus thermoglucosidasius*. Microbiology. 2013;159:1267-75.

[11]. Du W, Li W, Sun T, Chen X, Liu D. Perspectives for biotechnological production of biodiesel and impacts. Applied Microbiology and Biotechnology. 2008;79:331-7.

[12]. Demirbas A. Progress and recent trends in biodiesel fuels. Energy Conversion and Management. 2009;50:14-34.

[13]. Siriwardhana M, Opathella GKC, Jha MK. Bio-diesel: Initiatives, potential and prospects in Thailand: A review. Energ Policy. 2009;37:554-9.

[14]. Foo KY, Hameed BH. Utilization of biodiesel waste as a renewable resource for activated carbon: Application to environmental problems. Renewable and Sustainable Energy Reviews. 2009;13:2495-504.

[15]. Janaun J, Ellis N. Perspectives on biodiesel as a sustainable fuel. Renewable and Sustainable Energy Reviews. 2010;14:1312-20.

[16]. Singh RP, Embrandiri A, Ibrahim MH, Esa N. Management of biomass residues generated from palm oil mill: Vermicomposting a sustainable option. Resources, Conservation and Recycling. 2011;55:423-34.

[17]. Umikalsom MS, Ariff AB, Zulkifli HS, Tong CC, Hassan MA, Karim MIA. The treatment of oil palm empty fruit bunch fibre for subsequent use as substrate for cellulase production by Chaetomium globosum Kunze. Bioresource Technology. 1997;62:1-9.

[18]. Ranganathan SV, Narasimhan SL, Muthukumar K. An overview of enzymatic production of biodiesel. Bioresource Technology. 2008;99:3975-81.

[19]. Junior II, Flores MC, Sutili FK, Leite SGF, de M. e Miranda LS, Leal ICR, et al. Fatty acids residue from palm oil refining process as feedstock for lipase catalyzed monoacylglicerol production under batch and continuous flow conditions. Journal of Molecular Catalysis B: Enzymatic. 2012;77:53-8.

[20]. Cerveró JM, Skovgaard PA, Felby C, Sørensen HR, Jørgensen H. Enzymatic hydrolysis and fermentation of palm kernel press cake for production of bioethanol. Enzyme and Microbial Technology. 2010;46:177-84.

[21]. Jorgensen H, Sanadi AR, Felby C, Lange NE, Fischer M, Ernst S. Production of ethanol and feed by high dry matter hydrolysis and fermentation of palm kernel press cake. Applied Biochemistry and Biotechnology. 2010;161:318-32.

[22]. Ma F, Hanna MA. Biodiesel production: a review. Bioresource Technology. 1999;70:1-15.

[23]. Talukder MMR, Wu JC, Van Nguyen TB, Fen NM, Melissa YLS. Novozym 435 for production of biodiesel from unrefined palm oil: Comparison of methanolysis methods. Journal of Molecular Catalysis B: Enzymatic. 2009;60:106-12.

[24. Marchetti JM, Miguel VU, Errazu AF. Heterogeneous esterification of oil with high amount of free fatty acids. Fuel. 2007;86:906-10.

[25]. Du W, Xu Y, Liu D, Zeng J. Comparative study on lipase-catalyzed transformation of soybean oil for biodiesel production with different acyl acceptors. Journal of Molecular Catalysis B: Enzymatic. 2004;30:125-9.

[26]. Lai CC, Zullaikah S, Vali SR, Ju YH. Lipase-catalyzed production of biodiesel from rice bran oil. Journal of Chemical Technology and Biotechnology. 2005;80:331-7.

[27]. Oliveira AC, Rosa MF. Enzymatic transesterification of sunflower oil in an aqueous-oil biphasic system. Journal of the American Oil Chemists' Society. 2006;83:21-5.

[28]. Helwani Z, Othman MR, Aziz N, Fernando WJN, Kim J. Technologies for production of biodiesel focusing on green catalytic techniques: A review. Fuel Processing Technology. 2009;90:1502-14.

[29]. Bajaj A, Lohan P, Jha PN, Mehrotra R. Biodiesel production through lipase catalyzed transesterification: An overview. Journal of Molecular Catalysis B: Enzymatic. 2010;62:9-14.

[30]. Samukawa T, Kaieda M, Matsumoto T, Ban K, Kondo A, Shimada Y, et al. Pretreatment of immobilized *Candida antarctica* lipase for biodiesel fuel production from plant oil. Journal of Bioscience and Bioengineering. 2000;90:180-3.

[31]. Noureddini H, Gao X, Philkana RS. Immobilized *Pseudomonas cepacia* lipase for biodiesel fuel production from soybean oil. Bioresource Technology. 2005;96:769-77.

[32]. Du W, Xu Y-Y, Liu D-H, Li Z-B. Study on acyl migration in immobilized lipozyme TL-catalyzed transesterification of soybean oil for biodiesel production. Journal of Molecular Catalysis B: Enzymatic. 2005;37:68-71.

[33]. Gao D, Lin DQ, Yao SJ. Patch controlled protein adsorption in mixed-mode chromatography with benzylamine as functional ligand. Biochemical Engineering Journal. 2008;38:355-61.

[34]. Freitas L, Da Rós PCM, Santos JC, de Castro HF. An integrated approach to produce biodiesel and monoglycerides by enzymatic interestification of babassu oil (*Orbinya sp*). Process Biochemistry. 2009;44:1068-74.

[35]. Won K, Kim S, Kim K-J, Park HW, Moon S-J. Optimization of lipase entrapment in Ca-alginate gel beads. Process Biochemistry. 2005;40:2149-54.

[36]. Sheldon RA. Cross-linked enzyme aggregates (CLEAs): stable and recyclable biocatalysts. Biochemical Society Transactions. 2007;35:1583-7.

[37]. Kuo C-H, Peng L-T, Kan S-C, Liu Y-C, Shieh C-J. Lipase-immobilized biocatalytic membranes for biodiesel production. Bioresource Technology. 2013;145:229-32.

[38]. Xie W, Ma N. Immobilized Lipase on $Fe_3O_4$ Nanoparticles as Biocatalyst for Biodiesel Production. Energ Fuel. 2009;23:1347-53.

[39]. Jin Z, Han S-Y, Zhang L, Zheng S-P, Wang Y, Lin Y. Combined utilization of lipase-displaying *Pichia pastoris* whole-cell biocatalysts to improve biodiesel production in co-solvent media. Bioresource Technology. 2013;130:102-9.

[40]. Kim S-j, Song JK, Kim HK. Cell surface display of *Staphylococcus haemolyticus* L62 lipase in *Escherichia coli* and its application as a whole cell biocatalyst for biodiesel production. Journal of Molecular Catalysis B: Enzymatic. 2013;97:54-61.

[41]. Schwab AW, Bagby MO, Freedman B. Preparation and properties of diesel fuels from vegetable oils. Fuel. 1987;66:1372-8.

[42]. Vicente G, Martinez M, Aracil J. Integrated biodiesel production: a comparison of different homogeneous catalysts systems. Bioresource Technology. 2004;92:297-305.

[43]. L.P. Christopher KH, V.P. Zambare. Enzymatic biodiesel: Challenges and opportunities. Applied Energy. 2014;119:497-520.

[44]. Thamsiriroj T, Murphy JD. How much of the target for biofuels can be met by biodiesel generated from residues in Ireland? Fuel. 2010;89:3579-89.

[45]. Ramachandran K, Suganya T, Nagendra Gandhi N, Renganathan S. Recent developments for biodiesel production by ultrasonic assist transesterification using different heterogeneous catalyst: A review. Renewable and Sustainable Energy Reviews. 2013;22:410-8.

[46]. Demirbas A. Biodiesel production via non-catalytic SCF method and biodiesel fuel characteristics. Energy Conversion and Management. 2006;47:2271-82.

[47]. Tan KT, Lee KT. A review on supercritical fluids (SCF) technology in sustainable biodiesel production: Potential and challenges. Renewable and Sustainable Energy Reviews. 2011;15:2452-6.

[48]. Li W, Du W, Liu DH. *Rhizopus oryzae* whole-cell-catalyzed biodiesel production from oleic acid in tert-butanol medium. Energy and Fuels. 2008;22:155-8.

[49]. Iso M, Chen BX, Eguchi M, Kudo T, Shrestha S. Production of biodiesel fuel from triglycerides and alcohol using immobilized lipase. Journal of Molecular Catalysis B: Enzymatic. 2001;16:53-8.

[50]. Szczęsna Antczak M, Kubiak A, Antczak T, Bielecki S. Enzymatic biodiesel synthesis – Key factors affecting efficiency of the process. Renewable Energy. 2009;34:1185-94.

[51]. Xie W, Ma N. Enzymatic transesterification of soybean oil by using immobilized lipase on magnetic nano-particles. Biomass and Bioenergy. 2010;34:890-6.

[52]. Akbarzadeh A, Samiei M, Davaran S. Magnetic nanoparticles: preparation, physical properties, and applications in biomedicine. Nanoscale Research Letters. 2012;7:144.

[53]. Cao L, Langen L, Sheldon RA. Immobilised enzymes: carrier-bound or carrier-free? Current Opinion in Biotechnology. 2003;14:387-94.

[54]. Govardhan CP. Crosslinking of enzymes for improved stability and performance. Current Opinion in Biotechnology. 1999;10:331-5.

[55]. Aytar BS, Bakir U. Preparation of cross-linked tyrosinase aggregates. Process Biochemistry. 2008;43:125-31.

[56]. Shah S, Sharma A, Gupta MN. Preparation of cross-linked enzyme aggregates by using bovine serum albumin as a proteic feeder. Analytical Biochemistry. 2006;351:207-13.

[57]. Wilson L, Illanes A, Abian O, Pessela BC, Fernandez-Lafuente R, Guisan JM. Co-aggregation of penicillin g acylase and polyionic polymers: an easy methodology to prepare enzyme biocatalysts stable in organic media. Biomacromolecules. 2004;5:852-7.

[58]. Cao L, van Rantwijk F, Sheldon RA. Cross-linked enzyme aggregates: a simple and effective method for the immobilization of penicillin acylase. Organic Letters. 2000;2:1361-4.

[59]. Chen JW, Wu WT. Regeneration of immobilized *Candida antarctica* lipase for transesterification. Journal of Bioscience and Bioengineering. 2003;95:466-9.

[60]. Vafiadi C, Topakas E, Christakopoulos P. Preparation of multipurpose cross-linked enzyme aggregates and their application to production of alkyl ferulates. Journal of Molecular Catalysis B: Enzymatic. 2008;54:35-41.

[61]. Schoevaart R, Wolbers MW, Golubovic M, Ottens M, Kieboom AP, van Rantwijk F. Preparation, optimization, and structures of cross-linked enzyme aggregates (CLEAs). Biotechnology and Bioengineering. 2004;87:754-62.

[62]. Kreiner M, Moore BD, Parker MC. Enzyme-coated micro-crystals: a 1-step method for high activity biocatalyst preparation. Chemical Communications. 2001:1096-7.

[63]. Shah S, Gupta MN. Kinetic resolution of (+/-)-1-phenylethanol in [Bmim]/[PF6] using high activity preparations of lipases. Bioorganic & Medicinal Chemistry Letters. 2007;17:921-4.

[64]. Kumari V, Shah S, Gupta MN. Preparation of Biodiesel by Lipase-Catalyzed Transesterification of High Free Fatty Acid Containing Oil from *Madhuca indica*. Energy and Fuels. 2006;21:368-72.

[65]. Shah S, Sharma A, Varandani D, Mehta B, Gupta MN. A high performance lipase preparation: characterization and atomic force microscopy. Journal for Nanoscience and Nanotechnology. 2007;7:2157-60.

[66]. Migneault I, Dartiguenave C, Bertrand MJ, Waldron KC. Glutaraldehyde: behavior in aqueous solution, reaction with proteins, and application to enzyme crosslinking. Biotechniques. 2004;37:790-6, 8-802.

[67]. Cipolatti EP, Silva MJA, Klein M, Feddern V, Feltes MMC, Oliveira JV, et al. Current status and trends in enzymatic nanoimmobilization. Journal of Molecular Catalysis B: Enzymatic. 2014;99:56-67.

[68]. Ansari SA, Husain Q. Potential applications of enzymes immobilized on/in nano materials: A review. Biotechnology Advance. 2012;30:512-23.

[69]. Tran DT, Chen CL, Chang JS. Immobilization of *Burkholderia sp.* lipase on a ferric silica nanocomposite for biodiesel production. Journal and Biotechnology. 2012;158:112-9.

[70]. Ngo TPN, Li AT, Tiew KW, Li Z. Efficient transformation of grease to biodiesel using highly active and easily recyclable magnetic nanobiocatalyst aggregates. Bioresource Technology. 2013;145:233-9.

[71]. Kuo C-H, Liu Y-C, Chang C-MJ, Chen J-H, Chang C, Shieh C-J. Optimum conditions for lipase immobilization on chitosan-coated $Fe_3O_4$ nanoparticles. Carbohydrate Polymers. 2012;87:2538-45.

[72]. He Q, Xu Y, Teng Y, Wang D. Biodiesel production catalyzed by whole-cell lipase from Rhizopus chinensis. Chinese Journal of Catalysis. 2008;29:41-6.

[73]. Ban K, Kaieda M, Matsumoto T, Kondo A, Fukuda H. Whole cell biocatalyst for biodiesel fuel production utilizing *Rhizopus oryzae* cells immobilized within biomass support particles. Biochemical Engineering Journal. 2001;8:39-43.

[74]. Li W, Du W, Liu DH. Optimization of whole cell-catalyzed methanolysis of soybean oil for biodiesel production using response surface methodology. Journal of Molecular Catalysis B: Enzymatic. 2007;45:122-7.

[75]. Sun T, Du W, Zeng J, Dai LM, Liu DH. Exploring the effects of oil inducer on whole cell-mediated methanolysis for biodiesel production. Process Biochemistry. 2010;45:514-8.

[76]. Fukuda H, Hama S, Tamalampudi S, Noda H. Whole-cell biocatalysts for biodiesel fuel production. Trends Biotechnology. 2008;26:668-73.

[77]. Matsumoto T, Takahashi S, Kaieda M, Ueda M, Tanaka A, Fukuda H, et al. Yeast whole-cell biocatalyst constructed by intracellular overproduction of *Rhizopus oryzae* lipase is applicable to biodiesel fuel production. Applied Microbiology and Biotechnology. 2001;57:515-20.

[78]. Lee SY, Choi JH, Xu Z. Microbial cell-surface display. Trends Biotechnology. 2003;21:45-52.

[79]. Demirbas A. Biodiesel production from vegetable oils via catalytic and non-catalytic supercritical methanol transesterification methods. Progress in Energy and Combustion Science. 2005;31:466-87.

[80]. Tamalampudi S, Talukder MR, Hama S, Numata T, Kondo A, Fukuda H. Enzymatic production of biodiesel from Jatropha oil: A comparative study of immobilized-whole cell and commercial lipases as a biocatalyst. Biochemical Engineering Journal. 2008;39:185-9.

[81]. Li L, Du W, Liu D, Wang L, Li Z. Lipase-catalyzed transesterification of rapeseed oils for biodiesel production with a novel organic solvent as the reaction medium. Journal of Molecular Catalysis B: Enzymatic. 2006;43:58-62.

[82]. Du W, Liu D, Li L, Dai L. Mechanism exploration during lipase-mediated methanolysis of renewable oils for biodiesel production in a *tert*-butanol system. Biotechnology Progress. 2007;23:1087-90.

[83]. Huang Y, Zheng H, Yan Y. Optimization of lipase-catalyzed transesterification of lard for biodiesel production using response surface methodology. Applied Biochemical and Biotechnology. 2010;160:504-15.

[84]. Jeong GT, Park DH. Lipase-catalyzed transesterification of rapeseed oil for biodiesel production with tert-butanol. Applied Biochemical and Biotechnology. 2008;148:131-9.

[85]. Mood SH, Golfeshan AH, Tabatabaei M, Jouzani GS, Najafi GH, Gholami M, et al. Lignocellulosic biomass to bioethanol, a comprehensive review with a focus on pretreatment. Renewable and Sustainable Energy Reviews. 2013;27:77-93.

[86]. Sarkar N, Ghosh SK, Bannerjee S, Aikat K. Bioethanol production from agricultural wastes: An overview. Renewable Energy. 2012;37:19-27.

[87]. Limayem A, Ricke SC. Lignocellulosic biomass for bioethanol production: Current perspectives, potential issues and future prospects. Progress in Energy and Combustion Science. 2012;38:449-67.

[88]. Cotana F, Cavalaglio G, Nicolini A, Gelosia M, Coccia V, Petrozzi A, et al. Lignin as Co-product of Second Generation Bioethanol Production from Ligno-cellulosic Biomass. Energy Procedia. 2014;45:52-60.

[89]. McMillan James D. Pretreatment of Lignocellulosic Biomass. Enzymatic Conversion of Biomass for Fuels Production: American Chemical Society; 1994. p. 292-324.

[90]. Sun R, Tomkinson J, Wang S, Zhu W. Characterization of lignins from wheat straw by alkaline peroxide treatment. Polymer Degradation and Stability. 2000;67:101-9.

[91]. Melo E, Kennedy JF. Cellulose hydrolysis (biotechnology monographs, Vol. 3) edited by L.-T. Fan, M. M. Gharpuray and Y.-H. Lee, Springer-Verlag, Berlin, Heidelberg, New York, London, Paris and Tokyo, 1987. pp. viii + 198, price DM168.00. ISBN 3-540-17671-3. British Polymer Journal. 1988;20:532-.

[92]. Balat M. Production of bioethanol from lignocellulosic materials via the biochemical pathway: A review. Energy Conversion and Management. 2011;52:858-75.

[93]. Mosier N, Wyman C, Dale B, Elander R, Lee YY, Holtzapple M, et al. Features of promising technologies for pretreatment of lignocellulosic biomass. Bioresource Technology. 2005;96:673-86.

[94]. Hendriks AT, Zeeman G. Pretreatments to enhance the digestibility of lignocellulosic biomass. Bioresource Technology. 2009;100:10-8.

[95]. Alvira P, Tomas-Pejo E, Ballesteros M, Negro MJ. Pretreatment technologies for an efficient bioethanol production process based on enzymatic hydrolysis: A review. Bioresource Technology. 2010;101:4851-61.

[96]. Oliva JM, Saez F, Ballesteros I, Gonzalez A, Negro MJ, Manzanares P, et al. Effect of lignocellulosic degradation compounds from steam explosion pretreatment on ethanol fermentation by thermotolerant yeast *Kluyveromyces marxianus*. Applied Biochemical Biotechnology. 2003;105 -108:141-53.

[97]. Lee HJ, Lim WS, Lee JW. Improvement of ethanol fermentation from lignocellulosic hydrolysates by the removal of inhibitors. Journal of Industrial and Engineering Chemistry. 2013;19:2010-5.

[98]. Jonsson L, Alriksson B, Nilvebrant N-O. Bioconversion of lignocellulose: inhibitors and detoxification. Biotechnology for Biofuels. 2013;6:16.

[99]. Negro MJ, Manzanares P, Ballesteros I, Oliva JM, Cabanas A, Ballesteros M. Hydrothermal pretreatment conditions to enhance ethanol production from poplar biomass. Applied Biochemical Biotechnology. 2003;105 -108:87-100.

[100]. Ballesteros I, Negro MJ, Oliva JM, Cabanas A, Manzanares P, Ballesteros M. Ethanol production from steam-explosion pretreated wheat straw. Applied Biochemical Biotechnology. 2006;129-132:496-508.

[101]. Zhao X, Song Y, Liu D. Enzymatic hydrolysis and simultaneous saccharification and fermentation of alkali/peracetic acid-pretreated sugarcane bagasse for ethanol and 2,3-butanediol production. Enzyme and Microbial Technology. 2011;49:413-9.

[102]. Zhong C, Lau MW, Balan V, Dale BE, Yuan YJ. Optimization of enzymatic hydrolysis and ethanol fermentation from AFEX-treated rice straw. Applied Microbiology and Biotechnology. 2009;84:667-76.

[103]. Parisutham V, Kim TH, Lee SK. Feasibilities of consolidated bioprocessing microbes: from pretreatment to biofuel production. Bioresource Technology. 2014;161:431-40.

[104]. Viikari L, Vehmaanperä J, Koivula A. Lignocellulosic ethanol: From science to industry. Biomass and Bioenergy. 2012;46:13-24.

[105]. Girio FM, Fonseca C, Carvalheiro F, Duarte LC, Marques S, Bogel-Lukasik R. Hemicelluloses for fuel ethanol: A review. Bioresource Technology. 2010;101:4775-800.

[106]. Abedinifar S, Karimi K, Khanahmadi M, Taherzadeh MJ. Ethanol production by Mucor indicus and Rhizopus oryzae from rice straw by separate hydrolysis and fermentation. Biomass and Bioenergy. 2009;33:828-33.

[107]. Srilekha Yadav K, Naseeruddin S, Sai Prashanthi G, Sateesh L, Venkateswar Rao L. Bioethanol fermentation of concentrated rice straw hydrolysate using co-culture of Saccharomyces cerevisiae and *Pichia stipitis*. Bioresource Technology. 2011;102:6473-8.

[108]. Olofsson K, Wiman M, Liden G. Controlled feeding of cellulases improves conversion of xylose in simultaneous saccharification and co-fermentation for bioethanol production. Journal of Biotechnology. 2010;145:168-75.

[109]. Khuong LD, Kondo R, De Leon R, Anh TK, Shimizu K, Kamei I. Bioethanol production from alkaline-pretreated sugarcane bagasse by consolidated bioprocessing using Phlebia sp MG-60. International Biodeterioration and Biodegradation. 2014;88:62-8.

[110]. Van Gerpen J. Biodiesel processing and production. Fuel Processing Technology. 2005;86:1097-107.

[111]. Mongkolbovornkij P, Champreda V, Sutthisripok W, Laosiripojana N. Esterification of industrial-grade palm fatty acid distillate over modified $ZrO_2$ (with $WO_3$–, $SO_4$ – and $TiO_2$–): Effects of co-solvent adding and water removal. Fuel Processing Technology. 2010;91:1510-6.

[112]. Yujaroen D, Goto M, Sasaki M, Shotipruk A. Esterification of palm fatty acid distillate (PFAD) in supercritical methanol: Effect of hydrolysis on reaction reactivity. Fuel. 2009;88:2011-6.

[113]. Petchmala A, Laosiripojana N, Jongsomjit B, Goto M, Panpranot J, Mekasuwandumrong O, et al. Transesterification of palm oil and esterification of palm fatty acid in near- and super-critical methanol with $SO_4$–$ZrO_2$ catalysts. Fuel. 2010;89:2387-92.

[114]. Robles-Medina A, Gonzalez-Moreno PA, Esteban-Cerdan L, Molina-Grima E. Biocatalysis: towards ever greener biodiesel production. Biotechnology Advance. 2009;27:398-408.

[115]. Shimada Y, Watanabe Y, Sugihara A, Tominaga Y. Enzymatic alcoholysis for biodiesel fuel production and application of the reaction to oil processing. Journal of Molecular Catalysis B: Enzymatic. 2002;17:133-42.

[116]. Lee TS, Vaghjiani JD, Lye GJ, Turner MK. A systematic approach to the large-scale production of protein crystals. Enzyme and Microbial Technology. 2000;26:582-92.

[117]. Gilham D, Lehner R. Techniques to measure lipase and esterase activity in vitro. Methods. 2005;36:139-47.

[118]. Halim SFA, Kamaruddin AH. Catalytic studies of lipase on FAME production from waste cooking palm oil in a tert-butanol system. Process Biochemistry. 2008;43:1436-9.

[119]. Yadav GD, Borkar IV. Kinetic Modeling of Immobilized Lipase Catalysis in Synthesis of n-Butyl Levulinate†. Industrial & Engineering Chemistry Research. 2008;47:3358-63.

[120]. Kreiner M, Parker MC. High-activity biocatalysts in organic media: Solid-state buffers as the immobilisation matrix for protein-coated microcrystals. Biotechnology and Bioengineering. 2004;87:24-33.

[121]. Wu JC, Yang JX, Zhang SH, Chow Y, Choi WJ. Activity, stability and enantioselectivity of lipase-coated microcrystals of inorganic salts in organic solvents. Biocatalysis and Biotransformation. 2009;27:1-7.

[122]. Murdan S, Somavarapu S, Ross AC, Alpar HO, Parker MC. Immobilisation of vaccines onto micro-crystals for enhanced thermal stability. International Journal of Pharmaceutics. 2005;296:117-21.

[123]. Harper N, Dolman M, Moore BD, Halling PJ. Acid-Base Control for Biocatalysis in Organic Media: New Solid-State Proton/Cation Buffers and an Indicator. Chemistry – A European Journal. 2000;6:1923-9.

[124]. Solanki K, Gupta MN. A chemically modified lipase preparation for catalyzing the transesterification reaction in even highly polar organic solvents. Bioorganic & Medicinal Chemistry Letters. 2011;21:2934-6.

[125]. Hernández-Martín E, Otero C. Different enzyme requirements for the synthesis of biodiesel: Novozym® 435 and Lipozyme® TL IM. Bioresource Technology. 2008;99:277-86.

[126]. Salis A, Pinna M, Monduzzi M, Solinas V. Comparison among immobilised lipases on macroporous polypropylene toward biodiesel synthesis. Journal of Molecular Catalysis B: Enzymatic. 2008;54:19-26.

[127]. Royon D, Daz M, Ellenrieder G, Locatelli S. Enzymatic production of biodiesel from cotton seed oil using t-butanol as a solvent. Bioresource Technology. 2007;98:648-53.

[128]. Wang L, Du W, Liu DH, Li LL, Dai NM. Lipase-catalyzed biodiesel production from soybean oil deodorizer distillate with absorbent present in *tert*-butanol system. Journal of Molecular Catalysis B: Enzymatic. 2006;43:29-32.

[129]. Souza MS, Aguieiras EC, da Silva MA, Langone MA. Biodiesel synthesis via esterification of feedstock with high content of free fatty acids. Applied Biochemical and Biotechnology. 2009;154:74-88.

[130]. Tongboriboon K, Cheirsilp B, H-Kittikun A. Mixed lipases for efficient enzymatic synthesis of biodiesel from used palm oil and ethanol in a solvent-free system. Journal of Molecular Catalysis B: Enzymatic. 2010;67:52-9.

[131]. Halim SFA, Harun Kamaruddin A. Catalytic studies of lipase on FAME production from waste cooking palm oil in a *tert*-butanol system. Process Biochemistry. 2008;43:1436-9.

[132]. Ciftci ON, Temelli F. Enzymatic conversion of corn oil into biodiesel in a batch supercritical carbon dioxide reactor and kinetic modeling. Journal of Supercritical Fluids. 2013;75:172-80.

[133]. Liu Y, Yan YJ, Hu F, Yao AN, Wang ZC, Wei FX. Transesterification for Biodiesel Production Catalyzed by Combined Lipases: Optimization and Kinetics. AIChE Journal. 2010;56:1659-65.

[134]. Liu Y, Tan H, Zhang X, Yan YJ, Hameed BH. Effect of monohydric alcohols on enzymatic transesterification for biodiesel production. Chemical Engineering Journal. 2010;157:223-9.

[135]. Maury S, Buisson P, Perrard A, Pierre AC. Compared esterification kinetics of the lipase from *Burkholderia cepacia* either free or encapsulated in a silica aerogel. Journal of Molecular Catalysis B: Enzymatic. 2005;32:193-203.

[136]. Nie KL, Xie F, Wang F, Tan TW. Lipase catalyzed methanolysis to produce biodiesel: Optimization of the biodiesel production. Journal of Molecular Catalysis B: Enzymatic. 2006;43:142-7.

[137]. Shimada Y, Watanabe Y, Sugihara A, Tominaga Y. Enzymatic alcoholysis for biodiesel fuel production and application of the reaction to oil processing. Journal of Molecular Catalysis B: Enzymatic. 2002;17:133-42.

[138]. Chongkhong S, Tongurai C, Chetpattananondh R. Continuous esterification for biodiesel production from palm fatty acid distillate using economical process. Renewable Energy. 2009;34:1059-63.

[139]. Lu J, Deng L, Zhao R, Zhang R, Wang F, Tan T. Pretreatment of immobilized *Candida sp*. 99-125 lipase to improve its methanol tolerance for biodiesel production. Journal of Molecular Catalysis B: Enzymatic. 2010;62:15-8.

[140]. Mendes AA, Giordano RC, Giordano RdLC, de Castro HF. Immobilization and stabilization of microbial lipases by multipoint covalent attachment on aldehyde-resin affinity: Application of the biocatalysts in biodiesel synthesis. Journal of Molecular Catalysis B: Enzymatic. 2011;68:109-15.

[141]. Abdulla R, Ravindra P. Immobilized *Burkholderia cepacia* lipase for biodiesel production from crude Jatropha curcas L. oil. Biomass and Bioenergy. 2013;56:8-13.

[142]. Lai J-Q, Hu Z-L, Sheldon RA, Yang Z. Catalytic performance of cross-linked enzyme aggregates of *Penicillium expansum* lipase and their use as catalyst for biodiesel production. Process Biochemistry. 2012;47:2058-63.

[143]. Noritomi H, Sasanuma A, Kato S, Nagahama K. Catalytic properties of cross-linked enzyme crystals in organic media. Biochemical Engineering Journal. 2007;33:228-31.

[144]. Yan J, Yan Y, Liu S, Hu J, Wang G. Preparation of cross-linked lipase-coated micro-crystals for biodiesel production from waste cooking oil. Bioresource Technology. 2011;102:4755-8.

[145]. Soares CM, Teixeira VH, Baptista AM. Protein structure and dynamics in nonaqueous solvents: insights from molecular dynamics simulation studies. Biophysical Journal. 2003;84:1628-41.

[146]. Zacharis E, Omar IC, Partridge J, Robb DA, Halling PJ. Selection of salt hydrate pairs for use in water control in enzyme catalysis in organic solvents. Biotechnology and Bioengineering. 1997;55:367-74.

[147]. Harper N, Dolman M, Moore BD, Halling PJ. Effect of water activity on the rate profile of *Subtilisin Carlsberg* in toluene in the presence of an organo-soluble acid-base buffer. Enzyme and Microbial Technology. 2001;29:413-6.

[148]. Partridge J, Halling PJ, Moore BD. Solid-state proton/sodium buffers: "chemical pH stats" for biocatalysts in organic solvents. Journal of the Chemical Society, Perkin Transactions 2. 2000:465-71.

[149]. Fontes N, Halling PJ, Barreiros S. Control of enzyme ionization state in supercritical ethane by sodium/proton solid-state acid–base buffers. Enzyme and Microbial Technology. 2003;33:938-41.

[150]. Fernandes MLM, Krieger N, Baron AM, Zamora PP, Ramos LP, Mitchell DA. Hydrolysis and synthesis reactions catalysed by *Thermomyces lanuginosa* lipase in the AOT/Isooctane reversed micellar system. Journal of Molecular Catalysis B: Enzymatic. 2004;30:43-9.

[151]. Christopher LP, Kumar H, Zambare VP. Enzymatic biodiesel: Challenges and opportunities. Applied Energy. 2014;119:497-520.

[152]. Hidawati EN, Mimi Sakinah AM. Treatment of glycerin pitch from biodiesel production. International Journal of Chemical and Environmental Engineering. 2011;2:309-13.

[153]. Xu W, Gao L, Wang S, Xiao G. Biodiesel production in a membrane reactor using MCM-41 supported solid acid catalyst. Bioresource Technology. 2014;159:286-91.

[154]. Wang B, Li S, Tian S, Feng R, Meng Y. A new solid base catalyst for the transesterification of rapeseed oil to biodiesel with methanol. Fuel. 2013;104:698-703.

[155]. Fjerbaek L, Christensen KV, Norddahl B. A review of the current state of biodiesel production using enzymatic transesterification. Biotechnology and Bioengineering. 2009;102:1298-315.

[156]. Du W, Xu YY, Liu DH, Zeng J. Comparative study on lipase-catalyzed transformation of soybean oil for biodiesel production with different acyl acceptors. Journal of Molecular Catalysis B: Enzymatic. 2004;30:125-9.

[157]. Freitas L, Da Ros PCM, Santos JC, de Castro HF. An integrated approach to produce biodiesel and monoglycerides by enzymatic interestification of babassu oil (*Orbinya sp*). Process Biochemistry. 2009;44:1068-74.

[158]. Meunier SM, Legge RL. Evaluation of diatomaceous earth as a support for sol–gel immobilized lipase for transesterification. Journal of Molecular Catalysis B: Enzymatic. 2010;62:53-7.

[159]. Abdulla R, Ravindra P. Immobilized *Burkholderia cepacia* lipase for biodiesel production from crude Jatropha curcas L. oil. Biomass and Bioenergy. 2013;56:8-13.

[160]. Watanabe Y, Shimada Y, Sugihara A, Noda H, Fukuda H, Tominaga Y. Continuous production of biodiesel fuel from vegetable oil using immobilized *Candida antarctica* lipase. Journal of the American Oil Chemists' Society. 2000;77:355-60.

[161]. Lv P, Wang X, Yuan Z, Tan T. Conversion of Soybean Oil to Biodiesel Fuel with Immobilized *Candida Lipase* on Textile Cloth. Energy Sources, Part A: Recovery, Utilization, and Environmental Effects. 2008;30:872-9.

[162]. Kuo CH, Peng LT, Kan SC, Liu YC, Shieh CJ. Lipase-immobilized biocatalytic membranes for biodiesel production. Bioresource Technology. 2013;145:229-32.

[163]. Verma ML, Barrow CJ, Puri M. Nanobiotechnology as a novel paradigm for enzyme immobilisation and stabilisation with potential applications in biodiesel production. Applied Microbiology and Biotechnology. 2013;97:23-39.

[164]. Lopez-Gallego F, Betancor L, Mateo C, Hidalgo A, Alonso-Morales N, Dellamora-Ortiz G, et al. Enzyme stabilization by glutaraldehyde crosslinking of adsorbed proteins on aminated supports. Journal of Biotechnology. 2005;119:70-5.

[165]. Tan YH, Schallom JR, Ganesh NV, Fujikawa K, Demchenko AV, Stine KJ. Characterization of protein immobilization on nanoporous gold using atomic force microscopy and scanning electron microscopy. Nanoscale. 2011;3:3395-407.

[166]. Demirel M, Kayan B. Application of response surface methodology and central composite design for the optimization of textile dye degradation by wet air oxidation. International Journal of Industrial Chemistry. 2012;3:24.

[167]. Campos E, Coimbra P, Gil MH. An improved method for preparing glutaraldehyde cross-linked chitosan–poly(vinyl alcohol) microparticles. Polymer Bulletin. 2013;70:549-61.

[168]. Bordbar AK, Rastegari AA, Amiri R, Ranjbakhsh E, Abbasi M, Khosropour AR. Characterization of Modified Magnetite Nanoparticles for Albumin Immobilization. Biotechnology Research International. 2014;2014:6.

[169]. Netto CGCM, Nakamatsu EH, Netto LES, Novak MA, Zuin A, Nakamura M, et al. Catalytic properties of thioredoxin immobilized on superparamagnetic nanoparticles. Journal of Inorganic Biochemistry. 2011;105:738-44.

[170]. Staros JV, Wright RW, Swingle DM. Enhancement by N-hydroxysulfosuccinimide of water-soluble carbodiimide-mediated coupling reactions. Analytical Biochemistry. 1986;156:220-2.

[171]. Richert L, Boulmedais F, Lavalle P, Mutterer J, Ferreux E, Decher G, et al. Improvement of stability and cell adhesion properties of polyelectrolyte multilayer films by chemical cross-linking. Biomacromolecules. 2004;5:284-94.

[172]. Alonso N, Lopez-Gallego F, Betancor L, Hidalgo A, Mateo C, Guisan JM, et al. Immobilization and stabilization of glutaryl acylase on aminated sepabeads supports by the glutaraldehyde crosslinking method. Journal of Molecular Catalysis B: Enzymatic. 2005;35:57-61.

[173]. Silva C, Silva CJ, Zille A, Guebitz GM, Cavaco-Paulo A. Laccase immobilization on enzymatically functionalized polyamide 6,6 fibres. Enzyme and Microbial Technology. 2007;41:867-75.

[174]. Barbosa O, Torres R, Ortiz C, Fernandez-Lafuente R. The slow-down of the CALB immobilization rate permits to control the inter and intra molecular modification produced by glutaraldehyde. Process Biochemistry. 2012;47:766-74.

[175]. Chui WK, Wan LS. Prolonged retention of cross-linked trypsin in calcium alginate microspheres. Journal of Microencapsulation. 1997;14:51-61.

[176]. Shao P, Meng X, He J, Sun P. Analysis of immobilized *Candida rugosa* lipase catalyzed preparation of biodiesel from rapeseed soapstock. Food and Bioproducts Processing. 2008;86:283-9.

[177]. Shah S, Gupta MN. Lipase catalyzed preparation of biodiesel from Jatropha oil in a solvent free system. Process Biochemistry. 2007;42:409-14.

[178]. Atadashi IM, Aroua MK, Abdul Aziz AR, Sulaiman NMN. The effects of water on biodiesel production and refining technologies: A review. Renewable and Sustainable Energy Reviews. 2012;16:3456-70.

[179]. Lam MK, Lee KT, Mohamed AR. Homogeneous, heterogeneous and enzymatic catalysis for transesterification of high free fatty acid oil (waste cooking oil) to biodiesel: a review. Biotechnology Advance. 2010;28:500-18.

[180]. Kalantari M, Kazemeini M, Arpanaei A. Evaluation of biodiesel production using lipase immobilized on magnetic silica nanocomposite particles of various structures. Biochemical Engineering Journal. 2013;79:267-73.

[181]. Guldhe A, Singh B, Rawat I, Bux F. Synthesis of biodiesel from *Scenedesmus sp.* by microwave and ultrasound assisted in situ transesterification using tungstated zirconia as a solid acid catalyst. Chemical Engineering Research and Design.

[182]. Du Z, Tang Z, Wang H, Zeng J, Chen Y, Min E. Research and development of a sub-critical methanol alcoholysis process for producing biodiesel using waste oils and fats. Chinese Journal of Catalysis. 2013;34:101-15.

[183]. Yan J, Zheng X, Li S. A novel and robust recombinant *Pichia pastoris* yeast whole cell biocatalyst with intracellular overexpression of a *Thermomyces lanuginosus* lipase: Preparation, characterization and application in biodiesel production. Bioresource Technology. 2014;151:43-8.

[184]. Fujita Y, Takahashi S, Ueda M, Tanaka A, Okada H, Morikawa Y, et al. Direct and efficient production of ethanol from cellulosic material with a yeast strain displaying cellulolytic enzymes. Applied and Environmental Microbiology. 2002;68:5136-41.

[185]. Matsumoto T, Fukuda H, Ueda M, Tanaka A, Kondo A. Construction of yeast strains with high cell surface lipase activity by using novel display systems based on the Flo1p flocculation functional domain. Applied and Environmental Microbiology. 2002;68:4517-22.

[186]. Schmidt-Dannert C. Recombinant microbial lipases for biotechnological applications. Bioorganic and Medicinal Chemistry. 1999;7:2123-30.

[187]. Minning S, Schmidt-Dannert C, Schmid RD. Functional expression of Rhizopus oryzae lipase in *Pichia pastoris*: high-level production and some properties. Journal of Biotechnology. 1998;66:147-56.

[188]. Yu M, Lange S, Richter S, Tan T, Schmid RD. High-level expression of extracellular lipase Lip2 from Yarrowia lipolytica in *Pichia pastoris* and its purification and characterization. Protein Expression and Purification. 2007;53:255-63.

[189]. Eom GT, Lee SH, Song BK, Chung K-W, Kim Y-W, Song JK. High-level extracellular production and characterization of *Candida antarctica* lipase B in *Pichia pastoris*. Journal of Bioscience and Bioengineering. 2013;116:165-70.

[190]. Zheng Y-Y, Guo X-H, Song N-N, Li D-C. Thermophilic lipase from *Thermomyces lanuginosus*: Gene cloning, expression and characterization. Journal of Molecular Catalysis B: Enzymatic. 2011;69:127-32.

[191]. Zhang AL, Luo JX, Zhang TY, Pan YW, Tan YH, Fu CY, et al. Recent advances on the GAP promoter derived expression system of *Pichia pastoris*. Molecular Biology Reports. 2009;36:1611-9.

[192]. Li P, Anumanthan A, Gao XG, Ilangovan K, Suzara VV, Duzgunes N, et al. Expression of recombinant proteins in *Pichia pastoris*. Applied Biochemistry and Biotechnology. 2007;142:105-24.

[193]. Park J, Oh B-R, Seo J-W, Hong W-K, Yu A, Sohn J-H, et al. Efficient Production of Ethanol from Empty Palm Fruit Bunch Fibers by Fed-Batch Simultaneous Saccharification and Fermentation Using *Saccharomyces cerevisiae*. Applied Biochemistry and Biotechnology. 2013;170:1807-14.

[194]. Afolabi KD, Akinsoyinu AO, Omojola AB, Abu OA. The performance and egg quality traits of Nigerian local hens fed varying dietary levels of palm kernel cake with added palm oil. The Journal of Applied Poultry Research. 2012;21:588-94.

[195]. Liu ZH, Qin L, Jin MJ, Pang F, Li BZ, Kang Y, et al. Evaluation of storage methods for the conversion of corn stover biomass to sugars based on steam explosion pretreatment. Bioresource Technology. 2013;132:5-15.

[196]. Zhang J, Zhu Z, Wang X, Wang N, Wang W, Bao J. Biodetoxification of toxins generated from lignocellulose pretreatment using a newly isolated fungus, *Amorphotheca resinae* ZN1, and the consequent ethanol fermentation. Biotechnology for Biofuels. 2010;3:26.

[197]. Richardson TL, Harner NK, Bajwa PK, Trevors JT, Lee H. Approaches To Deal with Toxic Inhibitors during Fermentation of Lignocellulosic Substrates. Sustainable Production of Fuels, Chemicals, and Fibers from Forest Biomass: American Chemical Society; 2011. p. 171-202.

[198]. Kadar Z, Maltha SF, Szengyel Z, Reczey K, De Laat W. Ethanol fermentation of various pretreated and hydrolyzed substrates at low initial pH. Applied Biochemistry and Biotechnology. 2007;137:847-58.

[199]. Roe AJ, McLaggan D, Davidson I, O'Byrne C, Booth IR. Perturbation of anion balance during inhibition of growth of *Escherichia coli* by weak acids. Journal of Bacteriology. 1998;180:767-72.

[200]. Ibraheem O, Ndimba BK. Molecular adaptation mechanisms employed by ethanologenic bacteria in response to lignocellulose-derived inhibitory compounds. International journal of biological sciences. 2013;9:598-612.

[201]. Cherrington CA, Hinton M, Chopra I. Effect of short-chain organic acids on macromolecular synthesis in *Escherichia coli*. Journal of Applied Bacteriology. 1990;68:69-74.

[202]. Ma M, Liu ZL. Comparative transcriptome profiling analyses during the lag phase uncover YAP1, PDR1, PDR3, RPN4, and HSF1 as key regulatory genes in genomic adaptation to the lignocellulose derived inhibitor HMF for *Saccharomyces cerevisiae*. BMC Genomics. 2010;11:660.

[203]. Uddin S, Hadi SM. Reactions of furfural and methylfurfural with DNA. Biochemistry and molecular biology international. 1995;35:185-95.

[204]. Heux S, Sablayrolles JM, Cachon R, Dequin S. Engineering a *Saccharomyces cerevisiae* wine yeast that exhibits reduced ethanol production during fermentation under controlled microoxygenation conditions. Applied and Environmental Microbiology. 2006;72:5822-8.

[205]. Sanchez B, Bautista J. Effects of furfural and 5-hydroxymethylfurfural on the fermentation of *Saccharomyces cerevisiae* and biomass production from *Candida guilliermondii*. Enzyme and Microbial Technology. 1988;10:315-8.

[206]. Atilio de Frias J, Feng H. Pretreatment of furfural residues with switchable butadiene sulfone in the sugarcane bagasse biorefinery. Green Chemistry. 2014;16:2779-87.

[207]. Iwaki A, Kawai T, Yamamoto Y, Izawa S. Biomass conversion inhibitors furfural and 5-hydroxymethylfurfural induce formation of messenger RNP granules and attenuate translation activity in *Saccharomyces cerevisiae.* Applied and Environmental Microbiology. 2013;79:1661-7.

[208]. Zhang J, Zhu Z, Wang X, Wang N, Wang W, Bao J. Biodetoxification of toxins generated from lignocellulose pretreatment using a newly isolated fungus, *Amorphotheca resinae* ZN1, and the consequent ethanol fermentation. Biotechnology for Biofuels. 2010;3:1-15.

[209]. Quevedo-Hidalgo B, Monsalve-Marin F, Narvaez-Rincon PC, Pedroza-Rodriguez AM, Velasquez-Lozano ME. Ethanol production by *Saccharomyces cerevisiae* using lignocellulosic hydrolysate from Chrysanthemum waste degradation. World Journal of Microbiology & Biotechnology. 2013;29:459-66.

[210]. Madhavan A, Srivastava A, Kondo A, Bisaria VS. Bioconversion of lignocellulose-derived sugars to ethanol by engineered *Saccharomyces cerevisiae*. Critical Reviews in Biotechnology. 2012;32:22-48.

[211]. Koppram R, Tomás-Pejó E, Xiros C, Olsson L. Lignocellulosic ethanol production at high-gravity: challenges and perspectives. Trends in Biotechnology. 2014;32:46-53.

# APPENDIXES

# APPENDIX A
# LIST OF PUBLICATIONS

## 1. International Journals

No 1. Raita M, Laothanachareon T, Champreda V, Laosiripojana N. Biocatalytic esterification of palm oil fatty acids for biodiesel production using glycine-based cross-linked protein coated microcrystalline lipase. Journal of Molecular Catalysis B: Enzymatic. 2011; 73:74-9.

Research topics have been submitted for publication

1. Modification of immobilized lipase on magnetic nanoparticle for biodiesel production from palm oil
2. Kinetic study on esterification of palmitic acid catalyzed by glycine-based crosslinked protein coated microcrystalline lipase
3. Biocatalytic methanolysis activities of cross-linked protein-coated microcrystalline lipase toward esterification/transesterification of relevant palm products
4. Bioethanol production from palm kernel cake by the ethanologenic thermophile *Geobacillus thermoglucosidasius* TM242
5. Biocatalytic synthesis of starch esters by immobilized lipase on magnetic nanoparticle (Co-author)

**2. International Conferences**

No. 1 Raita, M., Champreda, V., and Laosiripojana, N., (2012) Development of Cross-Linked Protein Coated Microcrystalline Lipase Biocatalyst for Biodiesel Production using Palm Oil Fatty Acids, the 4 th International Conference on Sustainable Energy and Environment (SEE 2011) : A paradigm Shift to low Carbon Society, February 27-29th 2012.

No. 2 Raita, M., Champreda, V., and Laosiripojana, N., (2012) Biodiesel Production using Cross-Linked Protein Coated Microcrystalline Lipase with Potassium Sulphate as Core Matrix, the 23rd International Symposium on Chemical Reaction Engineering (ISCRE 23), September 7-10th 2014.

## APPENDIX B
## AGAROSE GEL ELECTROPHORESIS FOR CELL SURFACE DISPLAY AND EXTRACELLULAR EXPRESSION OF LIPASE

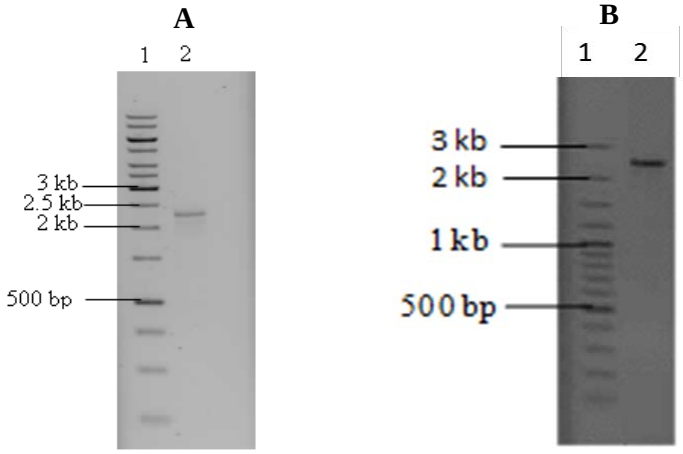


**Figure B1** Purification of LipaseTL_agg and LipaseCA_agg gene.

A: Lane 1; GeneRuler$^{TM}$ 1 kb DNA ladder, Lane 2; purified lipaseTL_agg gene

B: Lane 1; GeneRuler$^{TM}$ 100 bp DNA ladder, Lane 2: purified lipaseCA_agg gene

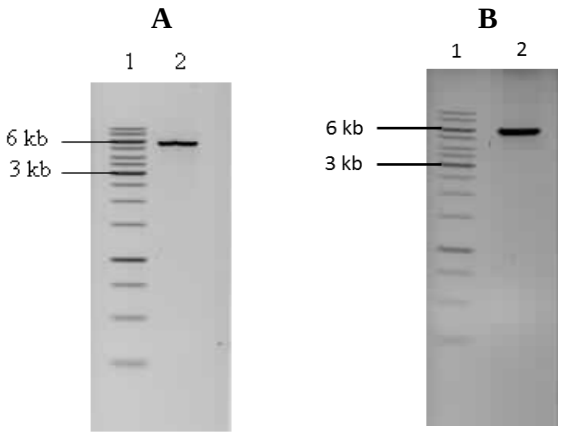


**Figure B2** Recombinant plasmid linearization of cell surface display form.

A: Lane 1; GeneRuler$^{TM}$ 1 kb DNA ladder, Lane 2: linearized pLipaseTL_agg plasmid

B: Lane 1; GeneRuler$^{TM}$ 1 kb DNA ladder, Lane 2: linearized pLipaseCA_agg plasmid

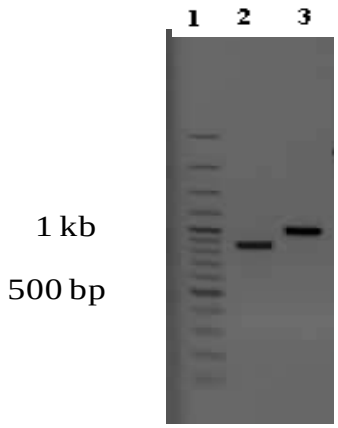


**Figure B3** Purification of LipaseTL_sec, and LipaseCA_sec gene. Lane 1: GeneRuler$^{TM}$ 100 bp DNA ladder, Lane 2: purified lipaseTL_sec gene, and Lane 3: purified lipaseCA_sec gene.

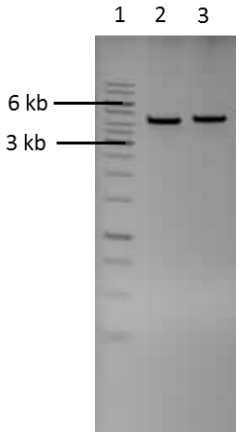


**Figure B4** Recombinant plasmid linearizations of extracellular lipase form. Lane 1: GeneRuler$^{TM}$ 1 kb DNA ladder, Lane 2: linearized pLipaseTL_sec plasmid, and Lane 3: linearized pLipaseCA_sec plasmid.